MICROSPHERE AND ENCAPSULATED CELL TRANSPORT IN A HETEROGENEOUS SUBSURFACE ENVIRONMENT

A Dissertation

Presented in Partial Fulfillment of the Requirements for the

Degree of Doctor of Philosophy

with a

Major in Geology

in the

College of Graduate Studies

University of Idaho

by

Christian R. Petrich

May, 1995

Major Professor: Dale R. Ralston, Ph.D.

Authorization to Submit Dissertation

This dissertation of Christian R. Petrich, submitted for the degree of Doctor of Philosophy with a major in Geology and titled "Microsphere and Encapsulated Cell Transport in a Heterogeneous Subsurface Environment," has been reviewed in final form, as indicated by the signatures and dates given below. Permission is now granted to submit final copies to the College of Graduate Studies for approval.

Major Professor _____ Date 5/17/95
Dale R. Ralston

Committee Members _____ Date 5/17/95
John H. Bush

_____ Date 5-18-95
Ronald L. Crawford

_____ Date 5-17-95
Stanley M. Miller

Department Administrator _____ Date 5-17-95
John H. Bush

College Dean _____ Date 5/17/95
Robert W. Bartlett

Final Approval and Acceptance by the College of Graduate Studies

_____ Date 5/24/95
Jean'ne M. Shreeve

Abstract

Indigenous subsurface microorganisms cannot easily degrade certain environmental contaminants. Non-indigenous microorganisms may be used in some cases to degrade these contaminants. The survival of non-indigenous microorganisms is crucial to the success of their use for *in situ* bioremediation; cell encapsulation has been shown to enhance the survival of some non-indigenous microorganisms. The use of encapsulated cells in a subsurface environment for *in situ* bioremediation depends, in part, on the transport characteristics of the encapsulated cells.

The objective of this study was to compare transport characteristics of encapsulated cells, polystyrene microspheres, and conservative tracers under field conditions, and to describe potential limitations of using encapsulated cells for subsurface bioremediation. The study included (1) the hydrogeological characterization of a shallow, confined, heterogeneous aquifer consisting of unconsolidated silts, sands, and gravels, and (2) a series of recirculating, uniform flow tracer tests with bromide; 2-, 5-, and 15-μm fluorescent polystyrene microspheres; and agarose encapsulated *Flavobacterium* tracers.

Tracer test results indicate significant influence of aquifer heterogeneity on solute and particle tracer transport. Differences in transport patterns of the solute and particle tracers point to transport in preferential ground water flowpaths. Results indicate that particle tracers and bromide migrated at approximately the same rate in certain flowpaths, but that particle tracers were excluded from some (or many) of the flowpaths carrying bromide. The combined use of solute and particle tracers may represent a method for evaluating preferential flowpath characteristics.

Encapsulated cell transport results were inconclusive. Preliminary results suggest that encapsulated cell transport was retarded with respect to the polystyrene microspheres. Microsphere transport results suggest that *in situ* bioremediation designs using encapsulated cells must accommodate differences in the migration characteristics of encapsulated cells and contaminants in a heterogeneous environment.

Acknowledgments

I would like to express deep appreciation to my major professor, Dr. Dale Ralston, and to faculty advisors Dr. John Bush, Dr. Ronald Crawford, and Dr. Stanley Miller for their guidance, advice, encouragement, and constructive criticism in completing this study. I would like to acknowledge the assistance of and discussions with Dr. Keith Stormo. I would also like to thank Vikranth Malyala and Govind Deshpande for many hours of counting spheres, Dr. Dave Knaebel for performing the PCR analysis, and Tom Mullen for conducting grain size analyses. Finally, I would to express gratitude to my loving wife, Susan Gelletly, for her ongoing patience, support, and encouragement throughout this entire process.

This work has been supported by grants from the Idaho Center of Hazardous Waste Remediation, the Idaho Water Resources Research Institute, and the U.S. Department of Ecology.

Dedication

I dedicate this work to my parents, Reinhard and Barbara Petrich, and to my wife, Susan Gelletly, who have inspired me to learn and to appreciate flowing water.

Table of Contents

APPENDICES

List of Tables

List of Figures

1. Introduction

1.1. Problem Statement

In situ biodegradation, the process of degrading xenobiotic compounds in a subsurface environment, is emerging as a promising method for restoring selected contaminated sites. Successful *in situ* biodegradation depends on a variety of factors, including contaminant type, aquifer materials and characteristics, availability of oxygen and nutrients, the presence of specific microbial populations, and other subsurface chemical and biological conditions.

Many contaminants are vulnerable to degradation by indigenous microbial populations. Some contaminants, such as pentachlorophenol, are not readily degraded by native microbes (Pignatello et al., 1983; Crawford et al., 1990). Non-indigenous bacteria have been identified that degrade some resistant contaminants (Crawford and O'Reilly, 1990). Such organisms might be introduced into the subsurface environment for *in situ* biodegradation of resistant contaminants.

Organism survival is a factor in the use of non-indigenous organisms for *in situ* bioremediation. Introduced microbes may disappear or be reduced to very low levels in days or weeks under marginal survival conditions. Microorganism survival may be limited by chemical concentrations; local contaminant concentrations may be biocidal, or non-contaminated water may not contain sufficient carbon/energy sources for biomass maintenance.

Microencapsulation of degradative organisms is a technique that enhances microorganism survivability (Stormo and Crawford, 1992). Preliminary findings showed that encapsulation increased microbial survivability by more than three orders of magnitude. Certain microencapsulated microbial enzymes may also be used for xenobiotic degradation, without the need for whole microbial cells.

One factor influencing *in situ* bioremediation using encapsulated cells is the migration of encapsulated cells in the subsurface. The encapsulated cells (or bacteria emanating from the encapsulated cells) must come into contact with the contaminant.

Encapsulated cell transport along primary ground water flowpaths may be desirable, or it may be desirable to have encapsulated cells remain stationary with contaminated ground water flowing past the encapsulated cells.

A fundamental understanding of subsurface encapsulated cell transport characteristics under field conditions is important to application of encapsulated cell technology for *in situ* bioremediation. This study therefore focuses on transport patterns of encapsulated cells and particle analogues in a subsurface field environment.

1.2. Purpose and Objectives

The purpose of this project was to aid in the development of encapsulated cell biodegradation methods by investigating particle transport characteristics. The general research objective was to compare transport characteristics of encapsulated cells, possible encapsulated cell analogues, and conservative tracers under field conditions, and to describe potential limitations of using encapsulated cells for subsurface bioremediation. Specific objectives included:

1. Conducting a review of pertinent scientific literature.
2. Preparing an experimental tracer test design.
3. Selecting an appropriate field site.
4. Conducting a detailed site investigation.
5. Evaluating hydraulic properties at the site.
6. Conducting a series of tracer experiments using a conservative, dissolved tracer, encapsulated cells, and a potential encapsulated cell analogue tracer under field conditions.
7. Comparing conservative and particle tracer transport results from the tracer experiments.
8. Describing potential limitations of using encapsulated cells for *in situ* bioremediation based on observed transport patterns.

1.3. Project Overview and Dissertation Organization

The general research objective for this project was to compare subsurface transport patterns of selected conservative and particle tracers in a field environment.

The project consisted of a conducting a scientific literature review, developing an experimental design, selecting a field site, conducting a site investigation and hydraulic characterization, conducting a series of tracer tests, and analyzing and comparing tracer test results. As with many field projects, individual project phases were influenced by findings made during previous phases. This dissertation therefore presents a description of project research activities in the approximate order in which they occurred.

The first step was to review the scientific literature pertaining to this project. Chapter 2 includes a review of factors affecting *in situ* bioremediation, cell encapsulation, and encapsulated cell survival. Particle filtration literature is also explored, followed by a brief review of common tracer test methods.

Chapter 3 presents a discussion of the general experimental design. Encapsulated cells are the primary tracer of interest; reasons for selecting additional tracers are described. The experimental setting (laboratory vs. field) is addressed; a rationale for the experimental scale is also presented. Field-site selection criteria are presented based on the tracers of interest and the desired experimental setting and scale. These factors led to a general experimental design under which monitoring-well design criteria were established.

The site selection process is presented in Chapter 4. A site was selected from two potential candidates on the basis of available information and on the drilling and installation of six exploratory monitoring wells. Chapter 4 describes the field site and its geological setting.

The site investigation is described in Chapter 5. The chapter begins with a general description of the field site and the geological setting. Site investigation tasks included installing additional monitoring wells, analyzing sediment samples for grain-size distribution, and periodically measuring water levels in the wells. A conceptual aquifer model was built from the results of the site investigation.

Three multi-well aquifer tests were conducted at the site to estimate hydraulic parameter values. Chapter 6 describes field methods used for the aquifer tests, followed by an analysis of aquifer test results.

Chapter 7 presents a detailed description of tracer test methods (this chapter builds on the general experimental design outlined in Chapter 3). The description of tracer test methods includes a description of the sampling system, the instrumentation system, and the tracer injection procedure.

Tracer test results are provided in Chapters 8, 9, and 10. These chapters present graphical comparisons of bromide, microspheres, and encapsulated cell tracer concentration patterns and replicate test results. A discussion of tracer test results is presented in Chapter 11

Conclusions formed on the basis of tracer test results are presented in Chapter 12. Recommendations for further study are also proposed in Chapter 12.

2. Background

2.1 Introduction

This chapter provides a brief review of scientific literature pertaining to the use of encapsulated cells for *in situ* bioremediation applications, beginning with a brief overview of factors that influence the success of *in situ* bioremediation. Enhancing microbial survival through the use of cell immobilization then is explored, followed by a discussion of cell encapsulation. Particle transport and filtration factors also are reviewed. The final sections provide a review of common tracer test techniques and a discussion of particle tracers.

2.2 Factors Affecting *in Situ* Bioremediation

Numerous factors contribute to the successful bioremediation of contaminated subsurface environments. These factors include the availability of appropriate organisms and adequate microbial growth conditions.

The presence of indigenous bacteria in ground water systems has been well documented (Harvey et al., 1984; Wilson et al., 1983; Aelion et al., 1987; and Fetter, 1994). Many hydrocarbon and other organic contaminants may be degraded by indigenous microbial populations (Mueller et al., 1991; Fetter, 1994).

Some organic compounds, however, such as chlorinated phenols, are resistant to biological degradation by indigenous organisms (Mueller et al., 1991; Crosby, 1981; Pignatello et al., 1983; and Crawford et al., 1990). Mueller et al. (1991) reported that while indigenous soil microorganisms removed from 87% to 100% of measured phenolic and lower-molecular-weight polycyclic aromatic hydrocarbons (PAHs), only 53% of higher-molecular-weight polycyclic aromatic hydrocarbons were degraded, and that pentachlorophenol was not removed. The authors suggested that indigenous microorganisms may not degrade these compounds in a reasonable time span.

Non-indigenous bacteria have been identified that effectively degrade chlorinated phenols such as pentachlorophenol (Martinson et al., 1984; Smallbeck and Strehler, 1987; O'Reilly et al., 1987; Crawford, 1987). Non-indigenous bacteria introduced to a

foreign subsurface environment may, however, succumb to new environmental conditions (Stormo and Crawford, 1994). Cells grown under rapid-growth conditions may undergo extreme physiological stress when exposed to new conditions in a subsurface environment.

Bacterial growth and survival of indigenous and non-indigenous microbes depends on a variety of factors. Subsurface bacterial growth requires sources of carbon, nitrogen, phosphorus and other inorganic nutrients (e.g., potassium, magnesium, sodium, iron) for the synthesis of nucleic acids. Bacterial growth requires electron acceptors, such as molecular oxygen. Bacteria can survive a variety of temperatures; freezing may stop growth but does not necessarily lead to death. All microorganisms require water. Some bacteria are very efficient at preserving moisture, which may be important in the vadose zone (Chapelle, 1993).

Bacterial growth may be limited by a variety of environmental factors such as a lack of substrate, production of toxic waste products, infection by viruses, or predation by protozoa (Chapelle, 1993). Xenobiotic compounds may inhibit microbial growth if local concentrations are biocidal.

Cell encapsulation is a technique that has been shown to increase microbial survival of non-indigenous cells under subsurface conditions (Stormo and Crawford, 1994). Encapsulation allows the inclusion of nutrients and carbon sources in the immediate cell environment, and offers a degree of protection from predators.

2.3 Cell Encapsulation

Microencapsulation is a process for immobilizing bacteria in a protective matrix to increase cell survival in subsurface environments. This section, based in part on Stormo (1993), presents a brief discussion of cell encapsulation.

The concept of using encapsulated cells for *in situ* subsurface bioremediation has been developed from aboveground applications. Bacteria, plant cells, animal cells and enzymes (Hulst et al., 1985; Dominguez et al., 1988; Fukushima et al., 1988; Pras et al., 1989) have been immobilized in a variety of matrices such as calcium alginate (Tramper et al., 1986a), K-carrageenan (Tramper et al., 1986b), and polyurethane (Renneberg et

al., 1988; Yang et al., 1988). Both fixed-film and batch reactors have been developed using bacteria immobilized in calcium alginate, agarose, and/or polyurethane foam (Stinson et al., 1991; Crawford and Chresand, 1990; Young, 1989; O'Reilly, 1989; Levinson, 1991; Tao, 1990).

Cell encapsulation offers several potential advantages for introducing organisms into the subsurface. Immobilization may increase the cell loading capacity (Nilsson et al., 1972; McGhee et al., 1984; Vournakis et al., 1989) and/or increase rates of production of microbial products (Lawton et al., 1987; Berry et al., 1988; Pundle et al., 1988) in bioreactors. A carrier material, such as agar (Jawson et al., 1989), peat (Aarons et al., 1986; Berg et al., 1988), alginate (Bashan, 1986), alginate-clay (Fravel et al., 1985), or fluid gels (Jawson et al., 1989) may represent a distinct advantage for organisms being introduced into the environment (Fravel et al., 1985; Aarons et al., 1986; Bashan, 1986; Berg et al., 1988; Jawson et al., 1989). These carriers can provide cells with nutrients and moisture, and may allow a higher concentration of organisms to be incorporated into the soil. Encapsulation materials can provide cells with increased protection from predators. Many researchers have shown that predation is an important biological factor affecting the survival of introduced organisms (van Elsas et al., 1986; Vargas et al., 1986; Corman et al., 1987; Acea et al., 1988; Compeau et al., 1988).

A major limitation to methods of entrapping bacteria within spherical immobilization matrices has been the difficulty of preparing beads (encapsulated cells) consistently in diameters of less than about 0.5 mm. Small diameters are required for transport under typical subsurface conditions. Stormo and Crawford (1992) developed a method for immobilizing large quantities of bacteria in calcium alginate, agarose, or polyurethane in diameters ranging from approximately 2 to 80 μm (Figure 2.3-1). Cell encapsulation in beads of small diameter presents the potential for using encapsulated cells under *in situ* aquifer conditions.

2.4 Encapsulated Cell Survival

Recent experiments using encapsulated and unencapsulated *Flavobacterium* ATCC 39723, a gram-negative aerobe capable of degrading a variety of chlorinated

phenols, indicated increased survival of the encapsulated cells. Stormo and Crawford (1993) evaluated pentachlorophenol degradation by microencapsulated *Flavobacterium* microbeads. Experiments were conducted in microcosms containing sand and gravel materials taken from the University of Idaho Groundwater Research Site from depths up to 5 m (Stormo and Crawford, 1994). Pentachlorophenol-spiked water was run through the microcosms for 150 days. The authors found no statistical difference in the degradation rates between microcosms containing free and encapsulated *Flavobacterium*. Flow through the microcosms was suspended following the degradation study and the temperature maintained at 20°C. After 400 days, selected microcosms were sacrificed. Encapsulated *Flavobacterium* were able to recover and degrade pentachlorophenol, whereas unencapsulated *Flavobacterium* were not. These results indicate that encapsulation enhanced the long-term survival of non-indigenous bacteria.

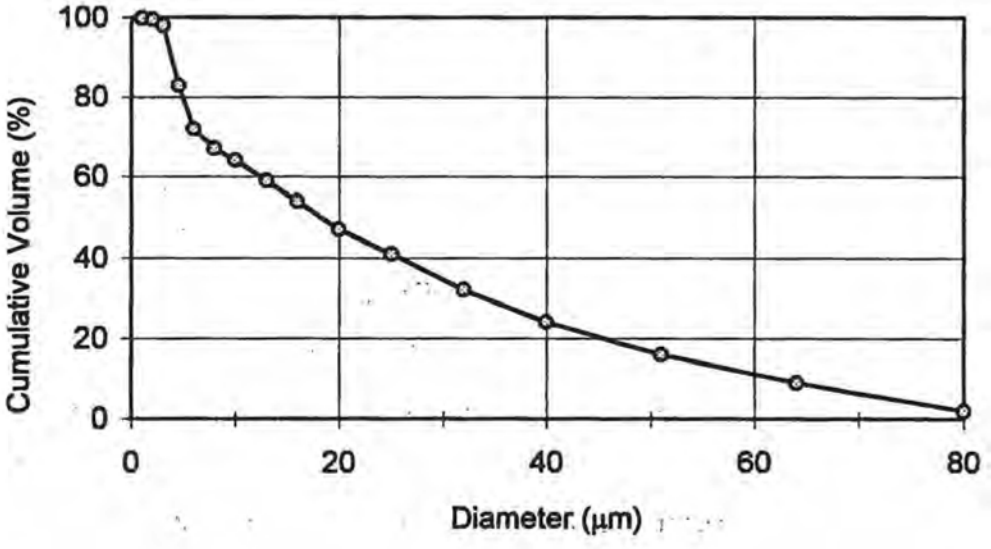

Figure 2.3-1: Bead size distribution of immobilized *Flavobacterium* cells (from Stormo and Crawford, 1992).

2.5 Particle Transport and Filtration

The success of *in situ* bioremediation using encapsulated cells is controlled, in part, by the extent of contact between encapsulated cells and the subsurface contaminant. Contact between the encapsulated cells and the contaminant may occur as the encapsulated cells are transported to or through contaminated zones, or as a dissolved contaminant migrates through zones containing encapsulated cells.

The extent of encapsulated cell transport is influenced by factors controlling the transport of other particles. Factors affecting particle transport include mechanical filtration, physiochemical filtration (adsorption/desorption), London-Van der Waals, and/or electrokinetic forces (Herzig et al., 1970). Mechanical filtration (straining) is the dominant process for large particles (diameter ≥ 30 μm), and results in particles being held in constrictions, crevices, and caverns by friction and fluid pressure forces. Physiochemical filtration results in particle capture on media grain surfaces of particles in the ≤ 3-μm range (typically approximately 1 μm). Both mechanical and physiochemical phenomena influence migration in particles ranging from approximately 3 to 30 μm (Herzig et al., 1970). London-Van der Waals and electrokinetic forces influence particle movement of colloidal-sized particles (≤ 1 μm).

Particles entering a porous medium may be mechanically strained in small pore spaces. Although such straining is frequently considered to be a major cause of particle removal from ground water, there are few reports of quantitative analysis of this phenomenon (McDowell-Boyer, 1986). Straining occurs when particles are captured within the matrix of the porous medium.

Particle capture may occur because of sedimentation, particle inertia, hydrodynamic effects, direct interception, and diffusion by Brownian motion (Herzig et al., 1970). Sedimentation occurs when particles of densities greater than that of the carrier fluid and velocities less than that of the carrier fluid settle into the surrounding matrix. Particle inertia can lead to filtration if a particle's weight prevents it from following bends in a streamline. Hydrodynamic effects can cause the lateral movement of non-spherical particles (forcing the particle into contact with media grains) in a non-uniform fluid shear field. Direct interception occurs when particles are too large to

follow the smallest tortuosities of carrier fluid streamlines. Finally, particles can reach zones outside of normal ground water flowpaths by Brownian motion and may thus be retained. Herzig et al. (1970) maintained that inertial forces are commonly negligible relative to gravity forces in an environment with laminar flow characteristics (suspension velocities of less than 0.1 cm/sec), and with media grain diameters on the order of 500 or 1000 μm; Brownian motion was also suggested to be insignificant under laminar flow conditions.

Once captured, particles may be retained at surface sites, crevice sites, constriction points, and cavern sites. Forces leading to the retention of suspended particles include axial fluid pressure, friction forces, and surface forces.

Particles larger than the porous medium grain size may form a surface mat or filter cake where flow is entering the medium. Substantial particle accumulation may lead to significant permeability reductions. Surface filtration is commonly used for filtering in chemical and process industries. Cheremisinoff and Azbel (1983) present a detailed review of the surface filtration literature.

Sakthivadivel (1972, reported in McDowell-Boyer, 1986) suggested that a critical factor determining filtration in porous media is d_m/d_p, where d_m and d_p are the media and particle diameters, respectively. Cake filtration would occur if d_m/d_p was less than 10 (relatively large particles compared to the medium size); i.e., no particle penetration would occur into the media. For d_m/d_p >20 (relatively small particles compared to the medium size), only 2 to 5% of the pore volume in a 45-cm column was occupied by retained particulate under equilibrium conditions, and permeability reductions were in the range of 10 to 15%. For $10<d_m/d_p<20$, Sakthivadivel found that media permeability was reduced by factors of 7 to 15, and that deposited particles occupied more than 30% of the media pore volume. Finally, he reported that increased flow rate would not dislodge filtered particles. These relationships are illustrated in Figure 2.5-1.

Sherard et al. (1984a, 1984b) conducted similar experiments, taking into account size distributions of both particles and media grains. The researchers conducted experiments to determine at what point fine sand would be filtered in coarse sand. The

investigators found that for $d_{m,15}/d_{p,85} < 9$ fine sand would not penetrate coarser sand, where 15% of the coarse filter sand (by weight) had a diameter of $d_{m,15}$ and 85% of the finer sand particles (by weight) had diameters $\cong d_{p,85}$.

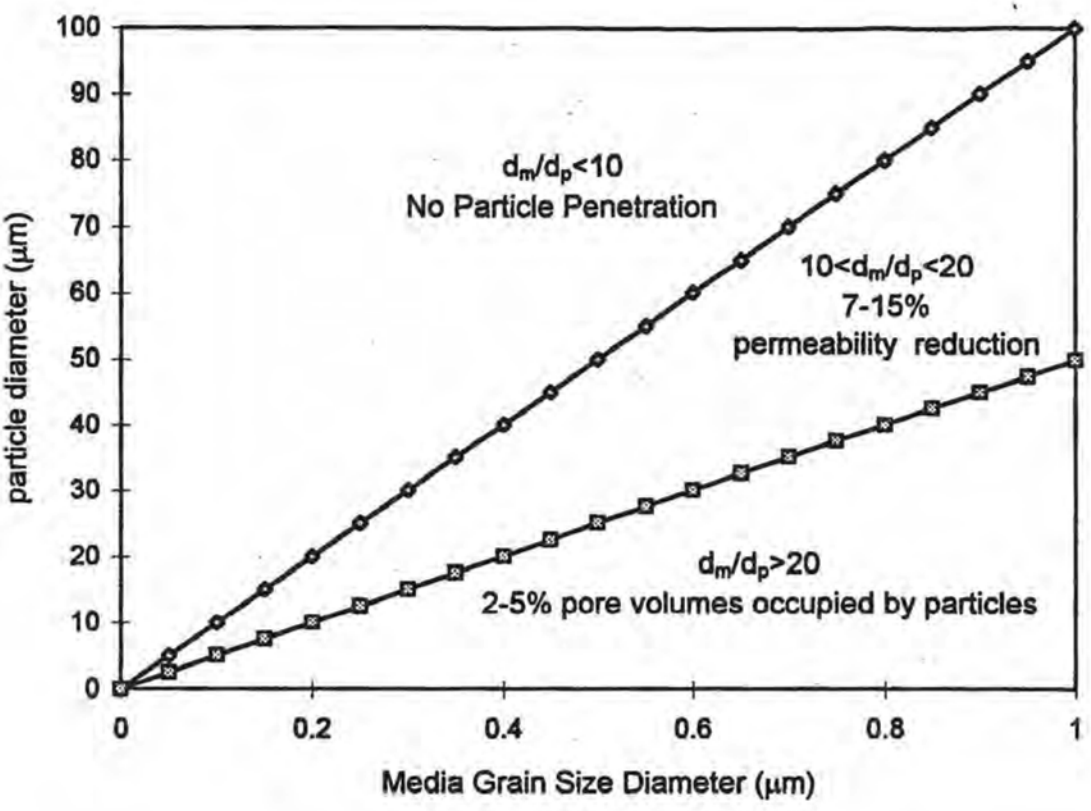

Figure 2.5-1: Media grain size and particle size relationships (based on Sakthivadivel, 1972, and in McDowell-Boyer, 1986).

Decolmotage (de-clogging, or a release of retained particles from the porous medium) processes are also important (Herzig et al., 1970). Spontaneous decolmotage may occur if local variations in pressure or flow rate change the flow in the immediate vicinity of a particle, or if a moving particle collides with a retained particle. Larger-scale decolmotage may occur if sudden variations in pressure or flow rate are applied, such as in the sphere of influence surrounding a changing pumping well.

Aquifer heterogeneity is an important factor in contaminant, microbial, and encapsulated cell migration under field conditions. Much of the particle transport

research has been conducted with homogeneous materials (Borchardt et al., 1961; Maroudas, 1965; Heertjes et al., 1967; Herzig et al., 1970; Sakthivadivel, 1972; Fitzpatrick and Spielman, 1973; and Darby and Lawler, 1990). Results from some of this work may not directly apply to poorly sorted, heterogeneous field conditions. Heterogeneous conditions are difficult to reproduce in laboratory settings. Smith et al. (1985) found that columns prepared from mixed, repacked soil filtered *Escherichia coli* more effectively than columns containing intact soils.

2.6 Tracer Tests

Tracer tests are a widely accepted tool in subsurface hydrology (Davis et al., 1985). Examples of extensive tracer tests include those conducted at field sites on Cape Cod, Massachusetts (Barber, 1987; Garabedian et al., 1987; LeBlanc et al., 1987; Smith et al., 1987a, b), and at Borden, Ontario (Curtis et al., 1986; Freyburg, 1986; Mackey et al., 1986; Roberts et al., 1986). Ground water tracers have included yeast, bacteria, viruses, spores, ions (e.g., chloride, bromide, iodide, etc.), various dyes, gases, stable isotopes, and radionuclides (Keswick et al., 1982; Davis et al., 1985). Many tracer tests are designed for unique combinations of tracers, local hydrogeologic conditions, injection methods, and desired sampling configurations.

General categories of tracer tests include radial flow and uniform flow tests (Davis et al., 1985). The first category, single-well techniques, include injection/withdrawal or borehole dilution methods. Two-well techniques include uniform flow or radial flow tests (Davis, et al., 1985).

Forced-gradient tracer tests, conducted in an induced gradient between two wells (Bianchi-Mosquera and Mackay, 1994), have been used to investigate transport processes with less time than required by natural-gradient tracer tests. Forced-gradient tracer tests have been used for investigating transport parameters within subsurface contaminant plumes (Mackay and Thorbjarnarson, 1990). Bianchi-Mosquera and Mackay (1994) conducted replicate forced-gradient tracer experiments with sorptive and conservative tracers.

2.7 Particle Tracers

Particle tracers have been used under laboratory conditions for filtration experiments (Maroudas et al., 1965; Herzig et al., 1970; Heertjes et al., 1967; Borchardt et al., 1961; Fitzpatrick et al., 1973; Gruesbeck et al., 1982; and Darby et al., 1990). Bacteria and other particles have been used as tracers under both laboratory and field conditions (Harvey et al., 1989; Champ and Schroeter, 1988; Smith et al., 1985; and Keswick et al., 1982).

Polystyrene microspheres have been used for emulating bacterial migration in ground water (Harvey et al., 1989; and Harvey et al., 1993). Tracer experiments were conducted with microspheres consisting of carboxylated latex, plain latex, and polyacrolein (having carboxyl surface groups), ranging in diameter from 0.2 to 1.3 μm, in a sandy freshwater aquifer. Multilevel monitoring was conducted at a distance of 6.9 m from the injection source.

Results suggested that carboxylated microsphere interaction with sediment led to greater retardation than occurred with fluorochrome-labeled bacteria, because of microparticle surface composition (Harvey et al., 1989). Retardation relative to chloride was also noted for polyacrolein microspheres; the breakthrough of uncharged latex particles occurred just slightly after chloride breakthroughs. Harvey et al. (1989) also noted greater dispersion for carboxylated microspheres relative to bacteria. The researchers suggested that the optimal size range for that site may be as much as several micrometers, based on unpublished data using neutral latex microspheres in the 1-, 3-, and 6-μm size range.

The researchers (Harvey et al., 1989) also reported evidence suggesting that transport of larger microorganisms through aquifer sediments is more rapid than that of smaller microorganisms. This phenomenon also appeared apparent in some of the microsphere data: the researchers noted an approximate 9-10 day retardation at 6.9 m for 0.23-, 1.53-, and 0.93-μm carboxylated latex particles (relative to chloride), but only a 2-day retardation for 1.35-μm diameter particles. Finally, the researchers noted a lack of apparent relationship between microsphere attenuation (immobilization within aquifer sediments) and retardation (slower transport).

Harvey et al. (1993) studied the effect of physical variability on the relative transport behavior of microbial-sized carboxylated microspheres, indigenous bacteria, and bromide. Data collected from both column and field experiments indicated the importance of aquifer sediment structure on microbial transport characteristics. The researchers noted the retardation of carboxylated microspheres in both field and laboratory tests with respect to bromide.

Champ and Schroeter (1988) investigated bacterial transport in a fractured crystalline rock environment (Chalk River) using conservative ion tracers, *Escherichia coli*, and "non-reactive particle" tracers. The particle tracers consisted of 0.83-, 1.17-, and 2.08-μm *Polybead Fluorescent* and *Fluoresbrite* microspheres (*Polysciences, Inc.*). Bacteria were counted by observing stained cells under a microscope and by plate counts on EMB agar. Microspheres were enumerated under a fluorescence microscope following collection under a filter. The researchers found that bacteria and particle tracer arrival times were the same or less than those for conservative tracers. Particle filtration was observed and was quantified by calculating filter factors. Filtration processes occurring in the fracture system were thought to be similar to those found in a gravel aquifer.

2.8 Summary

Cell encapsulation has been shown to increase the survival of non-indigenous microbes in a foreign environment (Stormo and Crawford, 1994). The successful use of encapsulated cells for *in situ* bioremediation depends on contact between encapsulated cells and subsurface contaminants. Factors having the most influence on encapsulated cell migration (because of particle size) are filtration and physiochemical processes. Relevant particle transport literature focused on understanding filtration processes or on the transport of bacteria and/or bacterial analogues (e.g., microspheres). Transport experiments conducted in laboratory columns may not adequately reflect the heterogeneous nature of typical field conditions (Smith et al., 1987). Results from experiments using microsphere tracers (Harvey et al., 1989; Harvey, 1993; Champ and Schroeter, 1988) indicate surface effects with carboxylated spheres, and that some larger particles may migrate faster than smaller particles in certain size ranges. No

citations describing encapsulated cell transport in natural-aquifer conditions were found in the scientific literature.

3. Experimental Design

3.1. Introduction

This chapter presents the development of and rationale for the general experimental tracer test design. The general experimental design evolved during the course of the field investigation, on the basis of initial observations and results. This chapter defines, however, a fundamental experimental design under which site investigation, hydraulic testing, and specific tracer test components were established.

The experimental design began with tracer selection, because the general research objective is driven by an interest in encapsulated cell migration. An experimental scale was defined based on anticipated tracer characteristics, potential encapsulated cell bioremediation applications, and logistics. Site-selection criteria were based on available sites, anticipated tracer characteristics, experimental scale, and generic contaminated-site characteristics. The general experimental design then was developed on the basis of tracer characteristics, experimental scale, and site characteristics.

3.2. Tracers

This study focuses on developing an understanding of encapsulated cell transport characteristics. Stormo and Crawford (1992) showed that microencapsulation enhanced *Flavobacterium* survival in microcosm experiments. The successful use of encapsulated *Flavobacterium* for *in situ* biodegradation depends on the degree of contact between the encapsulated cells and the subsurface contaminant. The degree of contact depends, in part, on the transport characteristics of the encapsulated *Flavobacterium*. This work is, in part, a continuation of encapsulated cell production and survival research by Stormo and Crawford (1991, 1992, 1994). The primary tracer selected for this project is therefore the same agarose-encapsulated *Flavobacterium* used in previous survival experiments.

Two encapsulated cell characteristics were expected to influence subsurface migration. First, the larger of the encapsulated cells (Figure 2.3-1) were expected to be

sizes (McDowell-Boyer, 1986; Sherard, 1984a, 1984b; Harvey et al., 1989; Harvey et al., 1993). However, it was hypothesized that a large portion of the encapsulated cells would be small enough to be transported at least some distance.

A second unknown encapsulated cell characteristic was the potential interaction between the encapsulation material (agarose) and aquifer sediments. No references were found in the scientific literature regarding agarose interaction in a subsurface environment.

A second particle tracer was chosen as a possible encapsulated cell transport analogue and as a conservative particle tracer for an experimental control. *Fluoresbrite* plain polystyrene latex microspheres (*Polysciences, Inc.*) have been evaluated as a bacterial analogue (Harvey et al., 1989), and were chosen as the second particle tracer because (1) they could be counted in large and small quantities under a microscope, (2) the particles were available in discrete, identifiable sizes, (3) they did not appear to adsorb to aquifer materials (Harvey et al., 1989), and (4) the author knew of no other commercially available particles with similar characteristics. Polystyrene microsphere sizes were selected to represent smaller-sized encapsulated cells.

A third tracer was desired to represent average ground water flow. Ion tracers, such as chloride and bromide, are commonly used for this purpose (Davis, et al., 1985). Chloride and bromide are inexpensive and can be monitored relatively inexpensively using selective ion probes. Chloride, bromide, and iodide have been shown to provide reproducible results in tracer tests (Bianchi-Mosquera and Mackay, 1994).

3.3. Scale

Tracer experiments are a method for analyzing tracer migration and aquifer transport characteristics. Aquifer transport characteristics depend, in part, on the scale of measurement. Tracer tests may be conducted over distances of centimeters (small scale), meters (intermediate scale), or tens or hundreds of meters (large scale). The applicability of results from any tracer test depends on the degree to which the tracer test scale is representative of the aquifer volume of interest.

In this work an intermediate scale (meters) for tracer tests was chosen for several reasons. First, the cost of conducting tracer tests (in terms of time, tracer, and sampling requirements) over an intermediate scale are less than the cost of tests conducted over a large scale. Second, intermediate-scale tests are not as sensitive to the micro-heterogeneities that may influence a small scale test. Third, an intermediate scale may represent some sites for which *in situ* bioremediation might be a treatment option, and represents near-well conditions for injection wells at a larger site.

3.4. Experimental Setting

Intermediate-scale tracer studies can be conducted under laboratory or field conditions. Various porous media materials can be used in laboratory columns or tanks, using either homogeneous, sieved material or retrieved aquifer sediments.

A field setting was chosen over a laboratory setting for several reasons. First, the author's experience and the literature (Smith, et al., 1985) reveals the inherent difficulty in representing the heterogeneous nature of typical field conditions in laboratory settings. Second, tracer tests conducted under field conditions were thought to be more representative of conditions at some typical contaminated sites. Third, field-based, rather than laboratory based, particle monitoring techniques provide a better test of monitoring system design.

The following criteria for selecting a field site were identified:

1. University of Idaho land ownership.
2. Access to University of Idaho laboratories.
3. Presence of the following aquifer characteristics: unconsolidated sediments, materials conducive to particle transport, uniform aquifer thickness, and relatively shallow aquifer depth.
4. Confining hydraulic conditions (for constant aquifer thickness during induced-gradient tracer tests).

The rationale for these criteria is as follows. First, University of Idaho ownership was required for site access. Second, ready access to University of Idaho laboratories was desired for ease of laboratory analysis. Third, many shallow aquifers vulnerable to contamination consist of unconsolidated sediments; selecting a field site in

unconsolidated sediments would provide results applicable to other similar sites. Fourth, sufficiently large aquifer grain sizes were required for particle and encapsulated cell transport. Fifth, a shallow aquifer depth was desired for well construction and sampling ease. Finally, constant areal aquifer thickness and confining hydraulic conditions were desired for two reasons: to allow comparisons of tracer test results from separate but nearby areas conducted under similar gradients, and to maintain uniform flow (and therefore ground water velocities) under induced-gradient tests.

3.5. General Tracer Test Design

Numerous types of tracer tests have been conducted for a variety of tracers under a variety of conditions (see Chapter 2). The tracer test design for this project was developed for encapsulated cell, polystyrene microsphere, and ion tracers on an intermediate tracer test scale, in a field setting. This section describes the general tracer test design, and a rationale for the design.

Two general categories of tracer tests have been described in the scientific literature: radial flow tests and uniform, natural gradient tests (Chapter 2). Radial-flow tests, by virtue of a non-linear gradient, yield varying ground water flow velocities with distance from the pumping/injection well. Natural gradient, uniform-flow tests generally involve extended tracer-transport times and a large number of monitoring wells.

A forced-gradient, uniform flow tracer test configuration was selected for this project. Forced-gradient tracer tests have been conducted at the Borden, Ontario, site (Bianchi-Mosquera and Mackay, 1994). The configuration developed for this project differs from the Borden tests since a hydraulic gradient was established by a water recirculation system. The forced-gradient, recirculating-loop configuration is described in the following paragraphs.

The forced-gradient tracer tests for this project were designed to be conducted along a linear transect of wells (Figure 3.5-1). A steady-state hydraulic gradient was established by means of pumping water from one end of each transect to the other for an extended period of time. Tracers were injected after steady-state flow conditions

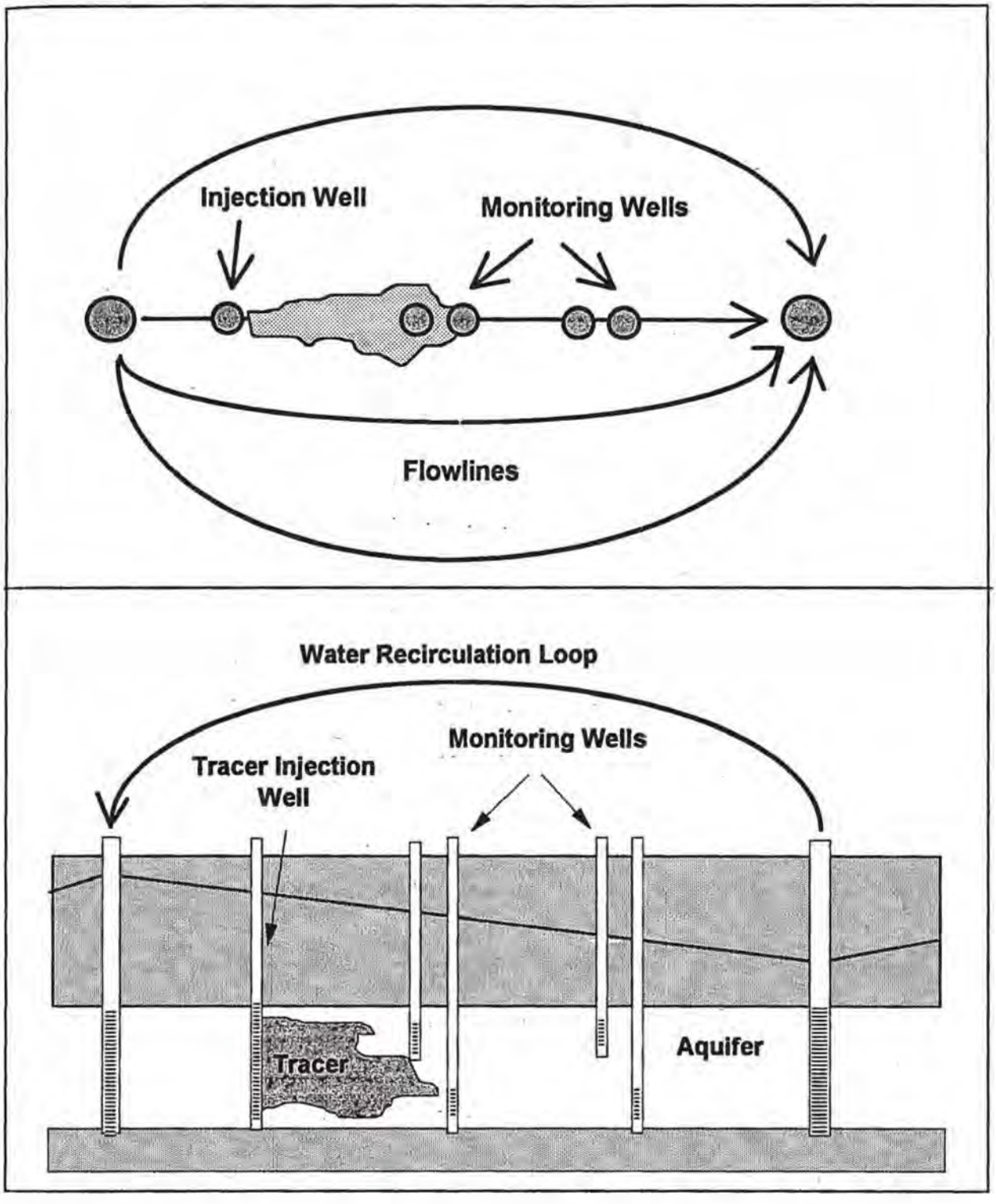

Figure 3.5-1: Generalized tracer test schematic in plan view and cross section.

were established and monitored in wells arranged in a straight line between the circulation wells.

Injecting and monitoring the tracers within the forced-gradient area reduces the dilution associated with injecting and monitoring the tracers in the primary pumping and injection wells. A reduced volume of tracer is required since it follows relatively linear flowlines between the pumping and injection well, although flowlines are influenced by local aquifer heterogeneities. A disadvantage of the forced-gradient, recirculating-loop system is the difficulty in calculating tracer mass balances, since the tracer eventually would be expected to recirculate within the recirculation loop.

The forced-gradient, recirculating-loop system is a prototype of possible remediation system design, because the recirculating water would allow repeated contact between encapsulated cells and subsurface contaminants. Such a recirculating-loop system could be coupled with an above-ground treatment system, if necessary.

The monitoring network along a transect could be designed for monitoring one-, two-, or three-dimensional transport. A three-dimensional network allows definition of transport parameters in a heterogeneous field environment; extensive three-dimensional monitoring networks have been constructed to evaluate advection and dispersion parameters in Massachusetts and Ontario (see Chapter 2). The goal in this project was not necessarily to define advection and dispersive characteristics, but to conduct an initial comparison of the *relative* advection rates of three tracers (bromide, polystyrene microspheres, and encapsulated cells). Thus, a monitoring network was designed consisting of monitoring wells along a straight line within the recirculation loop.

Tracer tests were conducted in a minimum of two different transects to compare possible differences due to aquifer heterogeneities. Replicate tracer tests (using the conservative tracer) were conducted in each of the two transects as a check on reproducibility. Replicate tracer tests would allow an evaluation of the tracer injection and sampling systems. Replicate tests might also provide an indication of pore-space clogging (if clogging occurs) due to particle injections.

3.6. Monitoring Well Design

The monitoring well design for this project evolved during the site-selection process. The final design was influenced by site conditions, available drilling and installation equipment, and sampling requirements for ground water monitoring.

Several monitoring well criteria were identified to guide the design process. Methods for installing monitoring wells had to allow for the description of aquifer sediments. Wells needed to be installed with screens at discrete depths, with known filter pack materials, and with annulus seals from the aquifer zone to ground surface. Monitoring well volume and casing screens had to be large enough to allow adequate well development in the casing vicinity, yet result in minimum disturbance to formation sediments. Finally, the monitoring wells had to be designed for hydraulic aquifer characterization (e.g., aquifer tests), and had to be of sufficient diameter to accommodate available pressure transducers and electrical water level indicator probes.

Monitoring wells also needed to be used for sampling tracer concentrations in ground water. Minimum sample requirements (for laboratory analysis) were estimated at approximately 10-15 ml fluid. This volume contained in a test tube would allow insertion of a selective-ion probe, and would provide sufficient filtration fluid for microscopic analysis. Flow rates for sample collection needed to be as small as possible to reduce the impact on hydraulic gradients in the vicinity of the sampling well (this also applies to sampler-purging rates). A minimum flow rate in the monitoring wells during sampling was desirable, however, to maintain particles (encapsulated cells and microspheres) in suspension.

4. Site Selection and Preliminary Site Investigation

4.1 Introduction

This chapter presents a description of the site selection process. The site selection process was based on criteria outlined in Section 3.4. A field site was selected using published information about two alternative locations and information gained during the installation of several monitoring wells at one of the locations.

4.2 Evaluation of Alternative Sites

Two sites were identified as potential field site candidates on the basis of University of Idaho (UI) ownership, availability, and proximity to UI laboratories. The Ground Water Research Site is located at the western end of the University of Idaho campus, adjacent to Paradise Creek (Figure 4.2-1). The University of Idaho Plant Science Farm is located approximately 3 km east of Moscow, Idaho. These sites were evaluated according to the site selection criteria outlined in Section 3.2.

Both sites have received approximately 64 cm of precipitation per year over the last 30 years (R. Patten, personal communication, 1994). Precipitation is generally of low intensity and occurs primarily during the winter and spring months.

Monitoring well logs for wells installed at the Ground Water Research site indicate approximately 2.7 to 3.6 meters of soil, clay, and silt underlain by approximately 0.6 to 3 meters of alluvial sand and gravel, which is in turn underlain by basalt (Li, 1991). The sand and gravel unit thins to the south with distance from nearby Paradise Creek; the sand and gravel unit is most likely associated with the ancient Paradise Creek Channel (Li, 1991). The areal extent of the sand and gravel unit in this area is unknown. The sand and gravel zone is underlain by fractured basalt assigned to the Lolo flow of the Priest Rapids basalt of the Wanapum Formation (Hooper and Webster, 1982).

A 1.2-hectare portion of the University of Idaho Plant Science Farm lies in an alluvial basin near the South Fork of the Palouse River. Several hand borings

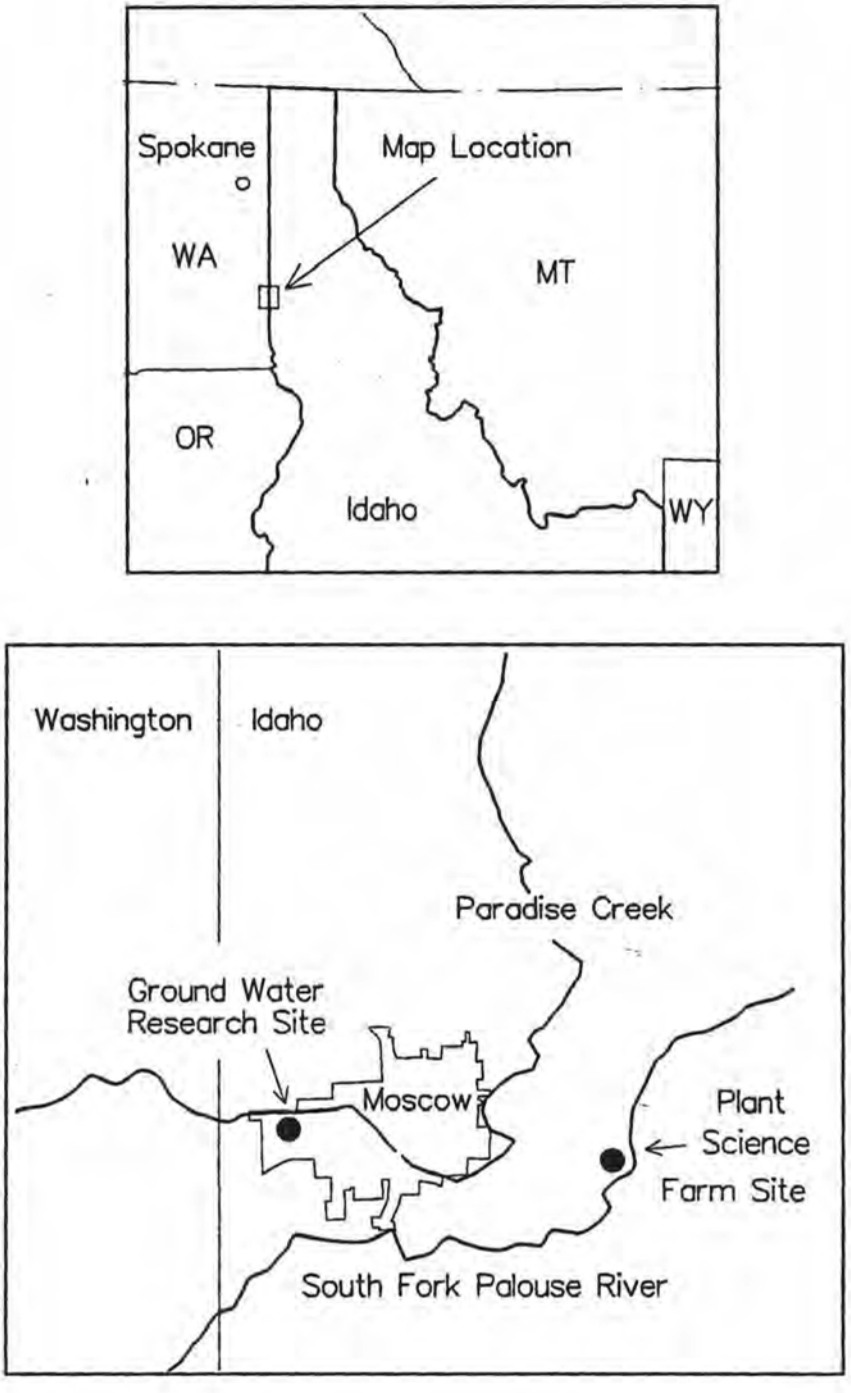

Figure 4.2-1: Locations of two alternative field site areas.

at the site (Figure 4.2-2) indicated a zone of unconsolidated silts, sands, and gravels beginning at a uniform depth of approximately two meters below ground surface. Water levels in the borings rose close to ground surface after penetrating the silt, sand, and gravel zone, indicating confined conditions. The aquifer thickness could not be determined with the hand augers because of borehole collapse in unconsolidated sediments. The hand auger boreholes were abandoned and filled with *Baroid Holeplug* (1.9-cm) pellets.

Based on preliminary results, the Plant Science Farm site fit the site selection criteria better than the Ground Water Research site. Thus, a second investigation phase was initiated at the Plant Science Farm site. Six exploratory boreholes (MW-1 through MW-6) were then drilled at the Plant Science Farm site (Figure 4.2-2). The purpose of these wells was to determine the aquifer thickness, the areal extent of the aquifer, and the potentiometric ground water surface. The wells were located east of the hand borings to take advantage of slightly higher ground surface elevation; vegetation types indicated slightly less soil moisture than in the hand-boring area.

Spacing of wells MW-1 through MW-6 was somewhat arbitrary, since these were exploratory wells. The rationale for varied well spacing was for potential geostatistical analysis of aquifer properties at wells located at various distances from one another.

The boreholes for MW-1 through MW-6 were installed with 10.1-cm hollow-stem augers mounted on a *SIMCO* 2800 drill rig. Use of the hollow-stem auger method allows relatively accurate description of cuttings, allows the installation of well screens and casings without the use of casing or drilling fluids, and allows the use of split-spoon samplers for obtaining sediment samples (Driscoll, 1986). Split-spoon sample aquifer samples were not consistently obtained from the aquifer zone because of gravels plugging the end of the sampler and sample loss during retrieval.

A limited number of aquifer samples were collected from the auger flight during drilling and taken to a small basement laboratory on the UI campus. A

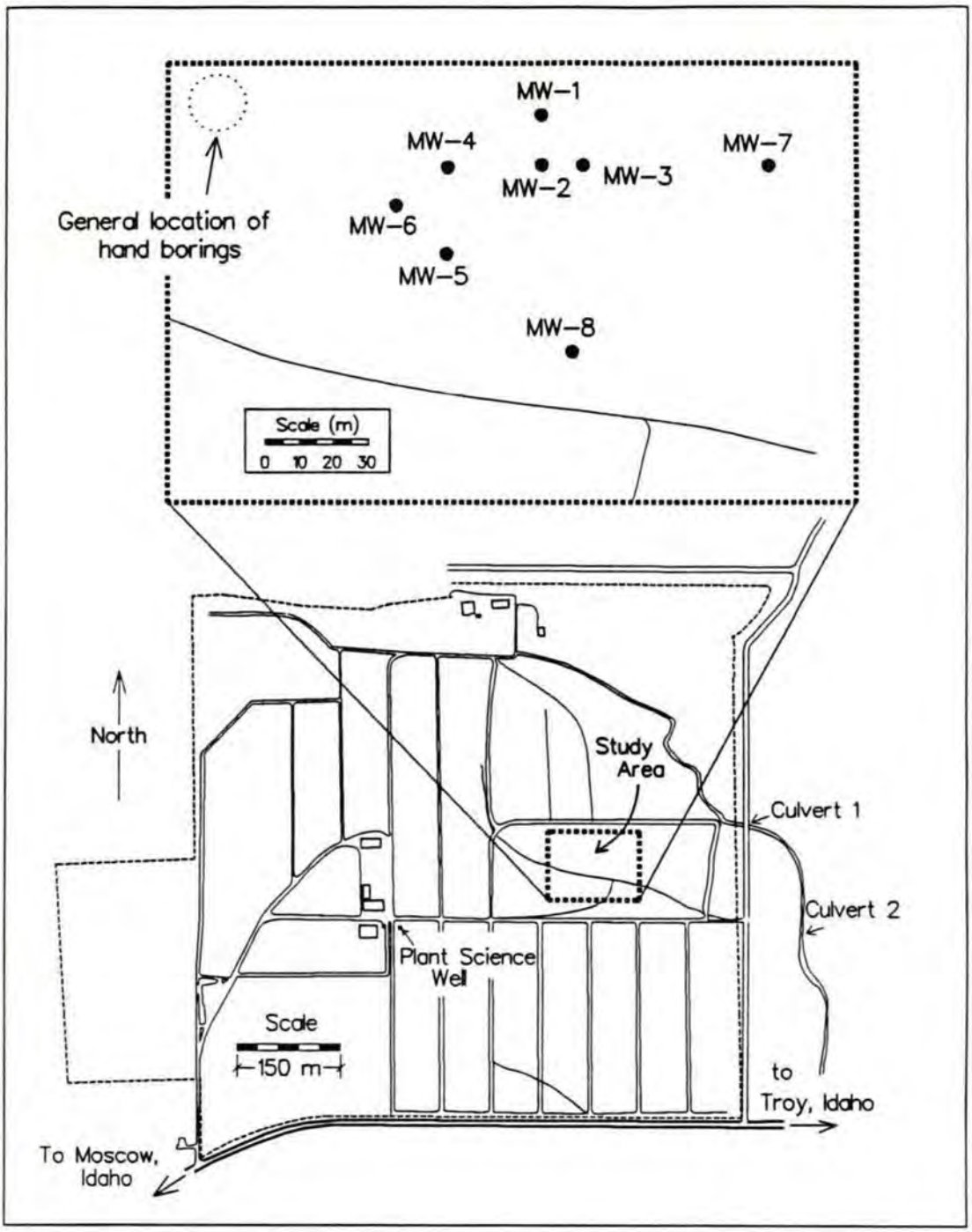

Figure 4.2-2: Plant Science Field Site area showing the locations of six monitoring wells and hand-auger holes.

broken water pipe above the laboratory in which samples were drying led to the loss of most of the samples that were collected. The six remaining samples were taken from MW-4 and MW-5. Grain-size distribution curves for these samples are shown in Figures 4.2-3 and 4.2-4.

Drilling logs from wells MW-1 through MW-6 indicated layers of silty loam, clayey silt, and silty clay to approximately 2.5 to 3 meters below ground surface, underlain by a horizontally continuous zone of silt, sand, and gravel, ranging in depth from approximately 2.5 to 3 meters below ground surface. Water levels in each borehole rose into the clayey silt and silty clay zone when the sand and gravel zone was pierced. Each borehole was extended into a zone of very stiff, light gray to bluish gray clay at a depth of approximately 4 meters.

The wells were completed with 5-cm diameter polyvinyl chloride (PVC) casings. PVC was selected as a well material because it is inert with regard to ground water containing bromide, polystyrene microspheres, or encapsulated cells, and it is relatively inexpensive. PVC is not susceptible to electrochemical or galvanic corrosion, is resistant to microbial degradation or degradation by soil, water, or other naturally occurring substances present in the subsurface, and is resistant to hazardous substances such as most acids, oxidizing agents, salts, alkalis, oils, and fuels (Nielson, 1991). PVC is vulnerable to certain chemical compounds, such as low-molecular-weight ketones, aldehydes, amines, chlorinated alkenes, and alkanes, but there was no evidence suggesting that any of these latter compounds would be present at the site. PVC is of adequate strength for shallow wells.

A filter pack method of well completion for these methods was used to prevent borehole collapse. Fine-grained materials from the silt and clay zone above the aquifer could potentially collapse into the aquifer zone in the absence of a filter pack.

The filter pack materials (and well screens) were ordered prior to drilling (to minimize waiting time for the drillers). The filter pack material was selected because finer-grained sediments were anticipated within or near the aquifer zone. Aquifer materials were expected to include silts, fine to coarse sands, and small gravels. Clean

Colorado silica (8-12) sand was selected for the filter pack material on the basis of an estimated D_{30} grain size diameter of 0.35 millimeters (medium sand).

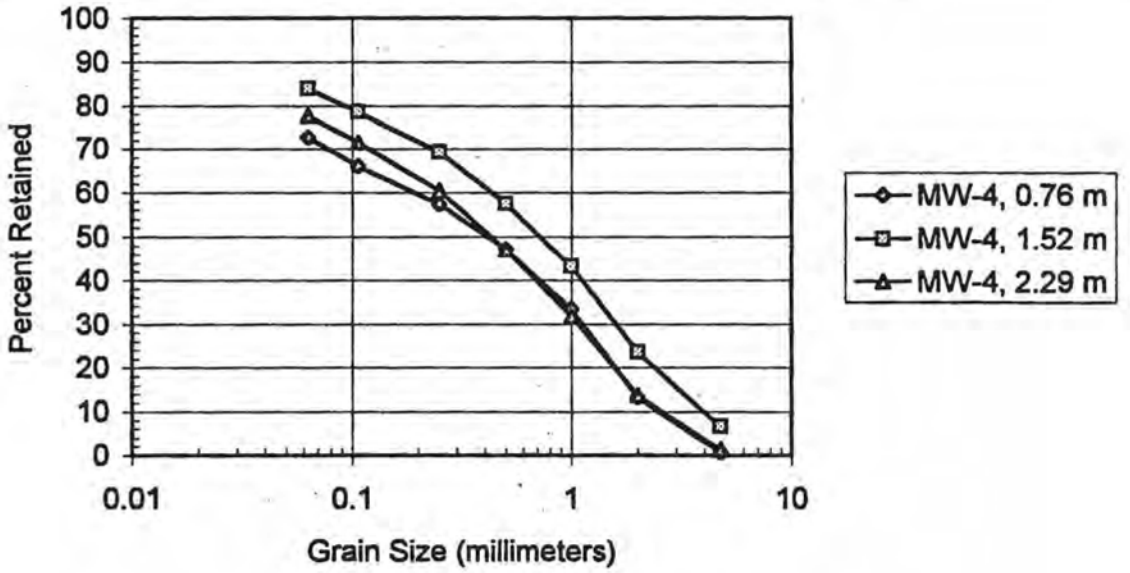

Figure 4.2-3: Grain-size distributions at various depths for MW-4.

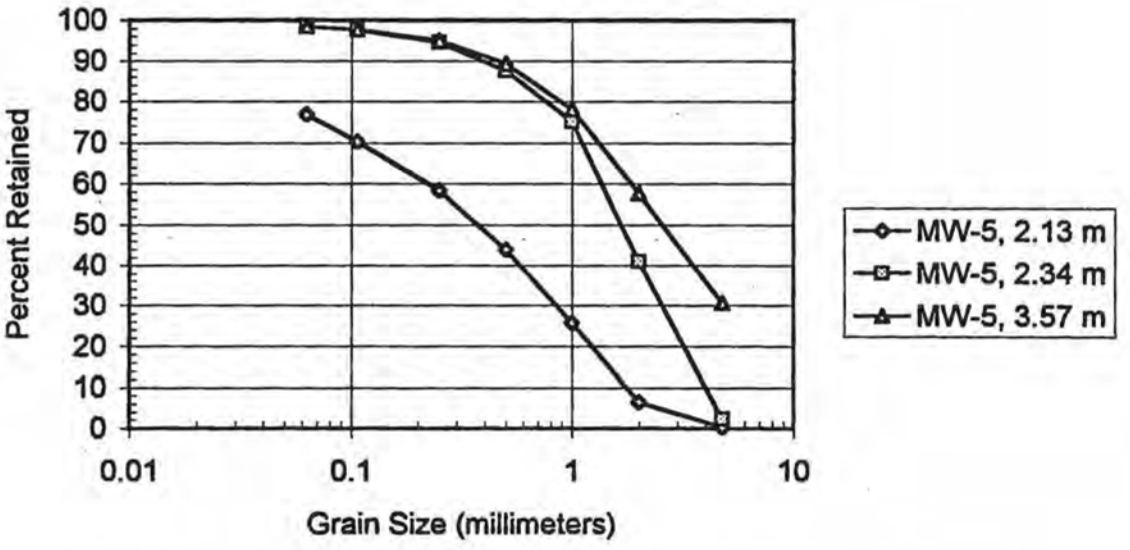

Figure 4.2-4: Grain-size distributions at various depths for MW-5.

PVC screen (152-cm length) was installed to span the silt, sand, and gravel aquifer zone. A 0.5-mm slot size was chosen as representing an approximate midpoint for the anticipated aquifer grain size distribution (silt, sand, and gravel).

Baroid Holeplug (1.9-cm) pellets were used to provide an annulus seal from approximately 15 centimeters above the top of the screen to ground surface in all wells. Protective steel casings with locking caps were installed in concrete to a depth of approximately 0.75 meters below ground surface.

Monitoring wells were developed by surging and pumping with compressed air or bailer. Differences in recovery times were observed during well development; monitoring well MW-5 appeared to recover more quickly than the other wells. The small slot size used in the monitor wells precludes pumping the maximum yield from the aquifer, and may have limited full development of the wells.

Information gained in these initial wells revealed the presence of a continuous, relatively thin (approximately 1.0 to 1.5 m thick) aquifer zone consisting of silts, sands, and gravels ranging from approximately 3 to 4.5 meters in depth. Rising water levels upon aquifer penetration indicated confining conditions. The stiff clay aquitard underlying the aquifer appeared continuous beneath the aquifer zone.

4.3 Site Selection

Two field sites were considered for this project. These sites were considered because they are owned by the University of Idaho, were available to this project, and were within a reasonable distance to university laboratories. The shallow aquifer at the UI Groundwater Research Site appeared to be highly heterogeneous and of limited areal extent. Initial wells in at the Plant Science Farm site indicated a shallow, confined aquifer consisting of unconsolidated sediments ranging in thickness from approximately 1 to 1.5 meters. Significant heterogeneities were noted in the aquifer materials, but the aquifer appeared continuous at a relatively constant thickness throughout the area penetrated by test wells.

The Plant Science Farm site was therefore chosen for this study on the basis of initial site investigation information and the site selection criteria. The Plant Science

Farm site offered confined aquifer conditions, shallower depths to water, and a relatively constant aquifer thickness. The Plant Science Farm site also had fewer competing uses (the Groundwater Research Site was used for cattle grazing) and had electricity available (within 250 meters)

The drilling of exploratory wells at the Plant Science Farm thus represented the first phase of a site investigation. Additional site investigation activities included installing additional monitoring wells, conducting sediment-size analyses, and monitoring water levels. These activities are described in the next chapter.

5. Site Characterization

5.1. Introduction

This chapter describes the second phase of site characterization conducted at the Plant Science Farm (the first phase consisted of the initial wells drilled during the site selection process). The second site characterization phase consisted of reviewing the local geological literature, installing additional monitoring wells, conducting grain size analyses of aquifer sediments, and collecting water level data. Site characterization led to the development of a conceptual hydrogeological model. The conceptual hydrogeologic model was used for designing aquifer and tracer tests and analyzing results from those tests.

The Plant Science Farm, situated three miles east of the city of Moscow, Idaho, is located in the eastern portion of the Pullman-Moscow Basin. The eastern portion of the basin is bordered on the north, east, and south by a broken horseshoe ring of mountains and hills consisting of granite, gneiss, and quartzite (Lum et al., 1990). The field site elevation is approximately 800 m. The closest surface water is the South Fork of the Palouse River, which flows near the eastern boundary of the Plant Science Farm. Land use in the field site area is primarily dry-land farming, although the field site itself has never been used for crops because of wet surface conditions during the spring.

5.2. Geological Setting

The Pullman-Moscow Basin is located near the eastern edge of the Columbia Plateau. Several major rock groups and ages are represented in the vicinity of the field site (Figure 5.2-1): the Precambrian metamorphic rocks, the Cretaceous granitic rocks, the Tertiary Columbia River Basalt Group and Latah Formation, and the Quaternary Palouse Formation and alluvium (Tullis, 1940; geological maps in the Plant Science Farm site area are currently being updated by Bush, Pierce, and Provant, University of Idaho).

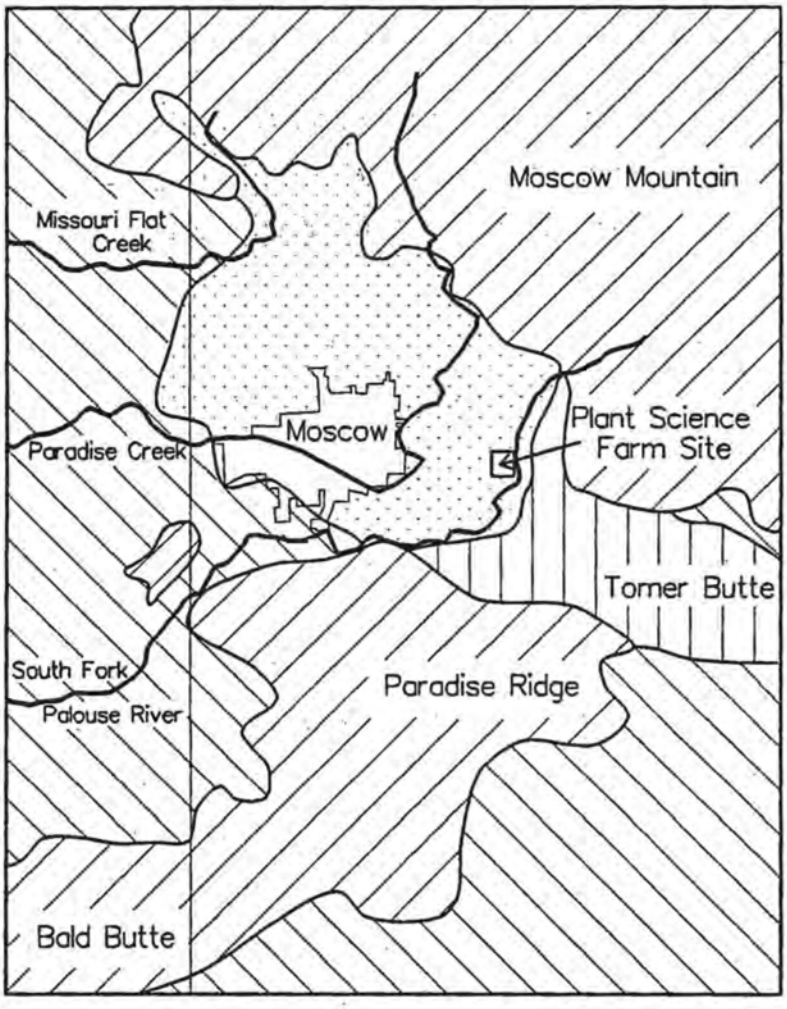

Adapted from J. Bush, J. Pierce, and A. Provant, 1995, unpublished map.

Figure 5.2-1: General bedrock geology in the Plant Science Farm area.

The oldest rocks in the field area consist of Precambrian sedimentary rocks metamorphosed into quartzite, gneiss, schist, and other related rock types (Tullis, 1940; Ralston, 1972). Precambrian metamorphics are exposed approximately 700 meters northeast of the field site.

Intrusive igneous rocks are exposed north, east, and south of the field site. These Cretaceous granites consist of quartz, diorite, granodiorite, monzonite, and granite (Ross, 1965), and are thought to have been formed as part of the Idaho batholith (Hyndman, 1989).

The Columbia River Basalts, which underlie the field site, consist of Miocene flood basalts that were extruded from vents in northeast Oregon and southeastern Washington from sixteen to six million years ago (Camp et al., 1982). The flood basalts flowed eastward into topographic lows of northern Idaho, filling valleys and covering foothills to elevations ranging from approximately 850 to 1100 m (Bond, 1963, Camp et al., 1982).

The basalts within the Pullman-Moscow Basin are described by Foxworthy and Washburn (1963) as dense, vesicular, medium gray to black on fresh surfaces, and lighter gray to brown where weathered. The Priest Rapids Member, which underlies the site (Figure 5.2-1), is further described by Hooper and Webster (1982) as a "medium-grained basalt with some phenocrysts of plagioclase and olivine in a matrix of intergranular pyroxene, ilmenite blades, and devitrified glass."

Tullis (1940) describes extensive sediment units found between or beneath basalt flows in south-central parts of Latah County, and small bodies of clay found either above, between, or beneath the upper basalt flows (collectively described as the Latah Formation). These sediments include sands, silts, and clays, ranging in color as light gray, light green, and tan to white. Tullis describes some layers as having a bluish color and some of the clays as ranging in color from dark bluish-gray, chocolate brown, and maroon to bright red. Coarse sediments (e.g., sands) associated with the Columbia River Basalts are characterized by their angularity, primarily consisting of quartz with significant amounts of muscovite. Bush, Pierce, and Provant (unpublished map) further describe Latah Formation sediments as "upwardly fining sequences (0.6 m to 1.5 m) of

poorly sorted and subrounded quartz gravels or coarse sand at the base grading upward into fine sand and in turn overlain by clay, generally kaolinite rich." Some of these Latah sediments present east of Moscow are interpreted by Bush, Pierce, and Provant as originating from eroded weathered exposures of crystalline rocks deposited in areas ponded by Priest Rapid basalt flows, and are referred to as sediments of Bovill. Further descriptions of these materials will be found in master's theses being prepared by Pierce and Provant.

Pleistocene-age loess, known as the Palouse Formation, covers much of the Palouse region. The loess is thought to have originated in the eastern margins of the Cascades and possibly the Pasco Basin (Breckenridge, 1986). The loess ranges from one meter to more than 50 m in thickness, and consists of even-textured tan or brown clayey silt (Foxworthy and Washburn, 1963). Quartz is a major constituent of the loess, although mica and feldspar are also present; montmorillonite is a major constituent of the clay fraction.

The most recent geologic deposits in the field site vicinity consist of Quaternary-age alluvium (Ross, 1965). These deposits consist of reworked loess and weathered basaltic material. At higher elevations or nearer to the bedrock hills the alluvium may consist of sand, silt, and clay formed by the decomposition of crystalline rocks (Foxworthy and Washburn, 1963).

The general geology in the field site area is reflected in the driller's log taken from a water supply well drilled at the Plant Science Farm. The well log (Crosthwaite, 1975) reveals the presence of clay, silt, sand, gravel, and basalt (Figure 5.2-1). The clay, silt, sand, and gravel zones are interpreted as Latah Formation sediments on the basis of the descriptions outlined above. Similarly, the basalt is interpreted as belonging to the Priest Rapids Member of the Wanapum Formation. The depth to crystalline basement rocks in the Plant Science Farm well is approximately 150 m.

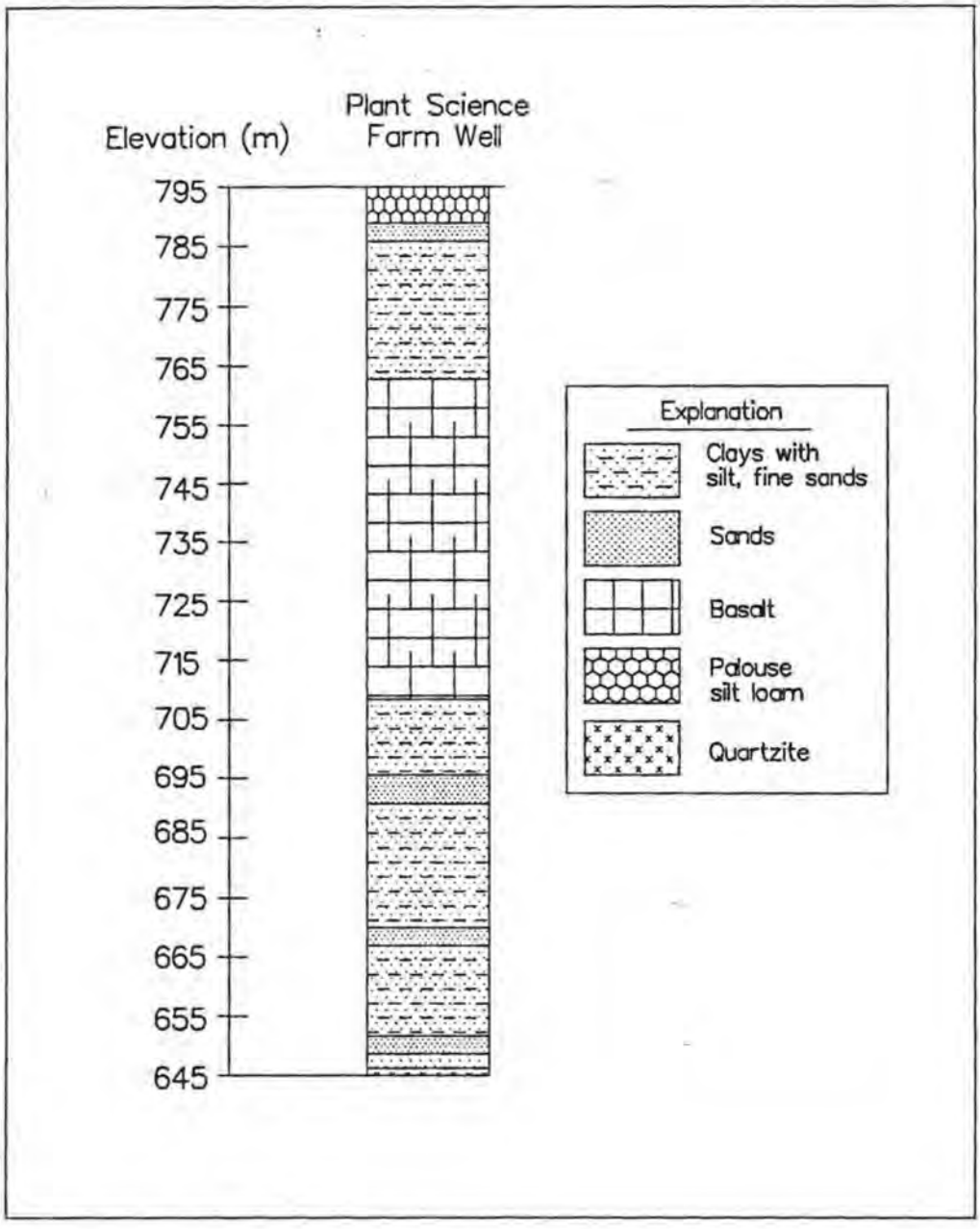

Figure 5.2-1: Well log for Plant Science Farm supply well.

5.3. Monitoring Well Design Criteria

Phase II of the site characterization consisted of the installation of additional monitoring wells at the Plant Science Farm site. This section outlines construction and location criteria for Phase II wells.

The purpose for Phase II monitoring wells at the field site was to (1) allow description of aquifer materials at the field site, (2) allow the monitoring of ground water levels during aquifer and tracer tests, and (3) to yield water samples with ion- and particle-tracer concentrations representative of those in the surrounding aquifer formation.

Monitoring well design criteria, which are discussed in the next several paragraphs, included:

1. Minimal borehole/casing storage.
2. Well design and construction that allows effective well development.
3. Sufficient well diameter for *Druck* pressure transducers and *Solinst* water-level indicator probes.
4. Minimal formation disturbance during well installation.
5. Discrete, known ground water sampling intervals.
6. The ability to retrieve aquifer sediment samples during well installation.

A small well volume was specified for two reasons. First, a small well volume would require less water removal for purging and sampling than a large well volume, and would require less time for purging and sampling. Low sampling rates would minimize local hydraulic effects during tracer experiments. Second, a minimum sampling rate would lead to higher flow velocities in a low-volume well, resulting in reduced particle settling.

Monitoring wells had to be designed to allow effective well development. The open screen area had to be large enough to allow the dislodging and removal of fine sediments in the well-screen vicinity. The monitoring well diameter had to be large enough for the removal of formation sediments from the well. However, excessive well

development was not desirable, since changes in formation sediments might skew tracer test results (removal of fine formation sediments in a borehole vicinity is usually desirable for water-production wells).

Monitoring wells needed to be large enough to accommodate *Druck* pressure transducers and *Solinst* water level indicator probes (this equipment was available to the project). The transducers and indicator probes are approximately 1.78-cm and 1.52-cm in diameter, respectively.

Minimal formation disturbance due to monitoring well installation was important for two reasons. First, formation disturbance might alter localized subsurface flow and particle transport characteristics. Second, a relatively large-diameter borehole surrounding a small-volume sampler could influence hydraulic testing results.

Discrete, multi-level sampling intervals were considered important because of heterogeneous aquifer characteristics. Layers of coarser material were noted in the aquifer zone during the installation of wells MW-1 through MW-6.

Well location criteria were influenced by the experimental scale and design, and by heterogeneous aquifer characteristics. Criteria for monitoring well placement included:

1. Locating monitoring wells so that tracer experiments would be conducted on a scale of meters (see Chapter 3).
2. Locating monitoring wells in transects, where each transect consists of a tracer injection well, monitoring wells, and a water-recirculation well at either end (see Chapter 3).
3. Spacing monitoring wells far enough apart to minimize formation disturbances (due to well construction).
4. Placing sampling ports and/or casing screens at multiple depths within the aquifer zone (to evaluate the effects of aquifer heterogeneity).
5. Providing for a variety of distances (lag distances) between wells for geostatistical analysis.

5.4. Monitoring Well Design Alternatives

The final monitoring well design for this project is a compromise shaped by various aquifer characteristics and limitations of drilling methods. This section provides a discussion of monitoring well alternatives considered for this project, and a rationale for the final monitoring well design.

In general, drilling methods include techniques for drilling with and without drilling fluids (Driscoll, 1986). Only methods for drilling without drilling fluids were considered to avoid the introduction of drilling fluids in the field site area.

Methods for drilling without drilling fluids include displacement "boring" or auger drilling (Nielson, 1991). Displacement "boring" consists of creating a borehole by means of forcing soil material into the borehole sidewall using a drive point method. Auger-drilling methods consist of using either solid-stem augers or hollow-stem augers to bring cuttings to the ground surface; the hollow-stem auger method allows the installation of well screens, filter packs, and an annulus seal inside the auger flight.

Three monitoring wells (MW-9, MW-10, and MW-11) were installed as drive point wells using 3.2-cm or 5-cm diameter drive point wells (61-cm long screens), manufactured by *Johnson Division, Inc.* Installation of these wells did not allow the retrieval (or description) of aquifer sediments.

Several attempts were made installing wells with a "drive pipe" method, which is an adaptation of the drive point method. A 2.54-cm I.D. schedule 80 steel pipe was driven into the ground to the desired depth; the steel pipe was pulled from the ground and quickly replaced with a 1.9-cm diameter PCV well casing containing multi-level samplers (Figure 5.4-1). In theory, a natural filter pack would develop around the PVC well as formation materials collapsed against the casing. This method produced a minimum diameter borehole, allowed for sediment retrieval (an aquifer sediment core was collected in the schedule 80 steel pipe), and enabled the installation of low-volume, multi-level samplers.

However, the drive pipe method yielded inconsistent sampler installations. Collection of core samples within the drive pipe was sporadic because cobbles blocked

the coring-pipe openings. Boreholes occasionally collapsed prior to sampler installation at the desired depth. It was not possible to obtain reliable formation seals between multi-level sampling points since the formation did not always collapse tightly against the sampler. Finally, low-volume tubing samplers (0.32-cm-diameter tubing in 1.9-cm-diameter PVC casing with a 2.54-cm length of 0.25-mm screen) were too small for proper well development.

The hollow-stem auger method was therefore selected for installing ground water monitoring wells. Selection of this drilling method led to a second monitoring well/sampler design.

The smallest common commercially available PCV well casing diameter is 5-cm. This casing diameter was thought to be too large for monitoring wells in this project, because it was feared that pumping the amount of water that would be required for purging and sampling would create excessive hydraulic disturbance in the well vicinity. Therefore 1.9-cm diameter PVC pipe was selected for well casing, which is the smallest diameter that would accommodate *Druck* pressure transducers. Screen openings would be cut by hand (see next section).

Well casing specifications were considered in conjunction with potential ground water sampler designs. The purpose of the samplers was to further reduce well casing volumes, allow placement of low-volume sampling tubing, and position pressure transducers for monitoring ground water levels.

A general sampler design for the 1.9-cm diameter monitoring wells is shown in Figure 5.4-2. The sampler consists of a 1.3-cm diameter PVC pipe with small-diameter sampling tubing attached to the outside. The Druck pressure transducer is installed in the bottom of the pipe. The effect of the pipe and transducer when installed in the monitoring well is to further reduce the amount of casing storage in the well. This sampler is further described in Chapter 7.

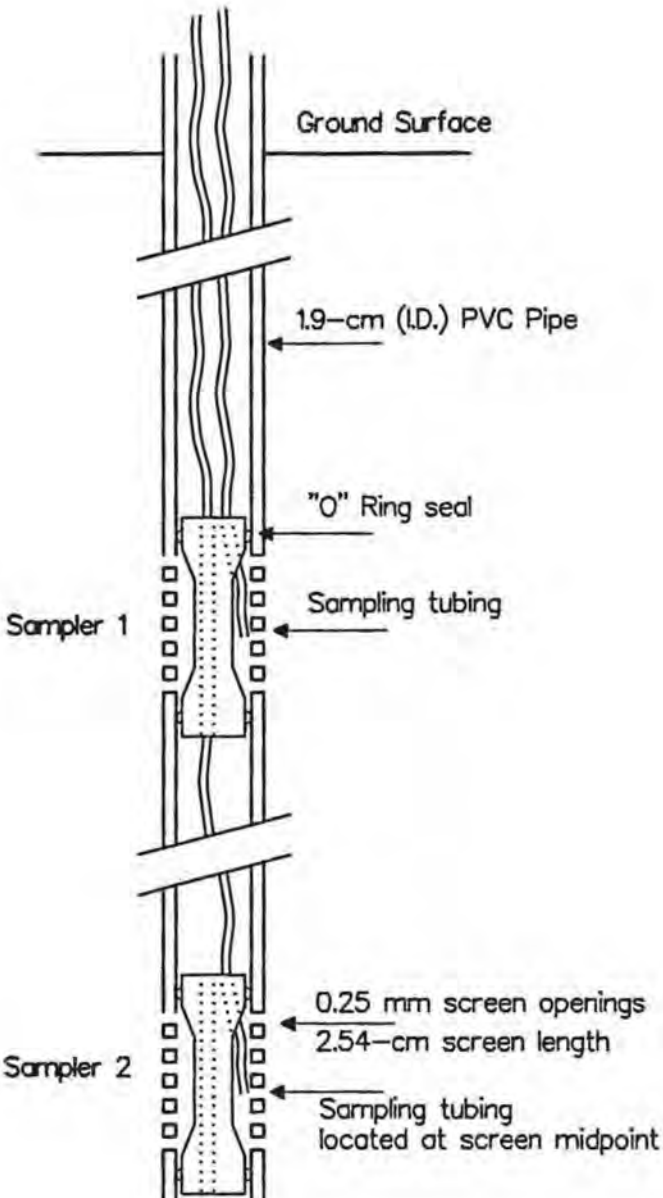

Figure 5.4-1: Multi-level sampling unit.

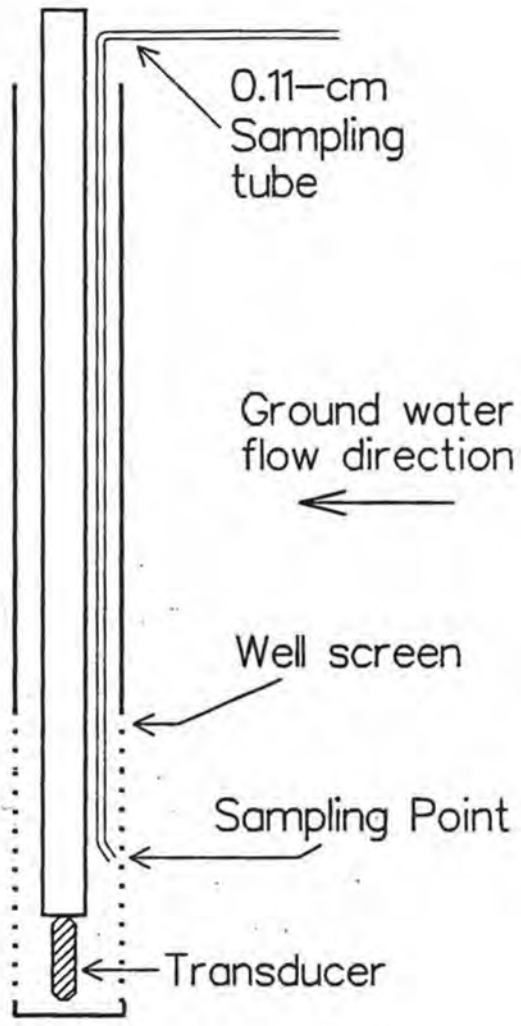

Figure 5.4-2: General monitoring well and sampler combination.

Advantages of the latter monitoring well and sampler combination include low casing volume (after the sampler is installed in the monitoring well), sufficient volume and flow capability for effective well development (prior to sampler installation in the monitoring well), sufficient diameter for *Druck* pressure transducers and water-level indicator probes, proven installation method (hollow-stem augers), and the ability to retrieve aquifer sediment samples during sampler installation. Disadvantages include a relatively large formation disturbance area (due to the outside auger diameters) and the inability of setting closely spaced multi-level sampling intervals (in an aquifer with an estimated thickness of 1.5 m) with a reliable annulus seal between sampling zones.

In summary, the hollow stem auger method was selected for installing monitoring wells because the method allows wells to be installed in an unconsolidated aquifer prone to caving, allows filter pack and bentonite seals to be installed at predetermined locations, and provides the opportunity for describing aquifer sediments via auger cuttings and split spoon sampling. Subsequent monitoring wells and samplers were thus constructed in the general form shown in Figure 5.4-2. Specific monitoring well design and construction details are provided in the next section. Sampler details are described in Chapter 7.

5.5. Monitoring Well Design and Installation

Design and construction details for monitoring wells MW-12 through MW-25 are presented in this section. A description of and rationale for monitoring well locations are presented first, followed by monitoring well design and construction details.

Monitoring wells MW-12 through MW-25 were installed in the vicinity of MW-5 (referred to as Cluster 1). Access to this area was good, and the aquifer near MW-5 appeared be more transmissive than near other areas, on the basis of observations made during well development.

The well cluster was designed with three transects of monitoring wells (Figure 5.5-1). A straight line of wells, as opposed to a more multi-dimensional monitoring array, was chosen to minimize costs and to minimize aggregate borehole disturbances.

Well locations within each transect were based on the general tracer test design shown in Figure 3.5-1. Each transect contains a 5-cm-diameter PVC well at both ends, for use as water recirculation wells. Each transect included a 1.9-cm-diameter well screened across the aquifer zone (to be used as a tracer injection well), followed (along the transect flowline) by at least one pair of 1.9-cm-diameter monitoring wells with screens 30.5 cm in length. The first well of each sampling pair, the down-gradient well closest to the injection well, was placed in the upper portion of the aquifer zone; the second well was placed in the lower portion of the aquifer zone (this arrangement was intended to minimize the hydraulic disturbances to sampling-well pairs). Transect C received two pairs of sampling wells; transects A and B received only one pair because of limited drilling funds.

Transect A begins with MW-5 and proceeds in a northerly direction (with wells MW-12, MW-13, MW-14, and MW-15; see Figure 5.5-1), so that Transect A wells would be in closer proximity to wells MW-4 and MW-6 (Figure 4.2-2). A second transect (Transect B) proceeds in a northwesterly direction from MW-5 (in proximity to wells MW-1 through MW-6 and Transect A wells), and a third transect (Transect C) trends southwest from MW-5.

The distances between wells were established on the basis of the criteria for intermediate-scale tracer tests (Chapter 3). The tracer injection wells were located approximately two meters from the water injection wells in each transect; the first sampling well (of a sampling pair) was located approximately 1.5 m from the tracer injection well, and sampling pairs were separated by approximately 0.5 m. Distances between Cluster 1 wells are provided in Table 5.5-1.

A typical well design is shown in Figure 5.5-2. Specific construction details for all monitoring wells (including those installed during the first site-investigation phase) are provided in Table 5.5-2.

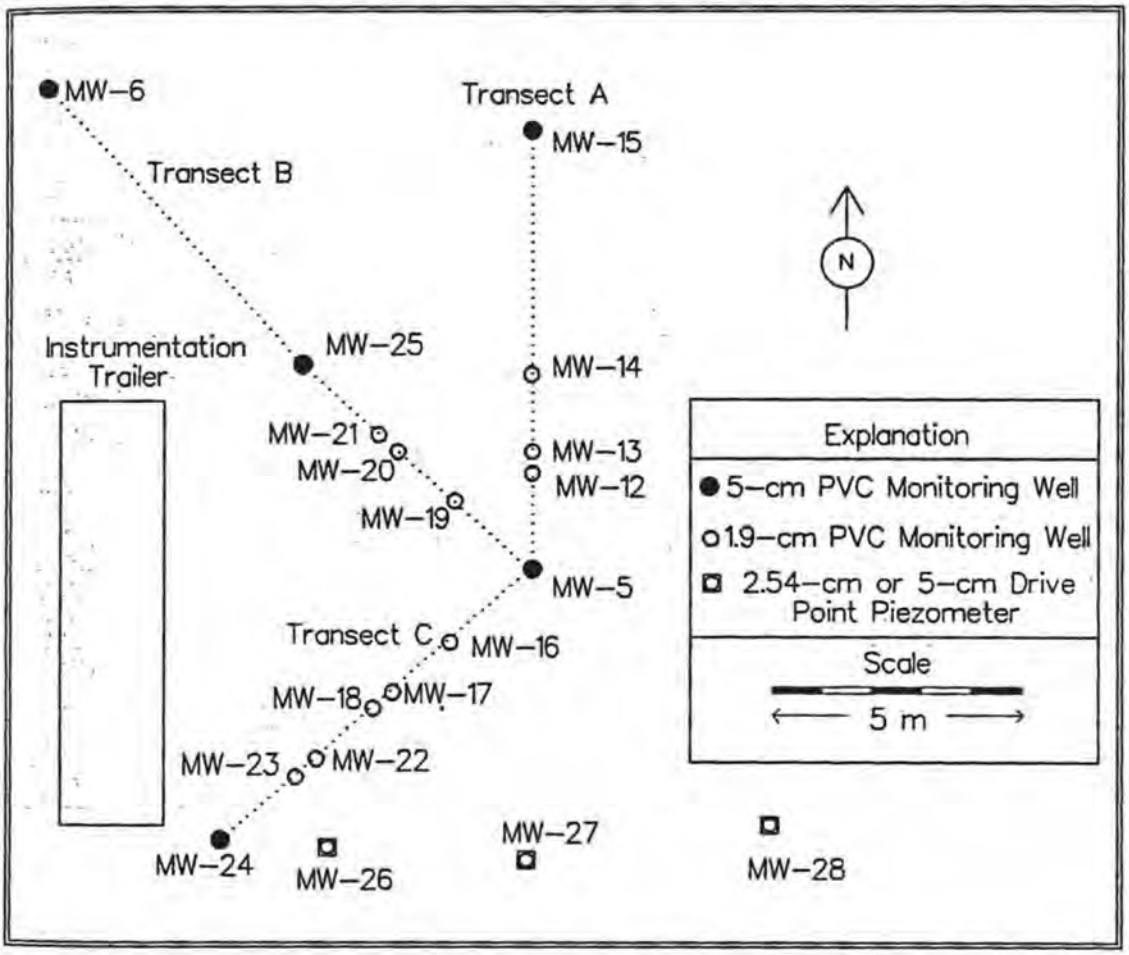

Figure 5.5-1: Cluster 1 well locations.

Transect A							
	MW-4	**MW-5**	**MW-12**	**MW-13**	**MW-14**	**MW-15**	
MW-4	0	1742	1538	1494	1338	869	
MW-5		0	204	249	404	874	
MW-12			0	45	200	670	
MW-13				0	156	625	
MW-14					0	469	
MW-15						0	
Transect B							
	MW-5	**MW-6**	**MW-19**	**MW-20**	**MW-21**	**MW-25**	
MW-5	0	36	218	370	417	627	
MW-6		0	253	406	453	663	
MW-19			0	152	199	410	
MW-20				0	47	257	
MW-21					0	210	
MW-24						0	
Transect C							
	MW-5	**MW-16**	**MW-17**	**MW-18**	**MW-22**	**MW-23**	**MW-24**
MW-5	0	213	373	418	570	618	836
MW-16		0	160	205	357	405	622
MW-17			0	45	197	245	462
MW-18				0	152	200	417
MW-22					0	48	265
MW-23						0	217
MW-24							0

Table 5.5-1: Distances (cm) between Cluster 1 wells.

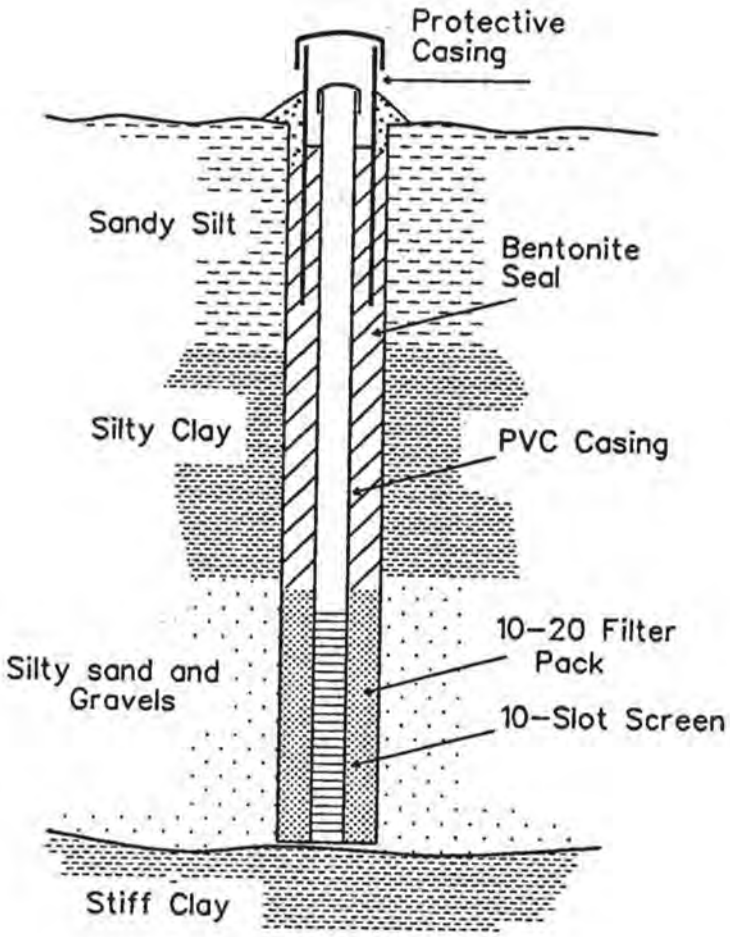

Figure 5.5-2: Typical well construction.

Well	Type (1)	Drilling Method (2)	Screen Interval (cm)	Screen Opening Size (mm)	Assumed Aquifer Penetration	Notes
MW-1	5-cm PVC	HSA	152	0.50	Full	(3)
MW-2	5-cm PVC	HSA	152	0.50	Full	(3)
MW-3	5-cm PVC	HSA	152	0.50	Full	(3)
MW-4	5-cm PVC	HSA	152	0.50	Full	(3)
MW-5	5-cm PVC	HSA	152	0.50	Full	(3)
MW-6	5-cm PVC	HSA	152	0.50	Full	(3)
MW-7	1.9-cm PVC	Drive pipe	152	0.25	Full	
MW-8	1.9-cm PVC	Drive pipe	152	0.25	Full	
MW-9	3.2-cm steel	Drive point	61	0.50		
MW-10	5.0-cm steel	Drive point	61	0.50		
MW-11	3.2-cm steel	Drive point	61	0.50		
MW-12	1.9-cm PVC	HSA	30.5	0.25	Lower	(4)
MW-13	1.9-cm PVC	HSA	30.5	0.25	Upper	(4)
MW-14	1.9-cm PVC	HSA	152	0.25	Full	(4)
MW-15	5-cm PVC	HSA	152	0.25	Full	(4)
MW-16	1.9-cm PVC	HSA	152	0.25	Full	(4)
MW-17	1.9-cm PVC	HSA	30.5	0.25	Upper	(4)
MW-18	1.9-cm PVC	HSA	30.5	0.25	Lower	(4)
MW-19	1.9-cm PVC	HSA	30.5	0.25	Full	(4)
MW-20	1.9-cm PVC	HSA	30.5	0.25	Upper	(4)
MW-21	1.9-cm PVC	HSA	30.5	0.25	Lower	(4)
MW-22	1.9-cm PVC	HSA	30.5	0.25	Upper	(4)
MW-23	1.9-cm PVC	HSA	30.5	0.25	Lower	(4)
MW-24	5-cm PVC	HSA	152	0.25	Full	(4)
MW-25	5-cm PVC	HSA	152	0.25	Full	(4)

Notes:
(1): Measurement indicates casing diameter
(2): Indicates screen length, in cm; "HSA" indicates wells that were drilled with a hollow-stem auger.
(3): Installed during site selection process.
(4): Indicates Cluster 1 wells.

Table 5.5-2: Monitoring well details.

Well casings consist of either 1.9- or 5-cm-diameter PVC. PVC was selected as a low-cost well material that is inert to ground water containing bromide, polystyrene microspheres, or encapsulated cells. The 5-cm-diameter casings were installed at the transect ends for pumping wells during aquifer tests and as water recirculation wells in the tracer tests (see next section). This size was selected because it was the smallest well diameter that would accommodate a *Grundfos Redi-Flow II* submersible pump. The Grundfos pump later proved unsatisfactory for long-term tracer test pumping. The 1.9-cm casing diameter was selected since it was the smallest well (in diameter) that could accommodate a *Solinst* water level indicator probe or the *Druck* pressure transducers (see Chapter 6). Tracer test samplers were designed to fit into the 1.9-cm wells (see Chapter 7).

Monitoring wells MW-12 through MW-25 were installed with hollow-stem augers using a University of Idaho *SIMCO* 2800 drill rig (as were MW-1 through MW-6; see Chapter 4). Boreholes for 5-cm casings were drilled with a 10.1-cm (I.D.) auger; boreholes for 1.9-cm casings were drilled with a 6.4-cm (I.D.) auger.

Sediment samples were taken in aquifer materials with a 3.8-cm split spoon sampler wherever possible. Samples were also taken from auger cuttings or the auger flight and/or the auger bit during auger removal. Sediment sampling is further discussed in Section 5.10.

The filter pack and screen sizes for wells MW-12 through MW-25 were specified on the basis of sediment samples collected from MW-5, the well closest to the new wells (see next section). The filter pack material was selected on the basis of the MW-5 sediment sample taken from approximately 2.13 m below ground surface. This sample was chosen over two other samples taken from within the aquifer zone (at depths of 2.34 and 3.57 m, respectively) for two reasons. First, finer-grained sediments in the two deeper samples may have washed from the auger flight during retrieval, biasing the samples (the 2.13-m sample was taken from an unsaturated environment, where cuttings were not washed during retrieval). Second, the filter pack was selected on the basis of finer-grained sediments since its purpose was to maintain formation

integrity in the borehole vicinity (i.e., prevent excessive amounts of fine-grained material from washing out of the formation).

Clean *Colorado* silica (10-20 sieve) sand was selected for the filter pack material. This filter pack material spans the grain size that is approximately four times the D_{50} sediment grain size (Nielson, 1991) for the MW-5, 2.13-m sample, and is approximately eight times the D_{70} grain size (Driscoll, 1986).

Pelletized bentonite extending from the top of the filter pack to the ground surface was specified to provide a reliable formation seal through the overlying aquitard. *Baroid Holeplug* (1.9-cm) pellets were used to provide an annulus seal from approximately 15 cm above the top of the screen to ground surface in all wells. Protective 10- or 15.2-cm-diameter (depending on well casing diameters) Schedule 40 PVC casings with slip-cap covers were installed for wells MW-12 through MW-25.

A 0.25-mm screen opening was chosen for wells MW-12 through MW-25 on the basis of the material observed within the aquifer. This opening size is larger than approximately 50% of the sediments contained in the MW-5, 2.13-m sample, which is the recommended opening size for naturally developed wells (Driscoll, 1986). This conservative size was selected, despite the use of a filter pack, to allow development adjacent to the casing (the filter pack) but not in the formation.

The 5-cm-diameter slot-cut PVC screens were purchased from commercially available stock. The 1.9-cm-diameter screens were not commercially available; these screens were therefore cut by hand using a circular 2.54-cm-diameter stainless-steel blade (0.25-mm thickness) mounted in a *Dremel* motor tool. A 30.5-cm section of 1.9-cm-diameter PVC screen would have approximately 145-150 cuts of approximately 1 cm each in length, resulting in an approximate open area of 3.8 cm^2 per 30.5-cm screen length (2% open area). These limited open areas were acceptable since these wells would not be used for significant pumping.

Wells were installed with either 30.5-cm or 152-cm screen intervals (see Table 5.5-2, or Appendix D). The 5-cm wells at the end of each transect were installed with 152-cm screens for full aquifer penetration. The tracer injection wells were also installed with 152-cm screens so that tracer could be simultaneously injected throughout

(along a vertical line) the aquifer zone. The remaining 1.9-cm monitoring wells were installed with 30.5-cm screens to allow for monitoring at different vertical zones within the aquifer. Pairs of wells with 30.5-cm screens were placed such that one well was screened in the upper portion of the aquifer and the other well was screened in the lower section. The two wells were placed 50 cm apart to reduce potential hydraulic interference between them. The shallower wells were placed in a flowline along a transect upgradient of the deeper well to reduce potential flow-field interference for the second well.

Monitoring wells were developed by bailing and/or surging and pumping with compressed air. It was found later that tracer test pumping wells were still producing small amounts of sediment that would clog the recirculation-loop system (see Section 8.2); these wells were further developed with the system shown in Figure 5.5-3. Water pumped through a radial nozzle was lowered into the well to dislodge fine sediments near the well screen (mode 1). Following agitation, two sediment aboveground collection basins were used to collect sediment. This system facilitated higher pumping rates and greater turbulence for well development than could otherwise be used in a low-production well, resulting in minimal subsequent sediment production.

5.6. An Aquifer Description

This section presents a description of shallow subsurface stratigraphy at the Plant Science Farm field site. The description is based on observations made during the installation and development of monitoring wells MW-1 through MW-6 and MW-12 through MW-25. These wells were installed with a hollow-stem auger, which allowed a visual description of borehole cuttings. Wells MW-7 through MW-11 were installed with drive points or drive pipes, methods not amenable to sediment description and/or sampling. Well logs are provided in Appendix A.

General subsurface stratigraphy for wells in transects A, B, and C (Cluster 1 wells) is shown in Figures 5.6-1 through 5.6-3 (stratigraphy in the vicinity of Cluster

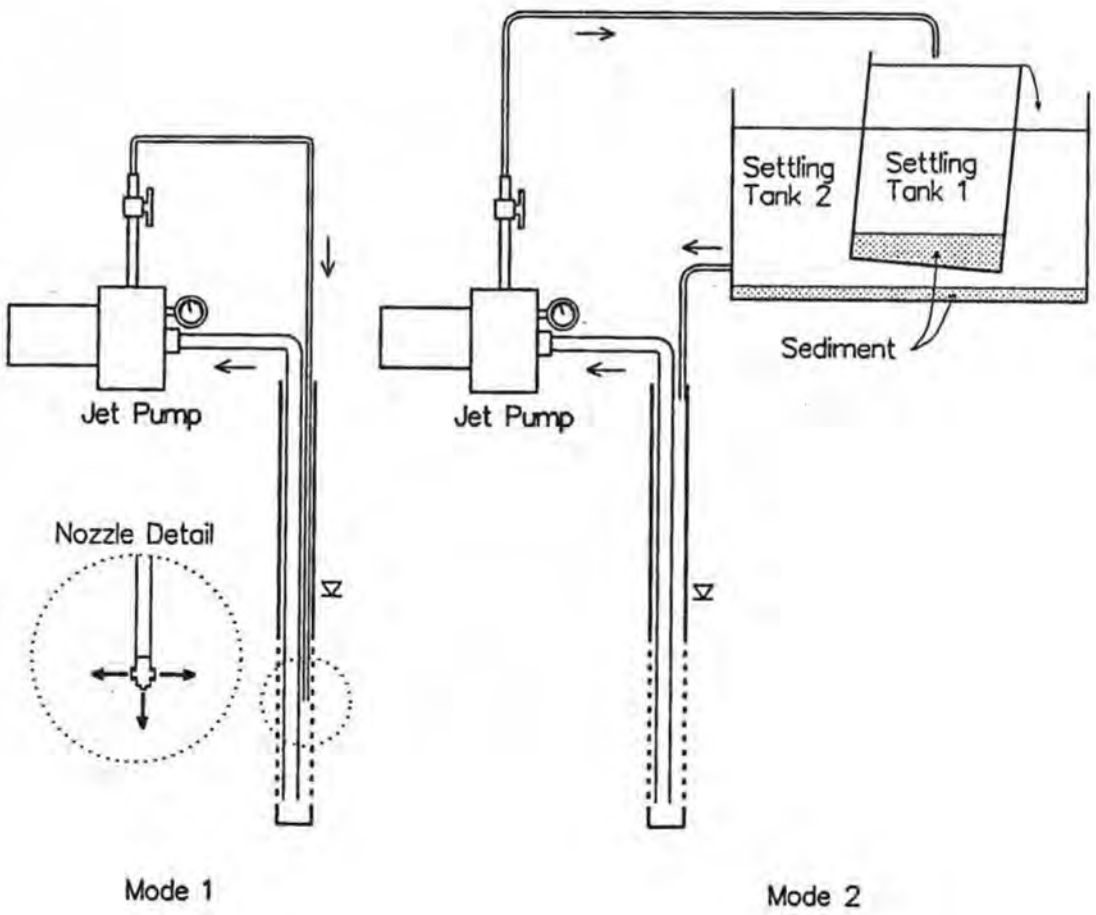

Figure 5.5-3: Well development system with a jet pump.

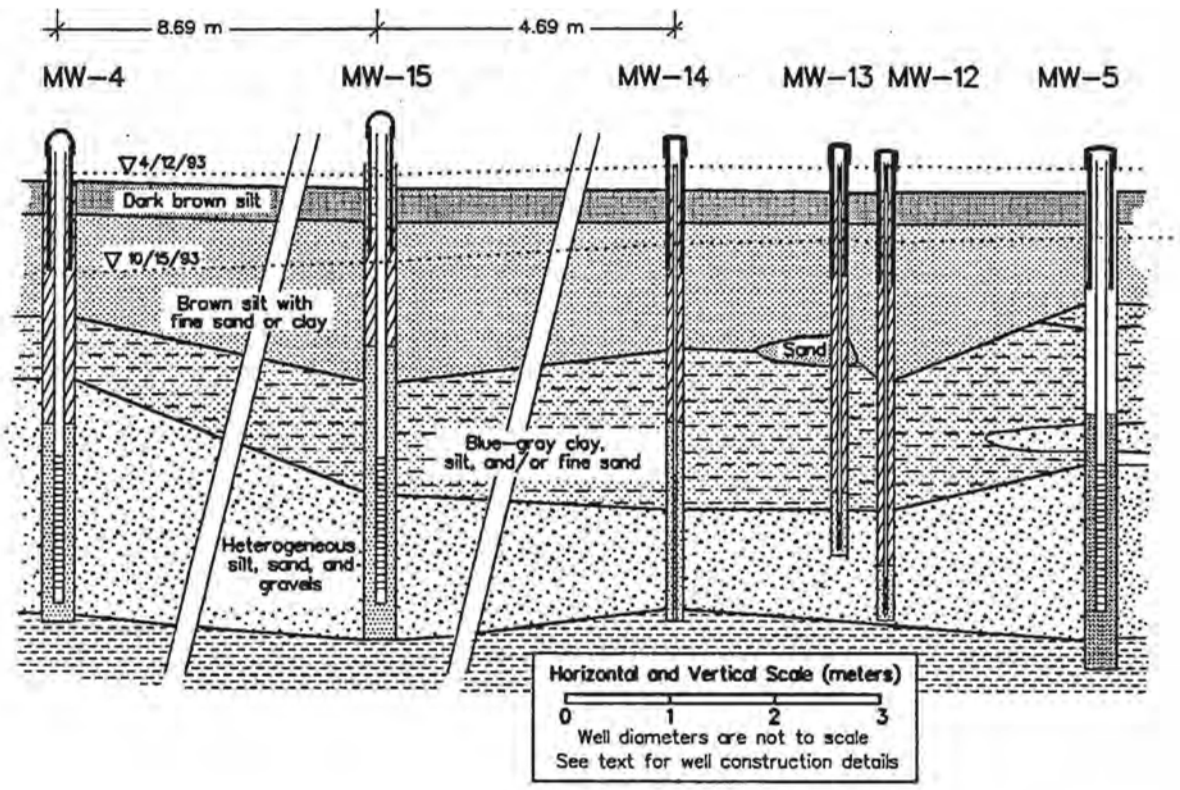

Figure 5.6-1: Transect A cross section.

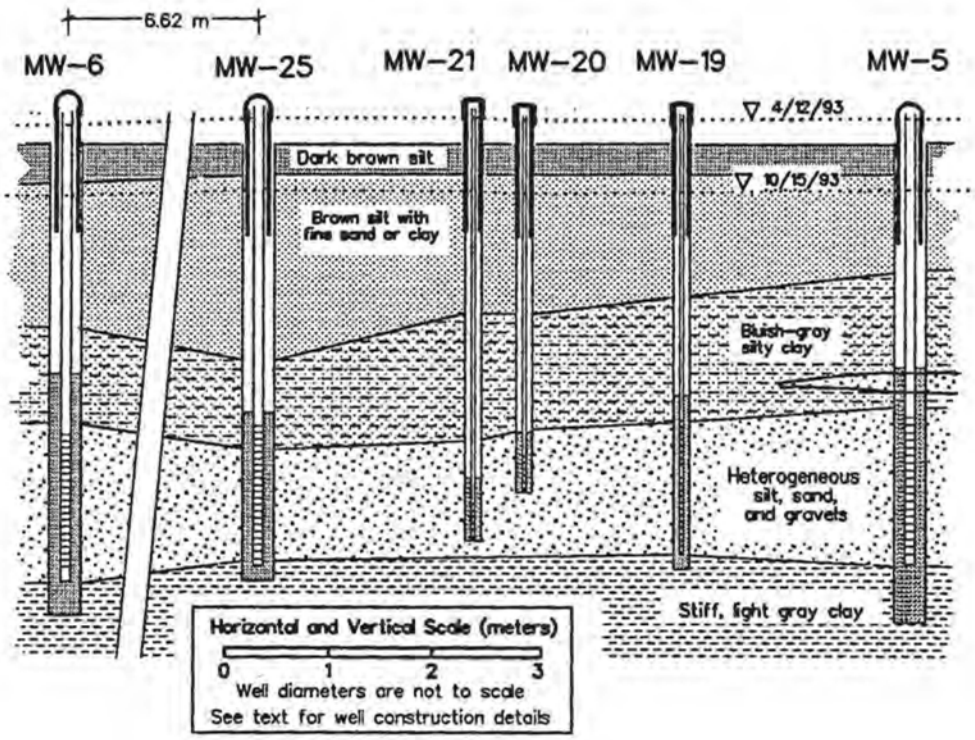

Figure 5.6-2: Transect B cross section.

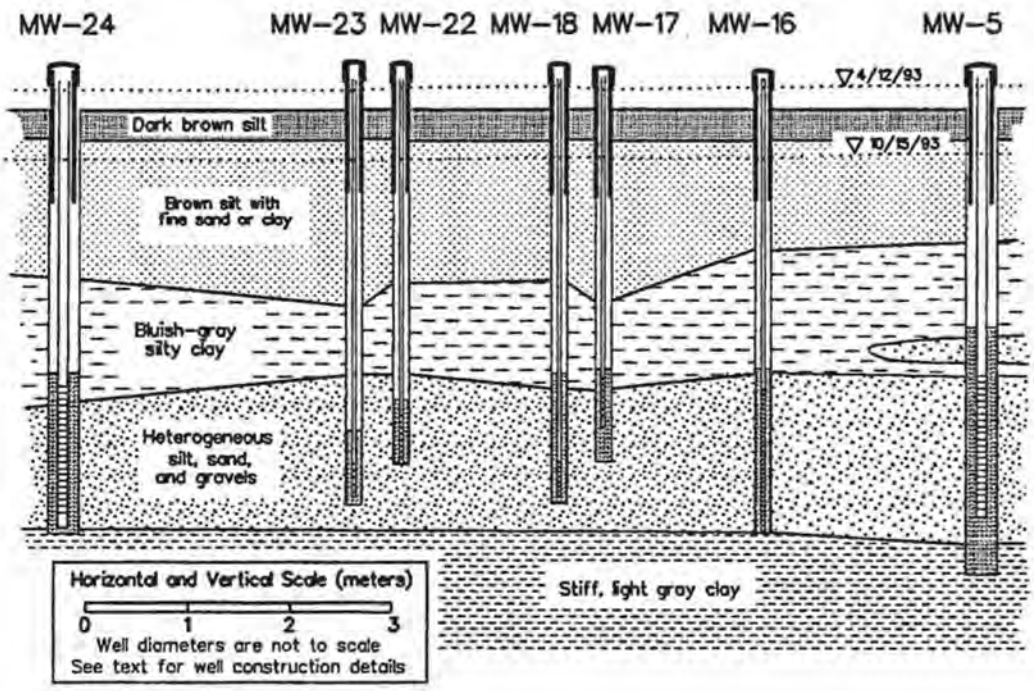

Figure 5.6-3: Transect C cross section

1 wells is emphasized since tracer tests were conducted in this area). The general stratigraphy consists of a shallow soil zone, a zone of brown silt containing various amounts of clay and/or fine sand, a bluish-gray zone of silty clay, a saturated aquifer zone consisting of silt, sand, pebbles, and gravel, and an underlying zone of stiff, dense, light gray clay. These zones are further described in the next several paragraphs.

A typical borehole penetrated approximately 30 cm through a medium- to dark-brown silty loam, with abundant roots from overlying grasses. Underlying the shallow soil zone was a zone of medium-brown silt containing varying amounts of fine sand and/or clay. This zone extended to depths of approximately 0.5 to 1.25 m below ground surface. In Transect B and C wells the medium-brown silt zone appeared to contain more clay than in Transect A wells. Increasing amounts of sand with depth were noted in some holes, whereas increasing clay was noted in others. The brown color in this zone also appeared to darken with depth in most wells.

Below the brown clayey silt lies a relatively sharp transition to a bluish-gray silty clay. Again, varying amounts of silt, fine sand, and clay were observed in this zone, with occasional sand lenses. Increasing amounts of silt and fine sand with depth were observed in numerous wells. All layers to this depth typically appeared unsaturated with water.

Under the gray silty clay at a depth ranging from approximately 2.5 to 4 m below ground surface lies a saturated silt, sand, and gravel zone. Significant heterogeneities in sorting, layering, grain size, and grain shapes were observed in drill cuttings from this zone. Gravels in this zone were granitic and/or quartzitic, poorly sorted, subangular to subround in shape, and ranging in size to 6-7 cm. Sands consisted of fine to very coarse, subangular to subround, poorly sorted quartzitic grains. Water from well development and split spoon samples contained silt and clay material having the same gray color as the silty clay overlying the aquifer. A reddish, pebbly sand zone (up to approximately 5-cm in thickness) was observed in MW-17, MW-18, MW-19, and MW-25 at approximately 3.2 m below ground surface. Some of the silt, sand, and gravels appeared to be interbedded, and some appear to be in a matrix of coarse and fine grained materials.

The silt, sand, and gravel zone was consistently saturated. Water levels in the borehole and/or well would typically rise to within approximately 0.5 to 1 m of the ground surface once the silt, sand, and gravel zone was penetrated. This zone is considered to be a confined aquifer because (1) it supplies water to wells, and (2) water levels rise above the top of the aquifer zone when the aquifer is penetrated.

The aquifer zone is underlain by a very stiff, very light gray to bluish gray clay. This stiff clay was seen in all of the deeper wells. This clay layer appears similar to Latah County clays described by Tullis (1940). None of the project wells penetrated through this clay zone.

5.7. Grain Size Analysis

Grain size analyses were conducted with sediment samples collected during the installation of monitoring wells. The purpose for conducting the grain size analyses was to (1) aid in the description of aquifer sediments, and (2) evaluate aquifer heterogeneities on the basis of the aquifer grain size distribution.

Sediment samples were taken with a variety of methods. First, 3.8-cm split spoon samples were taken in aquifer materials wherever possible. Split spoon samples were limited by cobbles blocking the split spoon entrance, or by the loss of saturated sands falling out of the sampler during retrieval. Water drainage from the cores removed from the saturated area may have resulted in the loss of fine-grained sediments. The use of a 9.5-cm-diameter *CME Continuous Sample Tube System* was attempted, but the drill rig was not capable of pushing it when significant gravels were present; aquifer samples were therefore not obtained with this method.

Sediment samples were also taken from auger cuttings, the auger flight, and/or the auger bit during auger removal. Some fine-grained materials may have been lost from the auger flight samples because of drainage or contact with other borehole sediments during retrieval. Sampling intervals and locations are given in Table 5.7-1. The depths from which auger cuttings samples were taken are approximate due to the nature of auger sampling. Grain size analyses were conducted using the ASTM method

	Upper Depth	Lower Depth	Sample Source	Notes
MW-5	2.3	2.4	Auger Flight	
MW-5	3.1	4.1	Auger Flight	
MW-7	2.7	3.7	Auger Flight	
MW-11	2.3	2.6	Auger Flight	
MW-12	2.7	3.1	Auger Flight	
MW-12	3.4	3.7	Auger Flight	
MW-13	3.1	3.4	Auger Flight	
MW-13	2.9	3.5	Core	
MW-14	2.7	3.4	Core	
MW-14	3.8	4.0	Core	
MW-15	2.7	2.9	Core	
MW-15	2.9	3.1	Core	
MW-15	3.1	3.2	Core	
MW-15	3.4	4.0	Auger Flight	
MW-15	4.0	4.0	Auger Flight	
MW-16	2.7	3.8	Auger Flight	
MW-16	3.7	3.8	Auger Cuttings	
MW-16	2.7	3.6	Core	
MW-17	2.7	3.6	Core	
MW-17	3.2	3.6	Core Bit	
MW-18	2.7	3.6	Core	
MW-19	2.7	3.6	SS Core	
MW-19	3.1	3.1	SS Core	
MW-19	3.7	4.0	SS Core	
MW-19	4.0	4.1	Core	
MW-20	2.7	3.4	SS Core	
MW-21	2.7	3.4	Core	
MW-22	2.7	3.4	Core	upper MW-25 cm recovery
MW-22	2.7	3.4	Core Bit	lower 1 cm recovery
MW-23	2.7	3.4	Core	30 cm recovery
MW-24	2.7	3.4	SS Core	
MW-24	2.7	3.4	SS Core	
MW-24	2.7	3.4	SS Core	
MW-25	2.7	3.4	SS Core	
MW-25	2.7	3.4	SS Core	

Table 5.7-1: Approximate sediment-sampling intervals (in m below ground surface); see text for discussion of limitations.

C 136-84a. Aggregate samples were oven-dried and sieved in a mechanical sieve shaker; sieves were weighed before and after on a scale to ± 0.01g. Sieve information is given in Table 5.7-2.

Sieve Number	Opening (mm)	Material	Size Range (mm)
4	4.76	Boulder	> 256
10	2	Cobble	64-256
18	1	Gravel	2-64
35	0.5	Coarse Sand	0.5-2
60	0.25	Medium Sand	0.25-0.5
140	0.106	Fine Sand	0.063-0.25
230	0.063	Silt	0.004-0.063
Pan		Clay	<.004

Table 5.7-2 Sieve details. (Size ranges are generalized from Driscoll, 1986)

A summary of grain size distribution data is presented in Figure 5.7-1 (results are given in tabular form in Appendix B). Cumulative grain size distribution curves are shown as averages at specific depth intervals in Figures 5.7-2 through 5.7-4. Standard deviations are plotted for depths in which multiple samples were taken. The greatest number of samples were taken in or near the aquifer zone since this was the primary zone of interest.

Several observations can be made from these graphs. First, samples taken from 2.5 to 4.5 m below ground surface were generally coarser than shallower samples. Averaged grain size distributions were very similar for the 2.5 to 3.5 m and the 3.5 to 4.5 m depths (Figure 5.7-1). Coarser materials correspond with samples taken from the aquifer zone. The error bands indicated by the standard deviation curves (Figures 5.7-2 through 5.7-4) indicate variability in grain size distribution (although the apparent variability is also caused by small sample numbers).

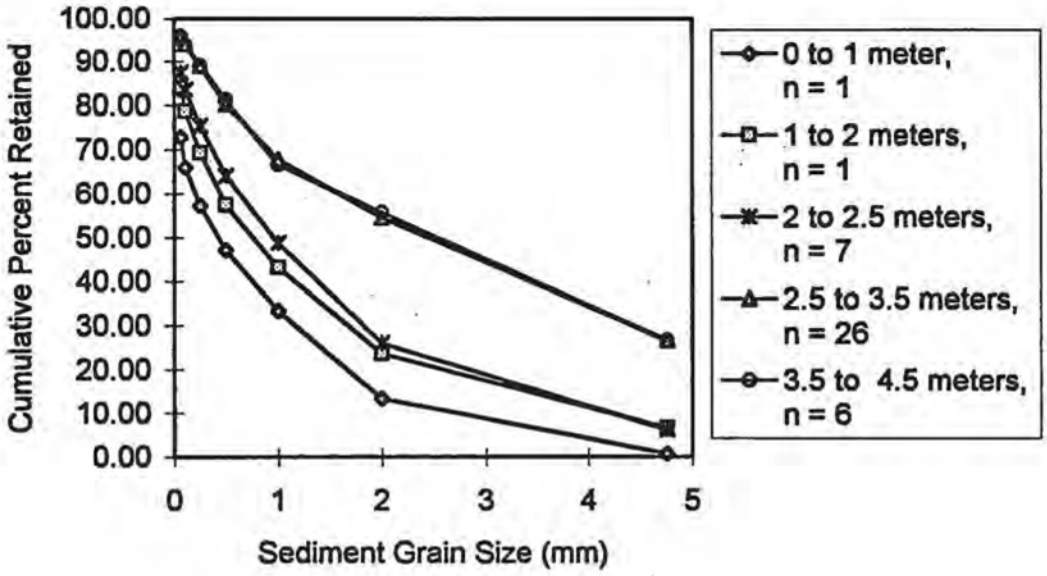

Figure 5.7-1: Average sediment grain size distributions

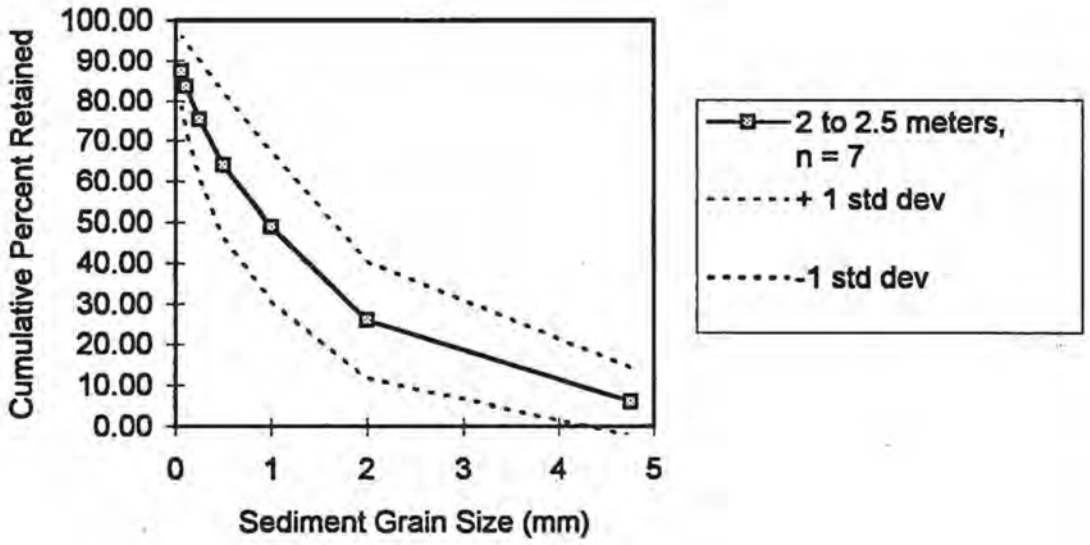

Figure 5.7-2: Average sediment grain size distribution (from 2 to 2.5 m depth).

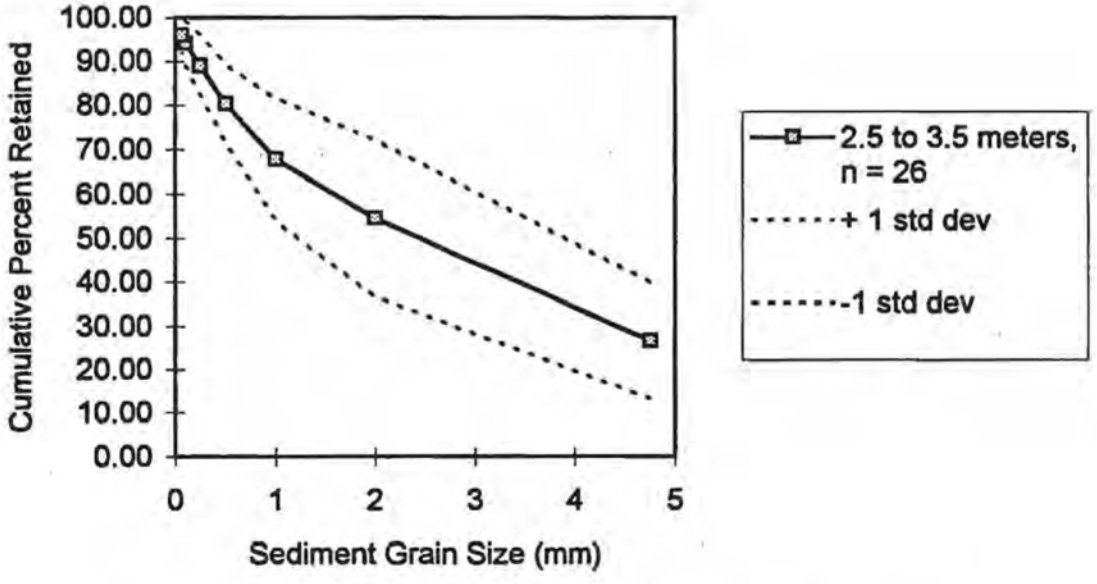

Figure 5.7-3: Average sediment grain size distribution (from 2.5 to 3.5 m depth).

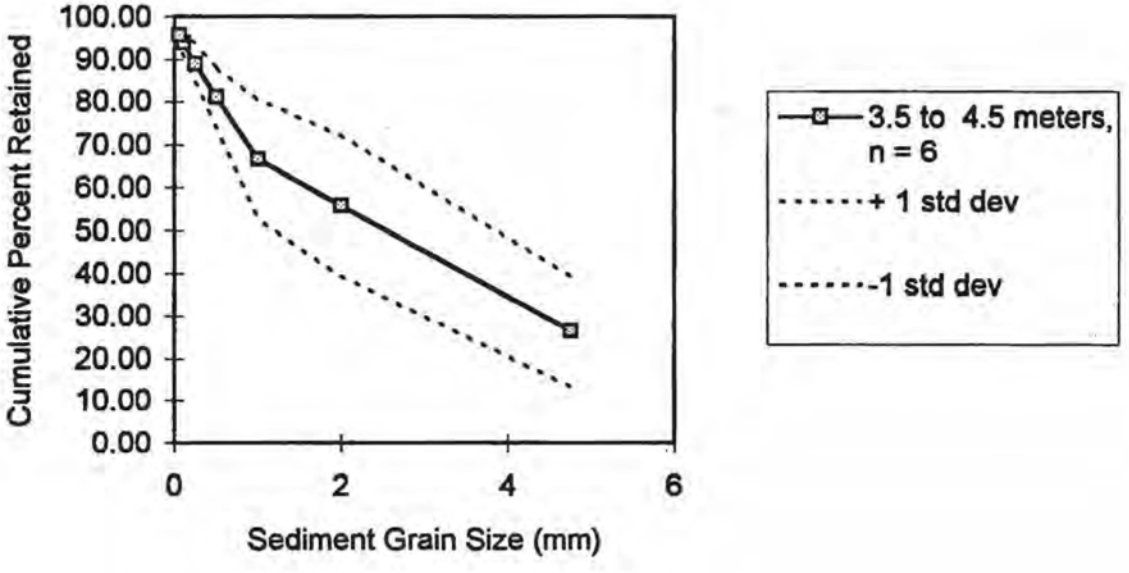

Figure 5.7-4: Average sediment grain size distribution (from 3.5 to 4.5 m depth).

5.8. Depositional Environment

Observations made of aquifer sediments during the installation of monitoring wells and subsequent grain size analyses provide a basis for considering potential depositional environments. Possible depositional environments resulting in the Plant Science Farm site aquifer sediments are discussed in this section.

In general, unconsolidated sediments can be created by rock weathering, or can be deposited by eolian, glacial, mass-wasting, or fluvial processes (Bloom, 1991). Aquifer sediments did not appear to be created by rock weathering at the Plant Science Farm site because the parent materials are not present in the immediate site vicinity. Although eolian deposits (loess) are present in the general field site area, the aquifer sediments are too large and too poorly sorted for eolian transport/deposition. Pleistocene glaciation did not extend to the Moscow area (Breckenridge, 1989); aquifer sediments were therefore not deposited by glacial processes. The degree of roundness in the field site aquifer sediments indicates transport over larger distances than would generally be expected with mass-wasting processes. Also, the quartzitic/granitic nature of the aquifer sediments indicates transport from sources other than the immediate field site area.

Aquifer sediments appear to have been deposited in a fluvial environment. University of Idaho researchers hypothesize (Bush, personal communication, 1994) that these aquifer sediments represent reworked sediments from nearby Moscow Mountain and/or quartzite outcrops to the north and east of the field site. The range of sorting, material sizes, and degree of roundness observed in field site aquifer sediments appears consistent with a fluvial depositional processes.

In general, alluvial deposits may include transitory channel deposits, lag deposits, channel fills, lateral accretion deposits, and splays (Vanoni, 1971). Alluvial sediment deposit characteristics depend on the channel slope, discharge, sediment load, and channel characteristics (Easterbrook, 1993).

Two general observations can be made regarding the depositional environment for field site aquifer sediments. First, the areal extent of aquifer sediments and the apparent limited aquifer thickness indicate a wide, shallow depositional zone. Second,

the degree of sorting (poor to moderate) and sediment size heterogeneity may indicate transitory channel deposits.

The shape and direction of ancient channels in the field site area cannot be determined from the available well data. The shape and direction of ancient field site channels is important since aquifer hydraulic conductivity (and particle transport capability) may be greater in the direction of ancient channels than perpendicular to ancient channels. The apparent source for aquifer sediments appears to be to the north and east of the field site. Similar deposits (similar composition, finer-grained) have been observed within the South Fork of the Palouse River drainage approximately 3 km downstream (south and west) of the field site. On the basis of these observations, and on the basis of general topography in the field site area, the general flow direction may have been from north to south, or from northeast to southwest, although local flow directions (on the scale of the field site) could have varied significantly.

5.9. Well Survey

Ground water monitoring wells at the Plant Science Farm site were surveyed to the nearest 0.3 cm on April 7 and 8, 1993. All elevations are based on the State of Idaho Public Works Benchmark (No. 5) located just northeast of the intersection of Idaho Highway 8 (Troy Highway) and Mill Road, southeast of the field site. The elevation of the benchmark is 790.19 meters above mean sea level. The approximate survey error for actual elevations is 1.8 ± 0.3 cm. The approximate survey error for relative elevations between wells is approximately ± 0.5 cm. Monitoring well elevations are given in Table 5.9-1.

Two locations for measuring water levels in the South Fork of the Palouse River were also surveyed. Water levels were measured at the west end of the Mill Road culvert and at the west end of the Elks Golf Course culvert.

5.10. Water Levels and Hydraulic Gradient

Water levels in all wells were taken periodically during the course of the project. Water-level readings were taken as part of the aquifer characterization to determine local ground water flow directions. Also, water level measurements were taken to

	Elevation (meters above mean sea level)	
Location	Inner Casing	Ground Surface
MW-1	791.05	790.68
MW-2	790.82	790.41
MW-3	790.82	790.43
MW-4	790.85	790.41
MW-5	790.80	790.29
MW-6	790.77	790.39
MW-7	790.95	790.64
MW-8	790.45	790.15
MW-12	790.74	790.31
MW-13	790.75	790.31
MW-14	790.66	790.33
MW-15	790.73	790.34
MW-16	790.68	790.33
MW-17	790.72	790.33
MW-18	790.74	790.32
MW-19	790.72	790.32
MW-20	790.71	790.33
MW-21	790.71	790.31
MW-22	790.75	790.33
MW-23	790.79	790.35
MW-24	790.76	790.36
MW-25	790.75	790.30
MW-26	790.90	790.33
MW-27	791.45	790.32
MW-28	790.87	790.29
Mill Road Culvert		790.70
Golf Course Culvert		789.26

Table 5.9-1: Well elevations.

determine whether the aquifer remains confined throughout the year (i.e., whether water levels in wells remain above the top of the aquifer.

Water levels were measured with a *Solinst* water level indicator probe. Readings were recorded to the nearest 0.3 cm. Water level readings are given in Appendix C.

Temporal water level data for monitoring wells in 1993 (the year during which tracer tests were conducted) are presented in Figures 5.10-1 through 5.10-5. Figure 5.10-1 presents water levels for monitoring wells MW-1 through MW-6; Figure 5.10-2 presents water levels for the drive point and drive pipe wells; Figures 5.10-3 through 5.10-5 present water levels for wells in Transect A, B and C, respectively.

The greatest difference in water levels between wells is seen in wells MW-1 through MW-6, presumably because these wells are separated by larger distances than some of the Cluster 1 wells.. The lowest water levels are seen in MW-7, which is the easternmost well. Water levels in wells in transects A, B and C followed similar patterns throughout the year. Water levels in sampling pairs completed in different aquifer zones (MW-12 and MW-13; MW-17 and MW-18; and MW-20 and MW-21) also remain similar throughout the year.

Three potentiometric surface maps showing water levels on April 12, June 15, and October 15, 1993, are shown in Figures 5.10-6 through 5.10-8. These data were chosen for the potentiometric surface maps to represent high and low water levels during the year in which tracer tests were conducted. A general east or northeasterly ground water gradient appears in all three measurements. Water levels in a series of shallow wells located approximately 300 m west of the site (near the Plant Science Farm buildings) also show a strong easterly gradient (Mosko, 1993).

A general water level depression appears to be present in Figures 5.10-6 and 5.10-7. The reason for this depression is unclear. However, the depression is created largely on the basis of water level readings in one well (MW-7) and thus may reflect measurement error. High water level readings in MW-7 may also indicate localized recharge. This well experiences the greatest water level change over the period of record.

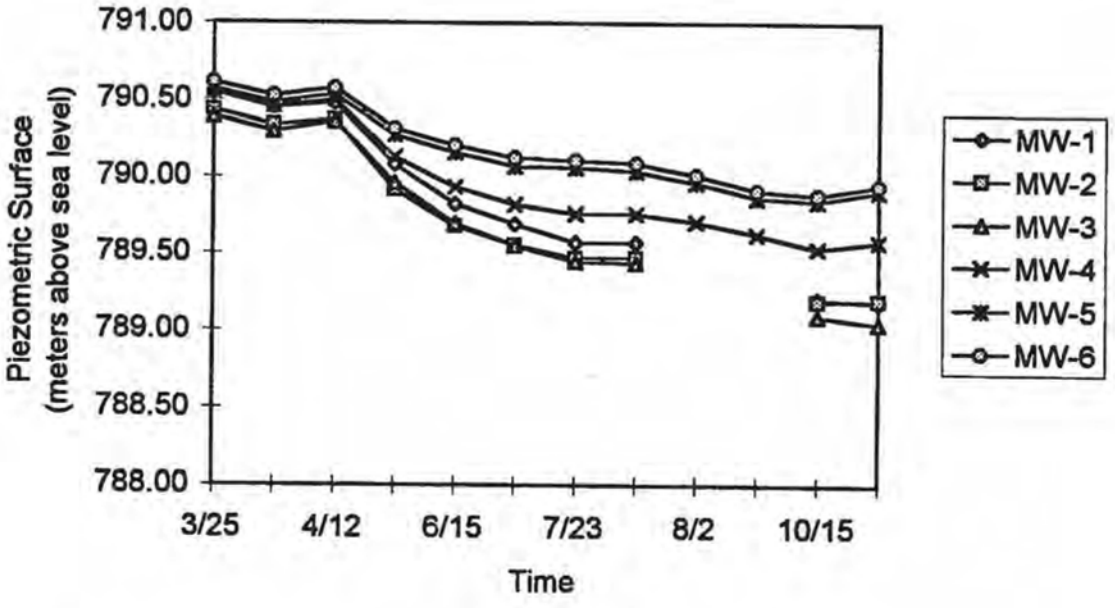

Figure 5.10-1: 1993 Water levels in monitoring wells MW-1 through MW-6.

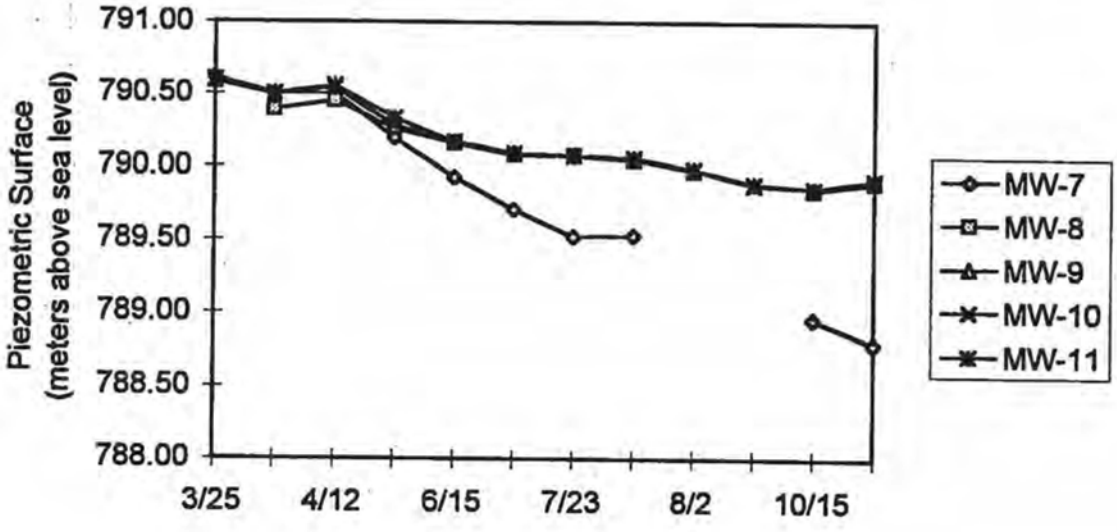

Figure5.10-2: 1993 Water levels in drive point, drive pipe wells.

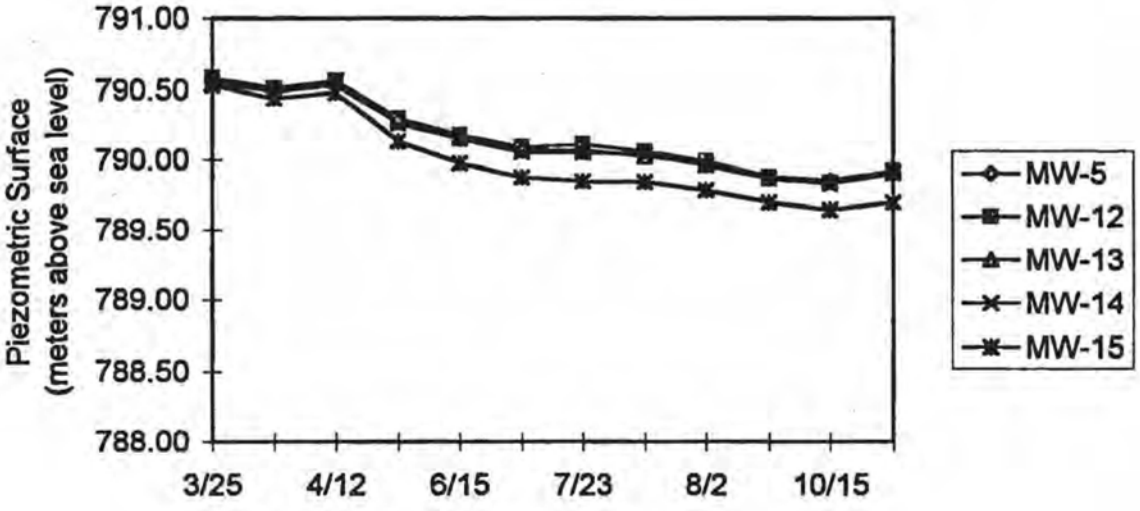

Figure 5.10-3: 1993 Water levels in Transect A wells.

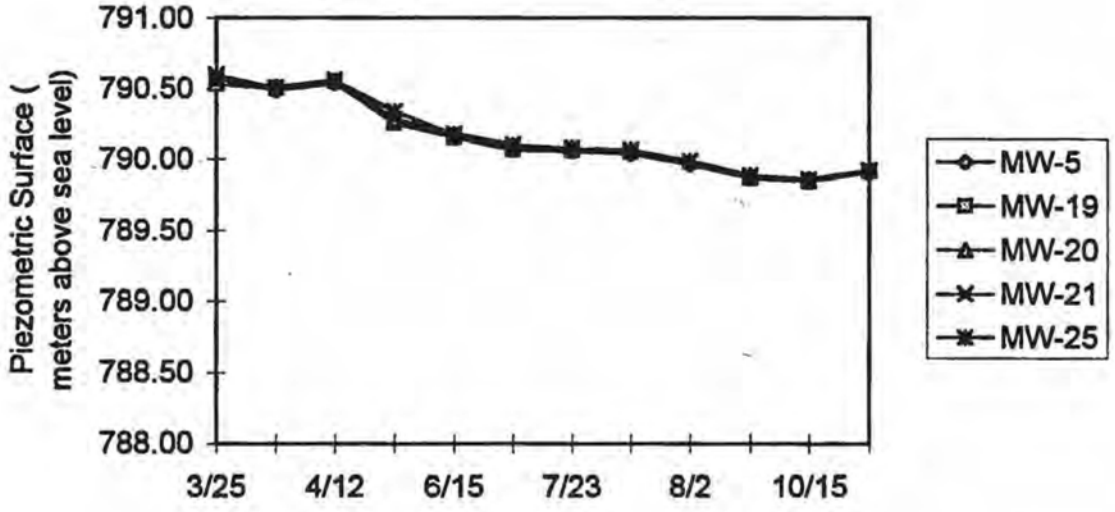

Figure 5.10-4: 1993 Water levels in Transect B wells.

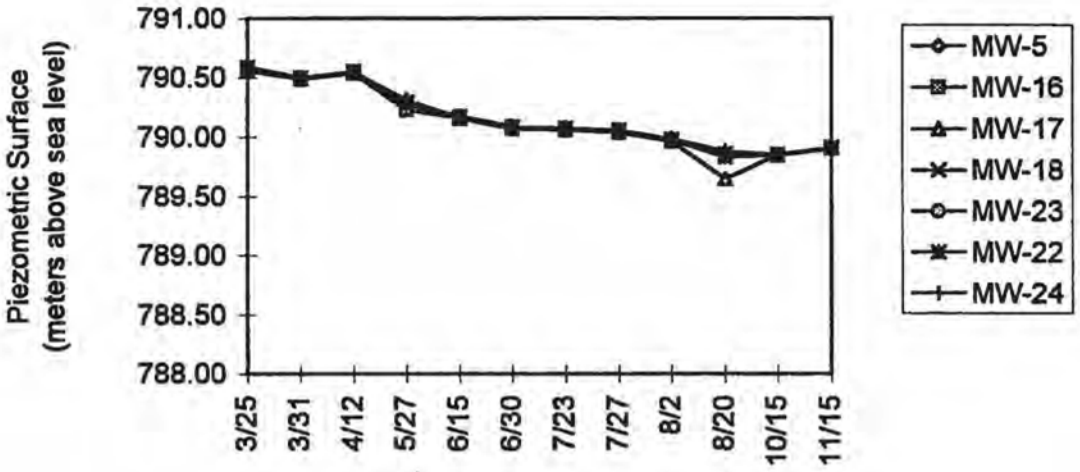

Figure 5.10-5: 1993 Water levels in Transect C wells.

The northeasterly ground water gradient in the field site area may be partially controlled by the South Fork of the Palouse River. The stream is located to the northeast and east of the field site (Figure 4.2.1), and is the only surface water in the vicinity of the field site. Water levels in the stream are lower than the field site; the creek probably is a local ground water discharge zone.

The April and June readings indicate a slight potentiometric depression in the vicinity of MW-1, MW-2, and MW-3. The reason for the potentiometric depression is unclear. The depression may be caused by heterogeneous aquifer characteristics, or may be an artifact of water-level measurement or survey error.

5.11. Conceptual Model

This section presents the development of a conceptual hydrogeologic model for the Plant Science Farm field site aquifer. The purpose of forming a conceptual model is to establish a framework (1) for selecting analytical models for aquifer test

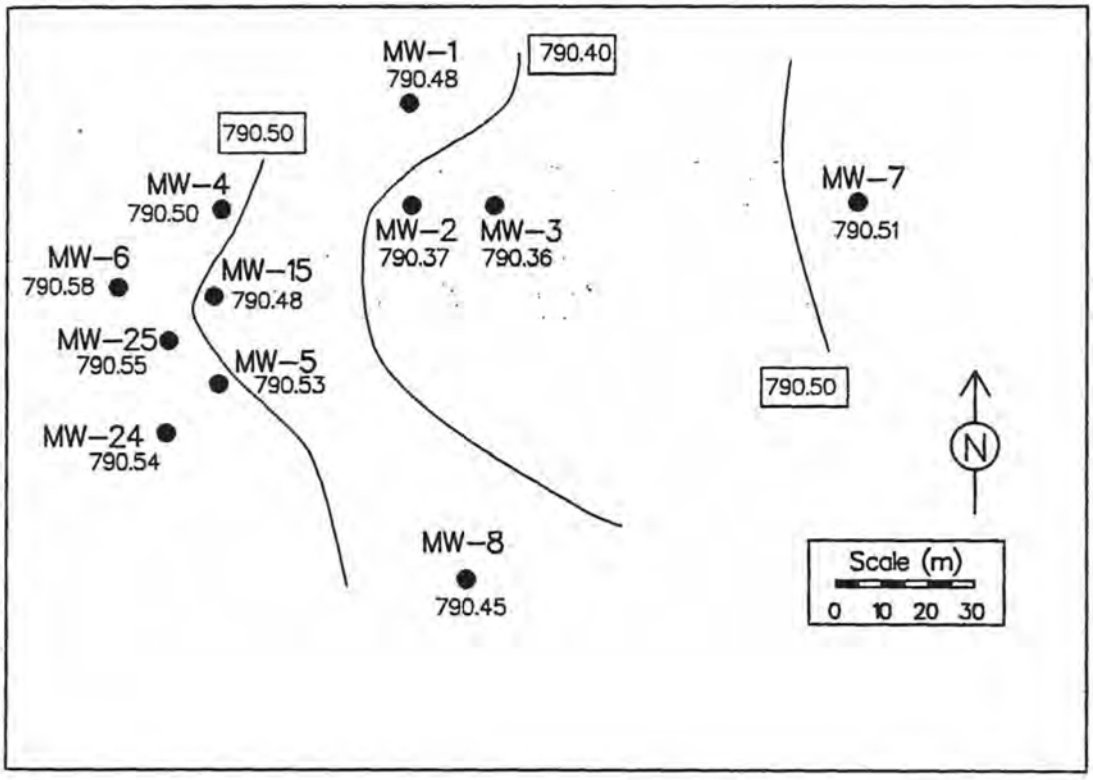

Figure 5.10-6: Potentiometric Surface on 4/13/93

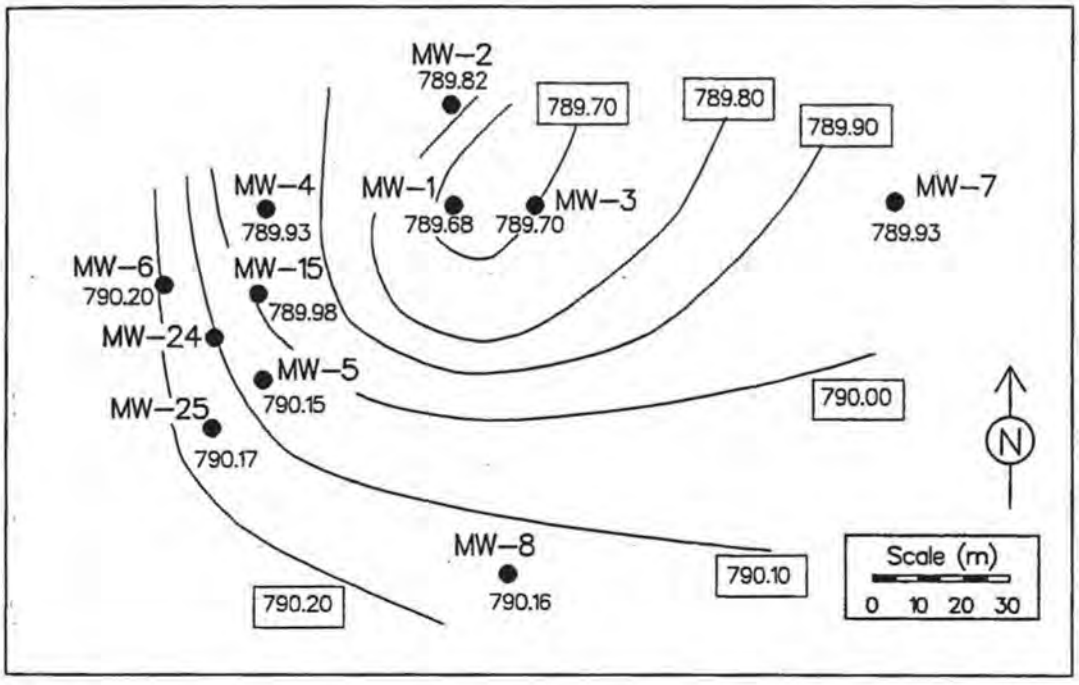

Figure 5.10-7: Potentiometric Surface on 6/15/93

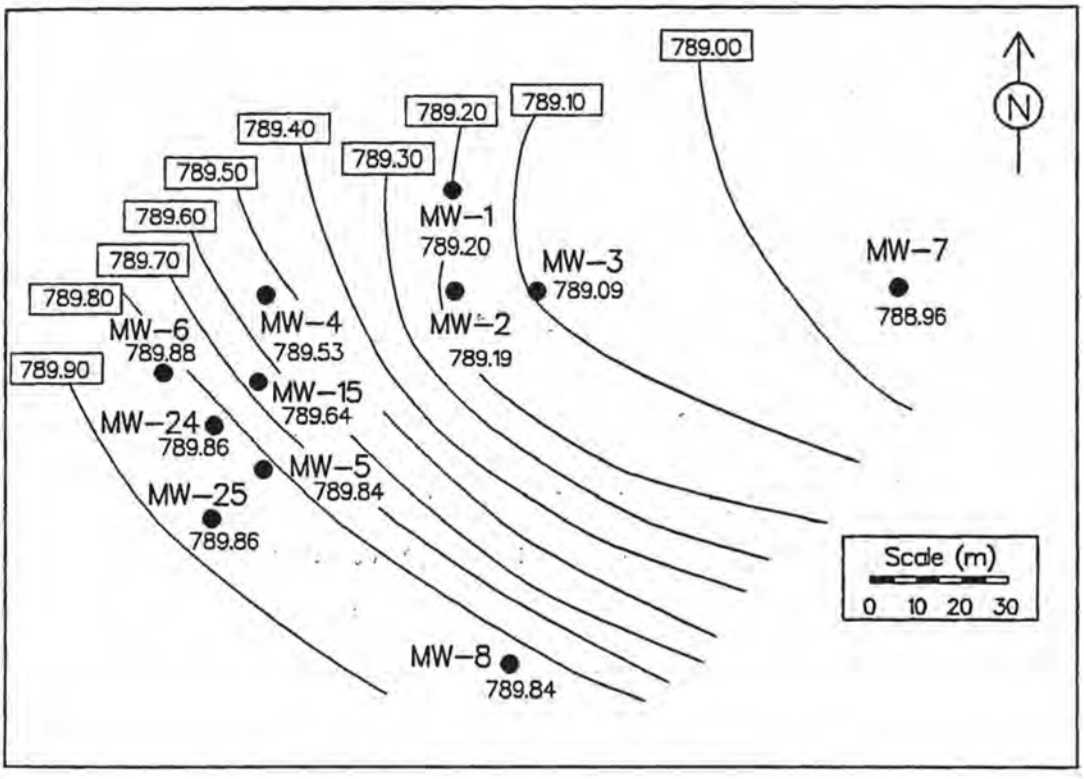

Figure 5.10-8: Potentiometric Surface on 10/15/93

analysis, and (2) for analyzing tracer test results in the context of aquifer characteristics. The conceptual model is based on observations and results from the field investigation, and on consideration of depositional environments.

Aquifer sediments at the Plant Science Farm field site consists of silt, fine- to coarse-grained quartzitic sand, and subangular to subround quartzitic gravel and cobbles ranging in size to approximately 7 to 9 cm. Aquifer sediments were described as being poorly to moderately well sorted, depending on the location. Similar aquifer sediments were encountered in all of the field site wells. The noise and feel of the auger provided an indication of relative difference in material sizes at different zones within the aquifer. The aquifer sediments were interpreted as belonging to the sediments of Bovill within the Latah Formation, and as having been deposited in a fluvial environment.

The thickness of aquifer sediments (in Cluster 1 wells) ranged from approximately 1 to 1.5 m. Overlying sediments frequently contained a transition zone grading from fine-grained sediments downward to coarse-grained aquifer sediments. This gradation suggests that aquifer sediments were not scoured following deposition.

Water rose within each borehole upon penetration of the aquifer zone, indicating confined hydraulic conditions. A stiff, light-gray clay observed in all of the deeper wells appears to be an underlying aquitard. A gray silt and clay zone above the aquifer materials is considered to be an upper aquitard. Cuttings from the upper aquitard generally appeared moist but not saturated during well construction. The upper aquitard zone contains varying amounts of silt and/or fine sand, generally near the transition to coarser aquifer sediments. The presence of some silt and fine sand in the upper aquitard may allow some water movement into or out of this zone corresponding to changes in aquifer head.

The areal extent of the aquifer zone is unknown. Sand and gravel deposits have been observed at similar depths in other parts of the Plant Science Farm (Mosko, 1993).

A conceptual model of the field site aquifer was developed from knowledge of the aquifer sediments and possible depositional environments. The conceptual model forms the basis for evaluating aquifer and tracer test results.

The conceptual model consisted of an aquifer zone containing silts, sands, gravels, and cobbles. These sediments are somewhat mixed, but zones of coarser and finer materials, in lensoidal and/or interbedded form, are present. The aquifer sediments are thought to have been deposited in a multi-channel environment covering the field site area; aquifer sediment heterogeneity may be the result of transitory channel deposition. Zones of coarser materials could be expected within ancient primary flow channels (primary flow channels would have carried a higher discharge, and therefore larger bedload materials).

The aquifer was assumed to be confined, as evidenced by rising water levels in boreholes following the penetration of the aquifer zone. Some vertical water movement occurs through the upper aquitard on a seasonal basis, although the upper aquitard was generally found to be moist but not saturated during drilling.

Two theoretical cross-sections of the conceptual model are shown in Figure 5.11-1. The first cross section illustrates a hypothetical cross-channel view of the conceptual aquifer model, and the second cross-section indicates a view along a hypothetical depositional channel. One or both of these cross-sections could describe aquifer sediments in the vicinity of Cluster 1 wells.

The hydraulic response anticipated in these aquifer sediments in response to stress (e.g., water pumping or water injection) would be dependent on the scale of measurement. On a small scale the aquifer might appear highly heterogeneous (in terms of hydraulic response). Over an intermediate to large scale the aquifer might still appear highly heterogeneous, or may appear to be "homogeneously heterogeneous." Apparent hydraulic boundaries could appear as a cone of depression (due to aquifer pumping) reaching multiple channel boundaries, or zones of increased or decreased hydraulic conductivity caused by multiple-channel stream deposition.

It is likely that ground water flow (and therefore tracer transport) in a heterogeneous environment is influenced by preferential flow in interconnected zones of larger pore spaces. The rates of particle and non-particle tracer transport along Cluster 1 depends, in part, on the patterns of interconnected pore spaces.

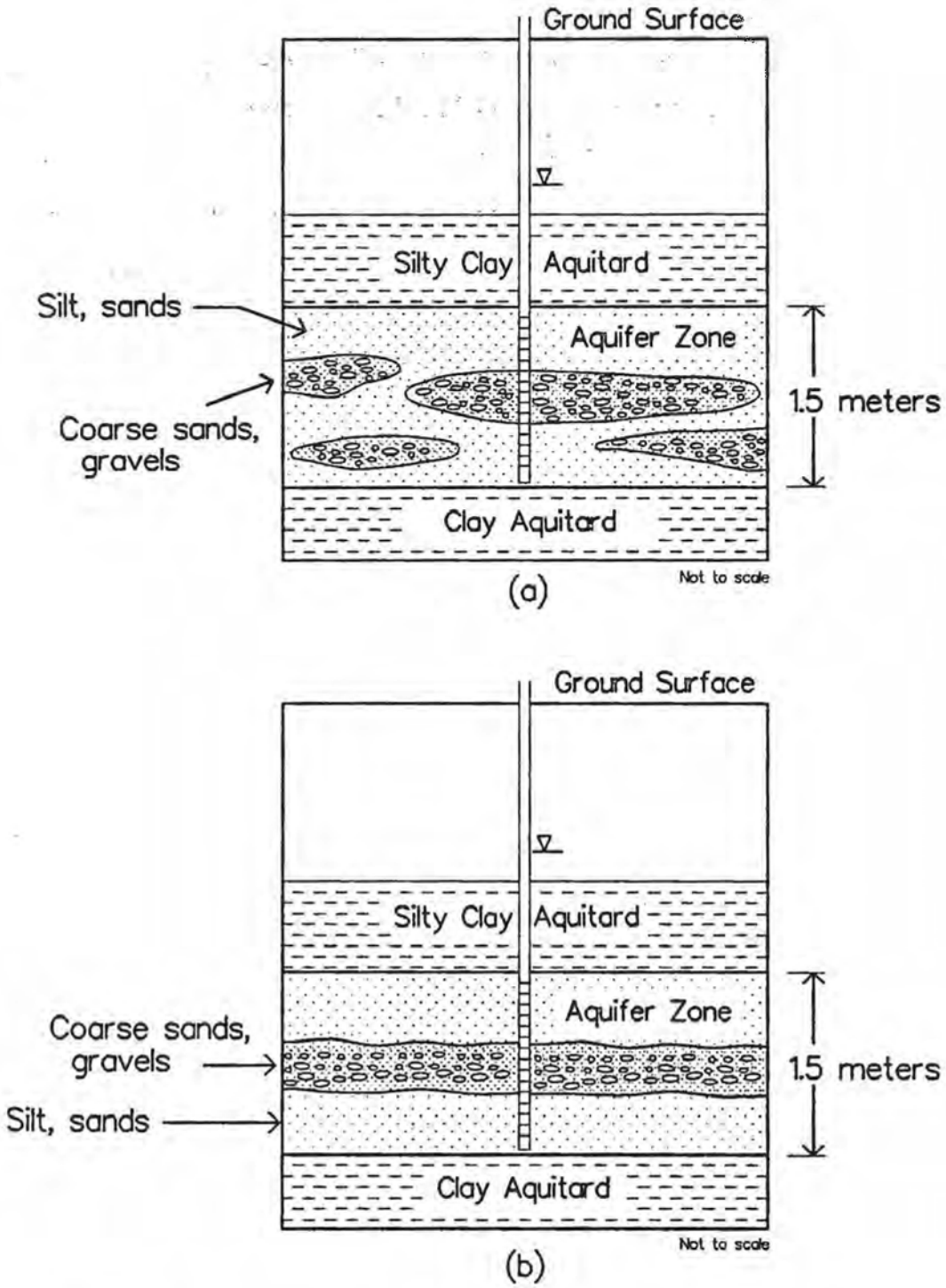

Figure 5.11-1: A conceptual Plant Science Farm aquifer model (two hypothetical cross-sections).

In summary, observations made during monitoring well installation are insufficient for a complete description of the aquifer sediment depositional environment. A conceptual aquifer model was developed from observations made during well construction and from knowledge of local geology. This conceptual model provided a context for designing hydraulic tests (Chapter 5) and tracer experiments (Chapter 7), and for interpreting results from the hydraulic tests (Chapter 5) and tracer experiments (Chapter 8).

6. Aquifer Tests

6.1 Introduction

Three multiple well aquifer tests were conducted during the course of this investigation. The purpose of aquifer tests was to estimate averaged subsurface hydraulic parameter values (i.e., aquifer transmissivity and storativity) along transects where tracer tests were conducted.

This chapter presents a description of three aquifer tests and an analysis of aquifer tests results. Aquifer test design considerations are discussed in Section 6.2. Field methods are described in Section 6.3, and aquifer test drawdown data are provided in Section 6.4. Techniques for analyzing drawdown data are in Section 6.5, and Section 6.6 provides an analysis of drawdown and recovery data. Finally, aquifer test results are summarized in Section 6.7.

6.2 Aquifer Test Design Considerations

Aquifer tests were designed and conducted on the basis of the experimental design and the conceptual field site aquifer model. A review of design considerations leading to the aquifer tests is provided here. Design components include the type of aquifer test (single or multiple well), the aquifer test configuration (selection of pumping wells, pumping rates, etc.), and a monitoring system.

Two general types of aquifer tests are commonly conducted. Multiple well tests yield parameter measurements representing hydraulic properties over an averaged aquifer area. Single well techniques are used to estimate hydraulic properties in the borehole vicinity. Multiple well tests were selected to obtain averaged hydraulic parameter estimates along Cluster 1 transects (along which tracer tests were conducted).

Wells MW-5, MW-24, and MW-25 were selected as aquifer test pumping wells. By design, 5-cm wells (sufficient diameter for a *Grundfos* submersible pump) were located at the end of each transect for this purpose. An aquifer test was not conducted in MW-15 because of time constraints.

Pumping rates were selected on the basis of general observations made during well development and several preliminary aquifer tests. An important criterion for selecting the pumping rate was that the water levels at the pumping well not drop below the top of the aquifer. The aquifer tests were designed to proceed until a sufficient number of data were collected to estimate aquifer parameters. Each test ended prematurely because of pump failure (see next section).

Drawdown was monitored in the wells closest to the pumping well. The purpose in monitoring the closest wells (as opposed to more distant wells) was to gain estimates of hydraulic parameters on an intermediate scale (meters) over the same areas in which tracer tests were conducted.

6.3 Field Methods for Multiple Well Aquifer Tests

This section presents a detailed description of the multiple well aquifer test methods and equipment used for this project. The aquifer test configuration was developed within the design considerations outlined in the previous section.

A schematic of the aquifer test apparatus used in aquifer tests M1, M2, and M3 is shown in Figure 6.3-1. Pumping test equipment components consisted of a pump and controller, a water level monitoring system, and water quality monitoring system.

The pumping tests were conducted with a *Grundfos Redi-flow 2* submersible pump and controller. The controller controls the voltage driving the submersible pump. This pump was selected because it fits into a 5-cm-diameter well, is theoretically capable of pumping at a steady rate over an extended period of time, and is capable of pumping within the desired range of discharge rates.

Pumps for aquifer tests M1 through M2 were powered by a portable *Honda* generator. Electrical cable was extended to the site following aquifer test M2; all subsequent aquifer and tracer tests were powered by on-site electricity.

The pump was equipped with 61 m of 1.3-cm-diameter Teflon tubing. A 0.32-cm-diameter copper tube was added to the pump discharge to create back pressure, which helped ensure a constant flow rate. The discharge rate was measured at the discharge point with a graduated 1-liter cylinder and a stopwatch. Back pressure in the

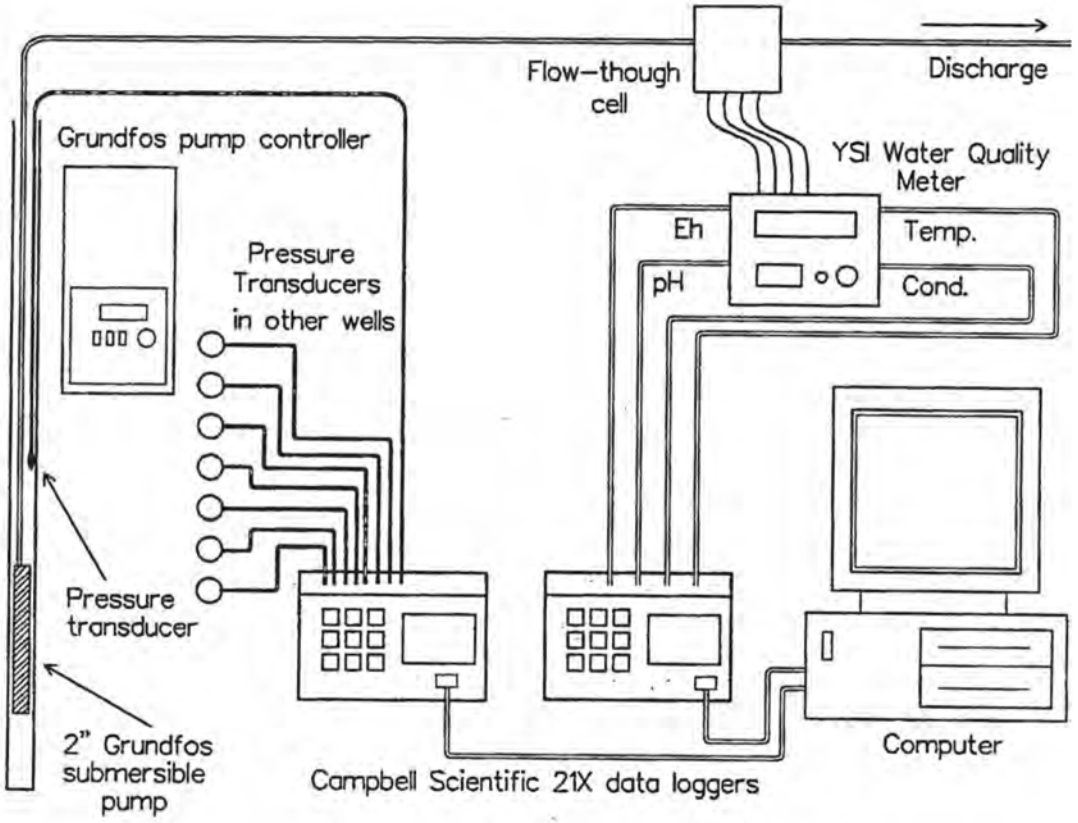

Figure 6.3-1: Schematic of aquifer test apparatus.

discharge line was monitored periodically (since back pressure correlates with the discharge rate); the pump controller voltage was adjusted as necessary to maintain a constant discharge rate. Discharge rates and back pressure readings are given in Table 6.3-1.

All three aquifer tests ended when the *Redi-flow* pump stopped functioning. The reason for pump failure was unclear. In retrospect, the recirculating jet pump system (used for subsequent tracer tests — see Chapter 7) would have allowed longer pumping times.

Water level monitoring components consisted of pressure transducers, a data recorder, an on-site data computer, and electric water level indicator probes. These components are described in the following paragraphs.

Water levels were monitored during each pumping test with one *Druck* 3.5 N/cm^2 (5-p.s.i.) and six or seven *Druck* 13.8 N/cm^2 (20-p.s.i.) pressure transducers. Transducers were calibrated in a laboratory water column before field use. Pressure transducers were installed in the wells closest to the pumping wells to allow frequent monitoring in wells in which the rate of water level change would be greatest. Table 6.3-2 lists the wells monitored with transducers during aquifer tests M1, M2, and M3.

Unused transducer cable was kept in the shade of the instrumentation trailer to reduce solar heating. In addition, exposed transducer cable was shielded with white 1.9-cm PCV pipe. The effects of solar heating on transducers was considered negligible because of these measures and because of moderate weather conditions during aquifer tests.

Pressure transducer data were collected in a *Campbell Scientific 21X* (8-channel) data recorder. The recording frequency was limited by available memory in the data recorder. As a compromise between recording frequency and data storage, the transducer readings were recorded every 10 minutes or at every 1-cm fluid level change in the pumping well (whichever was less). Recorder data were periodically downloaded into an on-site computer. The data recorder and computer were housed in an on-site instrumentation trailer.

Aquifer Test M1 Date: 11/12/92 Start time: 10:06 A.M. Weather: mild, overcast, rain				Aquifer Test M2 Date: 11/21/92 Start Time: 11:30 A.M. Weather: cool, rain and snow				Aquifer Test M3 Date: 5/27/93 Start Time: 10:30 A.M. Weather: warm, partly cloudy			
Time (min)	Back Pressure (N/cm^2)	Freq.* (Hz)	Rate (ml/min)	Time (min)	Back Pressure (N/cm^2)	Freq.* (Hz)	Rate (ml/min)	Time (min)	Back Pressure (N/cm^2)	Freq.* (Hz)	Rate (ml/min)
0	55.2	270	1172	0	56.58	270	955	2.4	49.7	282	1340
186	55.2	269		17	56.58	270	952	37.3	49.7	280	1300
212	55.2	270		28	56.58	270	968	65	49.7	281	1316
281	55.2	270		62	56.58			105	49.7	281	
326	55.2	269		539	56.58			213	49.7	281	1316
412	55.2	271		174	56.58			343	49.7	281	1310
470	55.2	269		315	56.58			635	19.3**	282	740
541	55.2	270		607	56.58						
616	55.2	270		704	56.58	270	1034				
725	55.2	270									
805	55.2	270	1188								

* Pump controller frequency

** Pump failed after approximately 600 minutes.

Table 6.3-1: Aquifer test details for M1, M2, and M3.

Test	Date	Pumping Well	Pumping Duration (ml)	Pumping Rate (ml/min)	Transducer Wells / Hand-Measured Wells*
M1	11/12/92	MW-5	775	1170	MW-5, MW-12, MW-13, MW-14, MW-16, MW-17, MW-18, MW-19 / MW-4, MW-6, MW-15, MW-20, MW-21, MW-22, MW-23, MW-25
M2	11/21/92	MW-25	1222	958	MW-12, MW-13, MW-14, MW-19, MW-20, MW-21, MW-25 / MW-6, MW-15, MW-16, MW-17, MW-18, MW-22, MW-23, MW-24
M3	5/27/93	MW-24	600	1320	MW-5, MW-16, MW-17, MW-18, MW-19, MW-22, MW-23, MW-24 / MW-12, MW-13, MW-14, MW-20, MW-21, MW-25, MW-26, MW-27, MW-28

* Denotes wells monitored with pressure transducers or measured by hand using an *Solinst* electrical tape.

Table 6.3-2: Multiple well aquifer test (M1, M2, and M3) summary.

Hand measurements were taken with *Solinst* water level indicator probes in monitoring wells not equipped with transducers. The number of wells monitored with indicator probes was limited by the number of available indicator probes and field assistants.

Water level monitoring focused on wells nearest the pumping well; the frequency of measurement was decreased during the first hour of each aquifer test as the rate of drawdown decreased. Water level measurements were then taken with available indicator probes in several more distant wells. Water level data from the more distant wells are of limited use to aquifer test analysis (since early drawdown data were missed) but were taken to provide an indication of drawdowns at more distant locations.

A *YSI* water quality meter (model 3500) connected to the pumping well discharge line was used to monitor pH, temperature, redox potential, and electrical conductivity. Water quality data from aquifer tests M1, M2, and M3 are presented in Section 6.4.

6.4 Aquifer Test Results

This section provides a summary of drawdown data taken during aquifer tests M1, M2, and M3. An analysis of aquifer test data is presented in the next section.

Table 6.4-1 provides a data summary for aquifer tests M1, M2, and M3. The data summary includes the first water level reading time (after the pumping test began) and the total number of data points for each well for each test. These data are provided as an indicator of reliability for subsequent parameter estimates. In general, water level readings were made sooner (after pumping began) and with greater frequency in wells monitored with the pressure transducer and data recorder equipment.

Drawdown curves for aquifer tests M1, M2, and M3 are provided in Figures 6.4-1 through 6.4-3. Drawdown curves are separated (for the sake of illustration) by arbitrarily assigning a different datum elevation to each well. The pumping well for each test is given the lowest datum. The pumping well drawdown patterns are an indication of discharge consistency. Variability in pumping well drawdown (e.g., M3, well MW-24, at approximately 350 minutes) was probably caused by minor fluctuations in pump discharge.

Table 6.4-2 presents aquifer thickness details for the pumping wells in pumping tests M1, M2, and M3. Data in Table 6.4-2 indicate that the aquifer remained fully saturated at all times throughout the aquifer test.

Periodic water quality readings taken during the aquifer tests with a *YSI* Water Quality meter are shown in Table 6.4-3. The purpose of these readings was to collect background water quality data in preparation for tracer tests.

Table 6.4-3 shows that pH is remains fairly constant throughout each test. Temperature differences between tests reflect differences in ambient air temperature, because discharge water traveled through approximately 61 m of 1.9-cm-diameter

	Aquifer Test M1			Aquifer Test M2			Aquifer Test M3		
Well	Method	First Point (min)	Total Points	Method	First Point (min)	Total Points	Method	First Point (min)	Total Points
MW-4	e-tape	47.67	12						
MW-5	trans*	0.02*	139*				trans	0.03	87
MW-6	e-tape	57	14	e-tape	1.63	58			
MW-9							e-tape	7.6	18
MW-10							e-tape	43	6
MW-11							e-tape	6.53	18
MW-12	trans	0.02	139	trans	0.14	994	e-tape	10.5	12
MW-13	trans	0.02	139	trans	1.08	992	e-tape	12.17	11
MW-14	trans	0.1	137	trans	0.4	998	e-tape	12.67	11
MW-15	e-tape	16.65	17	e-tape	31.5	8			
MW-16	trans	0.02	139	e-tape	110	7	trans	0.03	87
MW-17	trans	0.15	138	e-tape	0.43	29	trans	0.4	86
MW-18	trans	0.02	139	e-tape	2.42	27	trans	0.4	86
MW-19	trans	0.02	139	trans	0.4	998	trans	0.8	85
MW-20	e-tape	1	36	trans	0.4	987	e-tape	5.13	18
MW-21	e-tape	2.45	36	trans	0.4	987	e-tape	7.32	18
MW-22	e-tape	2.1.	40	e-tape	3.2	26	trans	0.03	87
MW-23	e-tape	2.67	38	e-tape	6.5	23	trans	0.03	87
MW-24				e-tape	115	7	trans*	0.03*	87*
MW-25	e-tape	9.4	20	trans*	0.04*	987*	e-tape	7.6	18

Notes: (1) "e-tape" indicates a *Solinst* water level indicator probe; "trans" indicates measurements taken by *Druck* pressure transducer and data recorder. (2) Aquifer test durations are provided in Table 6.3.3-1. "*" denotes pumping wells.

Table 6.4-1: Aquifer test data summary.

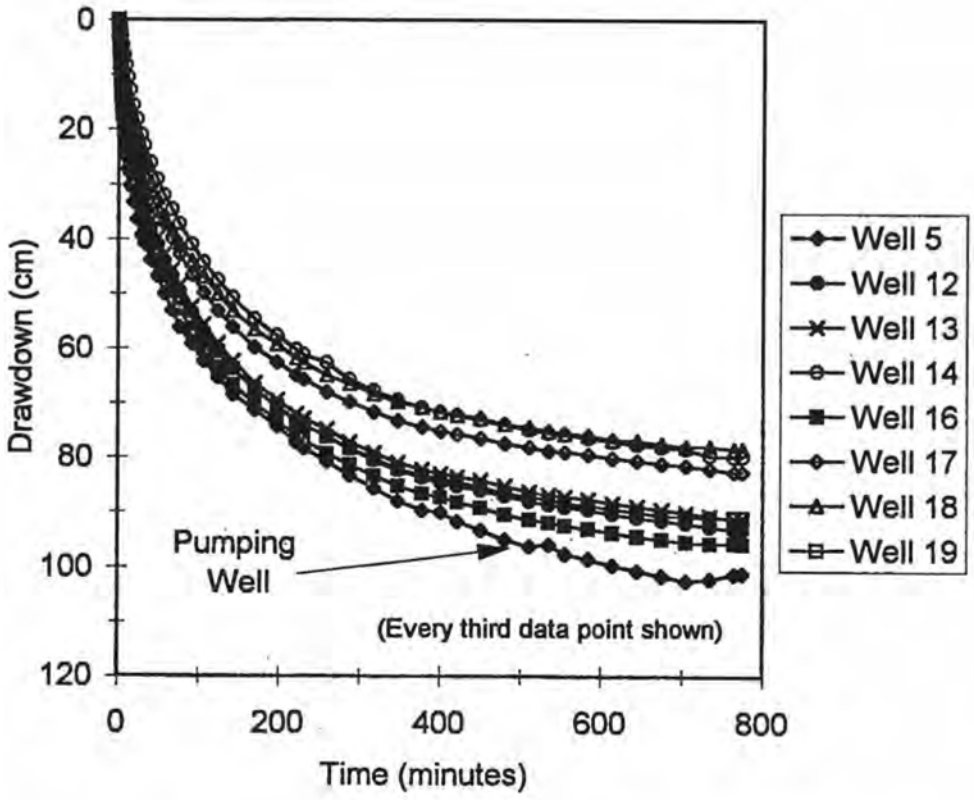

Figure 6.4-1: Aquifer test M1 drawdown curves (transducer-monitored wells only).

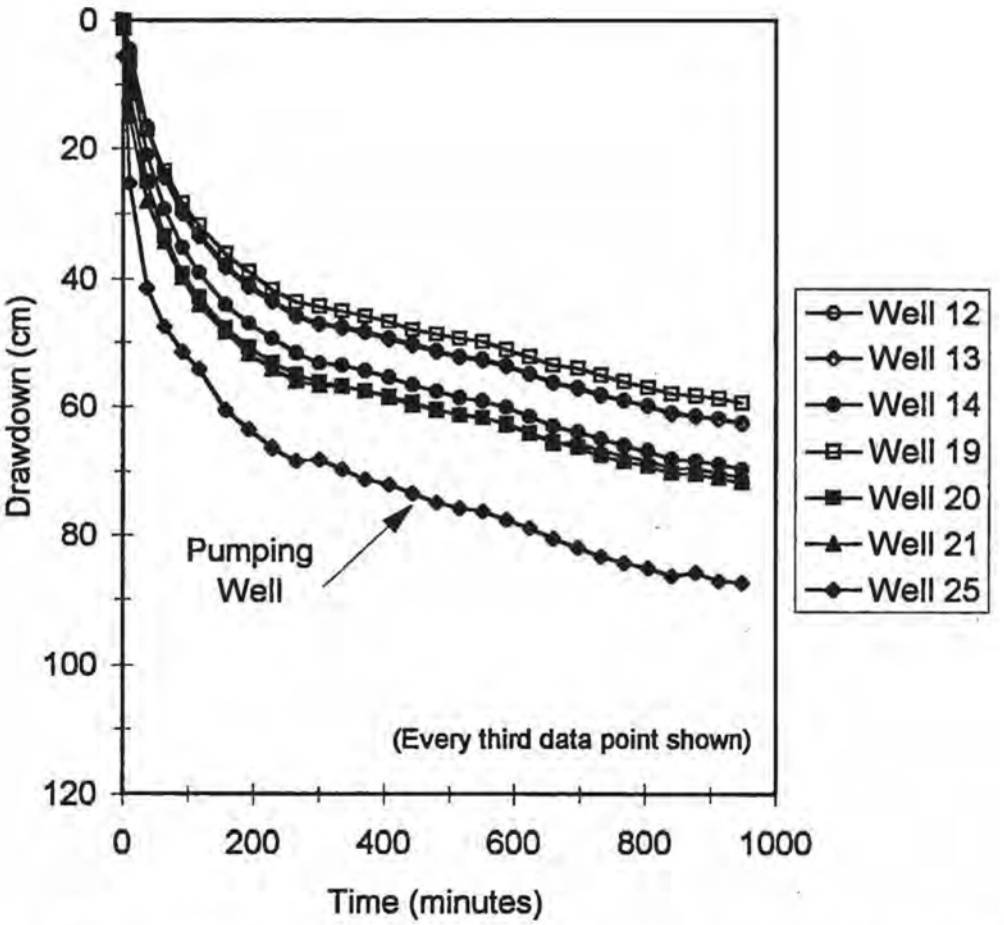

Figure 6.4-2: Aquifer test M2 drawdown curves (transducer-monitored wells only).

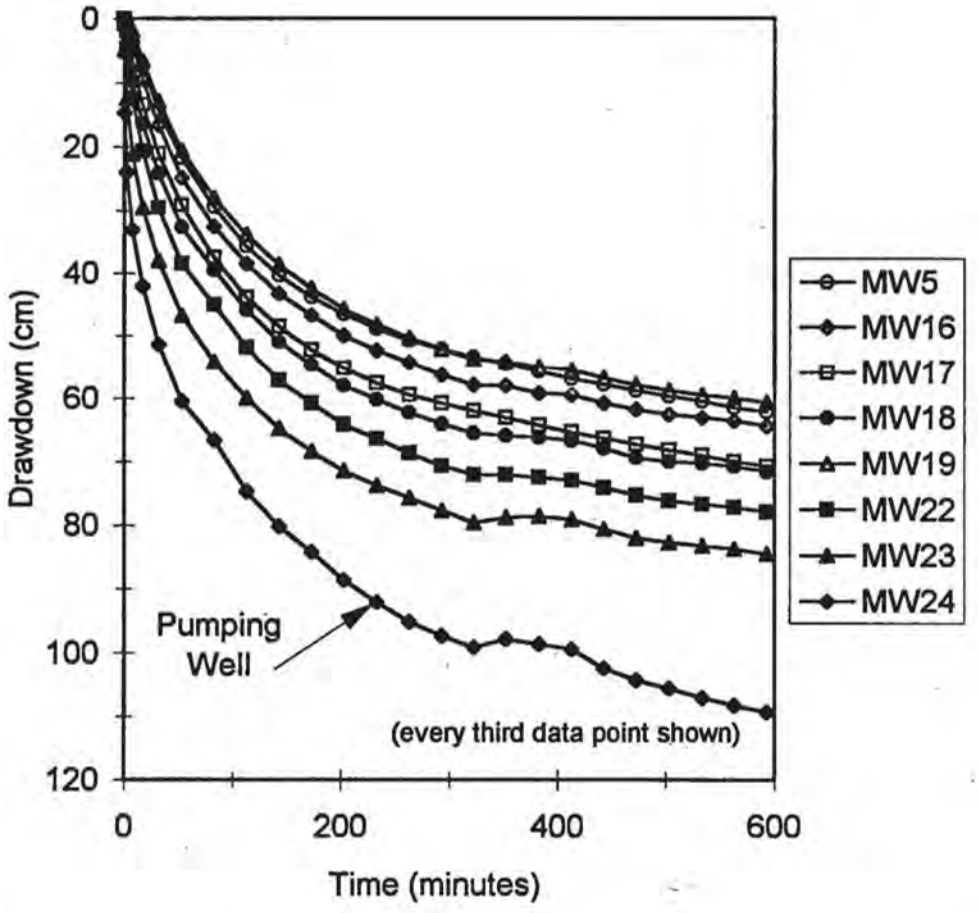

Figure 6.4-3: Aquifer test M3 drawdown curves (transducer-monitored wells only).

Pumping Well	MW-5	MW-24	MW-25
Aquifer Test	M1	M3	M2
Initial water level (m)	790.10	790.29	790.27
Minimum water level during aquifer test (m)	789.08	789.19	789.39
Estimated upper aquifer boundary elevation	787.9	787.9	787.9

Table 6.4-2: Comparison of initial and minimum water level elevations (in meters above M.S.L.) of the pumping wells in aquifer tests M1, M2, and M3, and for MW-19.

Aquifer Test M1				
Time (min)	**pH**	**Temp (°C)**	**Conductivity (µS)**	**Eh (mV)**
64	7.01	11.9	248	-22
70	7.01	11.8	135	-56
96	6.92	12.4	104	-101
122	6.9	12.5	120	-114
191	6.82	12	253	-116
236	6.8	13	256	-120
Aquifer Test M2				
Time (min)	**pH**	**Temp (°C)**	**Conductivity (µS)**	**Eh**
62	7.12	6.5	216	56
174	6.93	6.7	163	35
315	7.02	6.5	275	14
405	6.97	7.7	260	12
539	6.98	7.2	155	19
607	6.98	7.6	140	22
712	6.93	12.3	190	31
Aquifer Test M3				
Time (min)	**pH**	**Temp (°C)**	**Conductivity (µS)**	**Eh**
37	6.43	15.5	277	-9
40	6.43	15.2	277	-9
67	6.38	15.9	278	-27
212	6.38	15.9	277	-106
216	6.41	16.1	279	-108
336	6.39	15.7	276	-89

Table 6.4-3: Water quality data for aquifer tests M1, M2, and M3.

Teflon tubing before reaching the *YSI* meter. Conductivity values range from approximately 104 to 280 μS.

Redox potential decreased with time during M1 and M3, and decreased slightly during M2. High Eh values are usually associated with dissolved oxygen in water, such as near a recharge zone (Fetter, 1994). Ground water flow systems have a tendency toward oxygen depletion and reducing conditions (Freeze and Cherry, 1979), because of hydrochemical and/or biochemical reactions that consume oxygen. The initial redox potential observed in these aquifer tests may be influenced by oxygenation through an open well, but the decreasing redox potential with extended pumping (in two of the pumping tests) appears to indicate minimal localized recharge to the aquifer.

Minimal local recharge (indicated by decreasing redox potential during extended pumping) is consistent with a confined aquifer conceptual model. Negative redox potential values indicate a minimal amount of aquitard leakage (if any) in at least two of the aquifer tests.

Redox potential data from aquifer test M2 appear inconsistent with redox potential data collected during aquifer tests M1 and M3. Reasons for the discrepancy could include aquitard leakage near the pumping well (MW-24) of aquifer test M2 or residual oxygenation due to well installation or development. It is hypothesized that if aquitard leakage were contributing to elevated redox values in the Cluster 1 area, the effects of this leakage would have been more apparent in redox values observed during aquifer tests M1 and M3 (given the proximity of aquifer test M1, M2, and M3 pumping wells). Thus, it may be more likely that elevated redox values in aquifer test M2 were due to well oxygenation or some other anomaly.

6.5 Aquifer Test Analysis Methods

The purpose of the aquifer tests was to estimate hydraulic parameter values (transmissivity and storativity) over the areas in which tracer tests would be conducted (Cluster 1 wells). Numerous methods and techniques are available for analyzing aquifer test drawdown data that yield hydraulic parameter estimates. This section presents a

discussion of applicable aquifer test analysis methods. Aquifer test results are analyzed in the next section.

Aquifer test analysis methods include numerical and analytical techniques. Numerical techniques may lead to non-unique solutions (and therefore erroneous parameter estimates) when multiple parameters are unknown (as is the case for this project). Analytical techniques are limited by assumptions regarding specific geological conditions and well construction, but are frequently used for estimating transmissivity and storativity from aquifer test data. The aquifer test analysis for this project is limited to analytical techniques.

Several analytical solutions were considered for analyzing aquifer test drawdown data. These include solutions for drawdown in (1) confined, unconsolidated aquifers, (2) unconfined, unconsolidated aquifers, (3) "leaky" aquifers (with and without aquitard storage), and (4) aquifers with partially penetrating wells. In particular, solutions by Theis (1935), Cooper and Jacob (1946), Neuman (1975), Hantush and Jacob (1955), Hantush (1960), Neuman and Witherspoon, (1969 and 1972), Hantush (1961a, b), Weeks (1969), and Papadopoulos and Cooper (1967) were considered.

Some of these analytical solutions can be solved with a curve-matching procedure using observed drawdown data and a specific "type curve." Drawdown data may match multiple type curves. Interpretation lies in (1) choosing the proper hydrogeologic model and appropriate analytical technique on the basis of site conditions, (2) analyzing differences between measured drawdown curves and a theoretical expectation, and (3) considering deviations between site conditions and method assumptions.

The Theis (1935) and Cooper and Jacob (1946) solutions are applicable to confined, unconsolidated, homogeneous, isotropic aquifers of uniform thickness and infinite areal extent. Additional assumptions include fully penetrating pumping and observation wells, a uniform, horizontal potentiometric surface prior to pumping, an infinitesimally small well diameter, and a constant pumping rate. Both solutions can be used to evaluate drawdown and recovery data in observation wells, and the Cooper and Jacob method (1946) can be used to evaluate pumping well data (Fetter, 1994).

Storativity cannot be determined with pumping well data because of borehole and casing storage and possible non-laminar flow conditions.

The field site aquifer is not homogenous nor of infinite areal extent, although it may be "homogeneously heterogeneous" at some scale. Most of the Cluster 1 wells are fully penetrating, with the exception of six wells (Table 5.5-2). The initial potentiometric surface was not completely uniform nor horizontal prior to beginning each test, although the initial gradient was considered negligible with respect to the pump-induced gradient. The long-term pumping rate was relatively uniform during each aquifer test, with the exception of the initial time taken to pressurize the Teflon discharge line (Section 6.6).

The method developed by Neuman (1975) for unsteady flow in an unconfined aquifer may be applicable to the field site aquifer if water levels fall below the top of the aquifer during the course of the pumping test. Water level data taken in the pumping wells indicate that water levels did not drop below the top of the aquifer zone (Table 6.4-2). The Neuman solution was therefore not considered applicable for this analysis.

The Plant Science Farm aquifer is clearly confined, since water levels rise in boreholes upon penetrating this zone. However, varying amounts of silt and/or fine sand in the aquitard overlying the aquifer may allow leakage through the upper aquitard. After periods of extended pumping, water may also be released from storage in the upper aquitard. Negligible leakage, if any, is thought to occur through the underlying thick, stiff clay.

Analytical solutions that apply to semi-confined, or "leaky," aquifers were considered because of possible leakage from the upper aquitard. The Hantush and Jacob (1955) method is based on the same conditions as the Theis method (1935), except that leakage occurs through an overlying or underlying aquitard of infinite areal extent, uniform vertical hydraulic conductivity, vertical flow, and uniform thickness. Use of the solution also implies that the aquitard is overlain or underlain by an infinite, constant head plane source, and that water is derived from storage in the aquitard. An overlying constant head source from which leakage occurs is not apparent at the site.

The clay zone underlying the aquifer is believed to be continuous throughout the field site area. Little is known about deeper sedimentary aquifers at the site.

Hantush (1960) developed a solution for flow to a well in a semi-confined aquifer that accounts for water released from aquitard storage. The solution is valid as long as drawdown does not occur in an overlying or underlying source aquifer. The Hantush type curves become the Theis curve for the case where no leakage occurs ($\beta = 0$).

Additional methods exist for analyzing leaky aquifer systems (Neuman and Witherspoon, 1969 and 1972). These require aquifer and aquitard drawdown data; no aquitard water levels were obtained during these aquifer tests.

Several monitoring wells in the Cluster 1 area were installed, by design, as partially penetrating wells (MW-17, MW-18, MW-20, MW-21, MW-22, and MW-23; see Table 5.5-2). Hantush (1961a,b) developed solutions for correcting the effects of partially penetrating wells in confined or semi-confined aquifers. Weeks (1969) also developed several methods for evaluating horizontal to vertical permeability based on data collected from observations wells near a partially penetrating pumping well. These methods may be applicable for data from the partially penetrating wells.

Of the available solutions, the Theis (1935), Cooper and Jacob (1946), and Hantush (1960) analytical solutions appeared to fit the field site aquifer conceptual model. Partial penetration methods also appeared applicable for partially penetrating wells. The Theis (1935) and Cooper and Jacob (1946) methods represent solutions to the same equation, and generally give comparable results. However, the Cooper and Jacob solution is only valid for small values of u, i.e., large values of time and/or small distances between the pumping and observation wells. The Theis (1935) and the Hantush (1960) solutions were therefore selected for an initial analysis of drawdown data in observation wells. These two solutions may apply to the field site aquifer if the aquifer is confined and non-leaky, or confined and leaky. Application of the Hantush (1960) method to drawdown in a confined, non-leaky aquifer yields the same solution as the Theis (1935) method.

Recovery data from selected wells were also analyzed. The purpose of conducting an analysis of recovery data was to provide an independent check on results of the drawdown data analysis. The Theis (1935) and Cooper and Jacob (1946) methods can be used for estimating transmissivity from recovery data. The Cooper and Jacob method for recovery analysis was used because it is included in the *AQTESOLV* package (Duffield and Rumbaugh, 1989) for recovery analysis. The same assumptions listed earlier for these methods apply here.

Two methods were used to estimate transmissivity values from pumping well drawdown data: the Cooper and Jacob (1946) and Papadopoulos and Cooper (1967) methods. Neither of these methods provides an estimate of storativity because of borehole storage in the pumping well and non-laminar flow conditions. The Papadopoulos and Cooper (1967) method was chosen for this project because the method takes into account borehole storage in the pumping well.

6.6 Aquifer Test Analysis using the Theis (1935) Solution

This section begins an analysis of data collected during multiple well aquifer tests M1, M2, and M3. An analysis of drawdown data using the Theis (1935) method is presented in this section. An analysis using the Hantush (1960) method is presented in Section 6.7. Recovery and pumping well data were evaluated with the Cooper and Jacob (1946) and Papadopoulos and Cooper (1967) methods, respectively (Section 6.8). The *AQTESOLV* (Duffield and Rumbaugh, 1989) aquifer test analysis software is used for the curve match solutions.

Drawdown data taken from fully penetrating wells during aquifer tests M1, M2, and M3 were first compared to the Theis "type" curves using the AQTESOLV software. Data matches are provided in Appendix F.

Drawdown data were selected from one well to illustrate drawdown patterns observed in other wells. Drawdown data from MW-19 are used in the following discussion as examples of curve match characteristics. Monitoring well MW-19 is the only non-pumping well in which water level readings were collected by transducer and data recorder during all three aquifer tests (transducer-equipped wells resulted in a

larger number of readings at earlier times than hand-measured wells). MW-19 is a fully penetrating, 1.9-cm-diameter well located in Transect B. Additional details for MW-19 are shown in Table 6.6-1.

	M1	M2	M3
Pumping well	MW-5	MW-25	MW-24
Pumping rate (ml/min)	1170	1034	1320
Distance to pumping well (cm)	217	410	834
Screen length (cm)	152	152	152
Approximate aquifer thickness at pumping well (cm)*	210**	150	150
Approximate aquifer thickness at MW-19 (cm)*	160	160	160

* Aquifer thicknesses are approximate since the transition between the aquifer and the overlying aquitard is indistinct.

** The MW-5 well screen does not span the entire aquifer thickness, but is considered to be a fully penetrating well because it is completed in the coarsest of aquifer materials.

Table 6.6-1: Aquifer test details for MW-19

Four general observations can be made from the drawdown data and Theis curve plots. First, the entire drawdown data set could not be matched to the Theis curve. Second, the greatest number of drawdown data points could be matched to the Theis curve (as illustrated in Figures 6.6-1 through 6.6-3) with a match from approximately 10 to 300 minutes (referred to hereafter as a "mid-time" match). Drawdown data collected at times less than 10 minutes typically fell above the Theis expectation with a mid-time match. Third, drawdown data appear to deviate from the Theis expectation after approximately 300 minutes with a mid-time match. This deviation can be observed in Figures 6.6-1 through 6.6-3. Fourth, drawdown data generally were also matched to the Theis curve (Figures 6.6-4 through 6.6-6) from times between approximately 0.3 minutes to approximately 5 minutes (referred to hereafter as an "early-time" match).

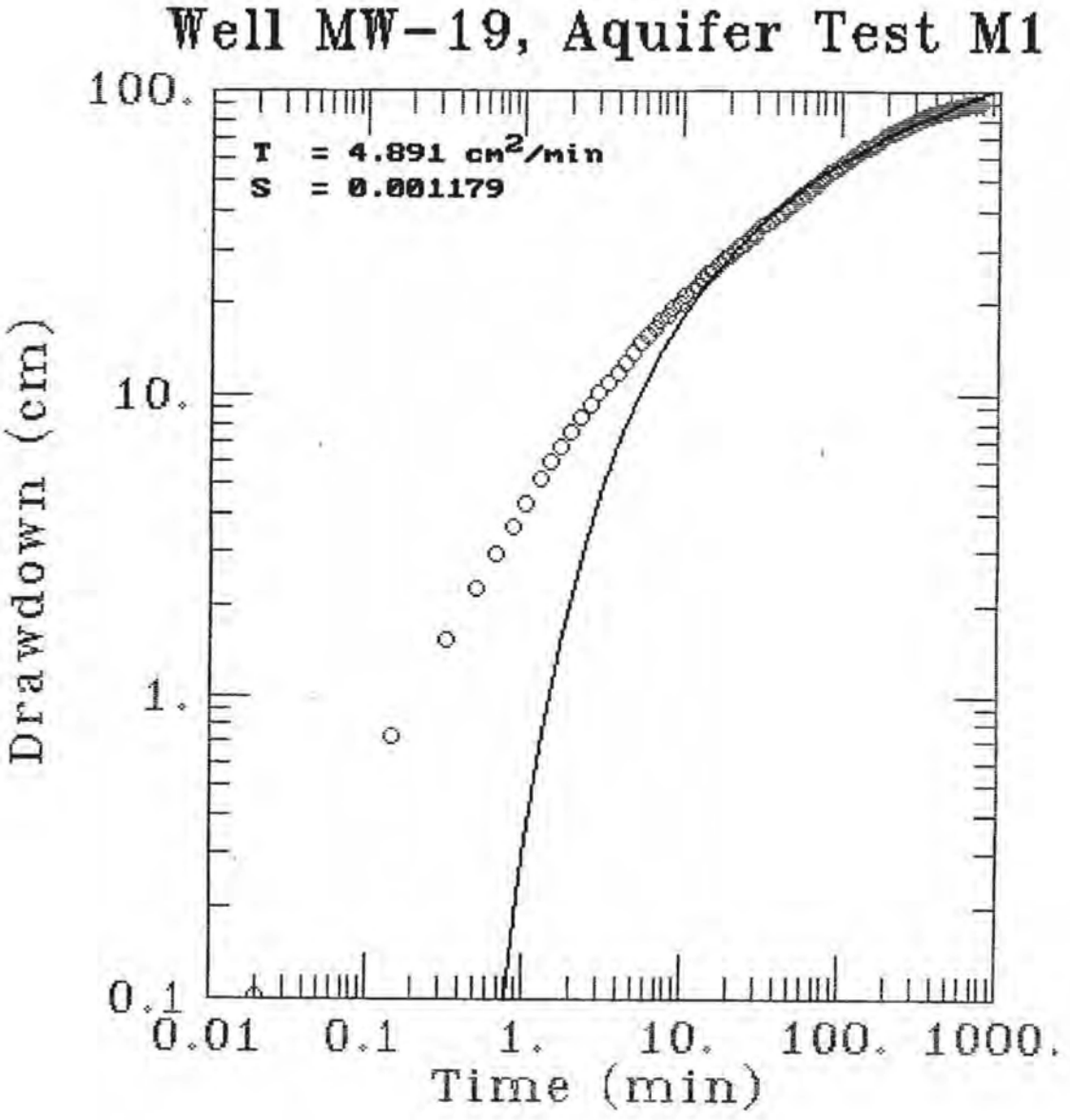

Figure 6.6-1: Mid-time drawdown/Theis curve match for MW-19, aquifer test M1.

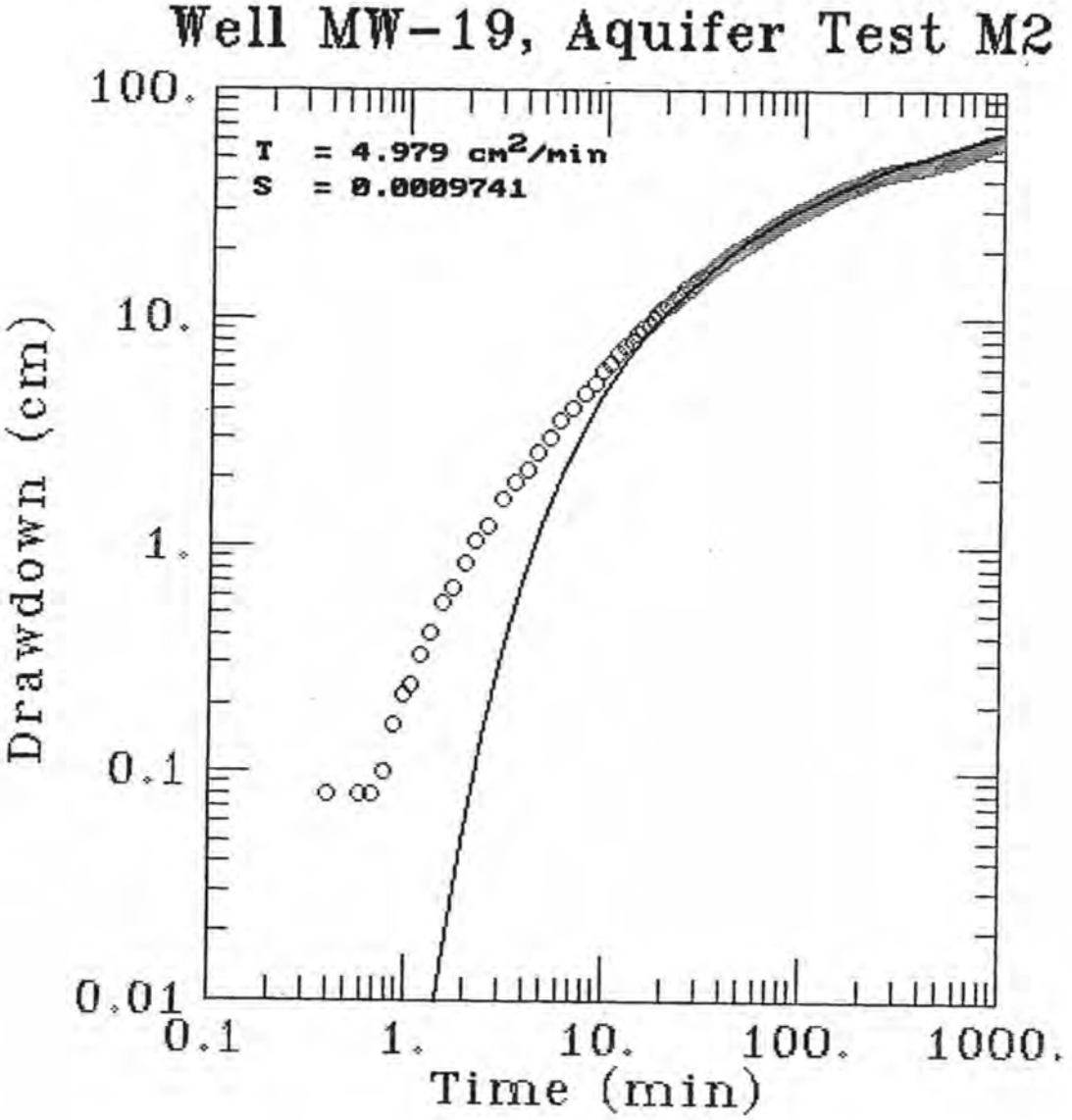

Figure 6.6-2: Mid-time drawdown/Theis curve match for MW-19, aquifer test M2.

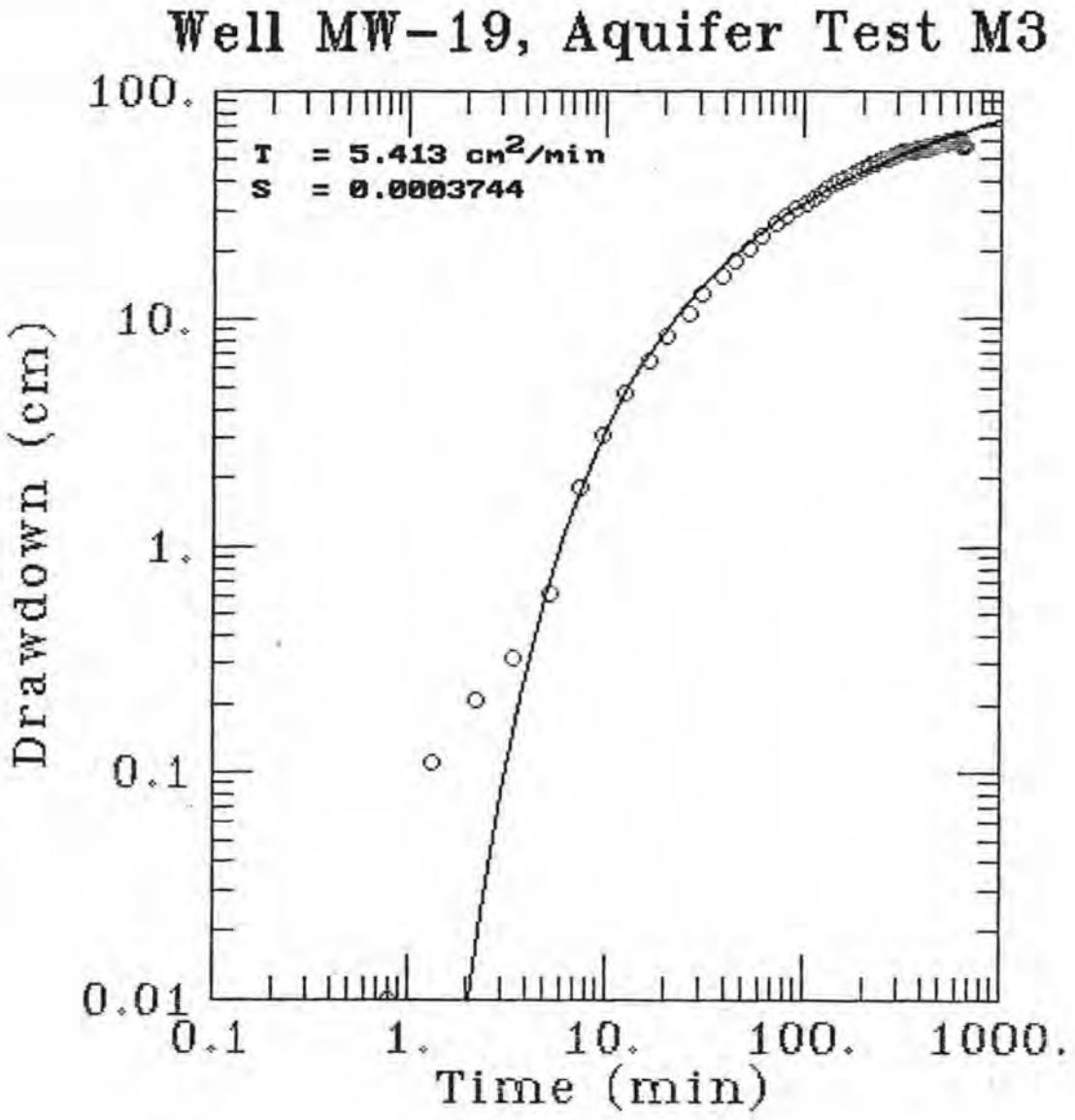

Figure 6.6-3: Mid-time drawdown/Theis curve match for MW-19, aquifer test M3.

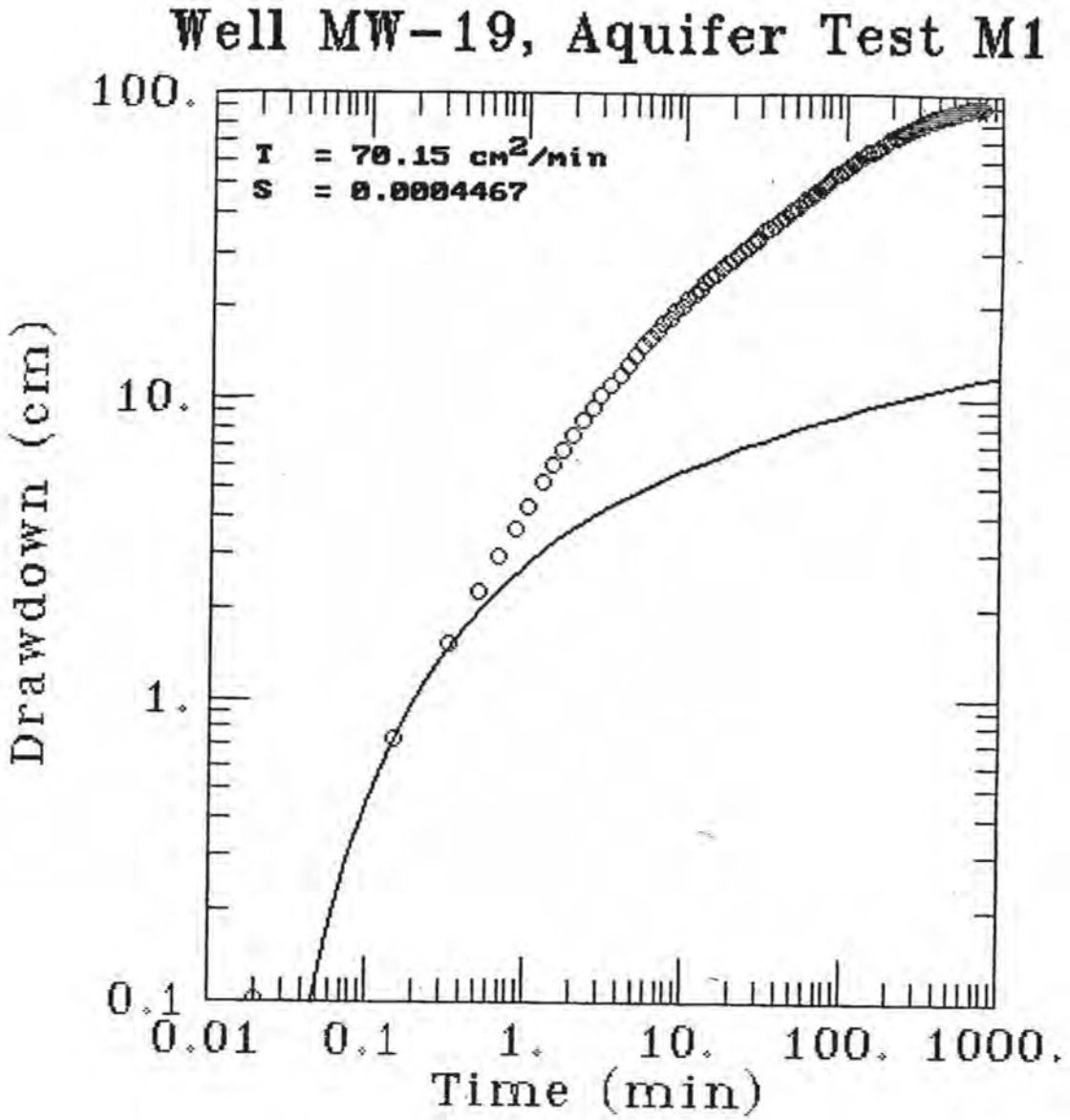

Figure 6.6-4: Early-time drawdown/Theis curve match for MW-19, aquifer test M1.

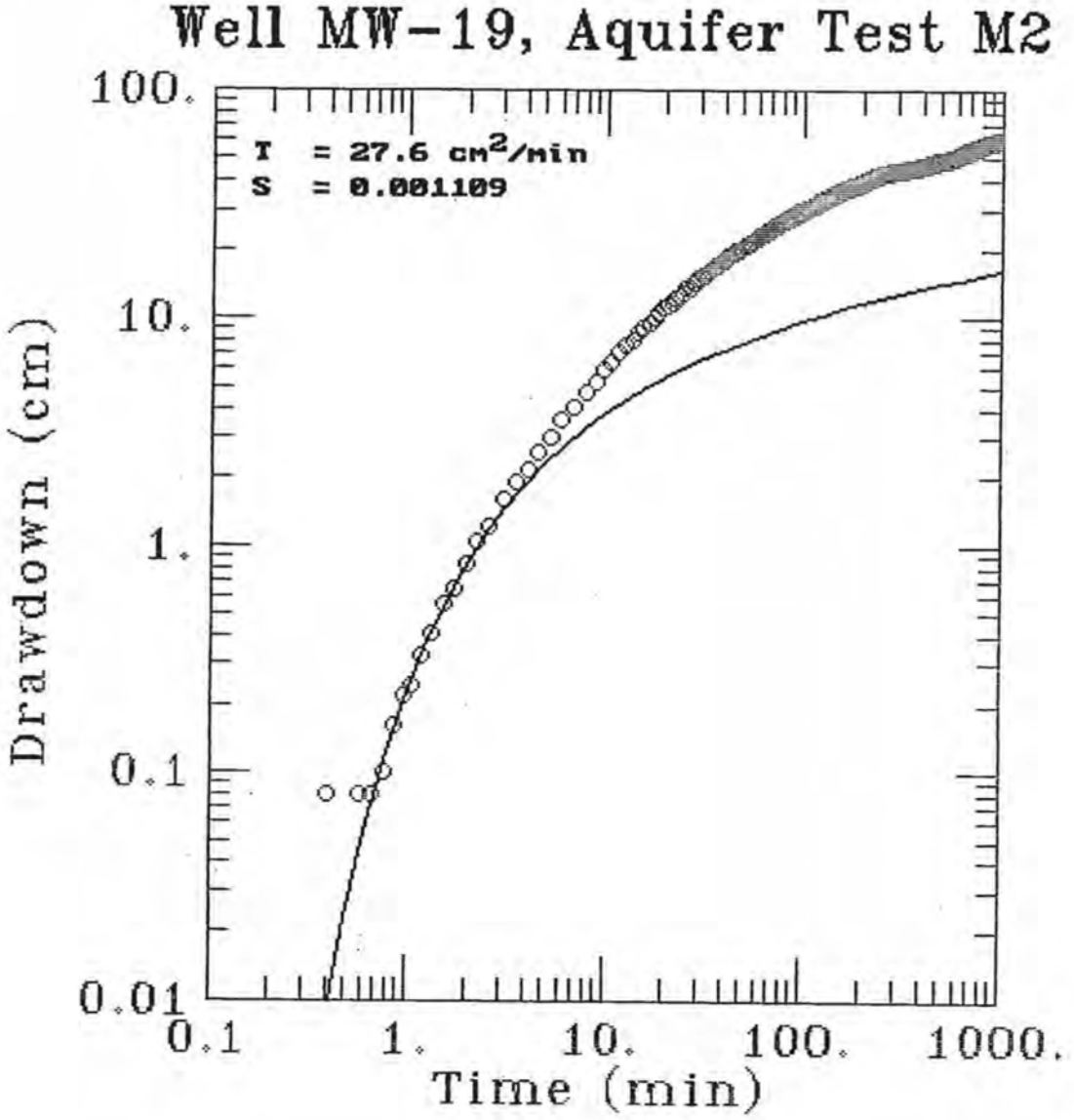

Figure 6.6-5: Early-time drawdown/Theis curve match for MW-19, aquifer test M2.

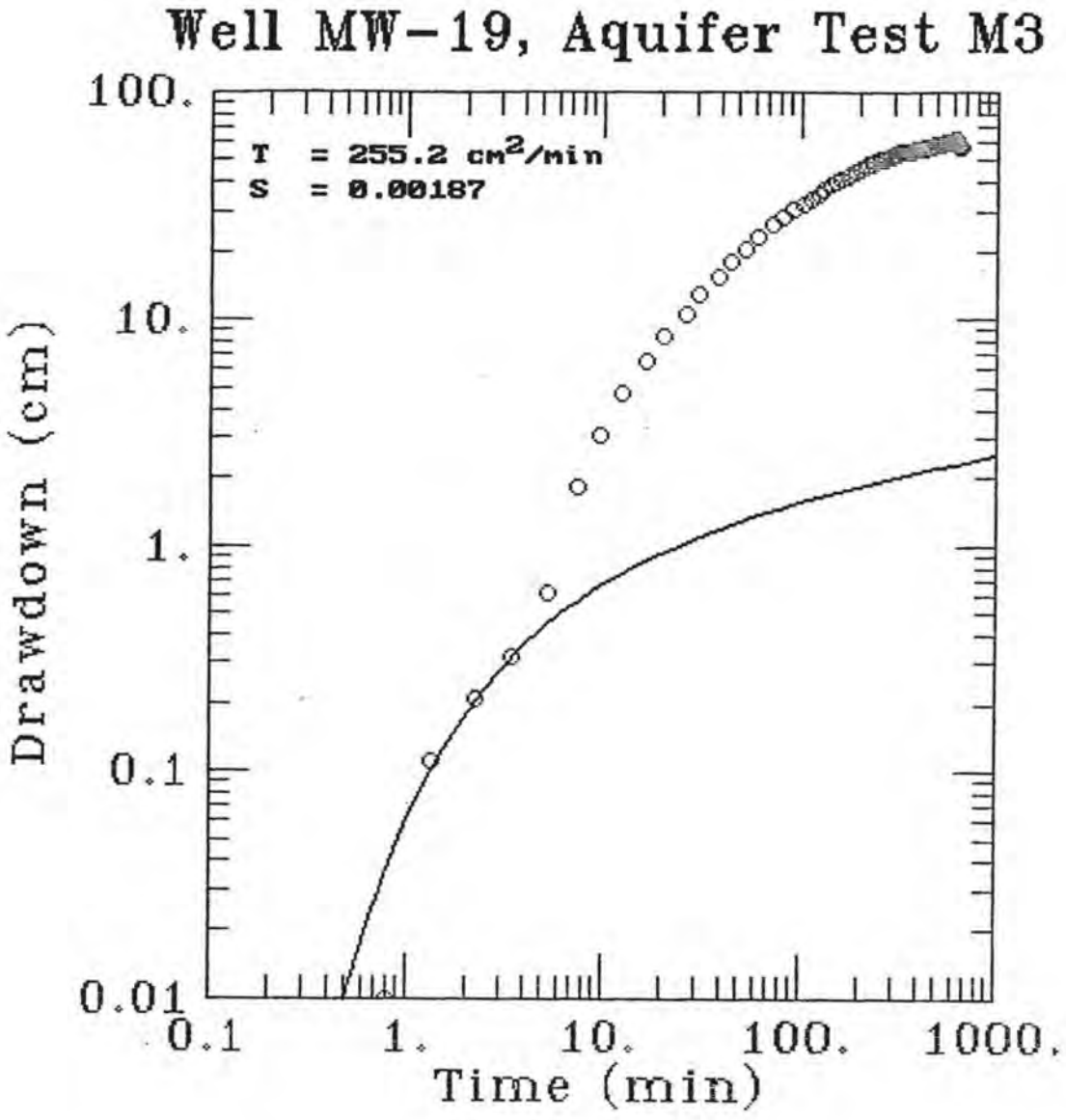

Figure 6.6-6: Early-time drawdown/Theis curve match for MW-19, aquifer test M3.

However, some of these matches were based on as few as two data points. Drawdown data generally began to deviate (trend above) the Theis curve at approximately 10 minutes with the early-time match.

Deviations between drawdown data and the Theis expectation are to be expected in a complex hydrogeological environment, and indicate a violation of one or more of the assumptions inherent to the Theis solution. Violation of Theis assumptions may preclude the use of the Theis solution, or may preclude the use of the Theis solution at certain times. Exploring reasons for the deviation between aquifer test drawdown plots and the Theis curve may reveal additional insight about the field site aquifer. The goal of the following analysis is to determine which drawdown data, if any, constitute a legitimate Theis curve match, leading in turn to an estimate of transmissivity and storativity values. Possible reasons for deviations from the Theis expectation with early-time and mid-time matches are considered below.

Deviations from the Theis expectation with an early-time match are considered first. Figures 6.6-4 through 6.6-6 show MW-19 drawdown data matched to the Theis curve at times less than approximately 5 minutes. Drawdown data recorded after 5 minutes of pumping fall above the Theis curve, indicating greater drawdown than predicted by the Theis method. Such drawdown patterns could indicate a variable pumping rate and/or "negative boundary" effects.

First, a constant pumping rate is assumed in the Theis solution. An increasing long term pumping rate could result in drawdown data that exceeds the Theis expectation. The long-term pumping rate was periodically monitored; no major fluctuations (increases) were observed.

Second, the Theis solution assumes an aquifer of uniform thickness and of infinite areal extent. Drawdown values may exceed the Theis expectation as a cone of depression (from pumping) encounters a negative (barrier) hydraulic boundary. Partial negative boundary effects might be observed in channel deposits as a cone of depression extends beyond the immediate channel alluvium. Apparent boundaries might be created by heterogeneities in aquifer materials; these boundaries might be expected to be multiple and non-parallel.

Analytical techniques have been developed for representing positive or negative boundary conditions through the use of image wells (Lohman, 1972; Ferris et al., 1962; Stallman, 1963). The method by Stallman (1963; as presented in Lohman, 1972) assumes the presence of one linear boundary at some distance from the pumping well. Early-time data from could not be matched using Stallman (1963) type curves (these curves are intended for single boundaries, which are unlikely at this site).

In summary, early-time drawdown data from aquifer tests M1, M2, and M3 generally could be matched to the Theis curve, although for many wells the match could only be made with very few points. Negative boundary conditions are likely at the site, because of the depositional environment. However, monitoring well drilling logs indicated that the aquifer materials are consistently present throughout the site. While not impossible, it appeared unlikely that boundary conditions would have been realized in the short time indicated by some of the data matches. Analysis therefore proceeded to consideration of the mid-time match between drawdown data and the Theis curve.

Drawdown data from aquifer tests M1, M2, and M3 were matched to the Theis curve between approximately 10 and 300 minutes (Figures 6.6-1 through 6.6-3). Again, MW-19 data are used here for the sake of illustration; Appendix F contains curve matches for other wells.

Early-time drawdown data fall above the Theis curve with a mid-time match, and late-time data (collected after approximately 300 minutes) appear to fall below the Theis curve. Possible reasons for the early-time deviations include (1) the effects of partially penetrating observation and/or pumping wells; (2) delayed yield effects; (3) the effects of borehole storage; or (4) the effects of variable pumping during the first 5 minutes of the aquifer test.

First, drawdown curve deviations from the Theis solution may indicate the effects of a partially penetrating pumping well or observation well. The Theis solution assumes horizontal flow between wells. Non-horizontal flow may occur because of a partially penetrating pumping well (Weeks, 1969). Partial penetration effects may lead to a drawdown curve that falls above or below the Theis curve, depending on well construction and local hydrogeology (Domenico and Schwartz, 1990).

Early-time deviations between drawdown data and the Theis expectation can be seen in partially penetrating wells, but also in all Cluster 1 wells thought to be fully penetrating (MW-5, MW-14, MW-15, MW-16, MW-19, MW-24, and MW-25; see Appendix F) for which early-time drawdown data (e.g., from 0 to 5 minutes) were collected. While it may be possible to realize partially penetrating well effects with fully penetrating wells in a highly heterogeneous environment (with multi-level preferential flow pathways) it appears unlikely that partially penetrating well effects would be seen in drawdown data from all fully penetrating wells. It is therefore unlikely that early-time Theis curve deviations observed in partially penetrating wells can be attributed to partially penetrating well effects.

Early-time drawdown data falling above the Theis curve may be characteristic of a delayed yield response in an unconfined aquifer. Initial drawdown in an unconfined aquifer is a response to the instantaneous release of water from a pumped aquifer; the initial release then becomes overshadowed by the effects of gravity drainage and vertical flow (Neuman, 1975). Delayed yield effects are unlikely in these tests because the aquifer appeared to remain fully saturated and confined throughout the duration of the aquifer tests (see Chapter 6).

The effects of borehole storage may give the appearance of a variable pumping rate. Significant pumping from borehole and/or casing storage gives a smaller effective pumping rate early in the test; the rate then increases with time as an increasing amount of water is pumped from the formation. The aquifer drawdown would be less than the Theis expectation if water is being removed from casing storage instead of the formation. Borehole and/or casing storage is believed not to be responsible for the drawdown/Theis curve deviation because the early-time drawdown deviation is above the Theis curve.

The second possible reason for drawdown data deviation from the Theis curve is a variable pumping rate. Variable pumping rates during the first 5 to 10 minutes of the aquifer test would lead to early-time drawdown data falling (1) above the Theis curve if the initial pumping rate was greater than the long-term pumping rate, or (2) below the Theis curve if the initial pumping rate was lower than the long-term pumping rate.

The discharge rate during the first minutes of each aquifer test was probably greater than the long-term discharge rate. Long-term pump discharge was uniform over extended pumping periods, and over the three meters of pumping well drawdown, on the basis of pre-test trials and data presented in Table 6.3-2. However, air in the discharge line (caused by drainage while the pump was turned off) and discharge line expansion during initial pressurization may have enabled the pump to discharge at a greater rate during the first minutes of operation until back pressure was established. A laboratory test done after the aquifer tests had been conducted showed that the discharge rate was significantly higher before the discharge line was fully pressurized. In retrospect, a check valve installed just above the pump housing may have reduced discharge variability before establishing a constant line pressure.

Discharge rates during the first minute(s) of the test were not measured because of other start-up activities (starting pump, starting data recorders, taking indicator probe measurements). Discharge measurements conducted prior to the aquifer tests indicated that pump discharge was insensitive to a drawdown of three meters.

An attempt was made to simulate the initial discharge rate from the observed drawdown in monitoring well MW-19. Figure 6.6-7 shows measured drawdown data from MW-19 during aquifer test M1 and two simulated drawdown scenarios. One simulated drawdown rate is based on a variable rate (i.e., a higher initial rate). A second simulated drawdown rate is shown for which a constant flow rate is assumed. The simulated rates are explained in the following paragraphs.

The drawdown attributed to a variable pumping rate is estimated using the Theis equation by assuming that the pumping well is initially pumped at a high rate, and that increasing amounts of water are injected into the well, such that the final composite flow rate equals the measured long-term flow rate. The variable discharge rate is simulated as a step function to represent the effects of an initially high discharge rate; the discharge rate decreases as pressure builds in the discharge line. The maximum pump discharge (on the basis of approximately 150 cm hydraulic head, no significant back pressure, maximum pump efficiency, and no friction loss) is approximately 17,000

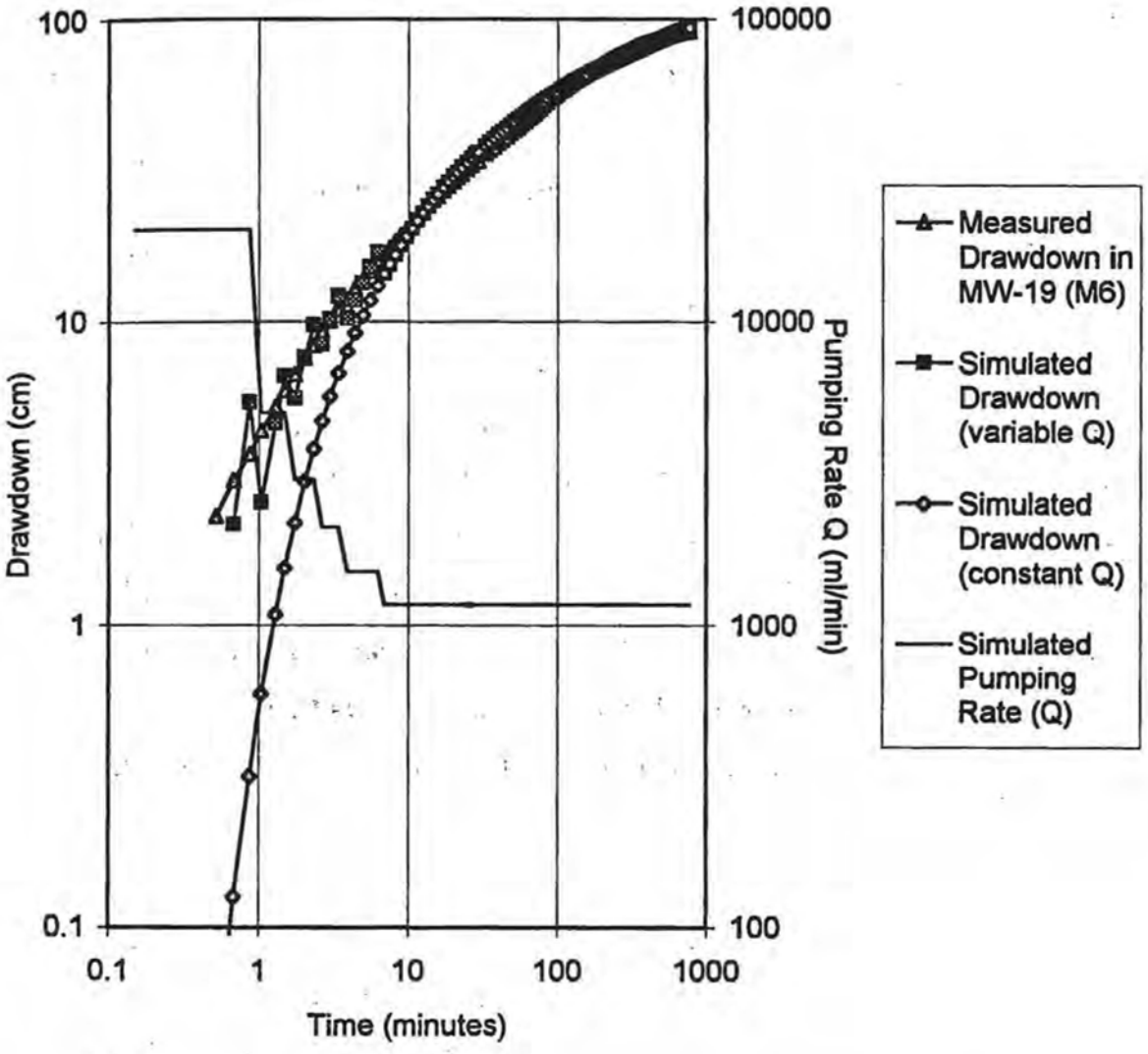

Figure 6.6-7: Simulated effects of a variable pumping rate in the first few minutes of aquifer test M1.

ml/min at 200 Hz, and approximately 26,000 ml/min at 300 Hz (*Grundfos* product literature). The initial simulated discharge rate was assumed to be 20,000 ml/min (on the basis of the actual pump controller setting). Transmissivity and storativity values are assumed to be those indicated by the mid-time Theis match for MW-19 (Figure 6.6-1). The rate of discharge decrease was determined empirically by attempting to reproduce the measured drawdown data. The simulated effective pumping rate is shown in Figure 6.6-7.

The drawdown resulting from constant discharge rate simulation was estimated using the same transmissivity and storativity values. The simulated pumping rate and associated drawdown patterns provide an indication that a variable pumping rate could have resulted in the observed drawdown patterns.

The mid-time drawdown data match with the Theis curve frequently resulted (depending on the well) in early-time data trending above the Theis curve and late-time data (after approximately 300 minutes) falling below the Theis curve. The previous discussion has focused on the early-time deviation. Possible reasons for the late-time deviation are considered next.

Drawdown data appear to deviate from the Theis curve beginning at approximately 300 minutes with a mid-time match. Possible reasons for this include a decrease in the long-term pumping rate, aquitard leakage, and/or a "positive" recharge boundary.

First, a decreasing pumping rate would create the effect of diminishing drawdown with respect to the Theis expectation. Discharge rates were monitored periodically by checking discharge line back pressure. Although major discharge fluctuations were not observed, some discharge variability was observed in the pumping well drawdown curves (Figures 6.4-1 through 6.4-3).

Next, the decrease in drawdown with respect to the Theis curve could be attributed to leakage from the overlying or underlying aquitards. A decrease in the expected aquifer drawdown may also have been caused by the effects of a recharge boundary or zones of increased transmissivity at some distance from Cluster 1 wells.

However, no streams or lakes are located close enough to the site to have had significant influence on test results.

Several conclusions can be drawn from the mid-time Theis curve match. A Theis match from approximately 10 to 300 minutes is possible with drawdown data from most wells. Early-time drawdown data are generally greater than the Theis expectation with the mid-time curve match. Partial penetration effects may lead to early-time drawdown data from the Theis curve, but the same early-time deviation is also present with fully penetrating wells. The early-time deviation is believed not to be caused by delayed yield effects since the aquifer remains saturated and confined throughout the aquifer tests. Borehole storage is not believed to cause early-time deviation since the deviation is greater than the Theis expectation, not less. A higher pump discharge during the first minutes of the tests appears to be the most likely reason for early-time drawdown deviation with a mid-time Theis curve match.

Drawdown data begin to fall below the Theis curve at approximately 300 minutes with a mid-time Theis curve match. Leaky aquitard conditions and/or a variable discharge rate are the likely reasons for the late-time water level deviations.

Transmissivity and storativity values using the Theis (1935) solution are provided in Tables 6.6-2 through 6.6-4 (estimates based on the Hantush solution, covered in the next section, are also provided in these tables). Values were not estimated for wells in which measurements were not taken during the first minutes of the aquifer tests. Transmissivity values based on a mid-time Theis match ranged from 4.2 cm^2/min to 6.3 cm^2/min. Storativity values ranged from 1.4×10^{-4} to 1.5×10^{-3}. Estimate reliability is limited by errors in data collection, by the number of data collected for any given well for any given test, by violation of assumptions inherent to the analytical solutions (e.g., homogeneous aquifer), and by the graphical curve-matching of the analytical solutions.

	Device	T (Theis) (cm^2/min)	S (Theis)	T (Hantush) (cm^2/min)	S (Hantush)	β (Hantush)
MW-5	trans	PW	PW	PW	PW	PW
MW-12	trans	4.8	1.5E-3	1.4	4.4E-6	9.0
MW-13	trans	4.7	1.0E-3	1.4	1.6E-6	12.6
MW-14	trans	4.5	8.2E-4	1.0	1.0E-5	4.7
MW-15						
MW-16	trans	5.3	9.4E-4	1.9	1.7E-5	2.8
MW-17	trans	5.0	6.3E-4	1.8	8.1E-6	3.5
MW-18	trans	5.3	5.8E-4	1.6	2.0E-6	7.4
MW-19	trans	4.9	1.2E-3	1.8	3.0E-6	7.9
MW-20	e-tape	4.6	9.1E-4	1.8	2.9E-4	0.6
MW-21	e-tape	5.2	7.3E-4	1.4	8.0E-5	1.4
MW-22	e-tape	5.0	5.0E-4	1.1	1.1E-5	3.7
MW-23	e-tape	5.0	4.6E-4	1.1	1.2E-5	3.4
MW-24						
MW-25	e-tape	4.2	8.3E-4	1.1	6.4E-5	1.7
Average		4.9	8.4E-4	1.5	4.2E-5	
Std. Dev.		0.3	3.0E-4	0.3	8.3E-5	

Notes: "T" represents transmissivity
"S" represents storativity
"β" represents the Hantush (1960) aquitard leakage coefficient
"trans" indicates that water levels were measured by transducer
"e-tape" indicates that water levels were measured with a water level indicator probe
"PW" denotes pumping well

Table 6.6-2: Estimated transmissivity and storativity values based on Theis (1935) and Hantush (1960) for aquifer test M1 (see text for further explanation).

	Device	T (Theis) (cm^2/min)	S (Theis)	T (Hantush) (cm^2/min)	S (Hantush)	β (Hantush
MW-5						
MW-6	e-tape	6.0	2.5E-4	2.0	7.6E-5	0.66
MW-12	trans	4.6	6.1E-4	1.4	1.3E-4	0.9
MW-13	trans	4.7	6.3E-4	1.2	7.2E-5	1.5
MW-14	trans	4.5	5.5E-4	1.0	3.0E-5	2.1
MW-15						
MW-16						
MW-17	e-tape	5.5	4.4E-4	1.5	2.8E-5	2.0
MW-18	e-tape	5.4	5.6E-4	1.1	2.8E-5	2.4
MW-19	trans	5.0	9.7E-4	1.2	3.8E-5	2.6
MW-20	trans	5.0	1.2E-3	1.4	9.9E-5	1.6
MW-21	trans	5.2	1.5E-3	2.6	2.5E-4	0.7
MW-22	e-tape	5.4	6.7E-4	1.1	4.9E-5	2.0
MW-23	e-tape	5.6	6.9E-4	1.4	1.3E-4	1.0
MW-24						
MW-25	trans	PW	PW	PW	PW	PW
Average		5.2	7.4E-4	1.5	8.3E-5	
Std. Dev.		0.5	3.7E-4	0.5	6.6E-5	

Notes: "T" represents transmissivity
"S" represents storativity
"β" represents the Hantush (1960) aquitard leakage coefficient
"trans" indicates that water levels were measured by transducer
"e-tape" indicates that water levels were measured with a water level indicator probe
"PW" denotes pumping well

Table 6.6-3: Estimated transmissivity and storativity values based on Theis (1935) and Hantush (1960) for aquifer test M2 (see text for further explanation).

	Device	T (Theis) (cm^2/min)	S (Theis)	T (Hantush) (cm^2/min)	S (Hantush)	β (Hantush
MW-5	trans	5.351	3.3E-4	5.6	3.1E-4	0.0
MW-6						
MW-12	e-tape	5.1	3.6E-4	4.7	3.4E-4	0.0
MW-13	e-tape					
MW-14	e-tape	4.2	3.5E-4	3.9	3.4E-4	0.0
MW-15						
MW-16	trans	5.4	5.2E-4	1.2	3.9E-5	1.9
MW-17	trans	5.5	7.7E-4	1.3	2.2E-5	2.9
MW-18	trans	5.7	7.1E-4	4.0	1.1E-7	30.7
MW-19	trans	5.4	3.7E-4	2.4	1.7E-4	0.4
MW-20	e-tape	5.4	1.4E-4	1.7	1.7E-5	1.2
MW-21	e-tape	5.1	5.0E-4	1.3	6.9E-5	1.3
MW-22	trans	5.1	1.3E-3	1.7	1.2E-5	4.8
MW-23	trans	6.3	9.3E-4	4.4	2.8E-8	47.6
MW-24	trans	PW	PW	PW	PW	PW
MW-25	e-tape	6.0	5.5E-4	5.6	5.3E-4	0.0
Average		5.4	5.7E-4	3.1	1.5E-4	
Std. Dev.		0.5	3.2E-4	1.7	1.8E-4	

Notes: "T" represents transmissivity
"S" represents storativity
"β" represents the Hantush (1960) aquitard leakage coefficient
"trans" indicates that water levels were measured by transducer
"e-tape" indicates that water levels were measured with a water level indicator probe
"PW" denotes pumping well

Table 6.6-4: Estimated transmissivity and storativity values based on Theis (1935) and Hantush (1960) for aquifer test M3 (see text for further explanation).

6.7 Aquifer Test Analysis using the Hantush (1960) Solution

This section presents an analysis of aquifer test data using the Hantush (1960) analytical solution. The purpose of the analysis was to evaluate possible hydraulic effects of aquitard leakage on hydraulic responses in the aquifer.

The Hantush (1960) method introduces a new variable (β) into the Theis solution. The β variable is used to represent water released from storage in an overlying or underlying aquitard. In the case of possible leakage from an overlying aquitard (as is the case with the Plant Science Farm field site), the expression for β is given as $\beta = \frac{r}{4b}\left(\sqrt{\frac{K' S_s'}{K S_s}}\right)$, where

r is the distance from the pumping well to observation point,

K' is the vertical hydraulic conductivity in the overlying aquitard,

K is the aquifer hydraulic conductivity,

S_s' is the specific storage coefficient in the overlying aquitard,

S_s is the specific storage coefficient in the aquifer, and

b is the aquifer thickness.

Aquitard leakage, as indicated by β, is large if values of r, K', and/or S' are relatively large, or if values of b, K, and/or S_s are relatively small.

As with most curve-matching methods, use of the Hantush (1960) requires a best fit interpretation. The Hantush β curves become more linear as the β values increase, and the difference in the shape between β curves becomes more indistinct (this is shown for MW-19 in Figures 6.7-1 and 6.7-2). Also, experimentation showed that matching a β curve to a series of drawdown data in which an early-time variable pumping rate caused greater drawdown yielded high β values and unreasonably low storativity values, e.g., less than 10^{-8}. Drawdown data were therefore matched to the β curves beginning with data recorded approximately 1 minute after pumping began.

Transmissivity and storativity data estimated using the Hantush (1960) method

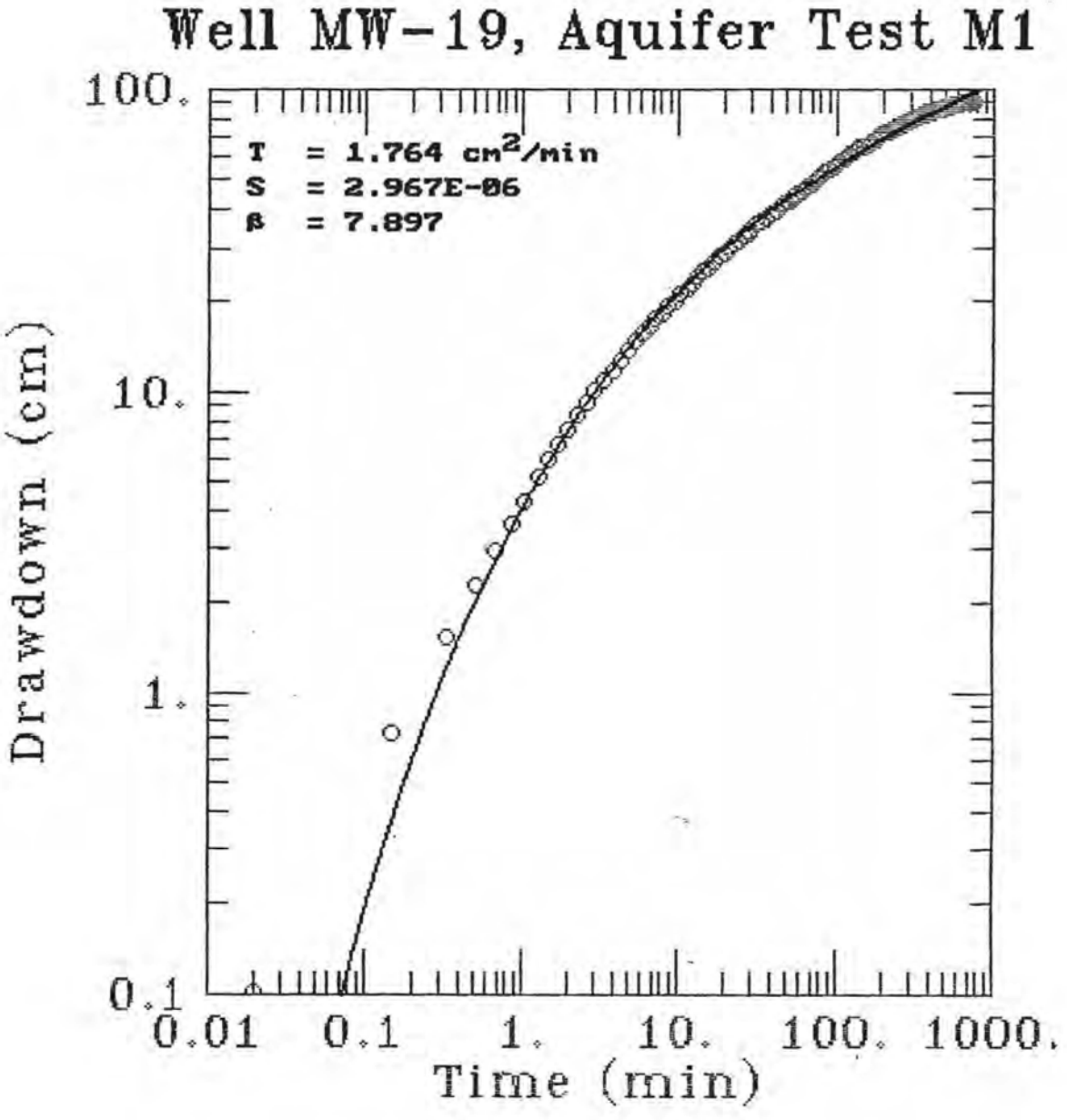

Figure 6.7-1: β curve match for MW-19 , aquifer test M1 data.

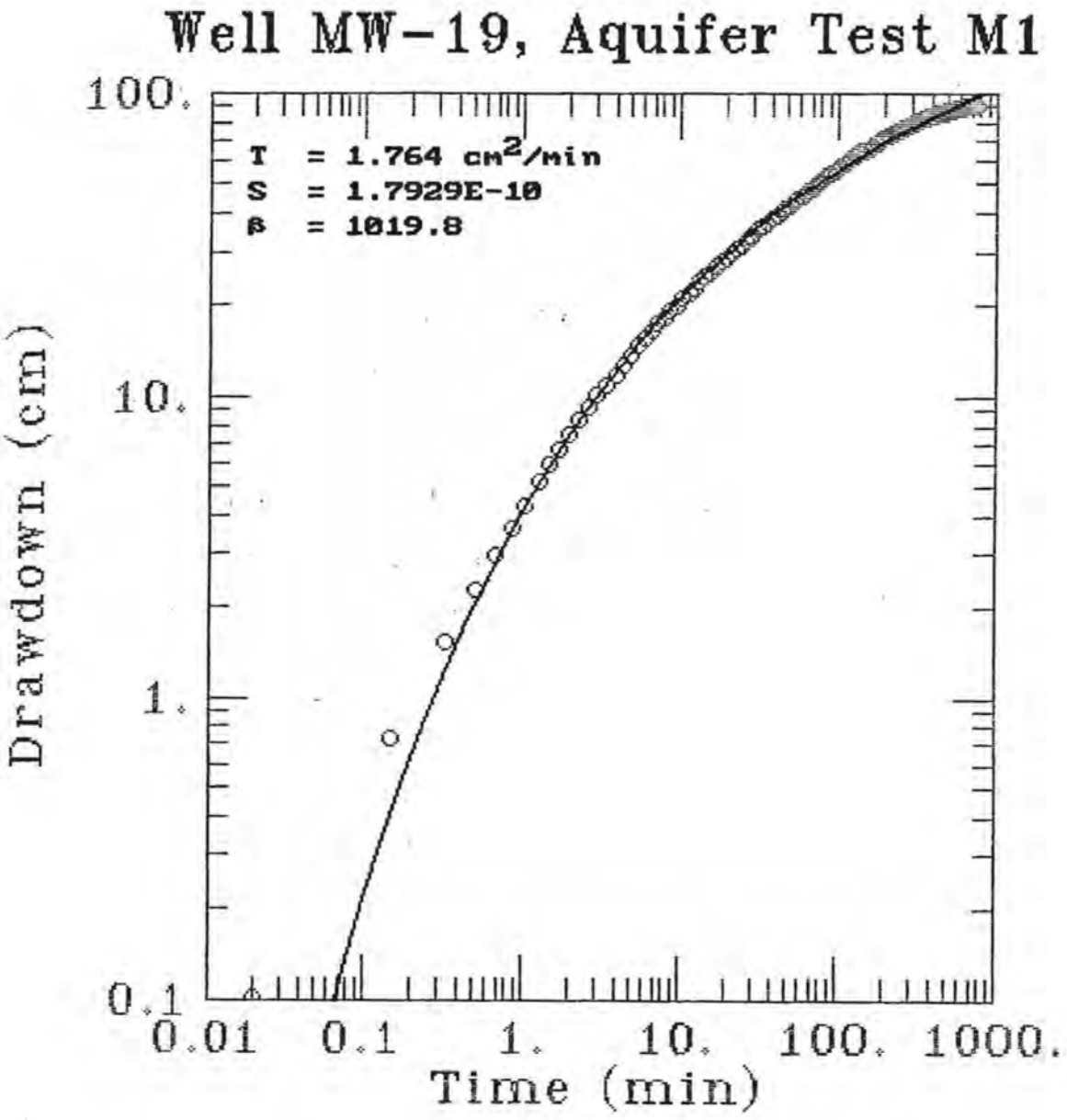

Figure 6.7-2: Alternative β curve match for MW-19 , aquifer test M1 data.

are presented in Tables 6.6-2 through 6.6-4. *AQTESOLV* plots are provided in Appendix F. Transmissivity estimates range from approximately 1.0 to 5.6 cm^2/s; storativity values range from approximately 2.8×10^{-8} to 5.3×10^{-4}, although all but two values were greater than 4.8×10^{-6}.

The Hantush (1960) leaky-with-storage method provided transmissivity values which generally were lower than the transmissivity values obtained with the Theis (1935) solution. Storativity values obtained with the Hantush (1960) solution are also generally less than those obtained with the Theis solution; some of the Hantush storativity estimates are unreasonably small, i.e., 10^{-6} or less.

Estimated β values were then evaluated for reasonableness. Table 6.7-1 provides values of $K'S_s'$, estimated using the expression $K'S_s' = \frac{\beta^2 KS_s}{\left(r/4b\right)^2}$, using β, T, and S values from the Hantush (1960) analysis of MW-19 drawdown data (MW-19 data were selected for consistency with the previous discussion). Resulting values of K' and aquifer compressibility (α) were then considered in the context of the observed aquitard material characteristics. Aquifer compressibility (α) was calculated from the expression

$S_s = \rho g(\alpha + n\beta)$, where

ρ is the density of water (1000 kg/m^3),

g is the gravitational constant (9.81 m/s^2),

n is the aquifer porosity (assumed to be 0.3), and

β represents the compressibility of water (4.6×10^{-10} m^2/N).

(Note that the β term used for the compressibility of water is different than the β used as a parameter in the Hantush method). Values of K' and α are presented in Table 6.7-2.

Several observations can be made from Tables 6.7-1 and 6.7-2. First, curve matches for MW-19 in tests M1, M2, and M3 using the Hantush (1960) method result in reasonable aquifer hydraulic conductivity values, judging on the basis of general values for aquifer materials (Freeze and Cherry, 1979) such as those seen at the site. Second, the aquifer storativity values, especially for some of the matches, appear

Test #	r (cm)	β	b (cm)	T (cm^2/min)	K (cm/sec)	S	S_s (1/cm)	$K'Ss'$ (1/sec)
M1	217	7.9	152	1.8	2.0E-4	3.0 E-6	2.0E-8	1.9E-9
M2	410	2.6	152	1.2	1.3E-4	3.8 E-5	4.9E-7	4.9E-10
M3	834	0.4	152	2.4	2.6E-4	1.7E-4	2.5E-6	2.5E-11

Notes:
- MW-19 data were selected for consistency with previous discussions.
- r represents the distance from the pumping well to MW-19.
- The aquifer thickness (b) is estimated on the basis of generalized drilling logs.
- T and S are estimated using the Hantush (1960) method.
- $K = T/b$; $S_s = S/b$

Table 6.7-1: Estimated values of $K'S_s'$ for MW-19.

$K'S_s'$ (1/sec)	K' (cm/sec)	S_s' (1/cm)	α (m^2/N)
1.9E-9	1E-6	1.9E-3	1.93E-9
4.9E-10	1E-6	4.9E-4	4.84E-10
2.5E-11	1E-6	2.5E-5	1.14E-11
1.9E-9	1E-8	1.9E-1	1.95E-7
4.9E-10	1E-8	4.9E-2	4.98E-8
2.5E-11	1E-8	2.5E-3	2.54E-9

Table 6.7-2: Estimated values of vertical aquifer hydraulic conductivity (K') and aquifer compressibility (α) for MW-19

somewhat low for the types of aquifer materials present at the site. Third, an assumed vertical aquitard hydraulic conductivity value of 10^{-6} cm/sec, which might be found in silty sediments (Freeze and Cherry, 1979) such as those found in the overlying aquifer, results in aquifer compressibility values in the 10^{-9} to 10^{-11} m^2/N range. These aquifer compressibility values might be typical for dense, sandy gravel, fissured rock, or sound rock (Domenico and Schwartz, 1990). If the vertical hydraulic conductivity in the aquitard is in the range of 10^{-8} cm/sec, which would be reasonable for unweathered clay or glacial till (Freeze and Cherry, 1979), the aquitard compressibility values would range from 10^{-7} to 10^{-9} m^2/N. These latter values would be consistent with clay, silt, or loose sand materials (Domenico and Schwartz, 1990).

The applicability of the Hantush (1960) method for analyzing drawdown data collected using the multi-well aquifer test data remains unclear. Curve matches resulting in very low aquifer storativity values appear unreasonable. Curve matches resulting in higher aquifer storativity values result in unreasonably low aquitard compressibility values for an assumed vertical hydraulic conductivity in the 10^{-6} cm/sec range. Reasonable aquitard compressibility values are obtained if it is assumed that the vertical hydraulic conductivity in the aquitard is in the 10^{-8} cm/sec range, but this vertical conductivity value seems too low for the observed aquitard materials. Thus, this analysis did not indicate with certainty whether or not significant aquitard leakage is occurring at the site. Aquifer transmissivity values estimated with the Theis and Hantush methods were fairly close for cases where the Hantush method led to reasonable aquifer storativity values (i.e., in the 10^{-4} range). In these cases β values were relatively small, indicating minimal leakage. In summary, on the basis of the analysis described above, the Theis method using a mid-time data match appears to represent the best analysis of aquifer test data.

6.8 Recovery and Pumping Well Data Analysis

An analysis of recovery data from observation wells provides a comparison with hydraulic parameter estimates made with the Theis (1935) and Hantush (1960) methods. Recovery data provide a useful basis for comparison because the recovery data were not significantly influenced by variability in the early-time pumping rate.

Recovery data were analyzed using the Cooper and Jacob (1946) method and *AQTESOLV* analysis software. Similar conditions are assumed with this method as with the Theis method; it is also assumed that values of u are small (i.e., r is small and t is large). The recovery analysis is limited to wells that were measured by pressure transducer; hand measurements were not taken during aquifer recovery.

Transmissivity values given by analysis of recovery data are provided in Table 6.8-1. Plots showing recovery data matches using this method are presented in Appendix E. Transmissivity values estimated on the basis of recovery data range from approximately 2.0 cm^2/min to 5.2 cm^2/min.

	Transmissivity (cm^2/min)		
Well	**M1**	**M2**	**M3**
MW 5	4.1		4.3
MW12	3.8	4.5	
MW-13	3.7	4.6	
MW-14	3.8	4.3	
MW-16	2.0		4.1
MW-17	3.8	4.8	4.3
MW-18	4.3		4.0
MW-19	4.0		4.7
MW-20		5.2	
MW-21		5.0	
MW-22			4.4
MW-23			3.6
MW-24			3.4
MW-25		4.6	

Table 6.8-1: Transmissivity values (cm^2/min) based on aquifer test recovery data. Recovery data were collected in transducer-monitored wells only.

Transmissivity values were also estimated from pumping well data using the Papadopoulos and Cooper (1967) method. Data collected in the first minute of the aquifer test were not used because a variable early-time pumping rate probably distorted early-time drawdown data.

Transmissivity estimates from the analysis of pumping well drawdown data are provided in Table 6.8-2. *AQTESOLV* (Duffield and Rumbaugh, 1989) plots are provided in Appendix F. Transmissivity values based on pumping well data ranged from 4.2 cm^2/min to 5.7 cm^2/min. These values are similar to transmissivity values estimated from (1) observation well drawdown data using the Theis (1935) method, (2) observation well data using the Theis (1935) method, and (3) drawdown data using the Hantush (1960) method.

Method	Transmissivity (cm^2/min)		
	MW-5 (M1)	MW-24 (M3)	MW-25 (M2)
Cooper and Jacob (1946)	4.5	5.1	5.7
Papadopoulos and Cooper (1967)	4.5	5.7	4.7

Table 6.8-2: Transmissivity values estimated from drawdown data collected in pumping wells during aquifer tests M1, M2, and M3.

6.9 Hydraulic Conductivity Values

Hydraulic conductivity values were estimated from the transmissivity values presented in the previous sections with the expression $K = \frac{T}{b}$, where K = hydraulic conductivity, T = transmissivity, and b = aquifer thickness. The hydraulic conductivity estimates are limited by the accuracy of the transmissivity and aquifer thickness estimates. The aquifer thickness was estimated from drilling logs.

Because of material heterogeneities in the aquifer zone, significant flow may occur along preferential ground water flowpaths. The hydraulic conductivity of these flow paths is much higher than the representative hydraulic conductivity estimated for the entire aquifer. The hydraulic conductivity values of the preferential pathways are of major significance in tracer studies.

Hydraulic conductivity estimates are therefore given in ranges, on the basis of the preceding transmissivity estimates and on aquifer thicknesses of either 150 cm or 30 cm (Table 6.9-1). The latter thickness might represent the coarsest, highest conductivity aquifer zones. These estimates are provided as a range of possible values rather than actual estimates.

6.10 Multiple Well Aquifer Test Discussion

Transmissivity values estimated with either the Theis (1935) or the Hantush (1960) solutions for most Cluster 1 wells fell into a relatively small range. If drawdown data collected in the first minutes of each pumping test were neglected the Hantush

Method for Estimating Transmissivity	Maximum and Minimum Transmissivity Estimates (cm^2/min)	Assumed Thickness (cm)	Estimated Hydraulic Conductivity (cm/sec)
Theis (1935)	4.2	150	4.7×10^{-4}
Theis (1935)	4.2	30	2.3×10^{-3}
Theis (1935)	6.3	150	7.0×10^{-4}
Theis (1935)	6.3	30	3.5×10^{-3}
Hantush (1960)	1.0	150	1.1×10^{-4}
Hantush (1960)	1.0	30	5.6×10^{-4}
Hantush (1960)	5.6	150	6.2×10^{-4}
Hantush (1960)	5.6	30	3.1×10^{-3}

Table 6.9-1: Possible range of hydraulic conductivity values.

solution provided better curve fits. However, some of the parameter values estimated using the Hantush (1960) method appeared unreasonable. Transmissivity values generated with drawdown data using the Theis (1935) and Hantush (1960) solutions, and with recovery data using the Cooper and Jacob (1946) solution, fell within a relatively close range. This observation indicates that (1) the mid-time Theis (1935) match appears more valid than the early-time match, and that (2) the effects of apparent heterogeneity observed during well installation appear to average out over the distances between Cluster 1 wells. The latter observation suggests that aquifer sediments approach being homogeneously heterogeneous on the scale represented by Cluster 1 wells.

7. Tracer Tests: Description and Methods

7.1 Introduction

This chapter presents a detailed description of tracer test methodology. The chapter begins with an overview of the tracer experiments, followed by a brief discussion of site applicability. A description of the recirculation loop and resulting hydraulic gradients is then presented, followed by a description of the tracer injection system. The sampling system, which was designed and constructed on the basis of the general experimental design and specific site characteristics, is then presented, followed by a description of water sample analysis techniques. The final section provides a brief description of the rationale for replicate tests. Tracer test results are presented in Chapters 8-12.

7.2 Tracer Test Overview

Four tracer experiments were conducted at the Plant Science Farm during the course of this project. The purpose of the tracer tests was to compare conservative and particle (polystyrene microspheres and encapsulated cells) tracer transport patterns in a heterogeneous field environment. This section provides an overview of the tracer experiments conducted for this project.

The general experimental design consisted of intermediate scale, forced-gradient, recirculating-loop tracer tests (see Chapter 3). Monitoring wells for aquifer characterization and tracer tests were designed, located, and installed according to the experimental design. The tracer test design, consisting of a water recirculation system, tracer injection system, and sampling system, was developed on the basis of the general experimental design.

The four tracer tests were conducted in Transects B and C (see Figure 5.5-1). Tracer tests T1 and T3 were conducted in Transects C and B, respectively, using potassium bromide, polystyrene microspheres, and encapsulated cell tracers. Tracer tests T2 and T4 were also conducted in Transects C and B, respectively, as replicates of tracer tests T1 and T3. Potassium bromide was used as a tracer in the replicate tests.

Several initial tracer tests were also conducted to develop and test injection and sampling methods. Tracers for these tests included chloride, distilled water, and bromide.

The first tracer tests were conducted in Transect C because this transect had more sampling wells than the other transects and therefore posed the greatest monitoring and instrumentation challenge. Transect B was chosen for the second tracer experiments, partly because of the proximity to the instrumentation trailer. Tracer tests were not conducted in Transect A because of the onset of cold weather (which caused freezing in the sampling lines).

Well MW-16 was used as the tracer injection well for Transect C; wells MW-17, MW-18, MW-22, and MW-23 were used as monitoring wells (Table 7.2-1). MW-17 and MW-22 are screened in the upper portion of the aquifer, MW-18 and MW-23 are screened in the lower portion. Well MW-19 was used as the injection well in Transect B; MW-20 and MW-21 were used as the upper and lower monitoring wells, respectively. Water samples were also taken from both pumping wells (MW-24 and MW-25), and from the injection well in Transect B (MW-19) beginning at two hours after injection. Distances between tracer injection and tracer monitoring wells are provided in Tables 5.5-1 and 7.2-2.

Tracer Test	Tracer Injection Well	Tracer Monitoring Wells	Sampling Method
T1	16	17, 18, 22, 23, 24	continuous sampling
T2	16	17, 18, 22, 23, 24	continuous sampling
T3	19	19*, 20, 21, 25	continuous sampling
T4	19	19*, 20, 21, 25	continuous sampling

* monitoring began 2 hours after last tracer was injected.

Table 7.2-1: Tracer test sampling details.

Transect B		Transect C	
Monitoring Well	Distance from MW-19 (cm)	Monitoring Well	Distance from MW-16 (cm)
MW-20	152	MW-17	160
MW-21	199	MW-18	205
MW-25	409	MW-22	357
		MW-23	405
		MW-24	622

Table 7.2-2: Distances (cm) between tracer injection wells and monitoring wells in Transects B and C.

7.3 Site Applicability for Particle Tracer Tests

This section presents a discussion regarding the applicability of the Plant Science Farm field site for particle tracer tests. Criteria for applicability include (1) a reasonable chance for at least some particle transport, and (2) aquifer materials representative of materials found at contaminated sites where encapsulated cells might be used. The site applicability discussion is based on the conceptual model (which evolved during the site characterization) and hydraulic testing results.

The conceptual model (Section 5.10.4) describes a heterogeneous confined or semi-confined aquifer containing silt, sand, gravel, and cobbles deposited in a transitory channel environment. Particle transport in such a heterogeneous environment depends on pore dimensions as indicated by aquifer sediment grain sizes and on the degree of interconnection between pore spaces. Heterogeneity in aquifer materials often leads to zones of larger interconnected pore spaces which in turn leads to preferential ground water flow. Some researchers have observed enhanced transport rates of small particles over dissolved tracers (Harvey et al., 1989; Harvey, 1993; Champ and Schroeter, 1989), possibly because of preferential ground water flow.

The degree of transport along well transects thus depends, in part, on the continuity and orientation of preferential ground water flowpaths. For instance, larger particles might be expected to migrate in preferential ground water flowpaths along

coarser channel deposits (see Figure 5.10.4-1), but not through finer-grained materials. Finer sediment zones may result in particle filtration.

The distribution of aquifer sediment grain sizes is an indication of particle transport potential. Sherard observed a relationship between the grain size distribution of a medium and the particle sizes that would migrate through the material (see Chapter 2). Sherard et al. (1984b) found that particle filtration would occur if $D_{m85}/D_{P15} < 9$, where D_{m85} indicates the 85% retained medium size and D_{P15} represents the 15% retained particle size. Figure 7.3-1 presents the 85% retained grain size data from samples collected at various depths during the installation of Cluster 1 wells. Figure 7.3-1 also shows the size thresholds for 2, 5, and 15-μm particles above which, on the basis of Sherard's relationship, particles should be filtered. On the basis of this relationship and grain-size data, 2-μm particles should be expected to migrate through aquifer materials at the site at depths between approximately 2.5 and 4.5 meters below ground surface. Encapsulated cells and microspheres with 5- and 15-μm diameters might be expected to pass through aquifer zones only between 3.5 and 4.5 meters.

The second criterion for site applicability was whether the Plant Science Farm site represents possible contaminated sites. Many contaminated sites are located over aquifers consisting of unconsolidated heterogeneous alluvial deposits. Although every site has unique characteristics, results from these tracer tests should be useful in considering particle transport at other sedimentary sites.

7.4 Recirculation Loop

A water recirculation loop was used to establish an hydraulic gradient along monitoring well transects B and C (see Figure 5.5-1). The recirculation loop is shown in Figure 7.4-1. Water was pumped from MW-25 to MW-5 in transect B, and from MW-24 to MW-5 in Transect C.

A pumping rate of approximately 2 liters/min was selected empirically. It was found that water levels in the wells remained above the top of the aquifer with this rate.

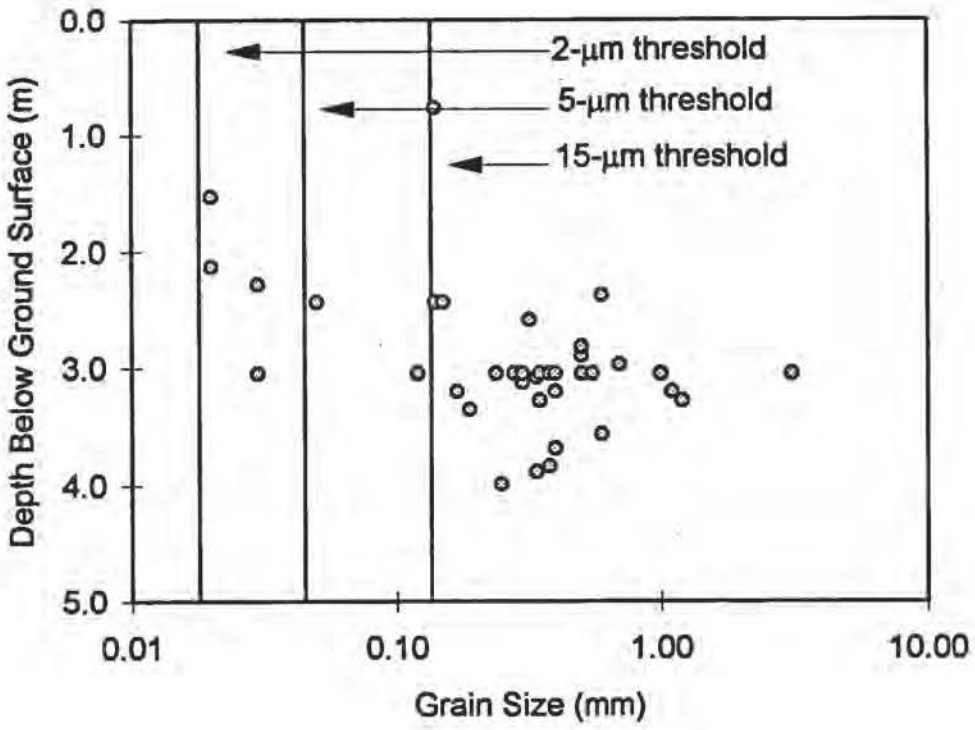

Figure 7.3-1: 85% retained grain size vs. depth below ground surface (see text for an explanation of "threshold" lines).

Three pump systems were used for pumping water through the transect circulation loop: the *Grundfos Redi-Flow* pump, a multi-cartridge *Cole-Parmer Masterflex* peristaltic pump, and a 1/2 HP *Berkeley* Jet Pump (model 25). The *Grundfos* produced a steady flow in the desired range, but could not be used for extended periods of time (Chapter 6). Flow in the peristaltic pump would decrease over time due to tubing wear. A *Berkeley* Jet pump, with plumbing modifications, was capable of pumping at a relatively steady rate for longer periods of time.

The *Berkeley* Jet pump is designed for a flow rate in excess of the desired two liters/minute; pump flow cannot be reduced by reducing the pump speed. The pump was therefore plumbed to circulate water (under pressure) within the pumping well, and

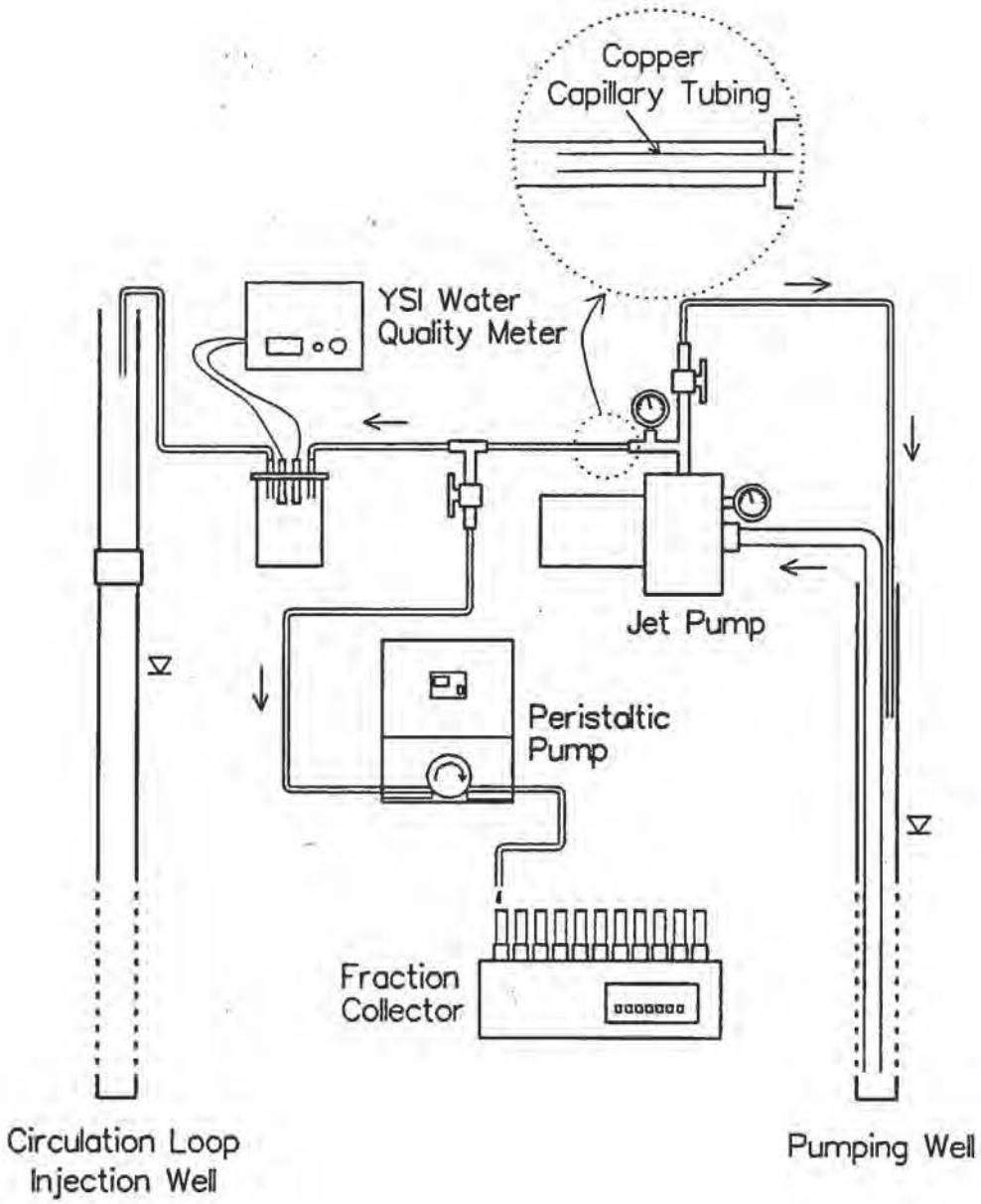

Figure 7.4-1: Transect circulation loop.

only the desired flow was ported to the transect circulation loop (Figure 7.4-1). Mixing volumes in the pumping well were consequently increased by the additional pumping well loop volume (approximately 1.3 liters).

Circulation-loop water flowed through 1-cm vinyl tubing from the pump to the water injection well. The injection well casing height was increased with a 122-cm extension to allow for increased head at the water injection well. Back-pressure in the circulation-loop tubing was required for constant flow; this was achieved with calibrated lengths of 0.32-cm copper tubing installed at the pump-recirculation loop valve.

Water in the circulation loop was also routed through a *YSI* Water Quality meter (model 3500) flow cell. Conductivity, pH, temperature, and redox potential readings were periodically taken throughout the tracer tests. Furthermore, 15-ml samples from the circulation loop were metered through a *Cole Parmer Digistaltic* pump and collected every 20 minutes using a *Buchler Alpha 200 Fractometer* (this sampling system is described in further detail below).

The purpose of the recirculation loop was to establish a uniform, steady-state hydraulic gradient within a transect. Average estimated gradients are shown in Table 7.4-1 for tracer tests T1, T2, T3, and T4. The estimates are based on water level readings taken in the pumping and injection wells at intervals of approximately every 10 minutes during the tracer tests. The standard deviation is a measure of gradient variability during the tracer test.

7.5 Tracer Injection System

Tracer test results are sensitive to injection methods, especially when injection wells are in close proximity to monitoring wells. This section describes the system used for injecting conservative and particle tracers for tracer tests T1, T2, T3, and T4.

Tracers may be injected continuously or as slugs over a short period of time. Continuous tracer injection was not desirable for this project because of high tracer costs. A system was therefore designed for injecting a tracer slug.

Tracer Test	Average Gradient	Standard Deviation
T1	0.147	0.002
T2	0.152	0.003
T3	0.137	0.003
T4	0.141	0.003

Table 7.4-1: Gradient between MW-5 and MW-24 in tracer tests T1 and T2; gradient between MW-5 and MW-25 in tracer tests T3 and T4.

The ideal slug-injection system allows instantaneous tracer mixing in the injection well with minimal hydraulic interference in the flow field surrounding the injection well. Any lingering tracer in the injection well above the screened area will slowly migrate toward the screened area, temporarily creating a continuous tracer source. Experimentation with several methods led to a circulation/injection system for the tracer injection well.

The tracer injection system is shown in Figure 7.5-1. A 1.27-cm I.D. PVC pipe was inserted in the 1.9-cm PVC well casing, with a pressure transducer installed in the bottom. This insert reduced the well casing storage (to 120 ml per meter of length). Attached to the outside of the insert were three 0.13-cm TFE tubes, which were extended to the bottom, middle, and top of the screened well casing area (tracer injection wells had 152-cm screen lengths, compared to 30-cm screen lengths in the sampling wells). A circulation loop was created by pumping water from the top of the screened interval and injecting water at the bottom of the screened interval at a rate of approximately 66 ml/min. A *Cole-Parmer Masterflex* peristaltic pump was used for pumping; a 0.5-m length of #13 *Pharmed* tubing was placed in a # 17 pump head and connected to the upper and lower well tubing. Tracer was injected directly into the remaining 0.13-cm TFE tubing (which extended to the middle of the screened casing interval) with hand-held syringes.

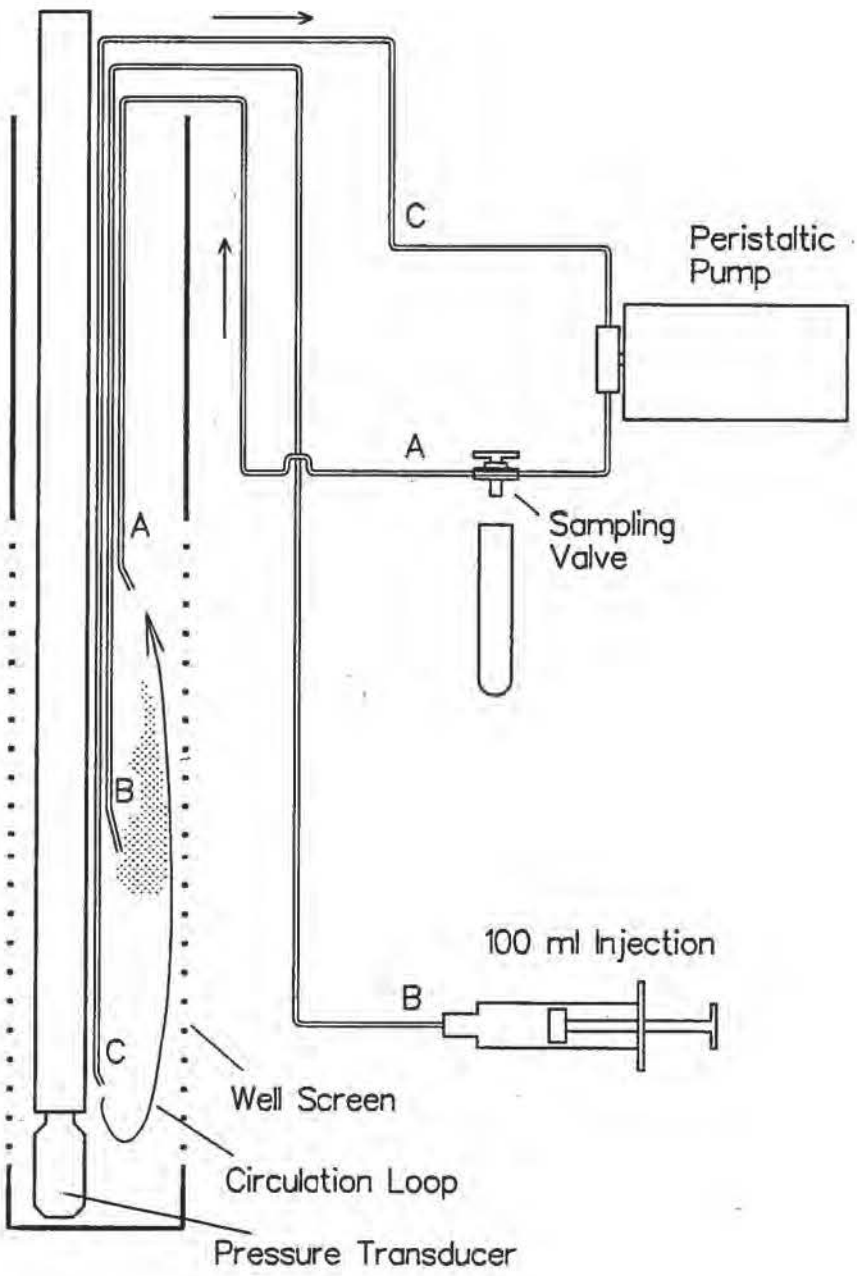

Figure 7.5-1: Tracer injection system

This circulation/injection system allowed constant mixing of water and tracer in the well casing, reducing the risk of a lingering tracer source (in the well casing) after the slug injection. The recirculation/injection system also minimized the flow field disturbance caused by injection, since less carrier fluid was required for adequate mixing.

Tracers were injected after a steady-state hydraulic gradient was approximated in the recirculation loop (as evidenced by minimal changes in water levels in the water-pumping and water-injection well). Tracer injections lasted for varying lengths of time due to the varying amounts of tracer being injected during each tracer test. In general, it took approximately 60 seconds to inject 100 ml of KBr solution, and correspondingly less time for 10-ml syringes with microspheres or encapsulated cells. These times represent slug injection relative to the tracer test time scale.

It was possible to note the arrival of these tracers in the tracer-injection circulation loop by the color of the microsphere and encapsulated cell solutions. Significant coloration was noted approximately 80 seconds after injection; color would fade quickly thereafter. These observations confirmed that the tracer was being introduced in slug form with rapid mixing in the injection well.

Immediately following injection, the injection tubing (tube B, Figure 7.5-1) was connected to the 3-way valve in the pressured side of the injection circulation loop at "A" and flushed. Sixty minutes after the last tracer injection in tracer tests T3 and T4 the injection tubing was connected to the outdoor *Buchler* fraction collector (via the *Digistaltic* pump) for periodic sample collection (Figure 5.6-1).

Samples from the circulation loop were collected by opening the 3-way valve at "A," flushing the valve briefly, and collecting approximately 15 ml in a glass tube. Each sample was capped and labeled immediately following collection and stored in an on-site refrigerator at approximately 5°C. Injection loop samples were taken immediately prior to injection, at 5 minutes and 20 minutes after each individual injection, and at intervals of every 20 minutes for at least three hours following the last injection.

7.6 Tracer Description

This section presents additional details regarding ground water tracers used in this project. Injectate concentrations, injection times, and estimates of initial aquifer concentrations are reported in this section.

Bromide, polystyrene microspheres, and encapsulated *Flavobacterium* cells were used in tracer tests T1 and T3; bromide was used in tracer tests T2 and T4. Table 7.6-1 provides tracer injection times for each test. Tracers were injected at 20-minute intervals to avoid any interference between tracers. The times given in Table 7.6-1 are based on the beginning of the first tracer injection. Tracer test concentration data (Chapter 8 results) were later normalized to the bromide injection time.

	T1	T2	T3	T4
Date	9/15/93	9/17/93	10/2/93	10/7/93
Bromide Injection	$t = 0$	$t = 0$	$t = 0$	$t = 0$
Polystyrene Microsphere Injection	$t = 20$	none injected	$t = 40$	none injected
Encapsulated Cell Injection	$t = 40$	none injected	$t = 60$	none injected

Table 7.6-1: Injection times (in minutes from when the tracer tests began) for tracer tests T1, T2, T3, and T4.

Potassium bromide was used as a conservative tracer to represent average ground water flow velocities. Background bromide concentrations at the site were very low; bromide was considered biologically stable and was assumed to not precipitate, absorb, or desorb (Davis et al., 1985). A 100-ml solution consisting of 10 g potassium bromide (KBr) and ground water collected from the circulation-loop pumping well was mixed just prior to each tracer test. The solution was poured into two 60-ml syringes and attached to a two-syringe manifold. KBr injection for each tracer test lasted

approximately one minute. The KBr injection was conducted at $t = 0$ minutes for each test, where t represents the time that the first injection began.

Injection well concentrations were sampled at 5-minute intervals beginning at 5 minutes after injection, and every 20 minutes thereafter for a period of 2 hours. An initial concentration was estimated on the basis of the injected potassium bromide mass and the fluid volume in the injection well. These estimated initial concentrations are given in Table 7.6-2. The actual concentration in MW-19 for T3 was somewhat less than indicated because of the accidental loss of approximately 10% of the injectate during injection. Measured bromide concentrations following injection are shown in Figure 7.6-1 (the first point on each curve is the estimated concentration from Table 7.6-2).

Injection Well	Approximate Initial Concentrations
MW-16 (T1 and T2)	16,100 ppm
MW-19 (T3 and T4)	14,800 ppm

Table 7.6-2: Estimated initial injection well bromide concentrations during tracer tests T1, T2, T3, and T4.

Fluorescent, monodispersed polystyrene (2.5% solids latex) microspheres (*Polysciences, Inc.*) were injected in Tracer Tests T1 and T3. Microsphere sizes are given in Table 7.6-3. Estimated numbers of particles per milliliter are also given in Table 7.6-3; particle counts may be calculated with the following equation (*Polysciences, Inc.*): microspheres/ml $= \dfrac{6W \times 10^{12}}{r \times \pi \times f^3}$ where

W = grams of polymer per ml in latex (0.025 g for a 2.5% latex).

f = Diameter in μm of latex particles.

r = Density of polymer in grams per ml (1.05 for polystyrene).

The estimated initial injection well sphere concentrations, calculated on the basis of the injection well fluid volumes, are also provided in Table 7.6-3.

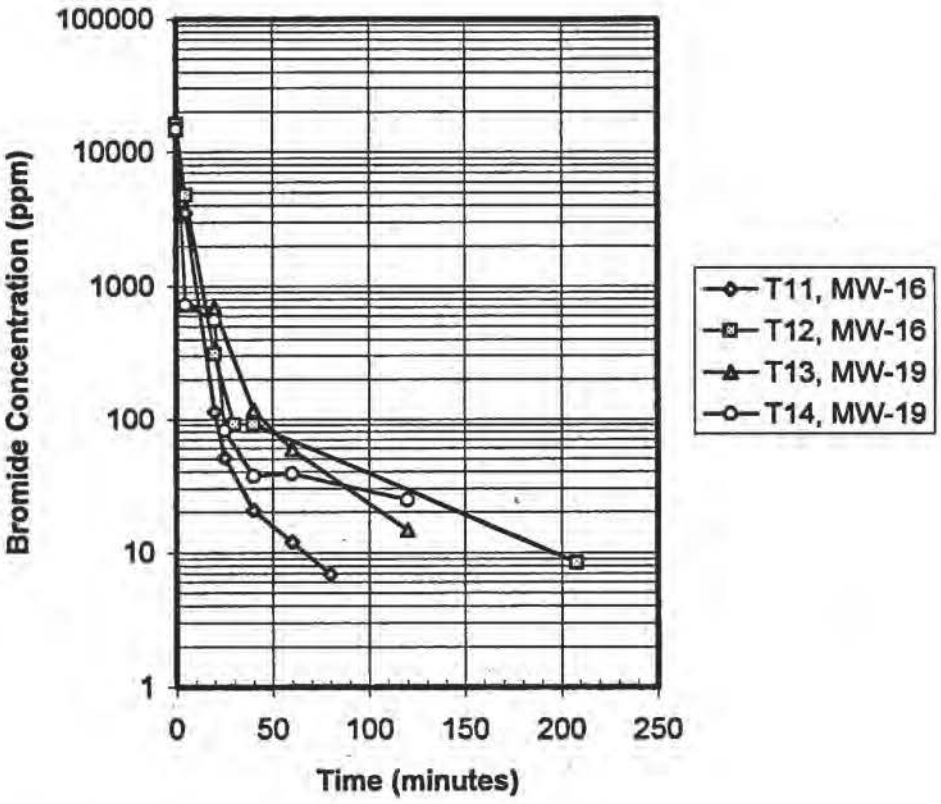

Figure 7.6-1: Bromide concentrations in injection wells.

Tracer Test	Size (μm)	Std Dev (μm)	Approx Volume (ml)	Approx # Spheres/ml*	Approx Total Spheres	Estimated Injection Well Concentration
T1	1.962	0.05	5	6.02×10^{9}	3.01×10^{10}	9.5×10^{7}
T1	5.475	0.42	2	2.77×10^{8}	5.54×10^{8}	1.75×10^{6}
T1	15.8	2.84	2	1.15×10^{7}	2.31×10^{7}	7.3×10^{4}
T3	1.962	0.05	5	6.02×10^{9}	3.01×10^{10}	8.5×10^{7}
T3	5.475	0.42	2	2.77×10^{8}	5.54×10^{8}	1.56×10^{6}
T3	15.8	2.84	2	1.15×10^{7}	2.31×10^{7}	6.5×10^{4}
* See equation in text						

Table 7.6-3: Injected microsphere sizes and approximate concentrations.

The polystyrene microspheres were removed from refrigerated storage immediately prior to each tracer test, vigorously shaken for approximately one minute, and decanted into a 10-ml syringe. Polystyrene microspheres were injected in the same manner as described for bromide.

The final tracer consisted of encapsulated *Flavobacterium* ATCC 39723, a gram-negative aerobe that degrades a variety of chlorinated phenols such as pentachlorophenol (PCP). *Flavobacterium* cells were grown in mineral salts using Na-glutamate as the carbon and energy source. Pentachlorophenol (PCP) was added (50 mg/liter) to induce the catabolic enzymes responsible for degradation of chlorinated phenols. Cell suspensions were passed through a low-pressure nozzle into an aqueous phase where matrix polymerization or gelation yielded beads of 2- to 80-μm diameter. A distribution of bead sizes is given in Figure 2.3-1. This method for the encapsulation of bacteria into microspheres of alginate, agarose, or polyurethane is further described in Stormo (1993).

Approximately 10 ml of solution (deionized water) containing encapsulated cells was injected in tracer tests T1 and T3. The 10 ml solution contained an estimated 10^7 to 10^9 beads (Stormo, unpublished data). Approximately 36% of the beads by volume were 10-μm or less in diameter (see Figure 2.3-1). On the basis of previous work, approximately 99% of the encapsulated cell microbeads (by number) were 10-μm in diameter or less; 94% by number were 5-μm in diameter or less (Stormo, personal communication).

Prior to injection, the encapsulated cells were stained with a 0.01% solution of acridine-orange dye. The encapsulated cells were then centrifuged at approximately 5000 × g, and excess fluid was carefully decanted. The encapsulated cells were rinsed five times by adding deionized water and repeating the centrifuging and decanting process.

Encapsulated cells were injected in tracer tests T1 and T3 as described above. A 10-ml volume of beads was injected by syringe at $t = 40$ minutes in tracer test T1 and at $t = 60$ minutes in test T3.

7.7 Sampling System

The ground water sampling system used during the tracer tests is described in this section. Components of the ground water sampling system include well samplers, the sample collection system, and a data collection system. Also described is a flow-through bromide probe system used for monitoring bromide in selected wells.

The purpose of the sampling system was to allow collection of approximately 15-20 ml of ground water for analyzing tracer concentrations with minimal disturbance to the flow field. Sampling frequency needed to be sufficient for adequately defining tracer concentration curves. Samples needed to be collected from a minimum of five wells over a period of at least 32 hours.

Ground water sampling frequently includes purging three or more well volumes prior to sampling. Removal of three or more well volumes prior to sampling every 10-20 minutes would affect the local hydraulic gradient, because of the relatively low transmissivity of the field site aquifer. A continuous sampling system was developed (1) to reduce the need for well purging, and (2) to automate the sampling process (because of multiple wells and frequent sampling requirements).

The sampling system developed for this project thus consisted of low-flow borehole samplers and an automated sample pumping and collection system. This system is outlined in Figure 7.7-1.

Ground water samplers consisted of 0.13-cm diameter TFE tubing (*Cole Parmer*) attached to the outside of a 1.6-cm PVC pipe (Figure 7.7-2). The purpose of the 1.6-cm PVC pipe was to reduce the volume of water in the monitoring well casing. The volume of water held in each monitoring well with sampler in place was approximately 120 ml per meter of casing length.

Samplers were placed in the 1.9-cm monitoring wells. Each sampler was placed such that the 0.13-cm tubing was located approximately 15 cm from the bottom of the 1.9-cm diameter well screen (centered over the well screen interval), and on the upgradient side of the well. A 3.5 N/cm^2 (5 p.s.i.) or 13.8 N/cm^2 (20

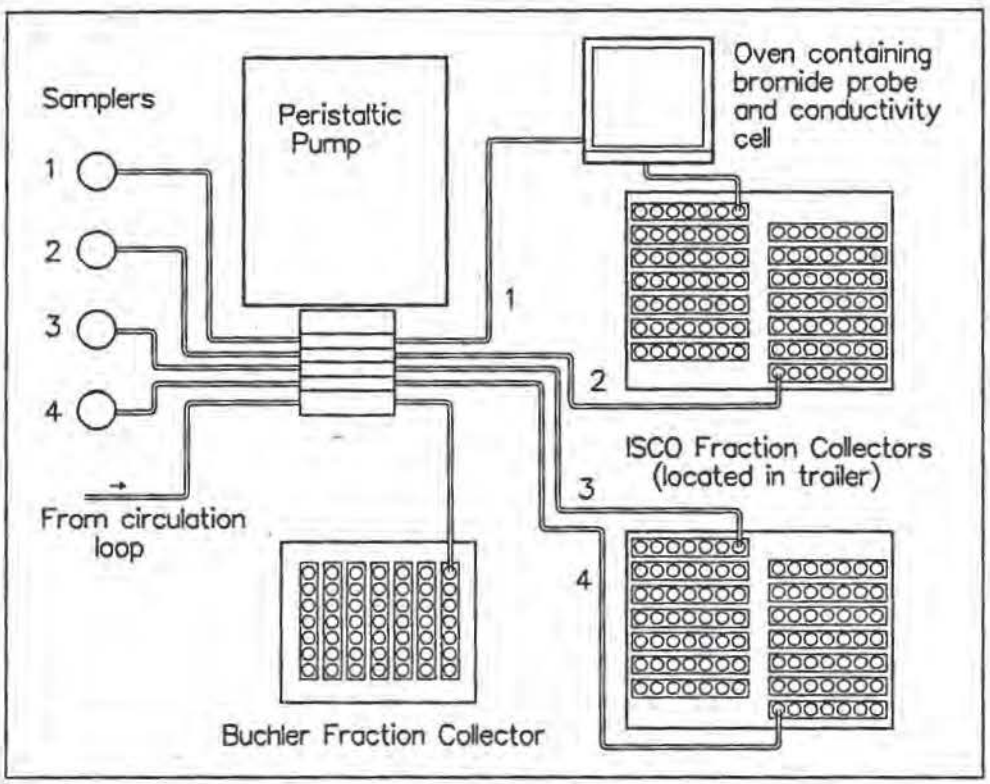

Figure 7.7-1: Continuous ground water sampling system.

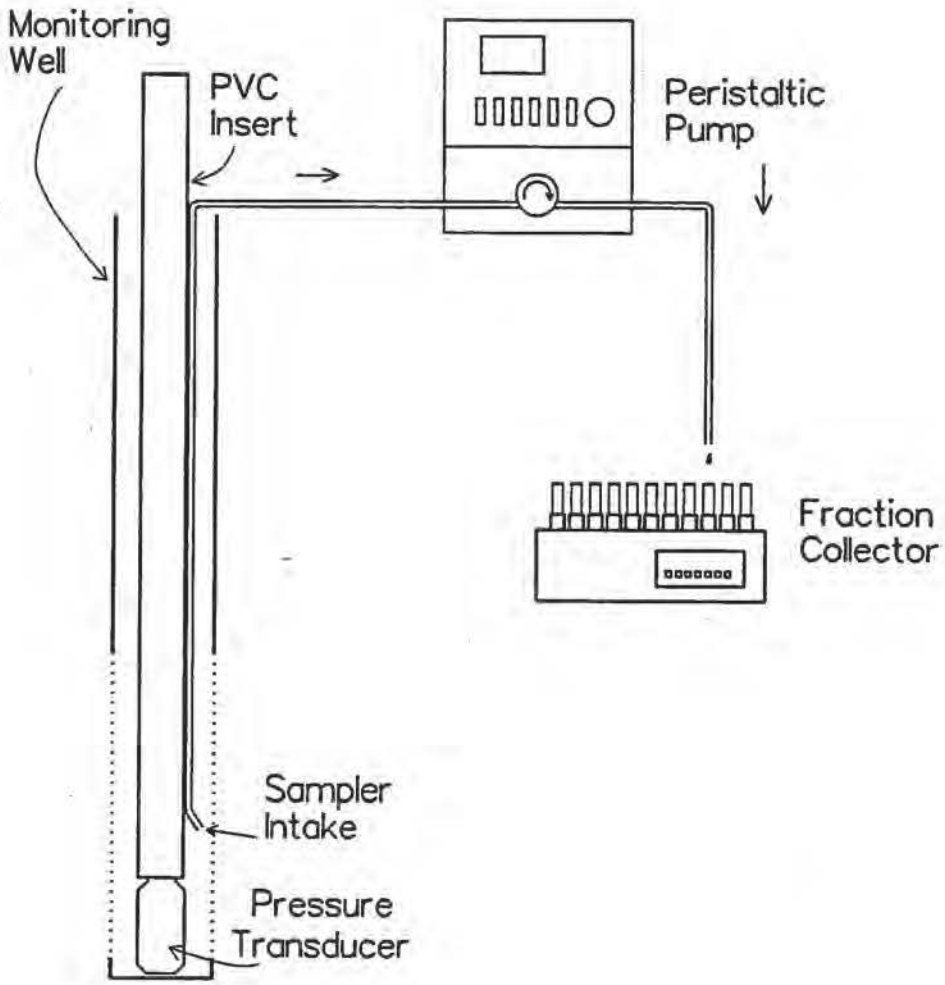

Figure 7.7-2: Sampler schematic.

p.s.i.) transducer for monitoring water levels (see Section 5.4) was threaded through the inner PVC pipe (and sealed to the end of the pipe) before placing the sampler into the well.

The TFE sampler tubing was routed from the well samplers to a *Cole Parmer Masterflex Digistaltic* pump (#7527-00). The pump, modified to accept a multiple-cartridge head, pumped fluid from all sampling wells and from the recirculation loop. The TFE sampler tubing was connected to 46-cm lengths of *Pharmed #13 Masterflex* tubing (0.08-cm diameter), which were routed through the pump cartridges and advanced periodically to minimize flow rate changes due to tubing wear. Occlusion screws in the pump cartridges allowed adjustment of flow rates in individual sampling lines. Finally, 0.11-cm TFE tubing carried sampling fluid from the digistaltic pump to fraction collectors.

Tubing sizes were selected by the following criteria. First, a sample flow rate of 1 ml/min or less was desired to minimize withdrawal effects on local hydraulic gradients. Second, it was desirable to keep fluid volumes in the sampling system at a minimum, to reduce sample mixing and to minimize sample travel times (to the collection system). Tubing diameters had to be large enough, however, to minimize the chance of clogging (limited particle clogging in sampling lines was experienced in the previous column experiments) and to avoid excessive tubing pressures. The 0.13-cm diameter tubing was therefore selected where the fluid pressures were negative (vacuum) and where friction losses would influence the depth from which samples could be removed; the 0.11-cm diameter tubing was selected for longer travel distances under positive pressure; the *Pharmed* tubing was selected where wear characteristics were important (e.g., in the pump cartridges). Finally, tubing lengths from all samplers within a transect were identical (see Table 7.7-1) so that fluid travel times from various samplers would be the same.

Water levels in sampling wells were monitored with the transducer attached to the bottom of the sampler. The *Solinst* water level indicator probe would not fit into 1.9-cm-diameter wells containing samplers (for hand measurements). A wire probe extension was fashioned that would extend into the annulus between the well casing and

the sampling apparatus in these wells. Water levels using the probe extension were taken in wells with transducers to provide calibration data.

Flow rates in the continuous samplers ranged from approximately 0.75 to 1.0 ml/min. Experimentation with this flow rate indicated negligible, if any, effect on local hydraulic gradients.

Transect	Tubing Material	Diameter (cm)	Length (cm)	Volume (ml)	Discharge (ml/min)	Travel Time (min)	Total Travel Time (min)
B	TFE	0.13	447	6.1	0.75	8.2	17.2
	Pharmed	0.08	46	0.2	0.75	0.3	
	TFE	0.11	726	6.5	0.75	8.7	
C	TFE	0.13	411	5.6	0.75	7.5	10.6
	Pharmed	0.08	30	0.1	0.75	0.2	
	TFE	0.11	244	2.2	0.75	2.9	

Table 7.7-1: Sampler tubing details.

A flow-through monitoring system was built to monitor bromide and electrical conductivity in one sampling line per test. The purpose of the flow-through probe was to (1) monitor bromide concentrations during individual tracer tests, (2) maintain data quality control (for comparison with subsequent laboratory analysis), and (3) evaluate sampling frequency (e.g., a 20-minute averaged sample would provide insufficient resolution if a bromide peak lasted less than 20 minutes). The flow-through probes were installed in sampling lines from MW-18 (tracer tests T1 and T2) and MW-21 (tracer test T3 and T4). These wells were the closest wells to the tracer injection well screened in the lower portion of the aquifer.

The flow-through bromide-monitoring system was constructed as shown in Figure 7.7-3 and was housed in the instrumentation trailer. A special glass housing was fabricated that would allow the fluid sample to come in contact with a *Cole-Parmer* single junction bromide electrode (#G-27502-05). It was found that diurnal temperature swings caused significant errors in bromide readings when the electrode

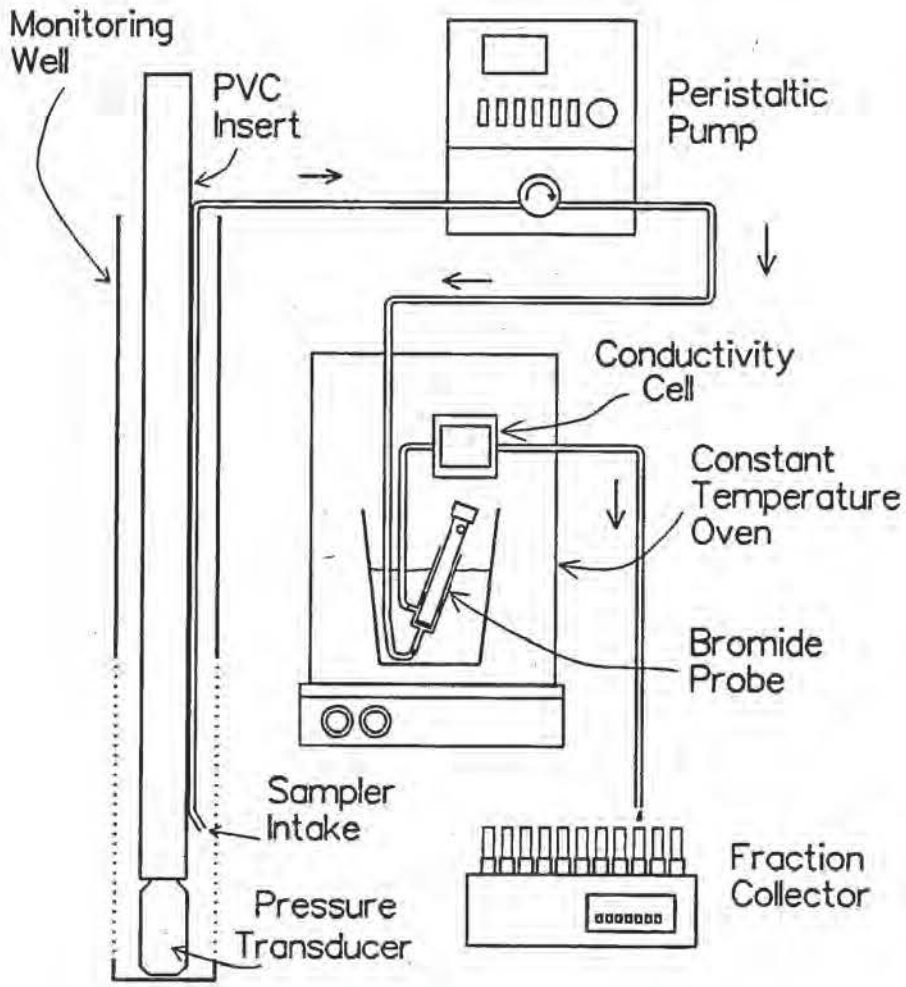

Figure 7.7-3: Flow-through bromide-monitoring system

was in use over a period of many hours. The probe and outer glass housing were therefore submerged in a water bath, which in turn was placed in a constant temperature oven; a thermometer was kept in the water bath for periodic temperature measurements. The oven was kept at approximately 35°C. The probe was positioned in the water bath at an angle so as to prevent the buildup of air bubbles at the bromide probe tip. The probe was calibrated by running known standards (made with ground water taken from the active pumping well before a tracer test began) through the bromide probe system at the same flow rate as the sampling system, i.e., approximately 0.75 ml/min.

Linear-log calibration curves are generally used for determining sample concentrations from the bromide electrode. A non-log-linear relationship (with assistance from the University of Idaho Mathematics Help Desk) was developed for this analysis to allow better calibration at low concentrations. Calibration curves were calculated using the expression $f = \ln(b) + \{p * \ln(a - (x - x'))\}$, where

$f = ln\{ln(y)\}$,

y is the concentration in parts per billion,

x is the mV reading from bromide probe, and

x' is the maximum x value.

The parameters a, b, and p are curve-fitting parameters. Individual x values were occasionally weighted by measurement confidence for better curve fits. This curve-fitting process provided better curve fits than commonly used regression fits due to non-linearity at low concentrations.

A flow-through conductivity cell was installed in conjunction with the bromide cell, and was also housed in the constant-temperature oven. The conductivity probe proved too insensitive for measuring bromide concentrations.

Fluid samples from monitoring wells were collected continuously with two *Isco* fraction collectors, located in the instrumentation trailer. The collectors were modified such that each collector could collect fluid samples from two wells. Samples were collected in 16 x 150 mm disposable glass tubes. Each fraction collector would collect approximately 70 tubes from each sample line before tube replacement was necessary. Sample tubes advanced every 20 minutes; after 20 minutes the sample tube contained

approximately 15 ml (at a flow rate of 0.75 ml/min), depending on pump head adjustment, tubing wear, outside temperature, etc. Sample tubes were removed from the samplers approximately every 10 hours, capped, labeled, and refrigerated on-site at approximately 5°C. Sample tubes were labeled with the tracer test number, the sampler (or well) number, and the tube number in indelible ink. Following each tracer test, sample tubes were transported to a University of Idaho laboratory and were refrigerated at 5°C.

Sediment samples from the bottom of each well were obtained following the last tracer test. The reason for sampling bottom sediments was to determine if tracer particles were settling to the bottom of the well casings (i.e., to determine if sampling velocities were too low to keep particles in suspension).

Two *Campbell Scientific 21X* data recorders (housed in the instrumentation trailer) were used to record data during the course of the tracer tests (Figure 7.7-4). The first data logger recorded pressure transducer readings from monitoring wells MW-5, MW-16, MW-18, MW-19, MW-20, MW-21, and MW-23 during tracer tests T1 and T2, and from monitoring wells MW-5, MW-6, MW-12, MW-14, MW-19, MW-20, MW-21, and MW-25 during tests T3 and T4. The second data logger recorded flow-through bromide probe data in tracer tests T1 through T4. Data files from the data logger were downloaded to computer, converted to ASCII files, and analyzed with spreadsheet software.

7.8 Laboratory Analysis

Laboratory analysis of bromide concentrations was conducted with the same *Cole-Parmer* bromide electrode (#G-27502-05) used for the flow-through bromide monitoring. Millivolt readings were given by a *Fisher Accumet Mini* pH meter (model 955). Samples and standards were prepared by warming them to room temperature before analysis (for consistency between analyses). The bromide probe was allowed to equilibrate in each sample for 6 minutes; a *Corning* magnetic stirrer was used to stir samples during this time. Temperature was monitored before and

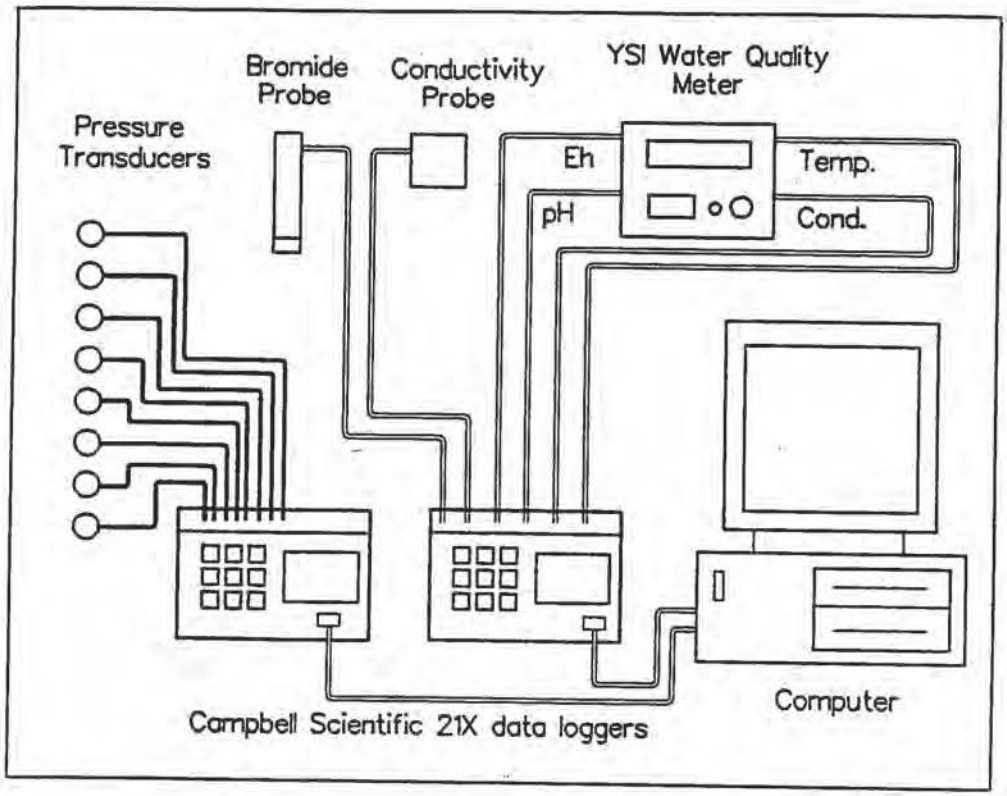

Figure 7.7-4: Data collection system.

after analysis. Calibration readings were taken using the same standards that had been prepared for flow-through calibrations (see previous section). Whenever possible, all samples from one observation well (and one tracer test) were analyzed at the same time.

Error sources for the selective ion electrode measurements include interference from other ions, temperature variation, and calibration. Selective ion electrodes were considered suitable for rapid estimation of ion constituents.

Polystyrene microsphere analysis was conducted by filtering water samples through porous filters and examining the filters under a microscope. Water samples with expected high concentrations were diluted with deionized water. Dilution was required to obtain a density that could be counted reliably. Water samples were shaken by hand prior to dilution or filtration. Hand-shaking with an up-and-down motion caused spheres to stay in suspension; vortexing or swirling the sample left spheres attached to tube. *Nuclepore* filters (0.2 or 1.0 μm) were used for filtration. The filter was placed on a microscope slide with a drop of immersion oil above and below the filter and covered with a cover slip.

The amount of fluid sample used for filtration depended on the expected microsphere concentration. Fluid volumes collected in the fraction collectors averaged approximately 15 ml. Fluid volumes removed for filtration ranged from one ml to approximately 10 ml. The filtration volume was diluted to as much as 1:1000, depending on the expected microsphere concentration.

Microsphere slides were counted using a Carl Zeiss microscope system equipped with an HBO-100 high-pressure mercury illuminator, a 10x ocular lens, and 4x, 10x, 40x, and 100x (oil) objectives. Individual bead sizes were counted at either 40, 100, or 400 magnifications, depending on the bead size and the quantity of beads. If possible, a full scan was made at 100 power. If the number of beads was too large, a minimum of 20 random fields were counted, from which an average and a standard deviation were calculated.

Only a small number of the total samples were analyzed for the presence of microspheres because of the analysis cost. Initial samples were selected on the basis of

expected tracer arrival; additional samples were selected, where possible, near times of observed higher concentrations.

Duplicate slides (approximately 10% of the counted slides) were prepared to evaluate error inherent to slide preparation. Duplicate counts of the same slide were conducted by different technicians to evaluate inherent counting error. Blank slides were also prepared following slides with high sphere concentrations as a check on apparatus cleansing. Duplicate slide counts are discussed in Chapter 9.

Slides prepared for polystyrene microspheres were also used for encapsulated cell counts. Random fields were scanned at 1000 magnifications because of the relative faintness of the encapsulated cells as compared to the microspheres. Significant problems were encountered in attempting to count encapsulated cells with this method. First, the polystyrene microspheres were much brighter than the encapsulated cells, making it difficult to count encapsulated cells in the vicinity of the microspheres. Second, the acridine-orange stain appeared to disappear fairly quickly when exposed to the ultraviolet light. Finally, the shelf-life of the acridine-orange stain appeared to be limited; very few encapsulated cells could be seen in duplicate slides prepared several months after the initial slide preparation. Encapsulated cell counts from microscope analysis are not reported because it was apparent that the method was leading to unacceptable results.

A polymerase chain reaction (PCR) technique was used for determining the presence of *Flavobacterium* deoxynucleotides (DNA), as an alternative to microscopic detection (this analysis was conducted by Dr. D. Knaebel, University of Idaho). The polymerase chain reaction techniques is a process that produces thousands or millions of copies of a certain DNA fragment. The polymerase chain reaction technique begins with separating DNA strands and annealing synthetic oligonucleotide "primers" (short, single-stranded DNA fragments) to specific sites of the separated *Flavobacterium* DNA strands. When DNA polymerases in the presence of deoxynucleotide triphosphates recognize the single-stranded DNA, they will synthesize the other strand of DNA. When repeated, this process can lead to an exponential increase in the number of copies

in the target DNA section. This technique can be used for other analyses to determine the presence (qualitatively) of a certain organism.

The primers for PCR were based upon a portion of the *pcpA* gene found on the chromosome of the *Flavobacterium* (Xun and Orser, 1991) In addition to detecting the wild type gene, PCR analysis was done in the presence of a plasmid (pKS412) construct that contained an internal ~101 base pairs (bp) deletion in *pcpA* (Stormo, 1993).

7.9 Data Analysis

This section presents a discussion of tracer test analysis methods. Analysis methods for this project were selected on the basis of the purpose and objectives outlined in Chapter 1, the type of data expected, and the quantity of data expected.

Tracer test analysis methods are available for evaluating a variety of hydrogeological and tracer transport characteristics. Uniform flow tests (such as those conducted for this project) can be used to estimate parameters such as dispersion and average ground water velocities (Davis et al, 1985). Data collected from extensive ground water monitoring networks have been used to evaluate aquifer anisotropy and hydraulic conductivity (Kenoyer, 1988; Hess et al., 1987; Garabedian et al., 1987), advection and dispersion (Freyberg, 1986; Mackey et al., 1986), spatial variability in hydraulic conductivity (Sudicky, 1986), and solute properties (Curtis et al., 1986; Roberts et al., 1986).

Both qualitative and quantitative analysis methods have been used in tracer tests. For example, Freyberg (1986) and Garabedian (1987) used spatial moments methods to evaluate advection and dispersion of nonreactive tracers on the basis of data from an extensive monitoring network. Analyses in which microspheres tracers were used (Harvey et al., 1989; Harvey, 1993; Champ and Schroeter, 1988) have consisted of qualitative comparisons of particle and conservative tracer concentrations.

Tracer test results from the experiments conducted for this project were evaluated on a qualitative basis, i.e., visual comparison of tracer concentration curves. Qualitative methods were chosen because the study objectives focused on an initial qualitative comparison of three tracers (bromide, polystyrene microspheres, and

encapsulated cells). The monitoring system was tailored to a comparison of tracer transport on two-dimensional basis. The monitoring system was not designed to collect extensive three-dimensional data such as might be used for investigating spatial aquifer properties, largely because of limited funds.

Mass balance calculations are frequently used for insight into tracer retardation processes. The recirculating-loop system as constructed for this project makes the mass balance calculation problematic, since tracer eventually begins to recirculate with in the loop. This is a desirable quality from a bioremediation perspective, since contact between contaminant and introduced microbes is enhanced, but it renders mass balance calculations less meaningful.

7.10 Replicate Tracer Tests

Tracer tests T2 and T4 were conducted with bromide tracer as replicates of tracer tests T1 and T3, respectively. The purpose of conducting replicate tracer tests was to evaluate sampling reliability and to monitor possible aquifer changes due to the tracer tests. Small-diameter sampling lines are susceptible to reductions in flow due to sample-tubing wear, film deposits, etc., which may lead to subtle changes in sampling system efficacy. Particle tracers could conceivably clog micro-flowpaths near the injection well, in the aquifer, and/or in the sampling system. Replicate tracer tests using a conservative tracer (e.g., bromide) were conducted after the bead injections as a check on bead-clogging in aquifer flowpaths or in the sampling system.

8. Bromide Transport Results

8.1 Introduction

This chapter begins the presentation of tracer test results. Bromide transport results from tracer tests T1 through T4 are presented in this chapter. Polystyrene microsphere transport data are presented and compared to bromide concentration data in Chapter 9. Encapsulated cell transport data are provided in Chapter 10. A discussion about bromide, polystyrene microsphere, and encapsulated cell transport results is presented in Chapter 11.

The bromide transport results are provided in the form of tracer concentration data and breakthrough curves. Tracer concentration data are reported for monitoring well samples and flow-through bromide probe readings. Bromide concentration data for tracer tests T1 and T3 are presented first, followed by bromide concentration data from replicate tests T2 and T4.

Data analysis consists primarily of visual comparisons between bromide tracer concentrations collected in different wells in different tracer tests. Such comparisons are consistent with the study objectives and with the type and quantity of data collected during these tracer tests.

The results of this project, as in many scientific endeavors, are limited by the experimental design and methods. The tracer tests were conducted on the basis of the goals and objectives outlined in Chapter 1, the experimental design formed in Chapter 3, and the specific methods described in Chapter 7.

8.2 Bromide Concentrations

Bromide concentrations for tracer tests T1 and T3 are shown in Figure 8.2-1 and 8.2-2. Concentrations are given for ground water samples collected from monitoring wells and from the flow-through bromide probe readings. Maximum bromide concentrations are listed in Table 8.2-1.

Several observations can be made from these bromide concentration graphs. First, the highest bromide concentrations in tracer test T1 (Transect C) were seen in

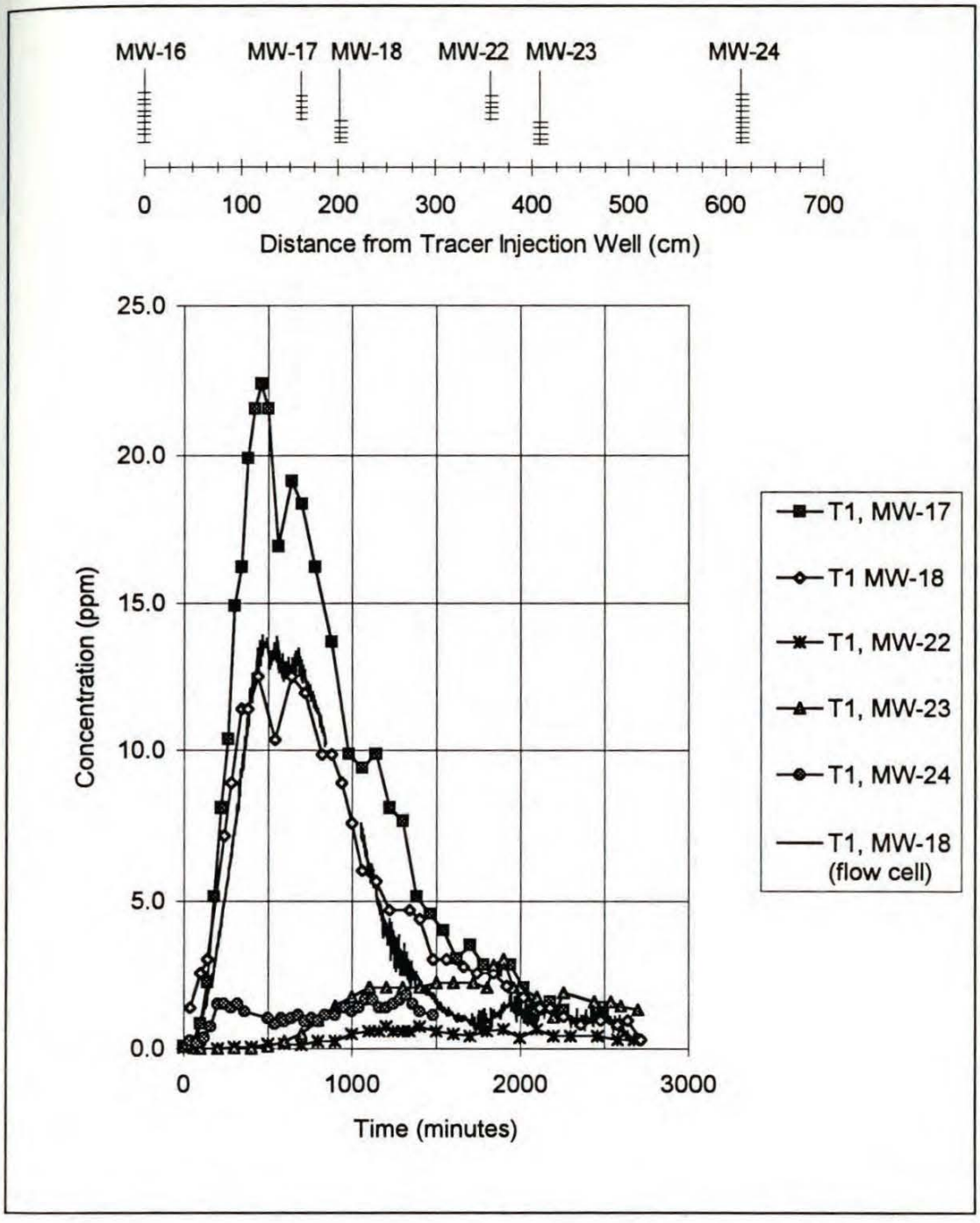

Figure 8.2-1: Bromide concentrations in Transect C during tracer test T1.

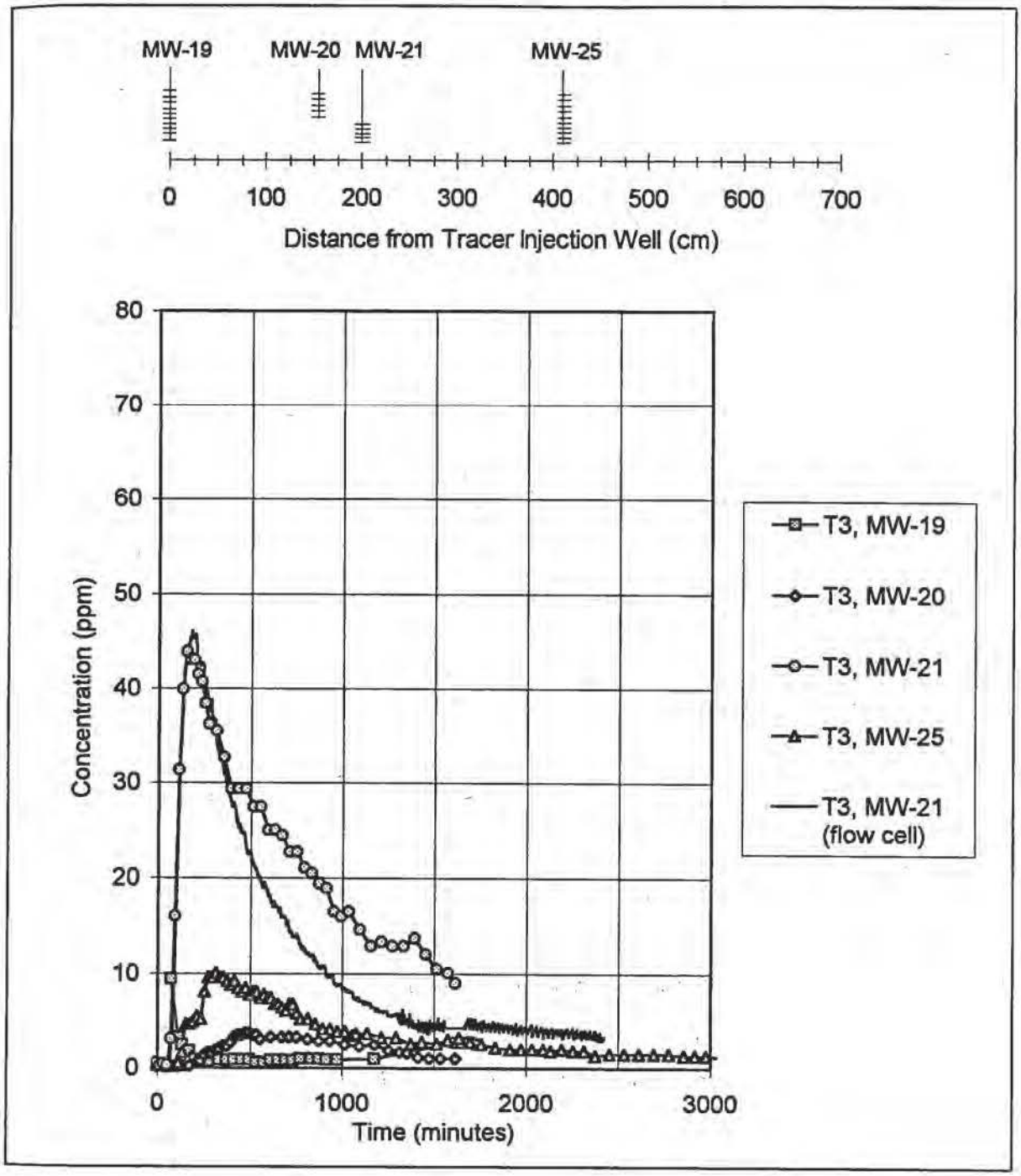

Figure 8.2-2: Bromide concentrations in Transect B during Tracer Test T3.

Well	T1	T2	Well	T3	T4
MW-17	22	19	MW-19*	9	1
MW-18	13	11	MW-20	4	2
MW-22	1	3	MW-21	44	55
MW-23	3	7	MW-25	10	6
MW-24	2	11			

Table 8.2-1: Maximum bromide concentrations (ppm) for tracer tests T1, T2, T3, and T4. (MW-19 concentration refers to peak concentrations after 1000 minutes of circulation).

MW-17 and MW-18. Higher tracer concentrations were observed in MW-17 than in MW-18 (MW-17 was completed higher in the aquifer than MW-18). The dip in bromide levels in wells MW-17 and MW-18 at approximately 550 minutes was caused by a glass tube jamming the fraction collector. The highest bromide concentration during tracer test T3 was observed in MW-21 (Figure 8.2-2). Concentrations in MW-21 were greater than in MW-20, despite MW-20 being closer to the tracer injection well than MW-21; MW-21 was completed in the lower portion of the aquifer, MW-20 was completed in the upper portion of the aquifer.

Second, the flow-through bromide probe measurements were generally similar to laboratory bromide measurements. The bromide flow-through cell installed in the sampling line of well MW-18 recorded bromide concentrations similar to those recorded from collected samples. The data anomalies seen from approximately 800 to 1100 minutes in the flow cell data were due to sample line freezing. The bromide concentrations in the flow cell connected to MW-21 closely correspond with laboratory bromide measurements from the same well up until approximately 400 minutes. The reason for the difference may be bromide probe calibration error, measurement error, or analysis error.

Discrepancies between flow-through cell readings and laboratory measurements, such as those seen between MW-21 bromide concentrations and the bromide probe measurements, may have been caused by using the bromide probe for extended

measurements without calibration. Frequent calibration was not feasible during the extended tracer tests.

Third, peak bromide concentrations in some wells (e.g., MW-21 during T3) were significantly asymmetrical. Asymmetrical bromide peaks were especially apparent in Transect B wells (e.g., MW-21).

Finally, bromide concentration increases in MW-19 were observed from about 1000 to 1600 minutes after injection (some data were lost during this time period due to sample-line freezing). This concentration increase probably reflects tracer recirculation in the well transect.

8.3 Bromide Breakthrough Curves

Tracer breakthrough curves are a means of comparing tracer arrival times at different wells. Breakthough curves are given in the form of C/C_{max}, where C represents the bromide concentration at any given time in a well and C_{max} represents the maximum concentration observed in the same well. The tracer breakthrough time is defined as the time span beginning when tracer was first observed in any given well through the time at which the tracer concentration reaches a maximum value. Breakthrough data are given as composite plots for each tracer test.

A bromide peak was considered to be significant if the concentration exceeded $3 \times s_d$, where s_d represents the standard deviation of averaged background samples. Breakthrough curves are based on C/C_{max} data from which the background concentration ($3 \times s_d$) has been subtracted. Estimated maximum background concentrations (based on $3 \times s_d$) are provided in Table 8.3-1.

The average background bromide concentration is higher in tracer tests T2 and T4 than in tracer tests T1 and T3. Initial bromide concentrations are higher in T2 and T4 because of the recirculating bromide remaining from tracer tests T1 and T3.

Breakthrough curves (based on C/C_{max} data) for tracer tests T1 and T3 are shown in Figures 8.3-1 and 8.3-2. Several observations can be made about bromide arrival from these figures.

	T1	T2	T3	T4
Average background Br^- concentration	0.2	2.5	0.6	1.1
s_d background Br^- concentration	0.45	1.76	0.56	0.85
Estimated maximum background concentration $(3 \times s_d)$	1.35	5.28	1.58	2.74
n	9	10	6	9

s_d represents the sample standard deviation of the averaged background samples, and n represents the number of background samples in each test.

Table 8.3-1: Estimated maximum background bromide concentration

First, Figure 8.3-3 shows tracer arrival in MW-17 and MW-18 (tracer test T1) soon after tracer injection. Second, the bromide concentration in MW-24 (the transect pumping well) increased soon after concentrations began rising in MW-17 and MW-18, and again when the bromide concentration increased in MW-23. The bromide concentration in MW-22 did not reach a level considered to be significantly above background.

Next, Figure 8.3-4 shows that bromide concentrations increased in MW-25 (tracer test T3, Transect B) before MW-20, despite MW-20 being significantly closer to the tracer injection well (MW-20 was completed in a higher aquifer zone than MW-21).

Average linear ground velocities were calculated from the bromide breakthrough curves. The average linear ground water velocity at any given monitoring well was calculated on the basis of the distance between the tracer injection well and the time that it took for the bromide to reach its maximum concentration. Average velocities are shown in Table 8.3-2.

The average linear velocity indicated in Table 8.3-2 for MW-24 is significantly larger than the other velocities calculated for Transect C wells. Because MW-24 is the pumping well in Transect C, tracer will be transported to MW-24 along the most conductive flowpath between the injection well and the pumping well. Increased gradients near the pumping wells (MW-24 and MW-25) may also have led to increased

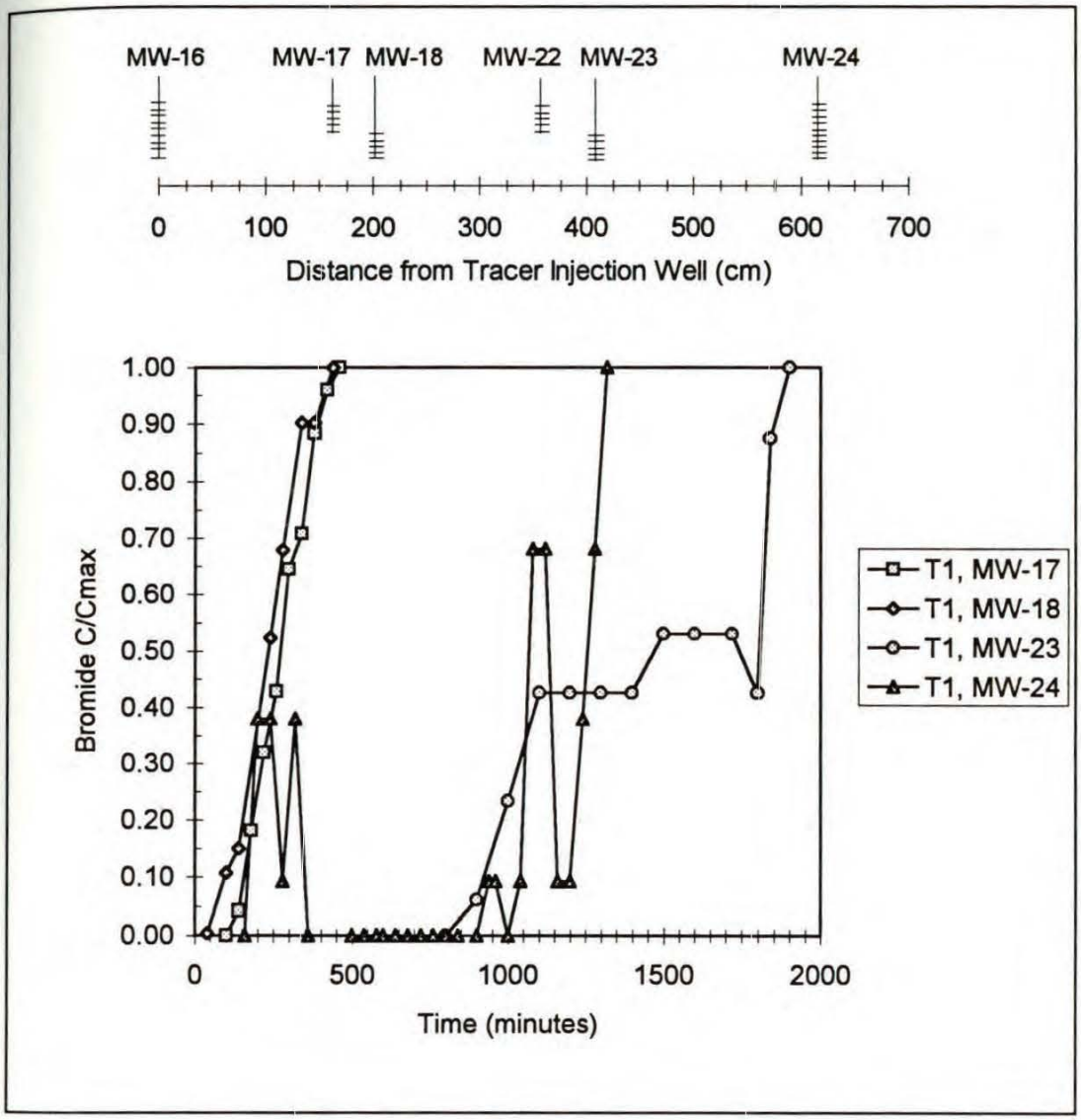

Figure 8.3-1: C/C_{max} for MW-17, MW-18, MW-23, and MW-24 in tracer test T1 (MW-22 did not reach a concentration above background levels).

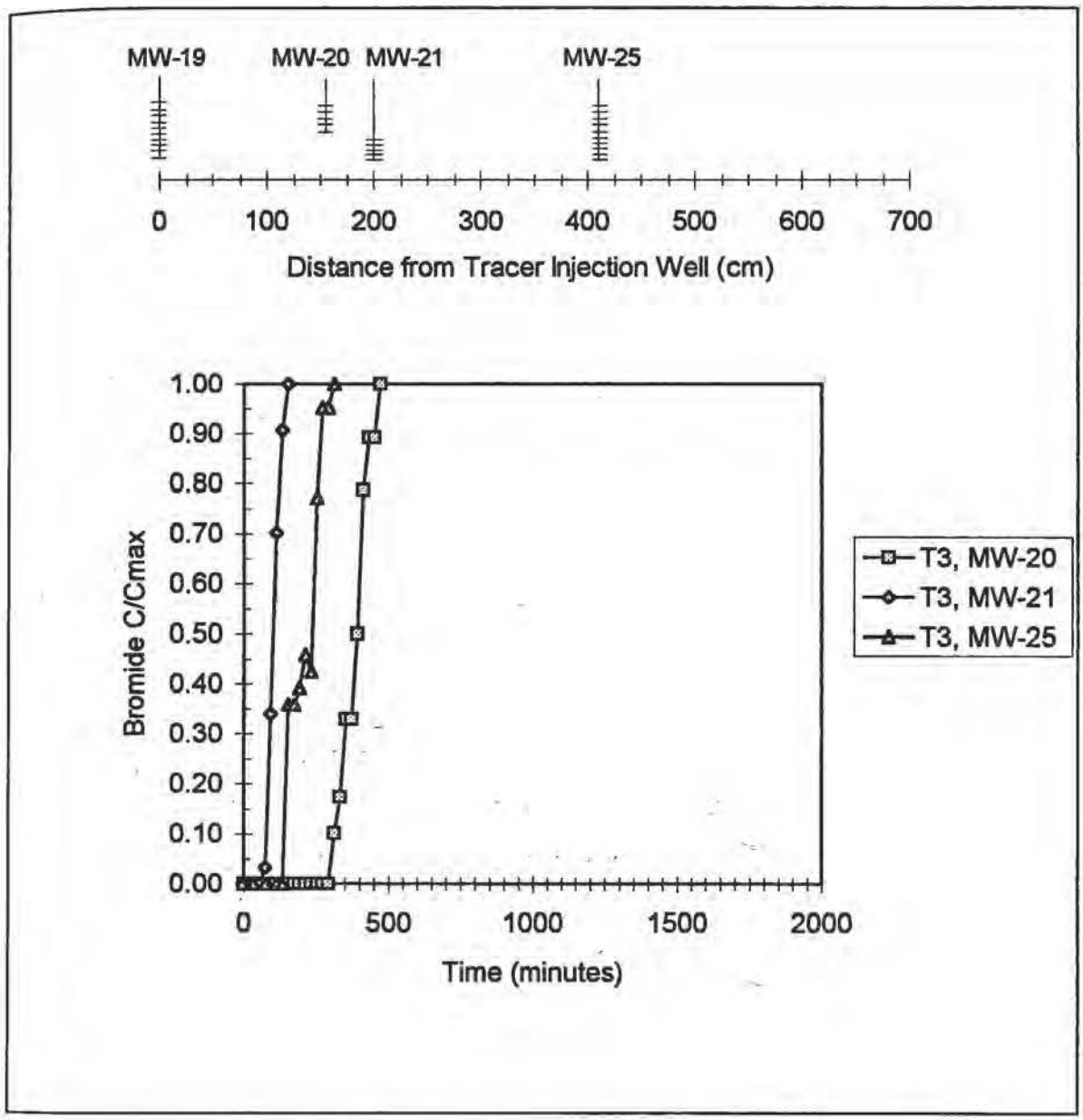

Figure 8.3-2: C/C_{max} for MW-20, MW-21, and MW-25 in tracer test T3.

Tracer Test, Monitoring Well	C_{max} Breakthrough Time (min)	Distance from Injection Well (cm)	Average tracer velocity (cm/min)
T1, MW-17	460	160	0.35
T1, MW-18	440	205	0.47
T1, MW-23	1900	405	0.21
T1, MW-24*	220	622	2.83
T3, MW-20	470	152	0.32
T3, MW-21	150	199	1.33
T3, MW-25	300	410	1.37

* Average tracer velocity for this well was estimated on the basis of the initial concentration increase at approximately 220 minutes (see Figure 8.3-1).

Table 8.3-2: Average bromide velocities in tracer tests T1 and T3.

average velocities, but do not account for tracer arrival in pumping wells before arriving in upgradient monitoring wells.

Monitoring wells downgradient of the tracer injection well and upgradient of the pumping well may or may not lie on the most conductive flowpath. The differences in average tracer velocities between monitoring wells and the pumping well in Transect C suggest that the most conductive flowpath between the tracer injection well and the pumping well does not lie in a straight line along the transect. Similar average tracer velocities between MW-21 and the pumping well in Transect B (MW-25) suggests that both of these wells intercept the most conductive flowpath between the tracer injection well and the transect pumping well.

8.4 Replicate Bromide Tracer Test Results

Replicate tracer tests were conducted in Transects B and C with bromide as a tracer. Tracer tests T2 and T4 were conducted as replicates of tests T1 and T3, respectively. Replicate tracer tests were conducted to evaluate injection and sampling consistency, and to identify possible pore-clogging effects of particle tracers.

Comparisons of bromide concentrations for MW-17, MW-18, and MW-24 in tracer tests T1 and T2 are provided in Figures 8.4-1 through 8.4-3. Comparisons of bromide concentrations are not provided for MW-22 and MW-23 since concentrations in these wells were very low.

Bromide concentrations in MW-17 in tracer tests T1 and T2 (Figure 8.4-1) were similar although the concentration in T1 increases somewhat faster than in T2. Bromide concentration curves for MW-18 during T1 and T2 (Figure 8.4-2) differed in magnitude and form. The bromide concentrations in MW-24 during T1 and T2 (Figure 8.4-3) began to rise at approximately the same time, but reached a different peak concentration (the background concentration in T2 was higher due to residual bromide remaining after T1).

Comparisons of bromide concentrations for wells MW-20, MW-21, and MW-25 in tracer tests T3 and T4 are provided in Figures 8.4-4 through 8.4-6. Bromide concentrations in MW-20 (Figure 8.4-4) remained relatively low in both tests; concentrations in T4 did not appear to rise significantly above background levels. Bromide concentrations in MW-21 during T3 and T4 (Figure 8.4-5) increased at approximately the same time, but reached different peak concentrations. Finally, bromide concentrations in MW-25 during T3 and T4 (Figure 8.4-6) showed similar responses.

Tracer arrival times should have been identical for the same wells if injection and transport conditions remained constant between replicate tests. In general, bromide concentrations in tracer tests T3 and T4 were more similar than concentrations in tracer tests T1 and T2. These differences in tests T1 and T2 were apparent in both flow-through probe concentrations and laboratory-measured data. The differences between bromide concentrations in replicate tests could have resulted from bromide probe calibration error, injection and/or sampling inconsistencies, differences in hydraulic gradient between tests, or clogging of aquifer sediments with particle tracers. Possible reasons for differences in replicate tests are addressed in Chapter 11.

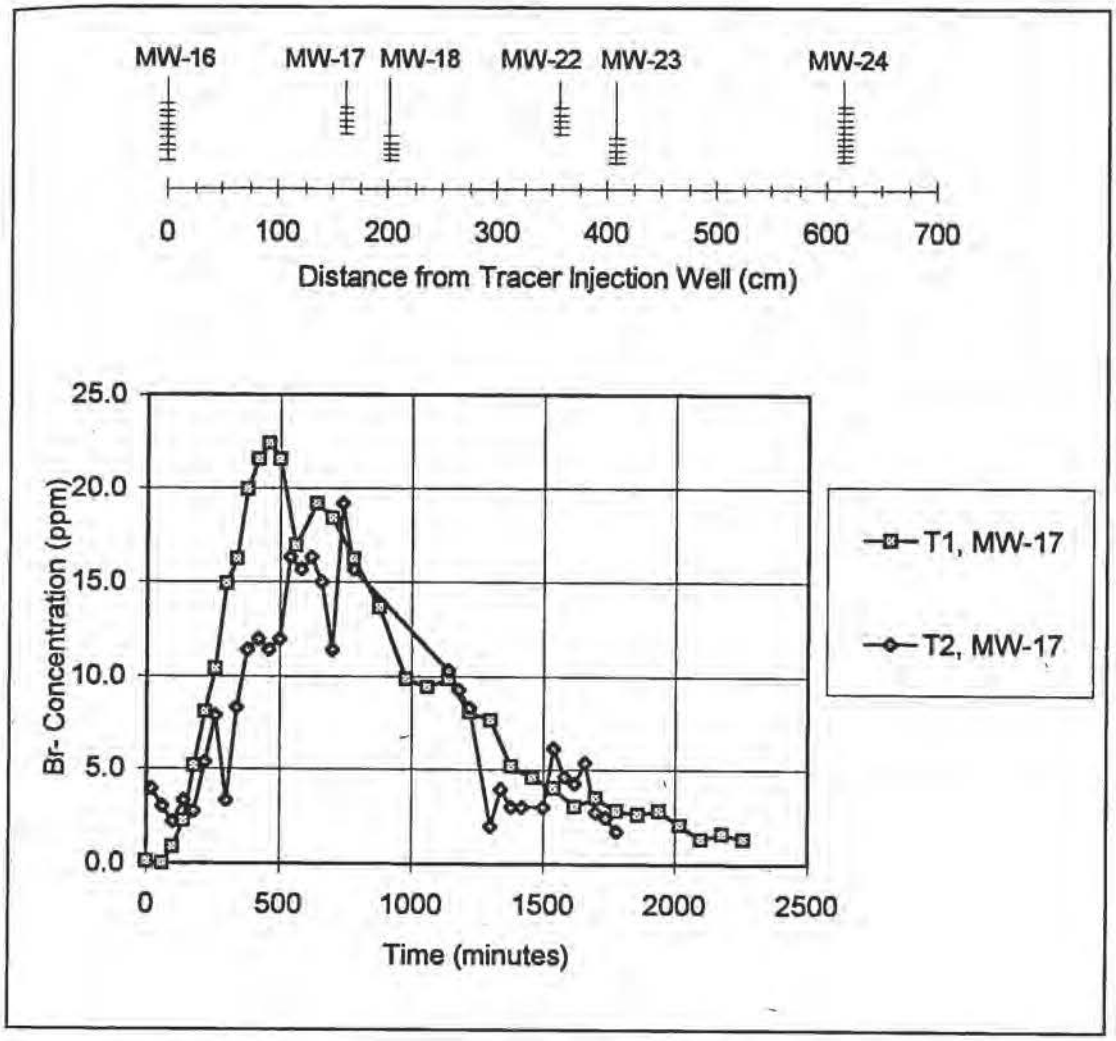

Figure 8.4-1: Bromide concentrations in MW-17 during Tracer Tests T1 and T2.

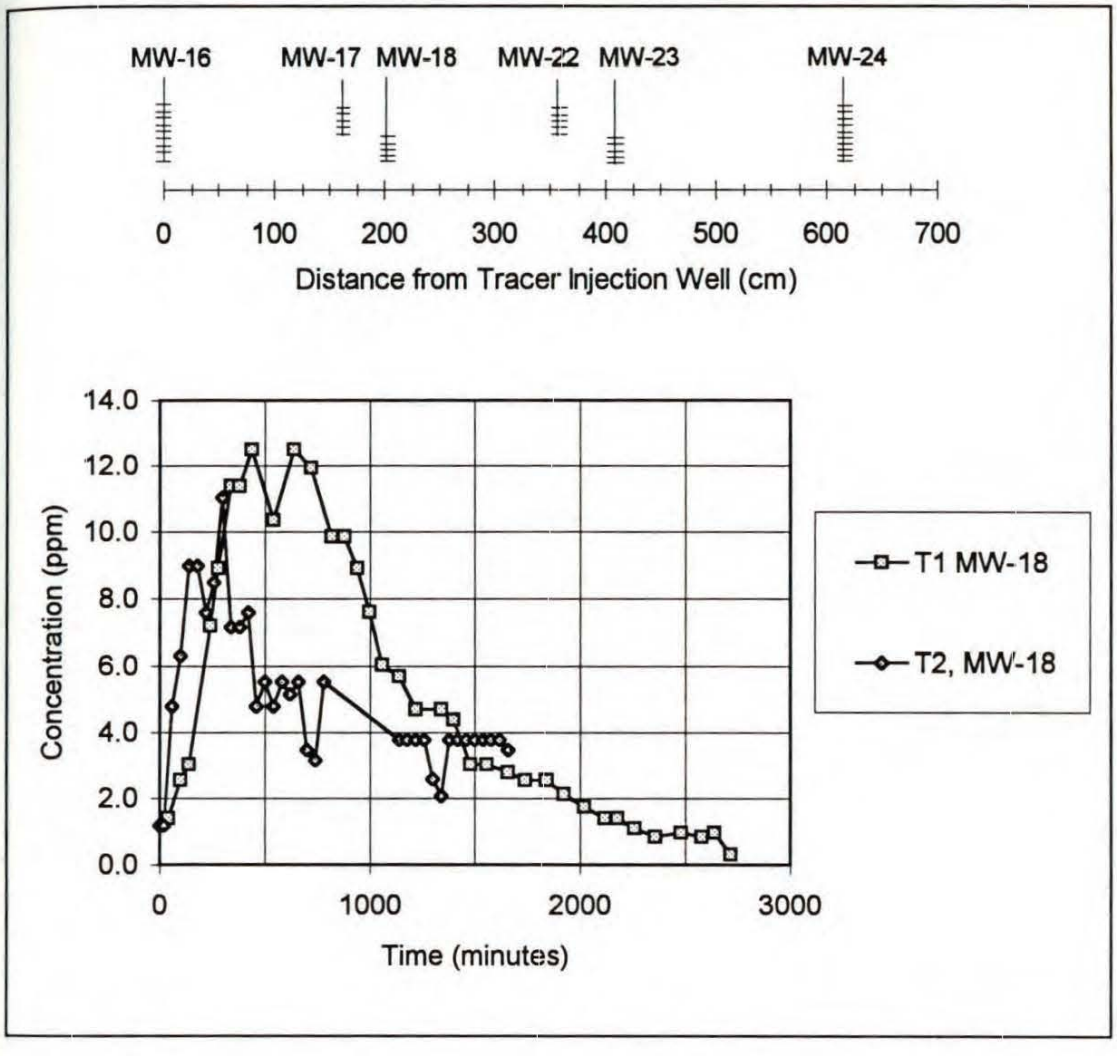

Figure 8.4-2: Bromide concentrations in MW-18 during Tracer Tests T1 and T2.

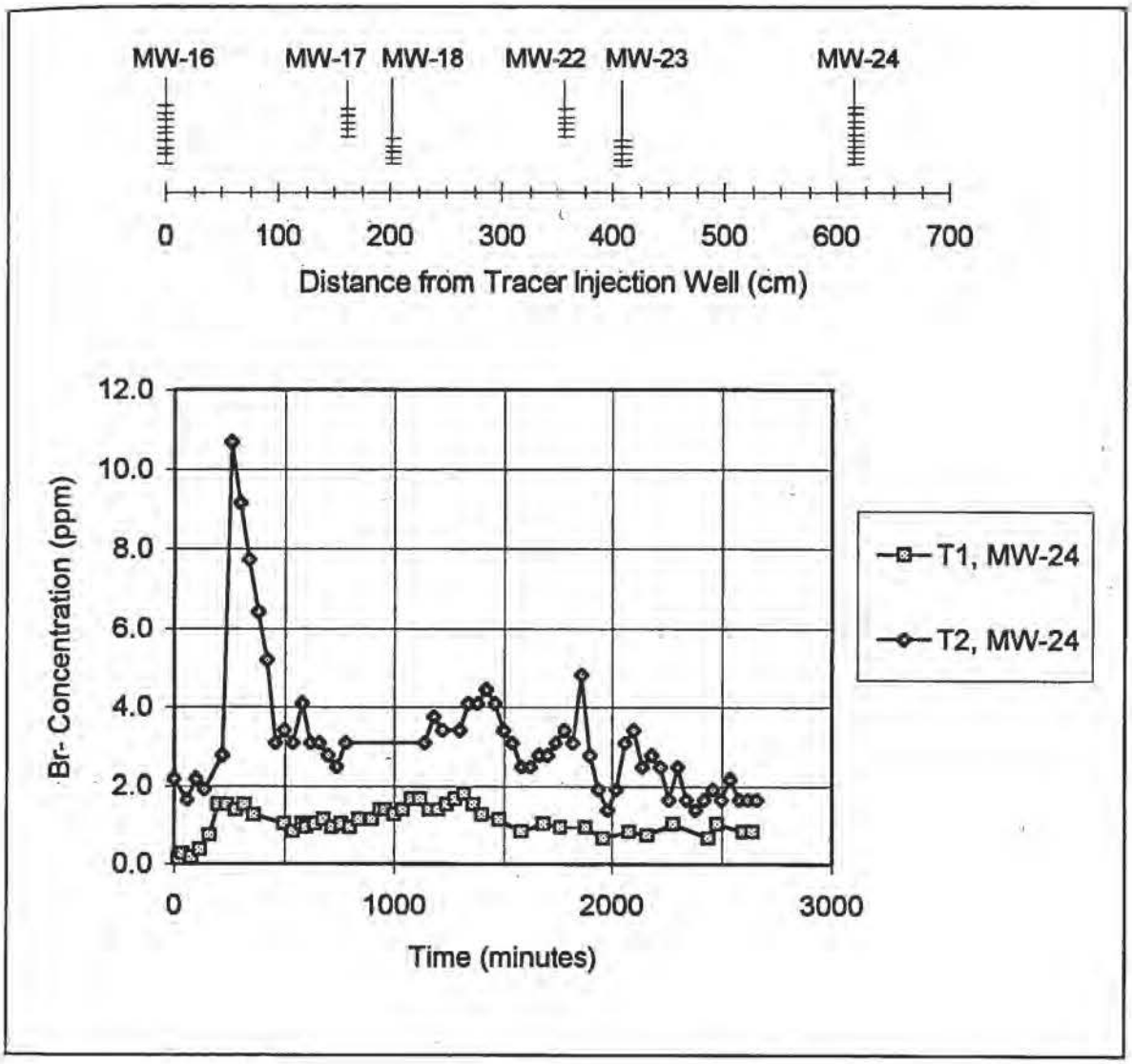

Figure 8.4-3: Bromide concentrations in MW-24 during Tracer Tests T1 and T2.

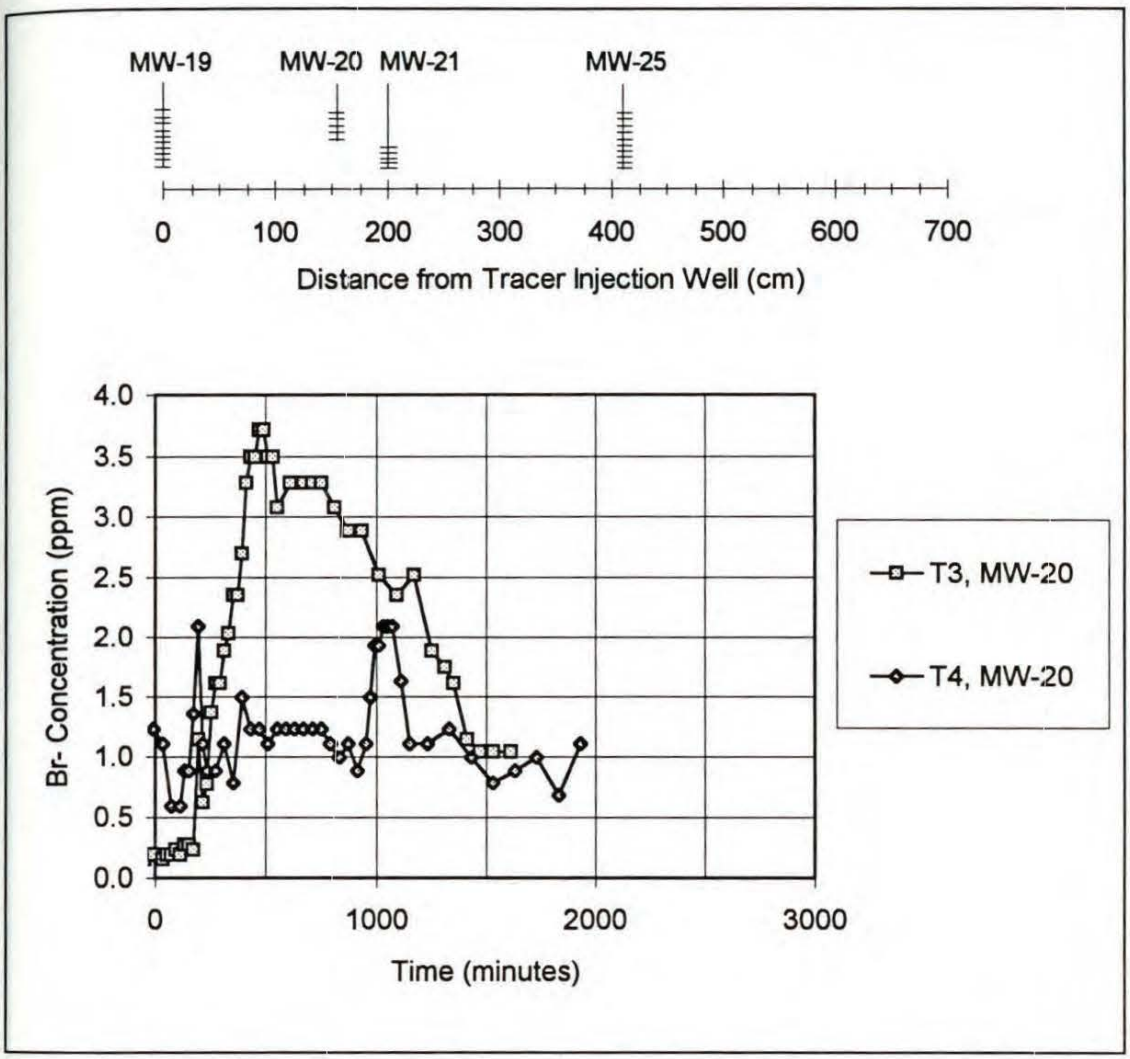

Figure 8.4-4: Bromide concentrations in MW-20 during Tracer Tests T3 and T4.

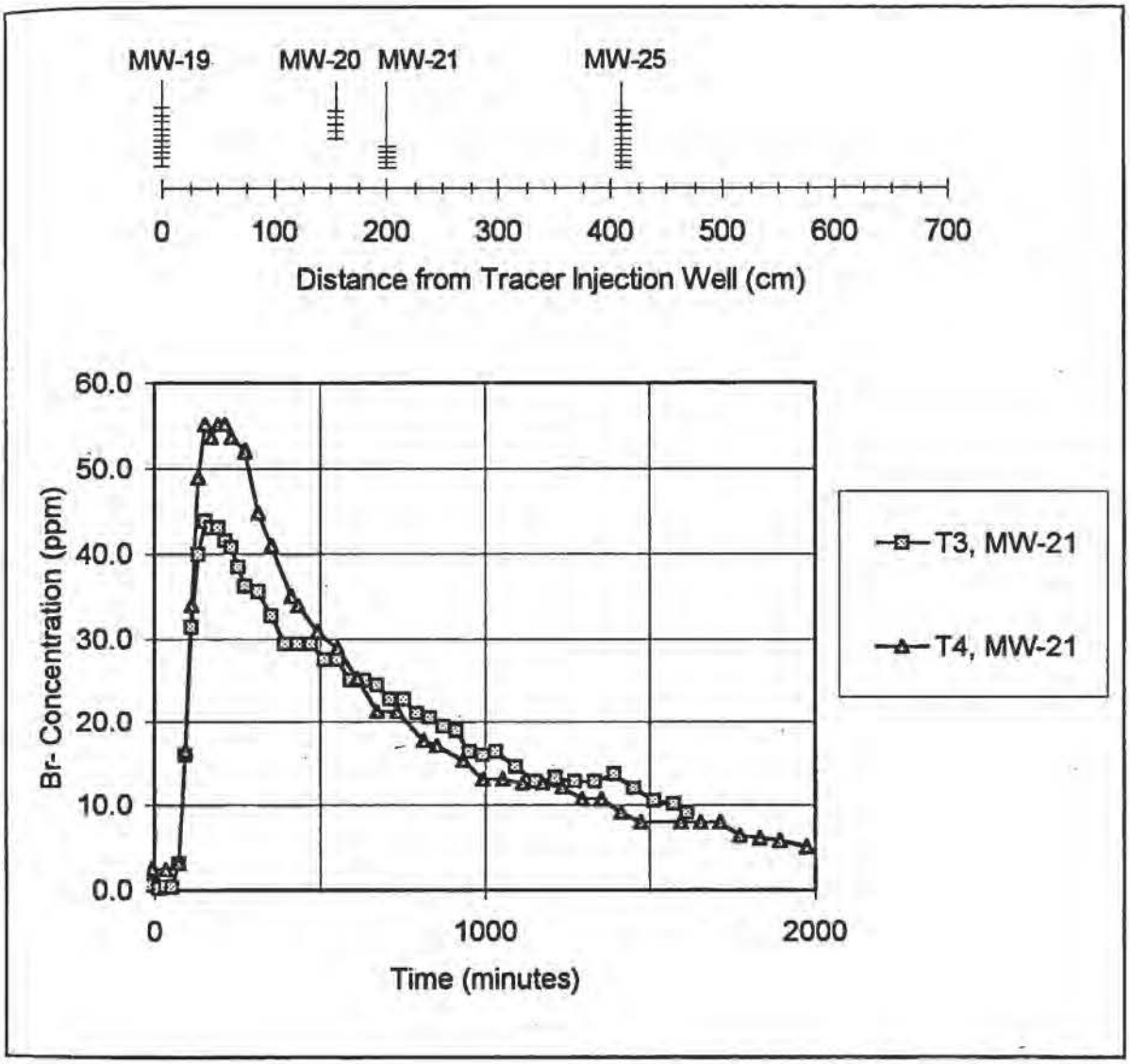

Figure 8.4-5: Bromide concentrations in MW-21 during Tracer Tests T3 and T4.

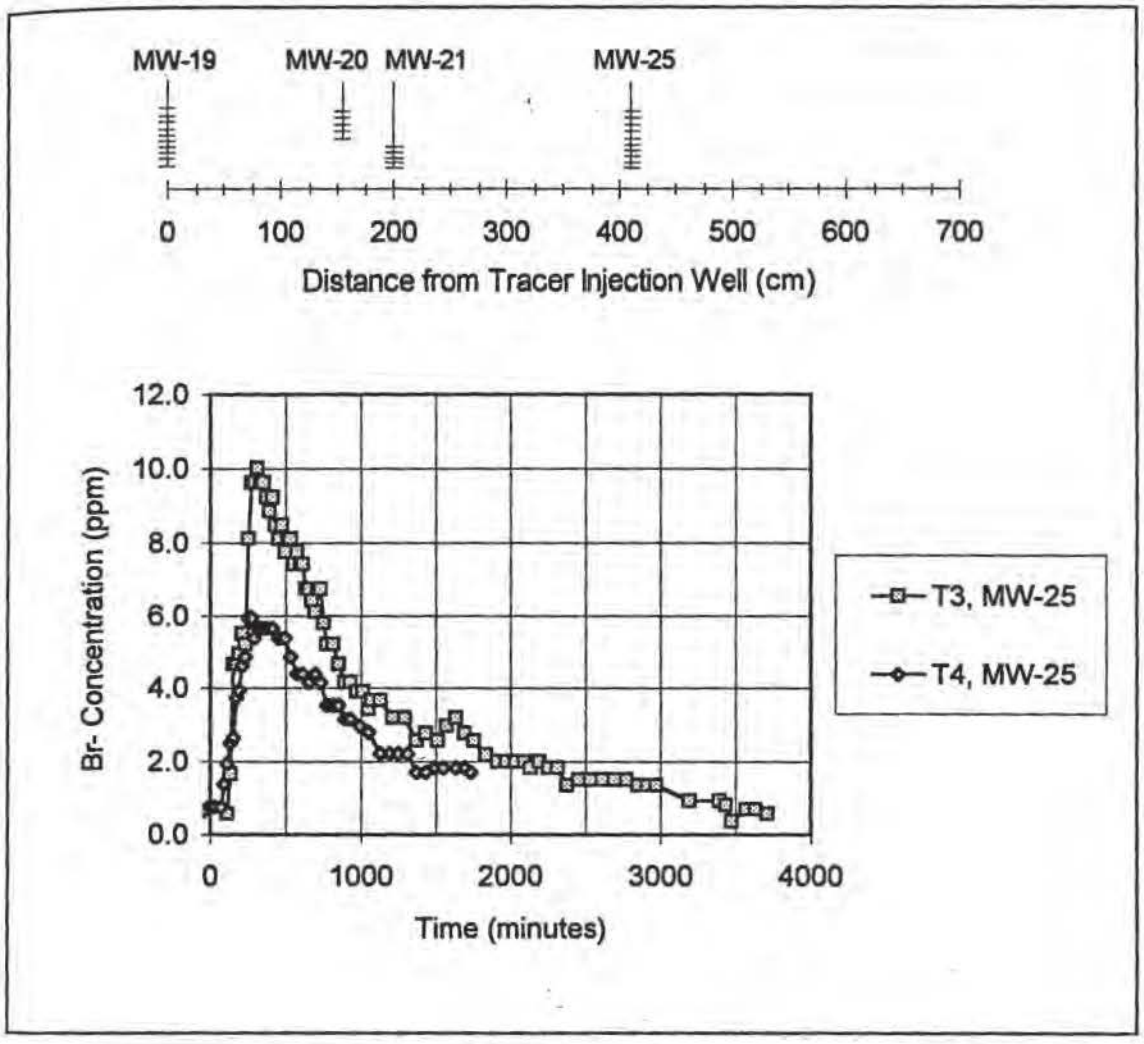

Figure 8.4-6: Bromide concentrations in MW-25 during Tracer Tests T3 and T4.

9. Polystyrene Microsphere Transport Results

9.1 Introduction

This chapter presents polystyrene microsphere transport data from tracer tests T1 and T3. The chapter includes (1) a presentation of concentration data, (2) a comparison of microsphere transport patterns with those of bromide (bromide concentration data are presented in Chapter 8), (3) a comparison of average tracer velocities (on the basis of maximum concentration peaks), and (4) an examination of duplicate microsphere analyses.

9.2 Polystyrene Microsphere Transport Results

This section presents polystyrene microsphere concentration data for tracer tests T1 and T3. Concentration data for 2-μm-diameter spheres are presented first, with comparisons of 2-μm microsphere and bromide arrival times. Concentration results are then presented for 5- and 15-μm-diameter spheres, with comparisons between 2- and 5-μm spheres. Finally, the maximum concentrations observed at each monitoring well are compared with the initial microsphere injection concentrations.

Concentrations for 2-μm polystyrene microspheres during tracer tests T1 are shown in Figure 9.2-1. The highest concentrations in tracer test T1 occurred in MW-17, with over 500 spheres per ml. The second highest concentrations (over 200 spheres per ml) were observed in MW-18. Both concentration peaks were noted at approximately the same time. Very few, if any, 2-μm polystyrene microspheres were confirmed in ground water samples collected from wells MW-22, MW-23, or MW-24.

Concentrations for 2-μm-diameter microspheres during tracer test T3 are shown in Figure 9.2-2. The highest sphere concentrations were observed in MW-21. Sphere concentrations in MW-20 were lower than in MW-21, and occurred approximately 20 minutes later. Microspheres were also observed in MW-25 at approximately 80 minutes after injection.

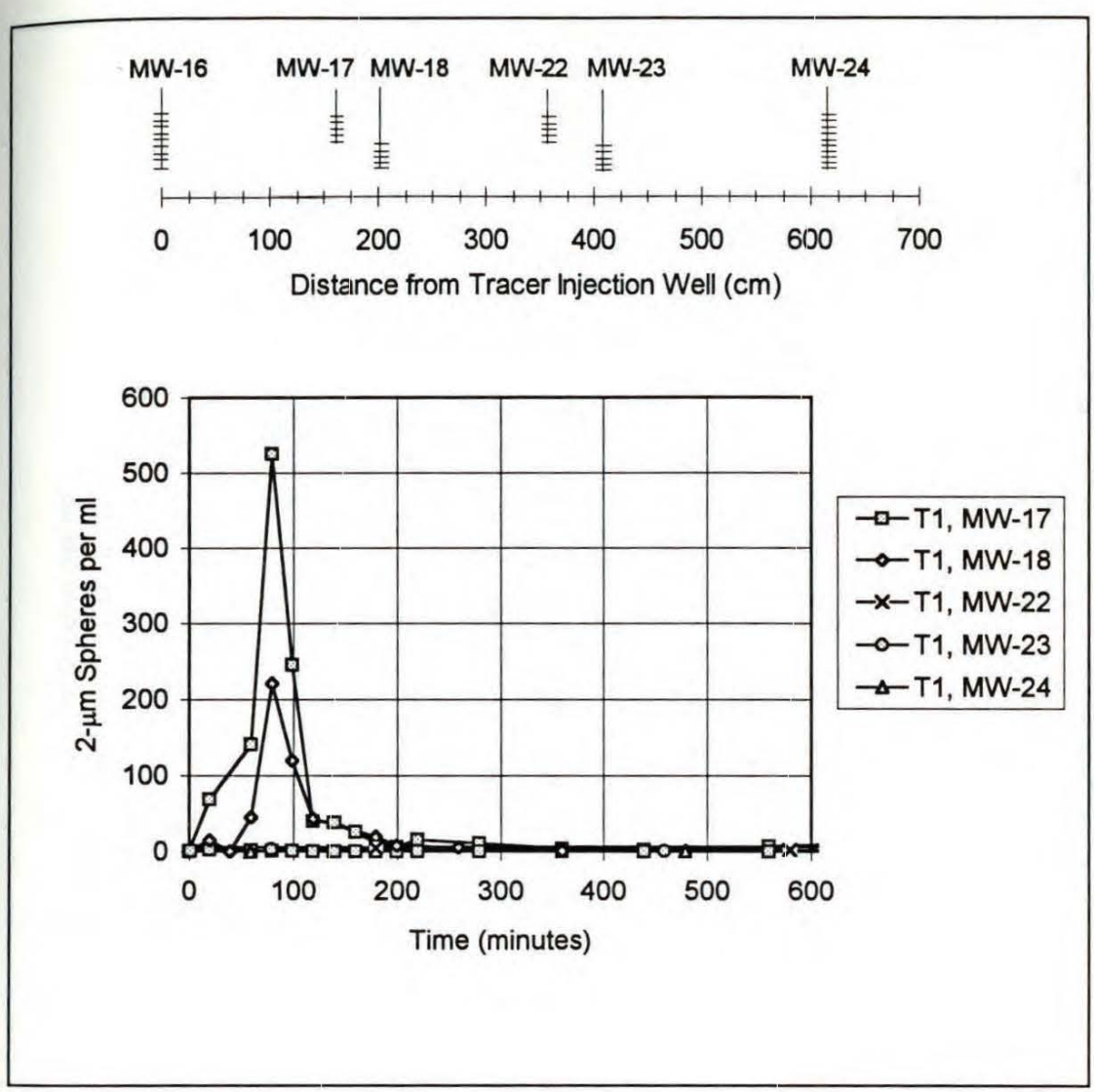

Figure 9.2-1: 2-µm polystyrene microsphere concentration in tracer test T1.

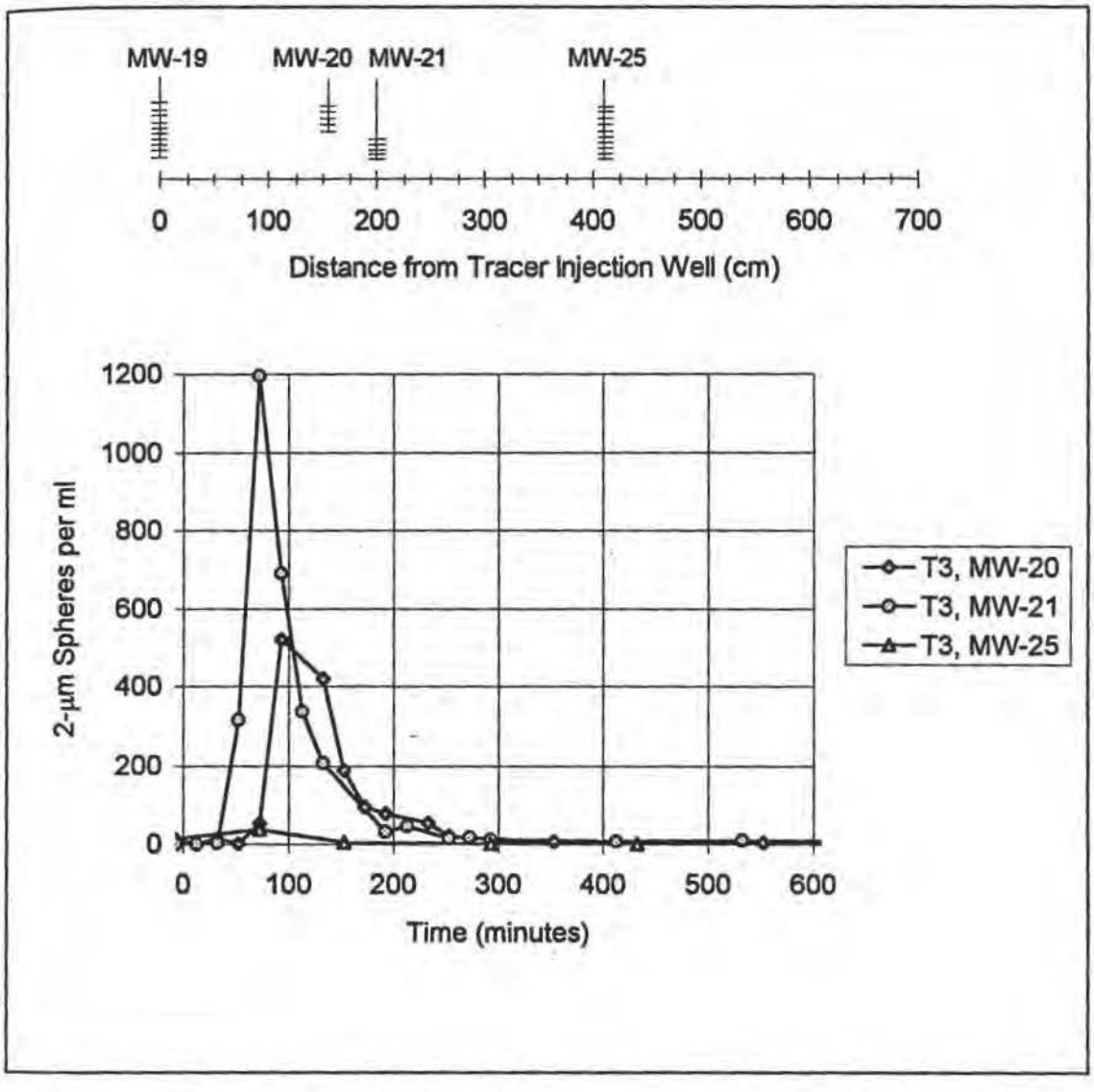

Figure 9.2-2: 2-µm polystyrene microsphere concentrations during tracer test T3.

Comparisons of 2-μm microsphere and bromide concentrations are shown in Figures 9.2-3 and 9.2-4. Several observations can be made from the comparisons. First, it appears that bromide and 2-μm microsphere concentrations begin to increase at approximately the same time in all wells except MW-20. Microsphere concentrations in MW-20 (during tracer test T3) appear to increase earlier than the bromide concentrations. Second, the 2-μm spheres reached peak concentrations earlier than bromide at each monitoring well. Third, the 2-μm concentration peaks were shorter in duration than the bromide concentration peaks.

Concentrations of 5-μm-diameter polystyrene microspheres in water samples collected during tracer tests T1 and T3 are shown in Figures 9.2-5 and 9.2-6. Five-μm spheres were observed in MW-17 and MW-18 during T1 (Figure 9.2-5). No 5-μm spheres were observed in MW-22, MW-23, or MW-24. Figure 9.2-6 shows that 5-μm spheres were observed in MW-20 and MW-21 during tracer test T3. Four 5-μm beads (approximately 0.7 spheres/ml) were observed in MW-25 at approximately 3370 minutes. The long delay period in this latter observation may indicate a data error (e.g., contaminated sample).

Figures 9.2-7 and 9.2-8 provide a comparison of 2-μm and 5-μm microsphere peak concentrations in MW-17 and MW-18 during tracer test T1. The 5-μm microsphere concentration peak appears to have occurred before the 2-μm sphere peak in both wells. Figures 9.2-9 and 9.2-10 show 2-μm and 5-μm microsphere concentrations in MW-20 and MW-21 during tracer test T3. Five-μm microsphere peak concentrations occurred at approximately the same time as the 2-μm peak concentrations. In both tracer tests T1 and T3 the 2-μm and 5-μm-diameter microspheres appear to arrive at approximately the same time. The 5-μm sphere concentrations were significantly lower than the 2-μm concentrations in both tests.

The observed maximum concentrations for bromide, 2-μm microspheres, and 5-μm microspheres were significantly different. Concentrations for bromide, 2-μm microspheres, and 5-μm microspheres are therefore compared in the form of C_{max}/C_0, where C_{max} is the maximum observed monitoring well concentration and C_0 is the

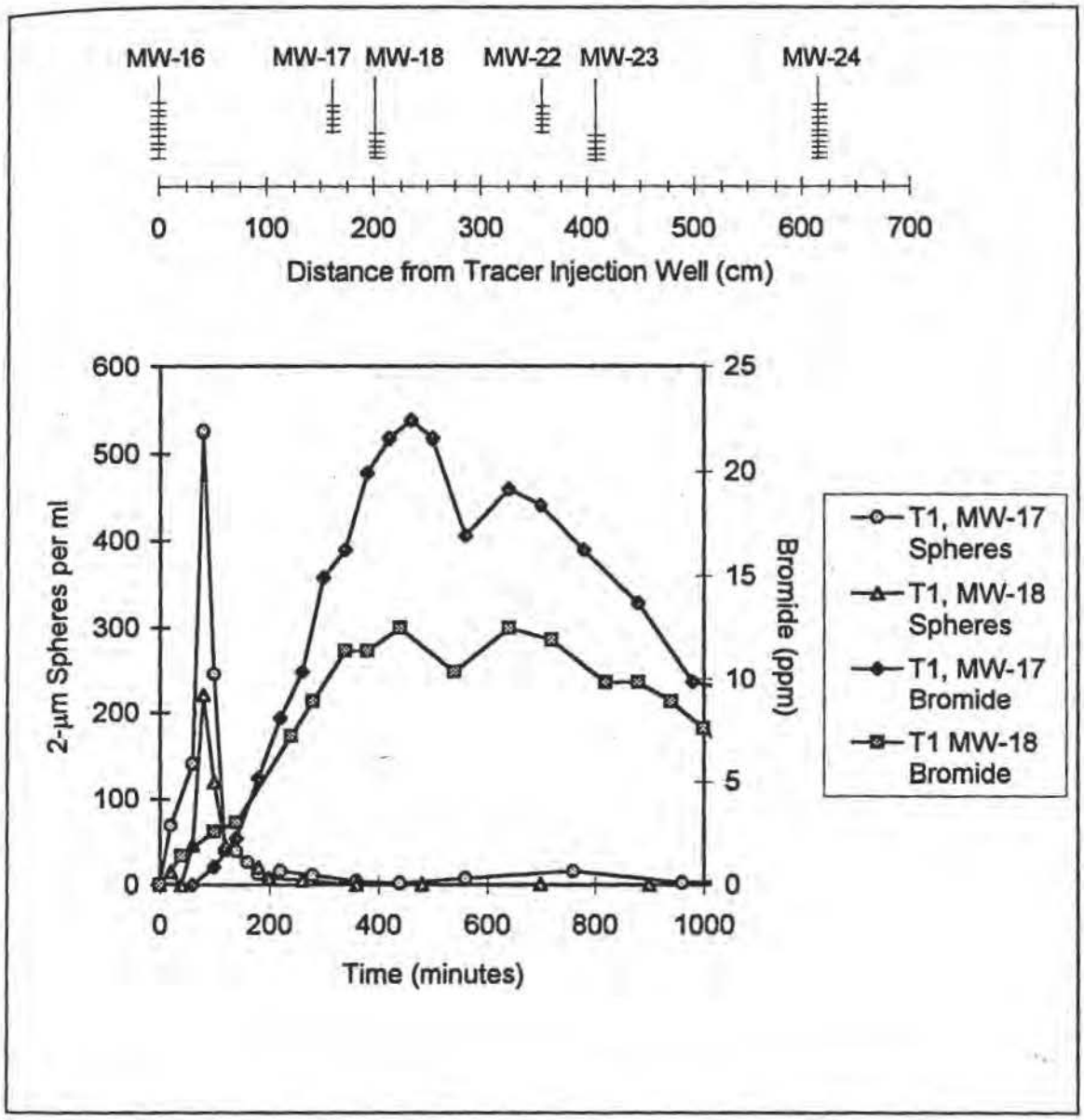

Figure 9.2-3: Bromide and 2-µm microsphere concentrations in tracer test T1.

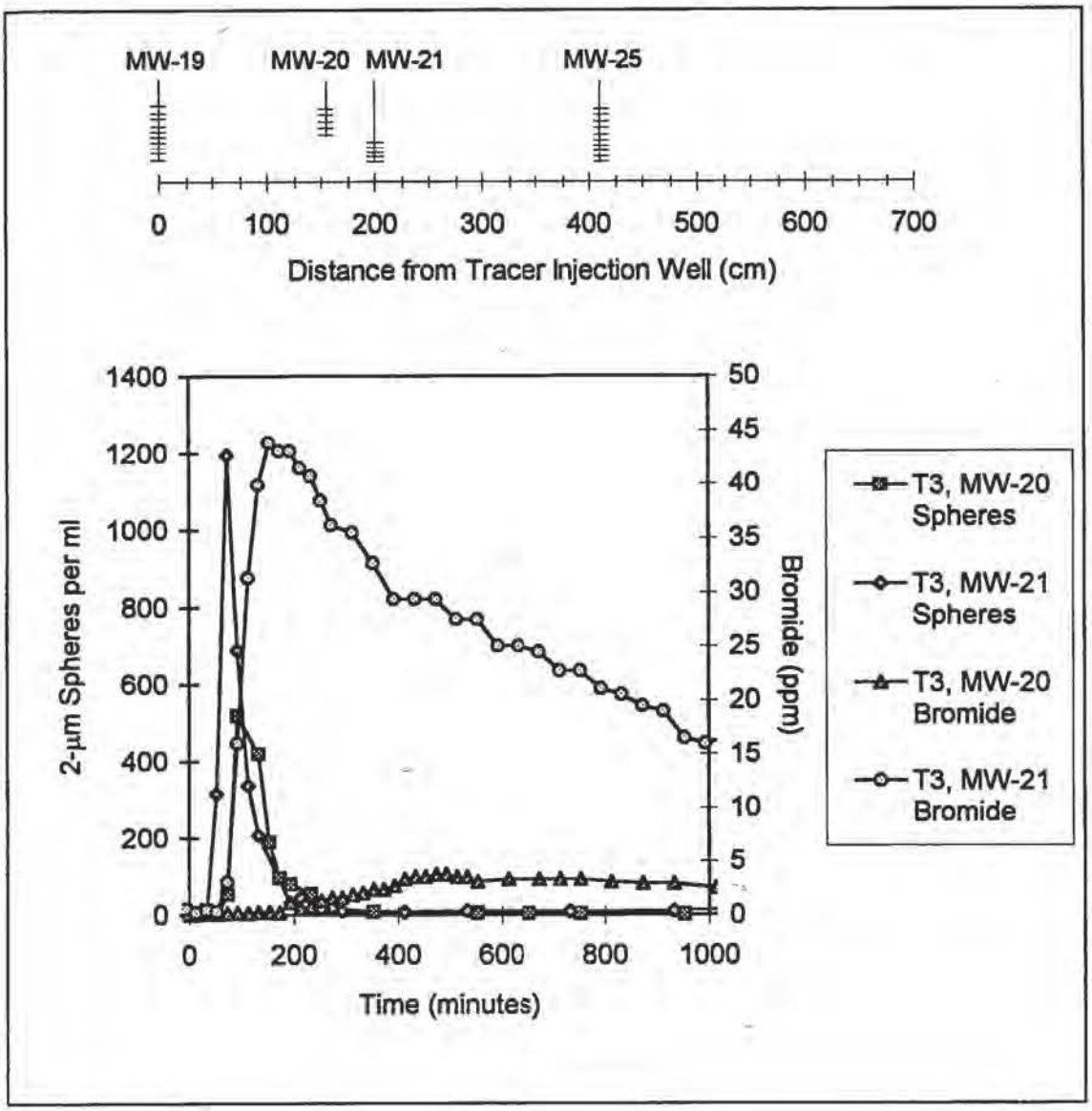

Figure 9.2-4: Bromide and 2-µm microsphere concentrations in tracer test T3.

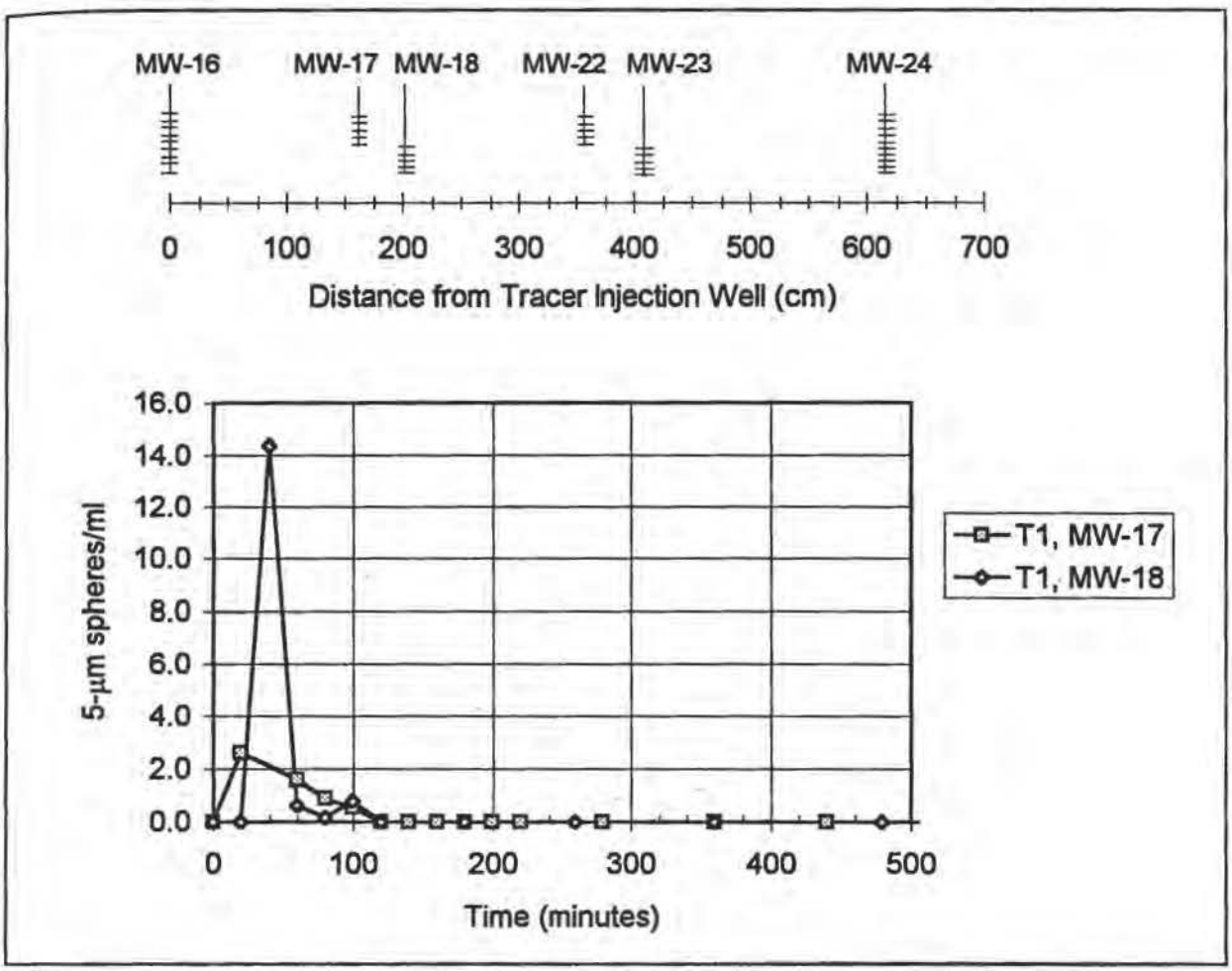

Figure 9.2-5: 5-µm polystyrene microsphere concentrations in tracer test T1.

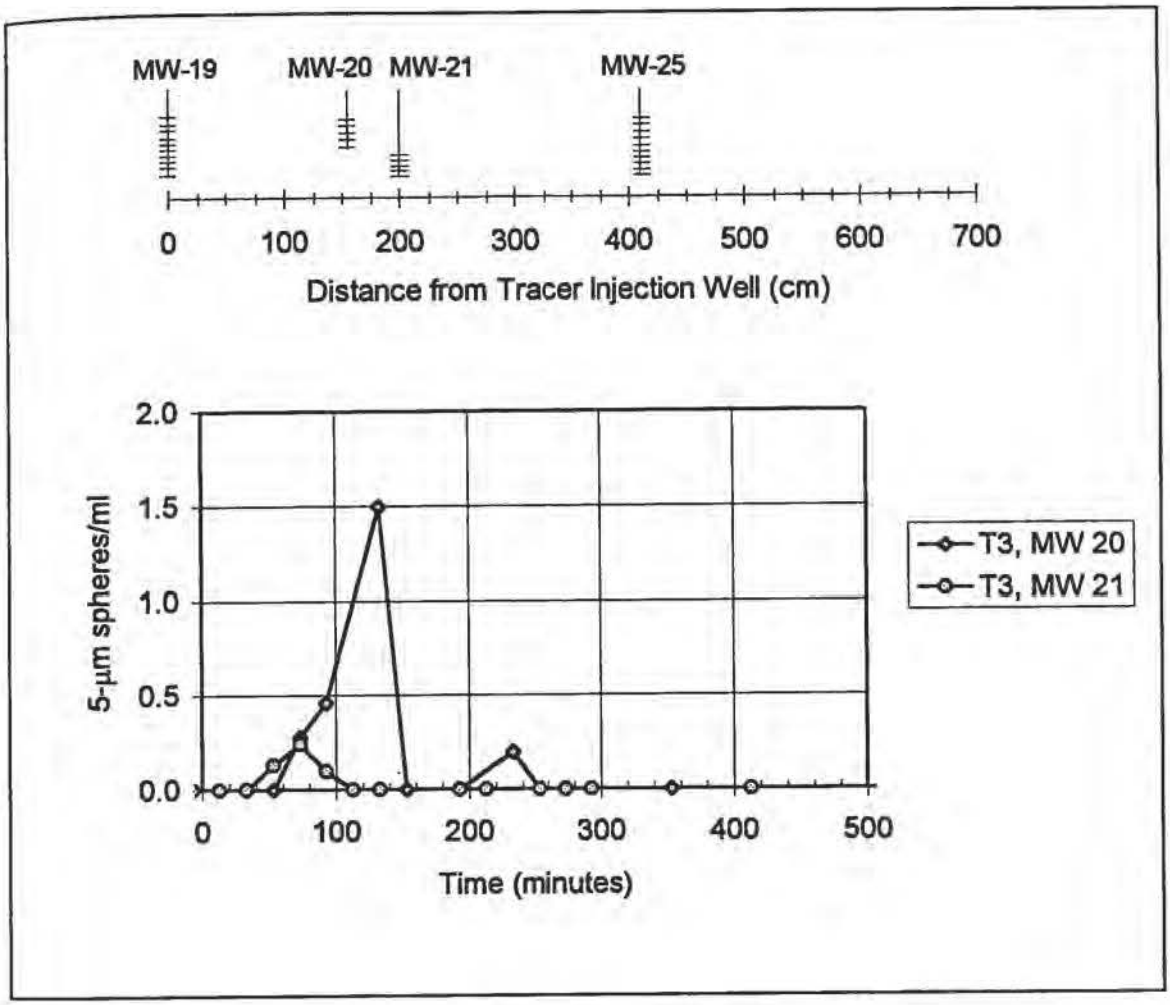

Figure 9.2-6: 5-µm polystyrene microsphere concentrations in tracer test T3.

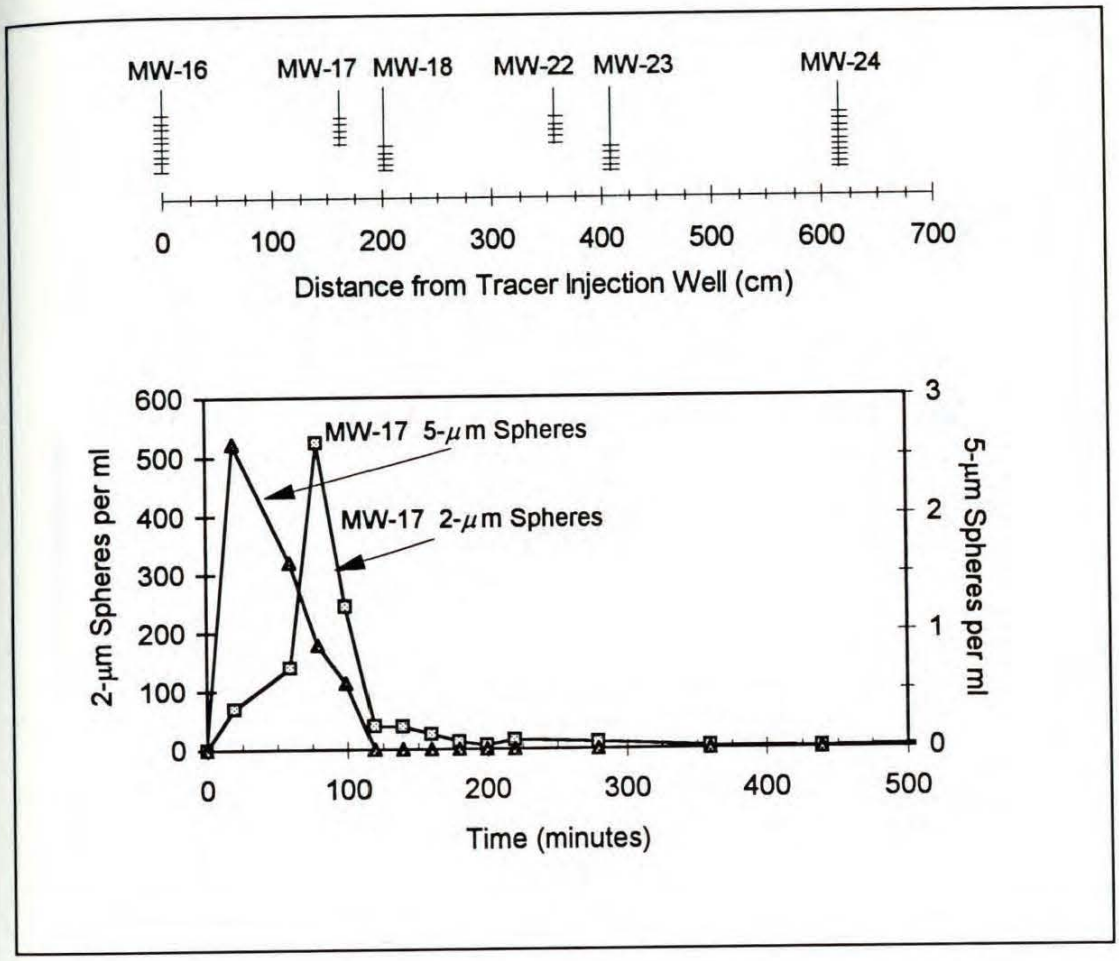

Figure 9.2-7: 2-μm and 5-μm polystyrene microsphere concentrations in MW-17 during tracer test T1.

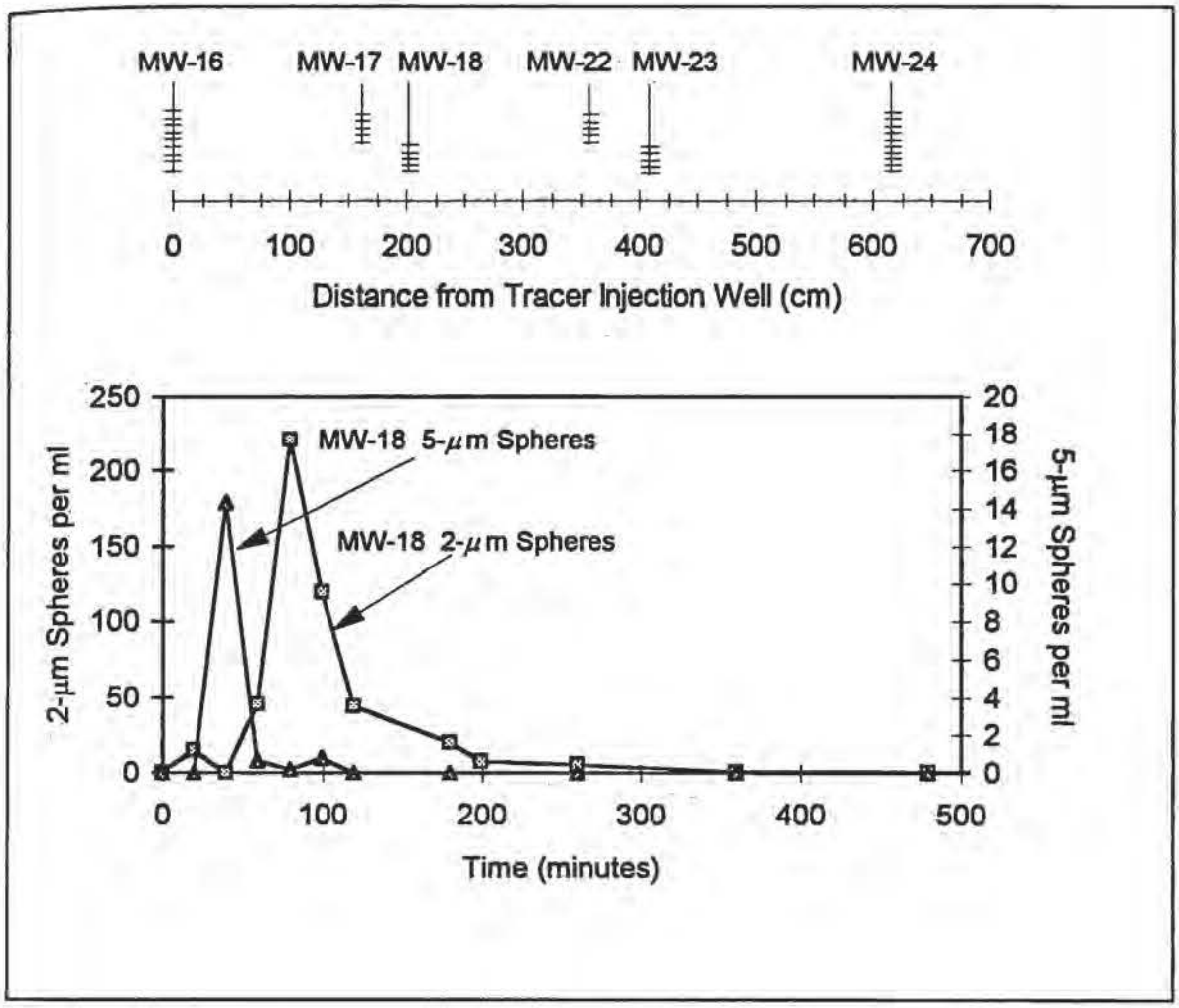

Figure 9.2-8: 2-μm and 5-μm polystyrene microsphere concentrations in MW-18 during tracer test T1.

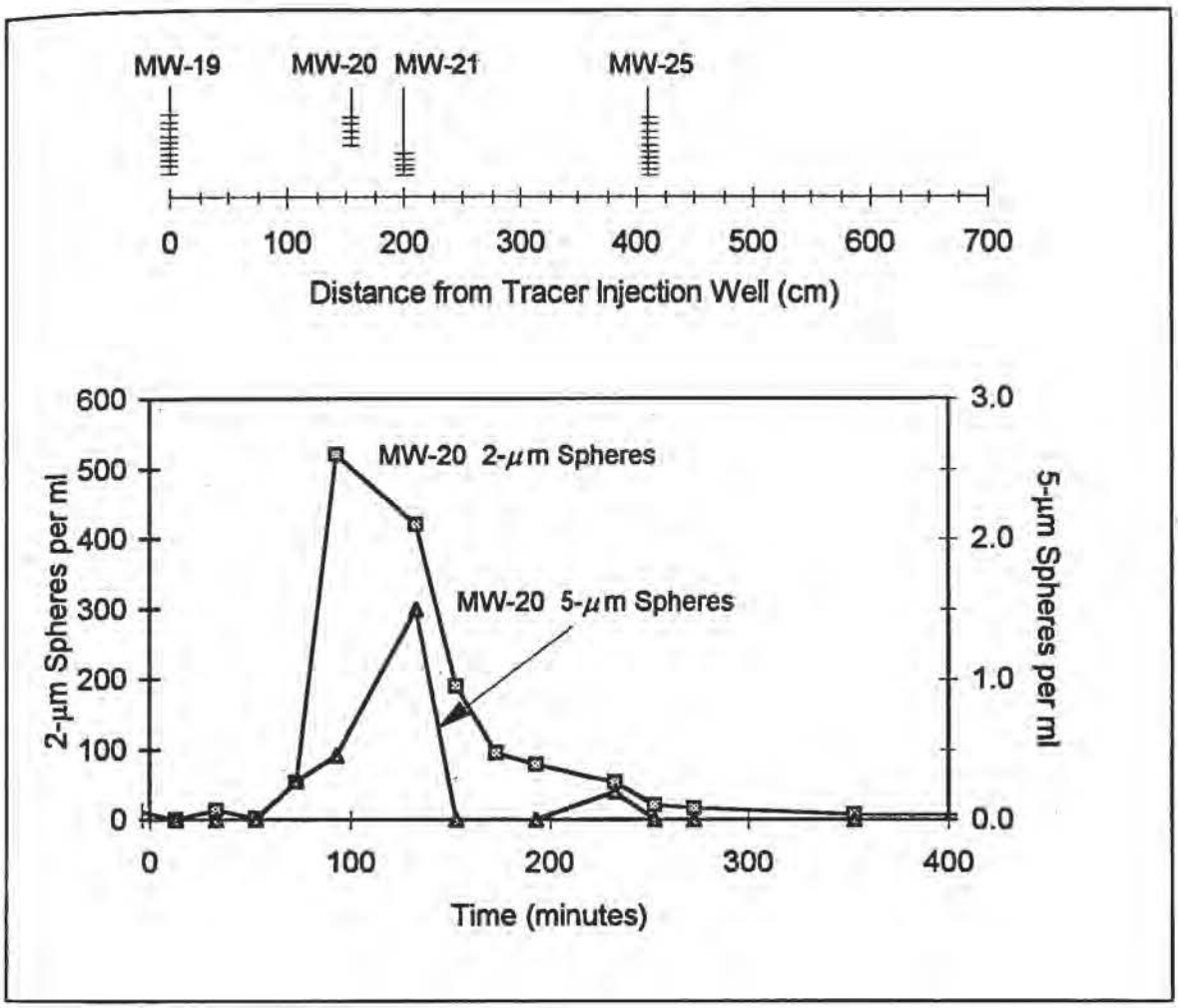

Figure 9.2-9: 2-μm and 5-μm polystyrene microsphere concentrations in MW-20 during tracer test T3.

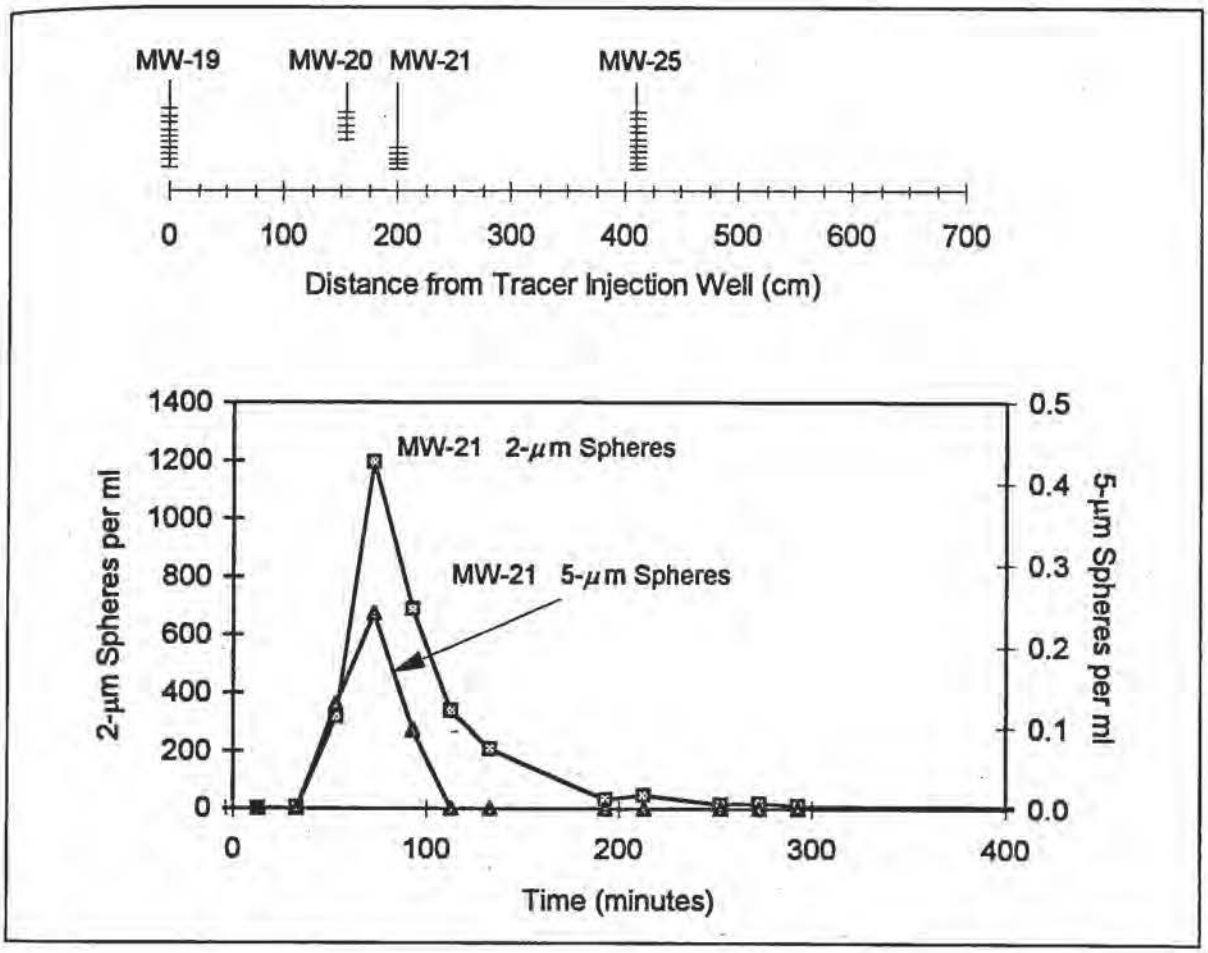

Figure 9.2-10: 2-µm and 5-µm polystyrene microsphere concentrations in MW-21 during tracer test T3.

concentration in the injection well immediately following tracer injection. This comparison takes into account the different initial tracer concentrations.

C_{max}/C_0 ratios for bromide and polystyrene microsphere concentrations in tracer tests T1 and T3 are presented in Figures 9.2-11 and 9.2-12. Several observation can be made from these figures. First, C_{max}/C_0 ratios for polystyrene microspheres are less than for bromide. Second, C_{max}/C_0 ratios for 5-μm microspheres in tracer test T1 are similar to those of the 2-μm spheres, but the ratios of 5-μm spheres in tracer test T3 are less than for 2-μm microspheres. Third, polystyrene microsphere C_{max}/C_0 ratios decrease with distance more than the bromide ratios. Finally, Figure 9.2-12 indicates that the maximum number of 5-μm spheres was higher in MW-20 than in MW-21, which is different than for bromide and 2-μm spheres (the number of 5-μm spheres in MW-21 water samples was very low, and may not necessarily be representative).

No 15-μm polystyrene microspheres were observed in ground water samples collected from the monitoring wells. However, bottom sediments from the casings of each monitoring well were sampled one week after tracer test T4. Sediment samples were taken by vacuum and do not necessarily represent a specific volume of sediment or water. Samples taken from MW-22 and MW-25 were inadvertently compromised and were therefore not analyzed.

Results from analyzing the bottom sediments are shown in Figure 9.2-13. Spheres 15-μm in diameter were observed in the bottom sediments of the two injection wells (MW-16 and MW-19) and in monitoring well MW-21. Also, 2- and 5-μm-diameter spheres were observed in the bottom sediments of most wells.

9.3 Comparison of Polystyrene Microsphere Tracer Velocities

This section provides a comparison of average bromide and polystyrene microsphere tracer velocities. The tracer velocities are estimated on the basis of the arrival times for concentration peaks. The purpose of this comparison is to quantify differences between the arrival times of various concentration peaks, which in turn can be used for evaluating tracer and aquifer characteristics.

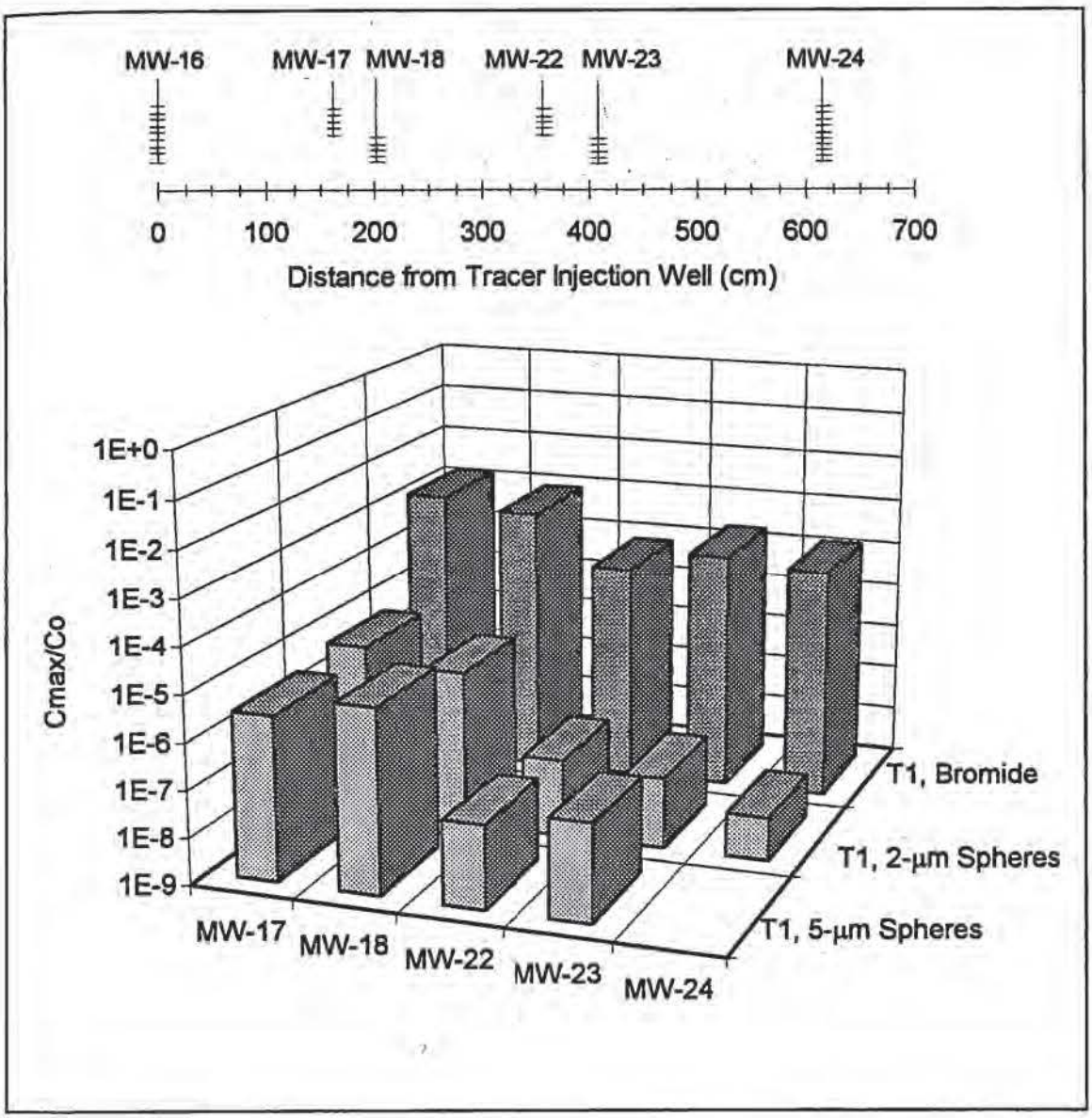

Figure 9.2-11: C_{max}/C_0 ratios (logarithmic scale) in Transect C during tracer test T1.

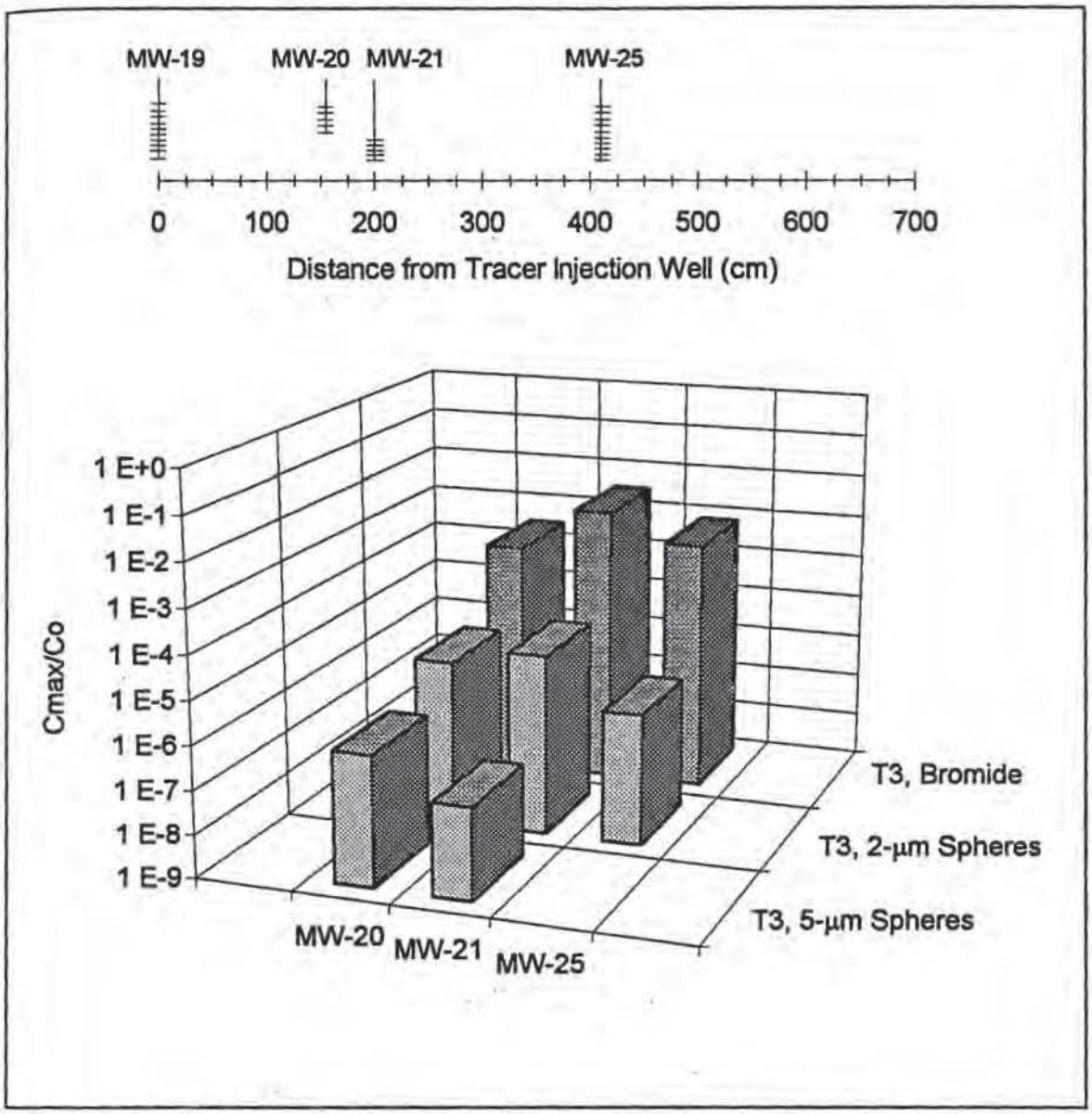

Figure 9.2-12: C_{max}/C_0 ratios (logarithmic scale) in Transect B during tracer test T3.

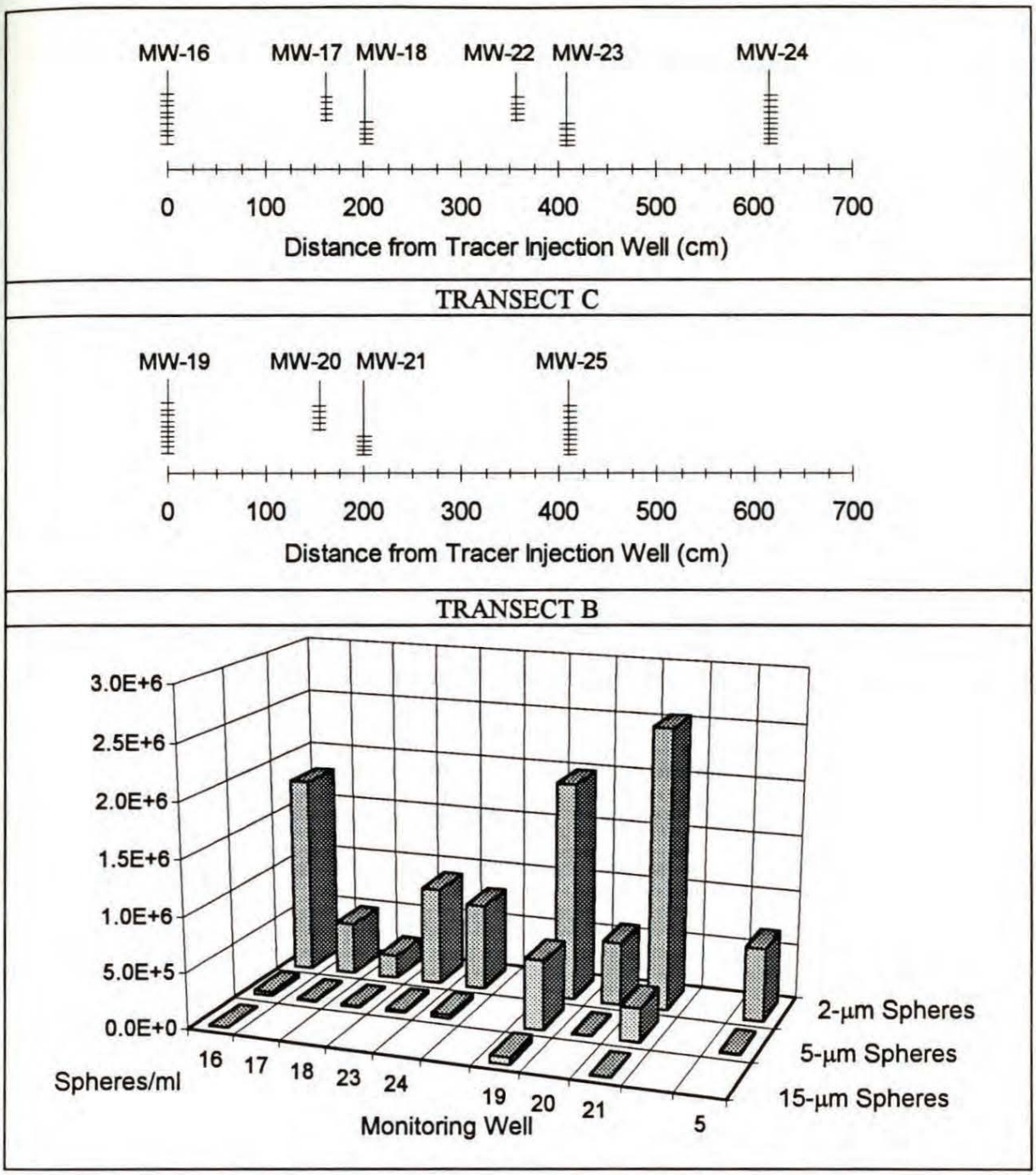

Figure 9.2-13: Polystyrene microsphere concentration in samples taken from the bottom sediments of selected wells.

Average tracer velocities are given in Table 9.3-1 for bromide and polystyrene microspheres. These average velocities were estimated on the basis of tracer arrival times and distances between the injection and monitoring wells. Data were limited to the four wells in which significant 2-μm sphere concentrations were observed.

Tracer Test, Monitoring Well	Distance from Injection Well (cm)	Bromide C_{max} Breakthrough Time (min)	2-μm Sphere Breakthrough Time (min)	Average Bromide Velocity (cm/min)	Average 2-μm Sphere Velocity (cm/min)
T1, MW-17	160	460	79	0.35	2.03
T1, MW-18	205	440	79	0.47	2.59
T3, MW-20	152	470	133	0.32	1.33
T3, MW-21	199	150	73	1.33	2.73

Table 9.3-1: Average bromide and 2-μm polystyrene microsphere velocities in tracer tests T1 and T3.

The average tracer velocities were compared to theoretical values on the basis of transmissivity values presented in Chapter 6. Average ground water velocities are estimated on the basis of Darcy's law. Darcy's law states that

$$Q = -KA\frac{dh}{dl} = -\frac{TA}{b}\frac{dh}{dl}$$

where

Q = the volumetric flux;

K = the hydraulic conductivity;

A = a cross-sectional aquifer area;

$\frac{dh}{dl}$ = the hydraulic gradient;

T = the aquifer transmissivity; and

b = the aquifer thickness.

The specific discharge, v, is given by the equation

$$v = \frac{Q}{A} = -\frac{T}{b}\frac{dh}{dl}$$

and the average linear ground water velocity (V_x), also referred to as the seepage velocity, is given by the equation

$$V_x = \frac{Q}{n_e A} = -\frac{T}{n_e b}\frac{dh}{dl}$$

where

n_e = the effective aquifer porosity.

Estimated theoretical average ground water velocities for the field site aquifer are presented in Table 9.3-2. It was assumed that transmissivity ranges from approximately 1.0 to 5.6 cm^2/min (Tables 6.7-1 through 6.7-3), and that the aquifer is 152 cm thick. It also was assumed that the porosity for unconsolidated mixed sand and gravel ranges from approximately 20 to 35%; it was assumed that the effective porosity of the field site aquifer is approximately 30%. The hydraulic gradient estimates for tracer tests T1 and T2 are listed in Table 7.4-1.

Tracer Test	Assumed Trans-missivity (cm2/min)	Assumed Aquifer Thickness (cm)	Porosity	Gradient	Estimated average velocity (cm/min)
T1	1.0	150	0.30	0.147	.0033
T1	5.6	150	0.30	0.147	.0183
T3	1.0	150	0.30	0.137	.0030
T3	5.6	150	0.30	0.137	.0170

Table 9.3-2: Average linear velocities assuming a homogeneous aquifer thickness of 150 cm.

The average estimated linear ground water velocities in Table 9.3-2 are much lower than the observed tracer velocities indicated in Table 9.3-1. This may be the result of incorrect estimates of transmissivity, porosity, or aquifer thickness. However, the magnitude of the difference, and the particle transport patterns, suggests that some

flow is occurring in preferential flowpaths. The velocities indicated in Figure 9.3-2 represent an average of velocities in a highly heterogeneous environment; i.e., some aquifer zones would be expected to have higher velocities than others.

An attempt was therefore made to estimate the apparent thickness of the preferential flowpaths on the basis of the estimated transmissivity values, an estimated porosity value, the measured gradients during tracer tests T1 and T2, and the estimated tracer velocities in Table 9.3-1. In estimating an apparent flowpath thickness it is assumed that there is a significant difference between the hydraulic conductivity of the materials in the preferential flowpath and the surrounding aquifer materials.

Solving for b in the equation for average linear velocity yields the equation

$$b_e = \frac{T}{n_e V_x \frac{dh}{dl}}$$

where b_e is the estimated preferential pathway thickness based on linear tracer velocities.

Preferential flowpath thicknesses, estimated on the basis of average bromide and polystyrene microsphere velocities, are shown in Tables 9.3-3 and 9.3-4, respectively. Estimated apparent flowpath thicknesses are very small: estimated thicknesses range from approximately 0.3% to 5.2% of the assumed 152-cm aquifer thickness. Polystyrene microsphere velocities yield much smaller apparent flowpath thickness values (less than 2% of the assumed 152-cm aquifer thickness) than those based on bromide velocities.

Implicit in the estimates of apparent flowpath thickness is the assumption that the flowpath maintains constant dimensions over the measured area. Constant flowpath dimensions are unlikely, given the heterogeneous nature of the aquifer sediments.

9.4 Duplicate Microsphere Counts

Water samples were analyzed for microspheres by preparing slides and counting microspheres under a microscope (Chapter 7). This section presents data derived from duplicate counts of the same slide and duplicate counts of duplicate slides. Duplicate microsphere counts provide an indication of data reproducibility.

Tracer Test, Monitoring Well Numbers	Average Bromide Velocity (cm/min)	Trans-missivity (cm^2/min)	Assumed Aqufier Porosity	Average Gradient	Estimated flowpath thickness (cm)
T1, MW-17	0.35	1.00	0.3	0.147	1.4
T1, MW-18	0.47	1.00	0.3	0.152	1.1
T3, MW-20	0.32	1.00	0.3	0.137	1.4
T3, MW-21	1.33	1.00	0.3	0.141	0.4
T1, MW-17	0.35	5.60	0.3	0.147	7.9
T1, MW-18	0.47	5.60	0.3	0.152	6.1
T3, MW-20	0.32	5.60	0.3	0.137	7.9
T3, MW-21	1.33	5.60	0.3	0.141	2.0

Table 9.3-3: Estimated aquifer thicknesses based on the average bromide velocity.

Tracer Test, Monitoring Well Numbers	Average Bromide Velocity (cm/min)	Trans-missivity Estimates* (cm^2/min)	Assumed Aqufier Porosity	Average Gradient	Estimated Aquifer Thickness (cm)
T1, MW-17	2.03	1.00	0.3	0.147	0.2
T1, MW-18	2.59	1.00	0.3	0.152	0.2
T3, MW-20	1.14	1.00	0.3	0.137	0.4
T3, MW-21	2.73	1.00	0.3	0.141	0.2
T1, MW-17	2.03	5.60	0.3	0.147	1.4
T1, MW-18	2.59	5.60	0.3	0.152	1.1
T3, MW-20	1.14	5.60	0.3	0.137	2.2
T3, MW-21	2.73	5.60	0.3	0.141	1.0

* from Tables 6.6-2 - 6.6-4.

Table 9.3-4: Estimated aquifer thicknesses based on the average polystyrene microsphere velocity.

Microsphere-counting reliability is limited by several factors. First, water from the ground water samples contained some non-microsphere particles fluorescing at the same wavelengths as the fluorescent marker contained in the microspheres; these non-microsphere particles were sometimes difficult to differentiate from the microspheres.

Second, some variability arose from differentiating larger beads from clusters of smaller beads (larger beads were verified at higher magnifications if few large beads were present). Third, variability in reliability could occur when conducting a full scan of a slide because of (1) counting error due to high numbers of spheres, or (2) potential overlap when conducting multiple passes across the filter with the microscope. Fourth, significant variability was noted between some random fields (random fields were used when the bead count was too high to count the entire filter). Variability between fields was attributed in part to preferential flow through the filter due to the grid shape of the underlying filter support. Finally, microsphere-counting reliability was limited by variability in filter and slide preparation.

Figure 9.4-1 shows variability between two operators counting 2-μm spheres on the same slide. Samples are indicated by the tracer test, the well number, and the sample number. For instance, T3-21-40 indicates test T3, monitoring well MW-21, and sample #40. Figures 9.4-2 through 9.4-4 show variability in 2-μm, 5-μm, and 15-μm sphere counts made from different slides and counted by two technicians. On the basis of these graphs it is apparent that slide preparation results in greater variability than counting spheres from the same slide. The variability range for sphere counts appears to fall within an order of magnitude.

Significant variability is also noted in the Standard Test Method of Enumeration of Aquatic Bacteria by Epifluorescence Microscopy Counting (ASTM D 4455-85). The standard deviation (bacteria per ml) was 45% and 17% of the mean count, respectively, for two samples sent to six independent labs for counting (repeatability, multiple operators). The first of these samples contained in the range of 10^4 beads per ml and the second sample contained in the range of 10^6 beads per ml.

In summary, duplicate microsphere counts indicate that there is a greater variability in preparing samples than in counting slides. Some errors were observed in duplicate analyses by different operators, but duplicate counts were consistently within one order of magnitude in variation. Significant variability is also noted in a similar ASTM method. From this analysis it is concluded that microscopic analysis of microsphere concentrations provided legitimate results.

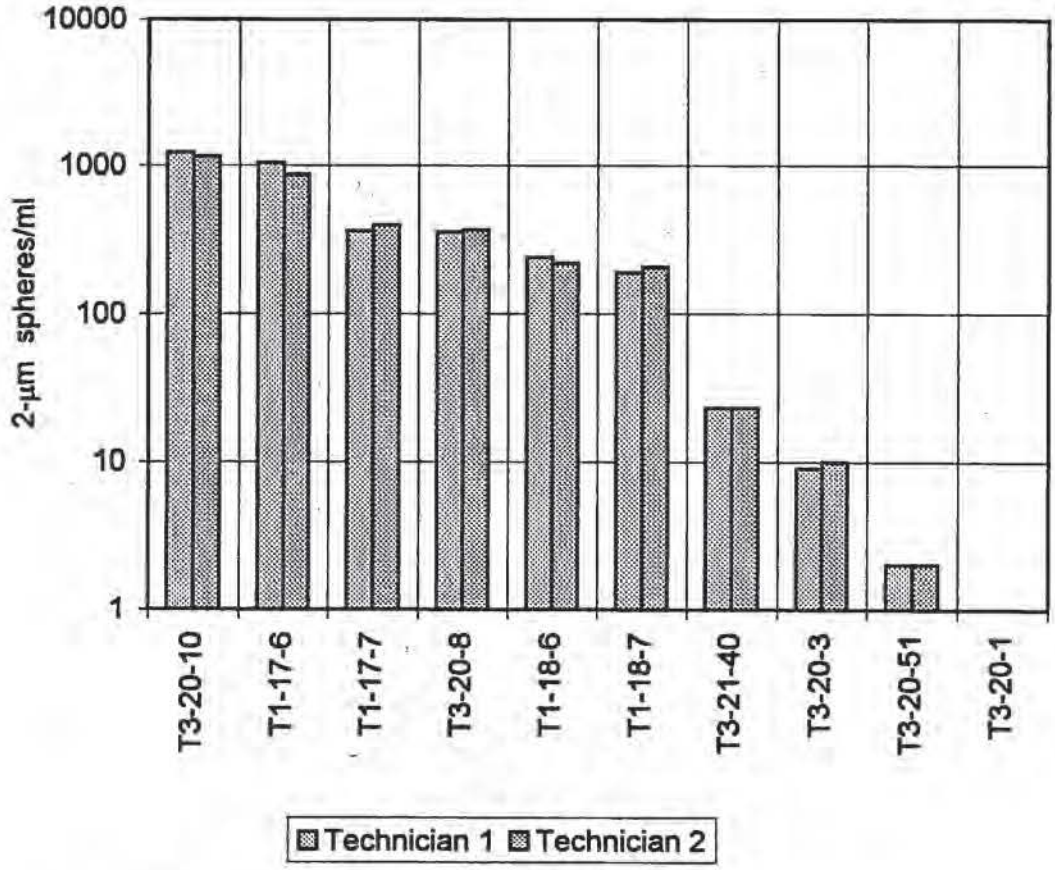

Figure 9.4-1: Duplicate slide counts of the same slide by two technicians.

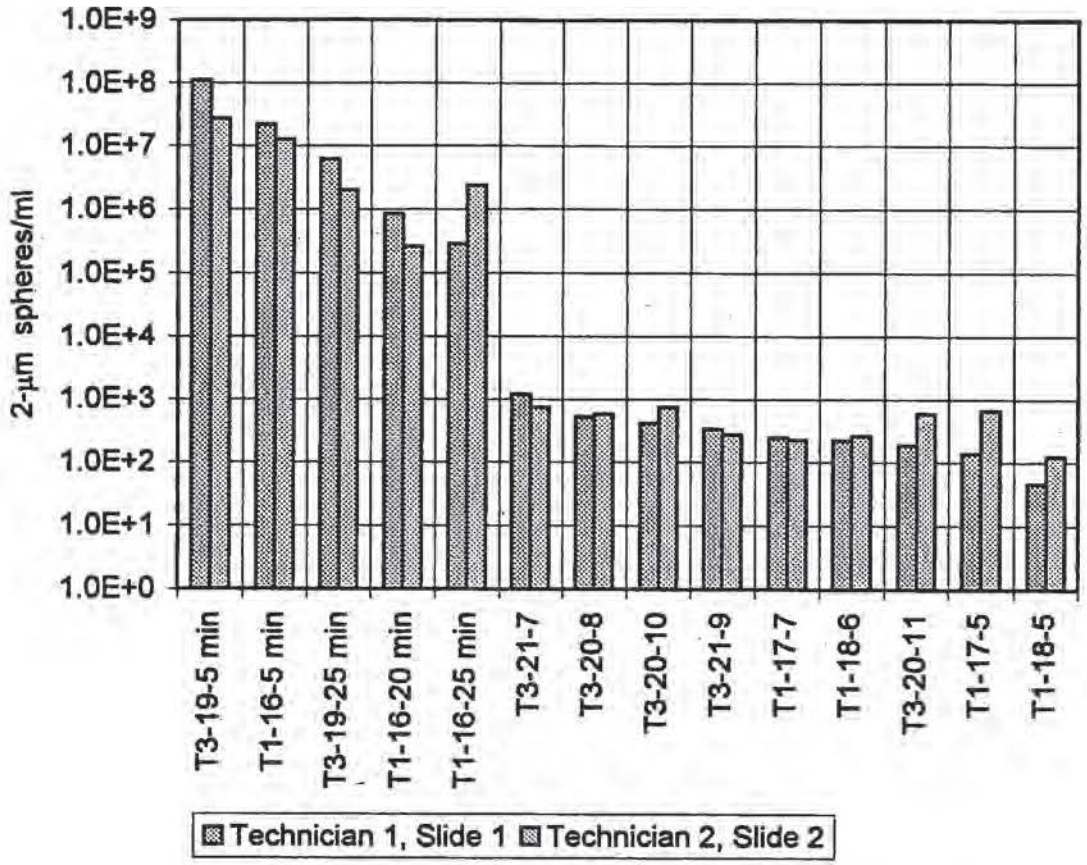

Figure 9.4-2: Duplicate slide counts; 2-µm spheres; different slides prepared (from the same water sample) and counted by two technicians.

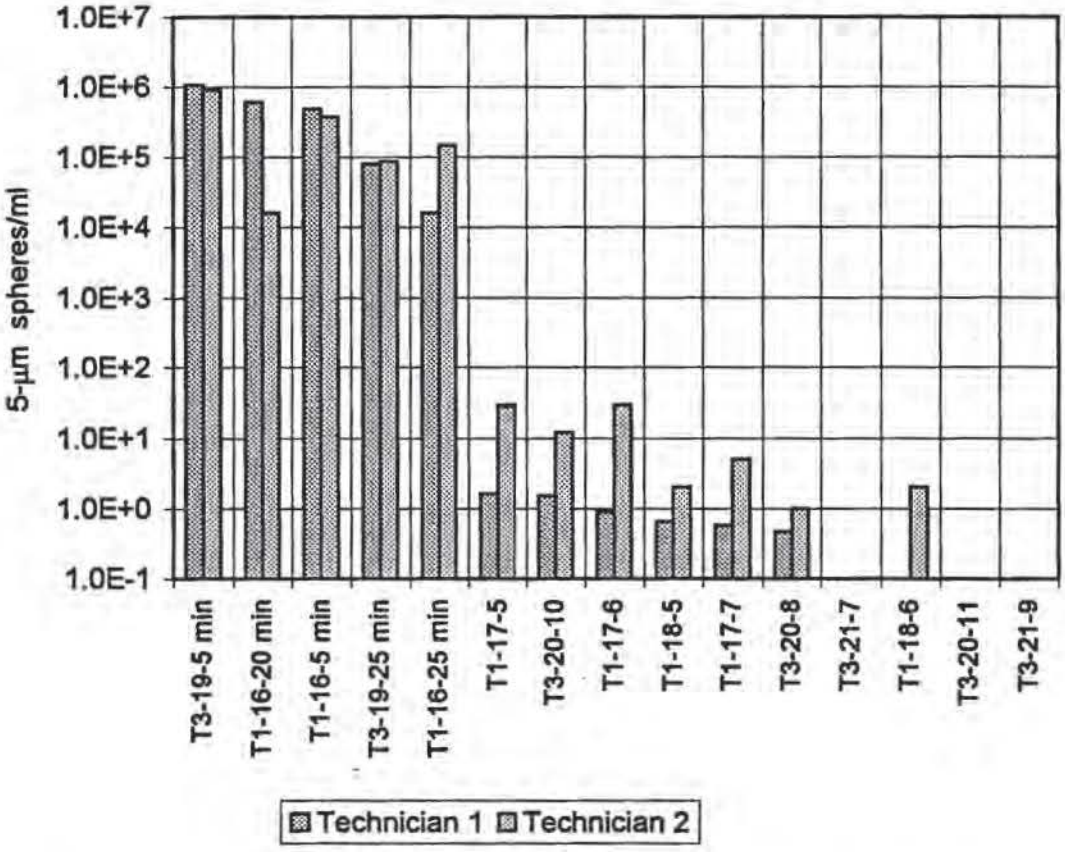

Figure 9.4-3: Duplicate slide counts; 5-µm spheres; different slides prepared (from the same water sample) and counted by two technicians.

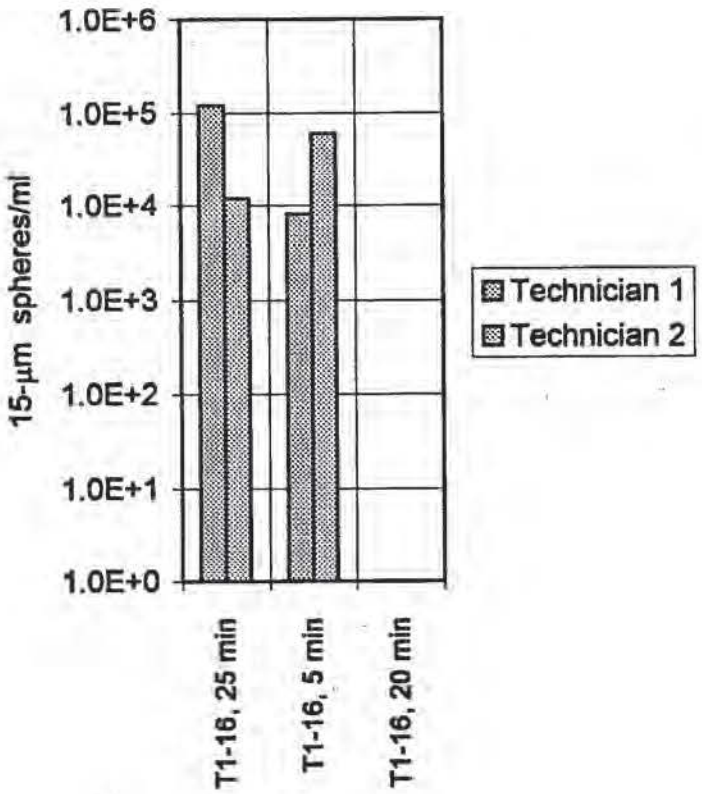

Figure 9.4-4: Duplicate slide counts; 15-µm spheres; different slides prepared (from the same water sample) and counted by two technicians.

10. Encapsulated Cell Transport Results

0.1 Introduction

This chapter presents results from analyzing ground water samples for encapsulated cell concentrations. A description of the encapsulated cells and analysis techniques used in this study is provided in Chapter 7.

0.2 Encapsulated Cell Concentrations

Several difficulties were experienced in attempting to quantify encapsulated *Flavobacterium* cell concentrations using fluorescent microscopy. First, the acridine-orange color held in the genetic material of the *Flavobacterium* cells appeared to fade after exposure to ultraviolet light. Second, the presence of similarly colored particles made it difficult to identify with certainty encapsulated *Flavobacterium* cells . Thus, particles that appeared to be encapsulated cells were observed (by microscope) in samples taken from the injection wells (MW-16 and MW-19), but few if any encapsulated cells were observed in monitoring well samples. It was unclear if the lack of observed encapsulated cells was a result of the detection technique or whether the encapsulated cells had not been transported in the aquifer. Abundant numbers of encapsulated cells appeared to be present in the injection well samples, but quantifying the number or sizes proved elusive for the reasons outlined above.

Because of these difficulties a PCR technique was then used to determine the presence of *Flavobacterium* cells. PCR is a qualitative technique for detecting the presence of specific DNA markers. The PCR analysis was conducted by Knaebel et al. (in progress); a description of methodology and results is provided in Appendix I.

A limited number of samples were analyzed because of the technique complexity. Ground water samples (including two negative controls and two duplicates) were taken from the injection wells immediately following encapsulated-cell injection, and from MW-21 in tracer test T3. MW-21 was chosen because this well experienced the highest concentrations of bromide and polystyrene microspheres during the tracer tests. Ground water samples taken from MW-21 at 73, 153, 233, 333, 473,

653, 693, 713, 733, 753, 773, 793, 813, 833, 853, 873, 893, 913, 933, 953, and 973 minutes following tracer injection were analyzed with the PCR technique (sample times represent the midpoint of a 20-minute sampling interval). Samples from MW-16 and MW-19 (tracer injection wells) were analyzed as positive controls.

PCR analysis results indicated a very strong presence of *Flavobacterium* cells in samples taken from the injection wells. The presence of *Flavobacterium* was also detected in the sample taken at 473 and at 793 minutes in MW-21 (Figure 10.2-1). This is a substantially longer arrival time than those for bromide and microspheres. The *Flavobacterium* signal in both of these samples appeared to be weak with respect to the injection wells.

The size of the encapsulated cells that were detected in MW-21 samples could not be determined with PCR analysis. The *Flavobacterium* signal may have been caused by encapsulated cell microbeads, or possibly by individual cells that had become separated from the encapsulation material.

These preliminary PCR results suggest that encapsulated-cell transport rates were highly retarded. Retarded *Flavobacterium* transport rates were indicated by a lack of *Flavobacterium* signal in the samples containing large amounts of bromide and/or polystyrene microspheres, and by a weak signal in the wells in which *Flavobacterium* was detected. Encapsulated cell retardation is indicated by longer arrival times for encapsulated cells than for microspheres.

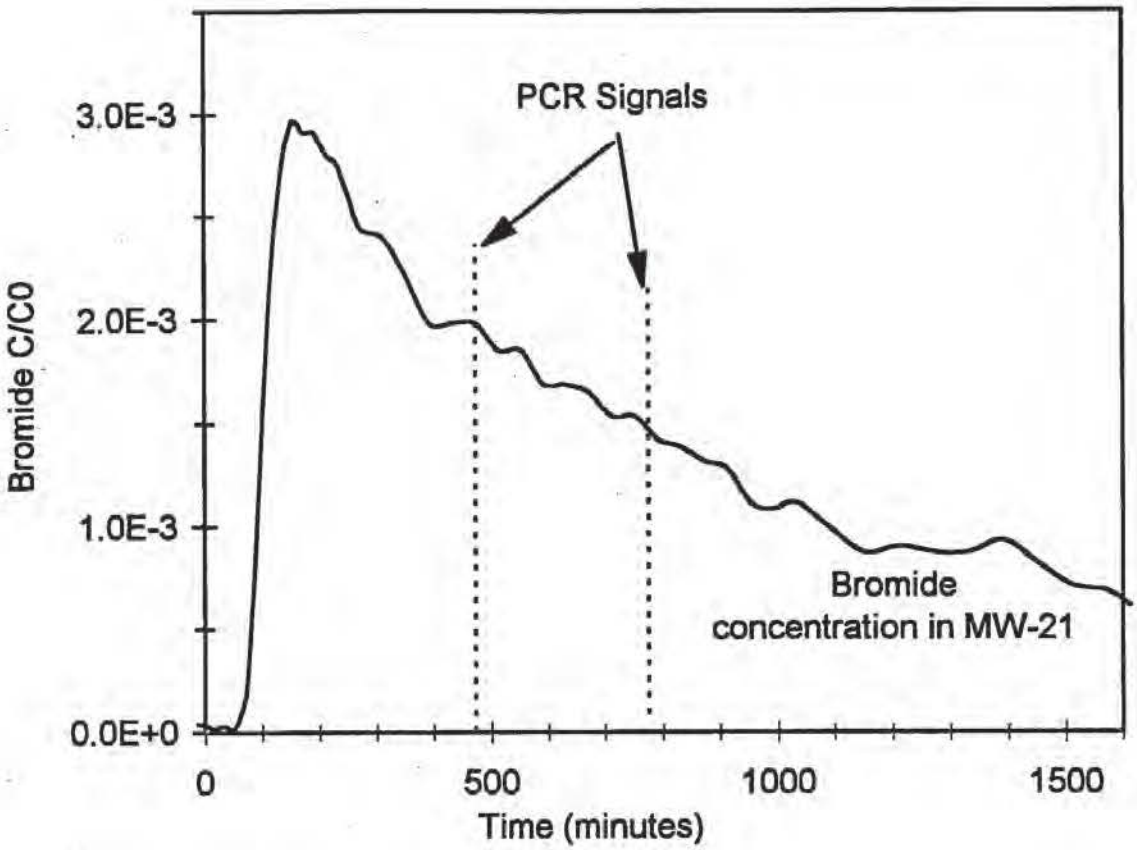

Figure 10.2-1: Occurrence of *Flavobacterium* (as indicated by positive PCR signals) in MW-21 ground water samples.

11. Discussion of Tracer Test Results

11.1 Introduction

This chapter provides a discussion of tracer test results. A discussion of observed tracer transport patterns is followed by a discussion of replicate tracer tests in which bromide was used. This is followed by a discussion of polystyrene microsphere transport results, focusing on the role of aquifer heterogeneity in the observed bromide and polystyrene microsphere transport patterns. This in turn leads to a general discussion about the possible role of particle tracers in a heterogeneous environment. Encapsulated cell transport patterns are addressed next, followed by a discussion about insights from polystyrene microsphere transport that might be applied to the use of *in situ* encapsulated cell applications.

11.2 Bromide Transport Patterns

The bromide transport patterns observed in this study are not those that might be expected under the ideal conditions in a homogeneous, isotropic aquifer. First, bromide concentrations in tracer test T3 were greater in MW-21 than in MW-20, even though MW-21 is further from the tracer injection well than MW-20 (Chapter 8). Second, bromide arrival occurred in MW-24 before MW-22 and MW-23, even though the latter wells are closer to the tracer injection well than MW-24. Similarly, bromide arrival occurred in MW-25 before MW-20; MW-25 is further from the tracer injection well than MW-20. Finally, estimated tracer velocities (Tables 9.3-3 and 9.3-4) indicate effective aquifer thicknesses that are significantly less than those indicated in the drilling logs.

Apparent anomalies in tracer concentrations, concentration peak arrival times, and apparent tracer velocities might be caused by (1) sampling error, (2) measurement error, and/or (3) aquifer heterogeneity. These reasons are explored below.

First, possible sampling errors during the tracer tests could include insufficient purge volumes and/or unrepresentative sample collection, or improper sample handling and/or storage. Ground water samples were collected continuously, and at the same

rate in each well. A lag period may have existed in which tracer concentrations in the aquifer formation changed at a faster rate than in the monitoring well, because of the borehole and casing volume, but this lag period probably was consistent between wells and over time. Improper handling and/or storage probably did not lead to the concentration anomalies described above, because samples from different tests and different wells were handled in a consistent manner.

Second, measurement error could have occurred during field (flow-through bromide probe) or laboratory measurements. Selective ion electrodes are generally considered suitable only for rapid estimation, but duplicate and replicate bromide measurements during laboratory analysis indicated consistent peak identification. Flow-through bromide probe measurements also indicated consistent peak identification with corresponding laboratory measurements.

The third possible explanation for unexpected differences in concentration peaks at different wells is the influence of aquifer heterogeneity. This appeared to be the most likely explanation, for the following reasons. First, significant heterogeneity in aquifer materials was observed during the installation of monitoring wells. Preferential ground water flow, occurring in zones with greater hydraulic conductivity than in surrounding areas, might be expected in a heterogeneous environment. Preferential ground water flow could account for the differences in bromide concentration peaks, bromide arrival times, bromide transport velocities, and asymmetrical bromide concentration peaks.

Bromide tracer transport results revealed the importance of preferential flowpaths in the movement of potential contaminants. Hydraulic testing results (on the basis of the multi-well aquifer tests) yielded a relatively small range of hydraulic conductivity estimates, in part because the multi-well aquifer tests result in the measurement of average aquifer characteristics . The bromide tracer test results revealed greater aquifer heterogeneity than indicated by hydraulic testing.

11.3 Replicate Bromide Tracer Test Results

Replicate tracer tests in Transects B and C using bromide tracer led to similar bromide concentrations in some wells, but not in others. Reasons for the differences

may include (1) bromide probe calibration error, (2) differences in injection and/or sampling methods, (3) differences in hydraulic gradient between tracer tests, (4) effects of elevated background concentrations (bromide concentrations remaining from the previous test), and (5) particle clogging in the aquifer.

First, bromide probe calibration error may be partially responsible for the differences. The electrode was found to be sensitive to temperature, concentrations, and immersion time (for tube samples), especially if concentrations remained fairly low (e.g., MW-20, tracer tests T3 and T4).

Second, extensive effort was made to ensure sampling and injection consistency between tracer tests. One observed difference was an approximate 10% (qualitative observation) loss in bromide injectate during injection in tracer test T3. T3 bromide concentrations were lower than T4 concentrations in well MW-21, but were higher in MW-20 and MW-25. The differences in T3 and T4 are not consistent with the inadvertent tracer loss during T3 injection.

Third, hydraulic gradient was kept as uniform as possible, but some differences were noted in the average hydraulic gradient (Table 7.4-1). Minor perturbations in the hydraulic gradient also may have caused slight differences in tracer arrival.

Fourth, elevated background concentrations were observed in the well transects at the beginning of the replicate tests (representing recirculating bromide from the previous test). Elevated background concentrations may represent a source of measurement error when measuring low concentrations in the replicate tests.

Finally, particle clogging in some flowpaths as a result of particle injections may have led to differences in bromide transport patterns between replicate tracer tests. Polystyrene microsphere and encapsulated cell transport results indicated that significant quantities of particles remained in aquifer materials. A rough approximation of the aquifer volume required to filter all of the particles injected in one tracer test follows. A total fluid volume of approximately 9 ml microspheres and 10 ml encapsulated cells were injected in each tracer test. If it is assumed that the particle volume is approximately half of the injected fluid amount (it was probably less than half), then the volume of aquifer required to hold that volume of particles (assuming a 30% aquifer

porosity) would be approximately 16 cm^3. It does not seem that enough particles were injected to lead to significant clogging.

In summary, the reasons for differences between the two replicate bromide tracer tests are unclear. It is believed that at least some of the difference lies in the bromide probe measurements and/or calibration. Additional replicate bromide tests conducted in series (with no particle injections between bromide tests), and the use of alternative analysis methods, might lead to further confidence in bromide sampling and analysis protocols.

11.4 Polystyrene Microsphere Transport Patterns

Several important polystyrene microsphere transport patterns were observed. First, the initial arrival of polystyrene microspheres occurred at approximately the same time as bromide in wells in which significant particle concentrations were observed, with the exception of MW-20, in which bromide arrival occurred later. Second, polystyrene microsphere concentration peaks consistently occurred before those of bromide in all wells in which significant concentrations of polystyrene microspheres were observed. Third, polystyrene microsphere concentration peaks were of shorter duration than the bromide peaks. Fourth, the 2-μm microspheres reached lower peak concentrations than bromide with respect to the original injection concentrations. Finally, the 5-μm microsphere concentration peaks appear to have occurred before the 2-μm sphere peaks in tracer test T1, but not in tracer test T3.

The observed differences in bromide and polystyrene microsphere peak concentration times may have been caused by (1) sampling and/or measurement error, (2) bromide concentration value errors, (3) bromide retardation, (4) polystyrene microspheres concentration peak value errors, or (5) flow in preferential ground water pathways. These possible factors are explored in the following paragraphs.

First, the differences in 2-μm-diameter microsphere and bromide concentration peak timing are consistent for both tracer tests in which particles were injected and among different observation wells in each test. There was no evidence for a consistent measurement error that might have led to these results.

Second, measurement error may have resulted in inaccurate bromide concentration peaks. Possible errors in bromide concentration values were addressed in Chapter 8. It appears unlikely that the timing of the bromide concentration peak is significantly different than that reported, although the actual magnitude of the peak may have been influenced by measurement error.

Third, the retardation of bromide tracer may have led to differences in concentration peak timing. While some bromide retardation may have occurred, bromide is generally considered not to be lost from a flow system by precipitation, absorption, or adsorption, and it is considered to be biologically stable (Schmotzer et al., 1973). Bromide is one of the most commonly used ion tracers for the determination of ground water flowpaths, ground water residence times, and the measurement of other aquifer properties (Davis et al., 1985). Anions are generally not affected by the aquifer medium (Davis et al., 1985), although clay minerals have an increasing capacity of holding anions as pH decreases. During aquifer tests the pH remained between 6.4 and 7.1 (Chapter 6). The amount of bromide retardation, if any, during the tracer tests is uncertain, but it seems unlikely that bromide retardation would have led to the bromide and polystyrene microsphere concentration peak differences observed in tracer tests T1 and T3.

Fourth, the differences in bromide and polystyrene microsphere concentration peak values may be an indication of inaccurate polystyrene microsphere peak concentration values. While significant variability was observed in the analysis of polystyrene microspheres (Section 9.4), the relative particle concentrations were consistent. In other words, there was agreement among technicians counting duplicate slides that samples contained either many spheres or few spheres, even though the actual count varied by as much as an order of magnitude. For that reason there is reasonable confidence that the polystyrene microsphere concentration peaks occurred for the times reported, although the actual magnitude of the peak may vary from the value reported.

Finally, the presence of preferential ground water flowpaths may led to the observed differences between bromide and polystyrene microsphere concentration peak times. The influence of preferential ground water flowpaths on microsphere transport is

consistent with the conceptual aquifer model and the interpretation of bromide transport results.

Differences in particle transport characteristics with respect to conservative tracers have been noted by other researchers. Earlier downgradient arrival of particle concentration peaks with respect to a conservative tracer are reported for *Escherichia coli* and particle tracers (Champ and Schroeter, 1988), yeasts (Wood and Ehrlich, 1978), and iron oxide colloids (Puls and Powell, 1992). Harvey et al. (1989, pp. 55) report that "unattenuated bacteria may be transported more quickly than a conservative tracer, simply on the basis of size." Harvey (1993) suggests that bacteria can move more rapidly than conservative tracers in an aquifer dominated by preferential flowpaths. Harvey et al. (1993), building on work by Bitton and Harvey (1992), suggest that microbial migration along preferred flowpaths or exclusion of particles from a portion of the total porosity on the basis of size may be responsible for the rapid migration of microorganisms with respect to conservative tracers.

Tracer test results indicate that the polystyrene microsphere peaks occur before bromide peaks, and that microspheres reach lower relative concentration peaks with respect to bromide. But despite differences in concentration peak timing, the initial arrival of the bromide and polystyrene microsphere tracers was at approximately the same time. Similar patterns may be present in transport comparison data of DAPI-stained bacteria and bromide in Harvey et al. (1989, Figure 3)) and bromide and *Escherichia coli* in Champ and Schroeter (1988, Figures 1, 2, and 3).

Similar arrival times for conservative ion and particle tracers suggests that the transport of particles may be just as rapid as *some* of the conservative solute tracer. However, the particle tracers are excluded by size from some (or most) of the ground water flowpaths. A portion of the conservative tracer also moves through zones of smaller interconnected pore spaces and is thereby subjected to longer, more tortuous flow paths. Transport of conservative tracer through more tortuous flowpaths may lead to greater dispersion, resulting in concentration peaks of longer duration. Therefore the aggregate conservative tracer concentration peak might be expected to occur after that

of the particle tracer, because the bromide concentration represents the aggregate flow through a greater volume of the total aquifer materials.

This concept is illustrated in Figure 11.4-1. Part (a) represents a hypothetical aquifer with four distinct preferential flowpaths (unlikely in an actual aquifer). The flowpaths represent varying degrees of hydraulic conductivity and tortuosity, with flowpath "A" being the most conductive. Part (b) of Figure 11.4-1 represents theoretical conservative tracer concentrations at the end of each flowpath.

It might be assumed that particles are only able to pass through flowpath "A", because flowpath "A" contains larger interconnected pore spaces than the other flowpaths (hence the greater hydraulic conductivity). Particles arriving through flowpath "A" probably migrate at approximately the same rate as the bromide tracer. However, the particle concentration peak would be observed before the aggregate bromide concentration peak, but at a lower peak concentration (because particles entering lower conductivity flowpaths are filtered)(Figure 11.4-1(c)). This hypothetical representation of particle and bromide migration in a highly heterogeneous environment may explain the different apparent transport rates and concentration peaks of 2-μm spheres and bromide in tracer tests T1 and T3.

The hypothetical representation of 2-μm spheres and bromide may also explain the different observed transport rates of 2- and 5-μm-diameter microspheres in tracer test T1. The 5-μm spheres arrive at approximately the same time as the 2-μm spheres, but the 5-μm sphere concentration peak occurs earlier. This would imply that available flowpaths are more limited for 5-μm spheres than for 2-μm spheres in the vicinity of Transect C.

The peak arrival of 5-μm-diameter microspheres in wells MW-20 and MW-21 occurred at or slightly after the arrival of 2-μm spheres. The 5-μm concentrations were very low, which limits confidence in the concentration peak timing. However, an arrival of the 5-μm peak at or after the 2-μm peak might indicate temporary filtration and subsequent release of 5-μm particles, or might indicate a small percentage of preferential pathways that are able to transmit uniformly both 2-μm and 5-μm spheres.

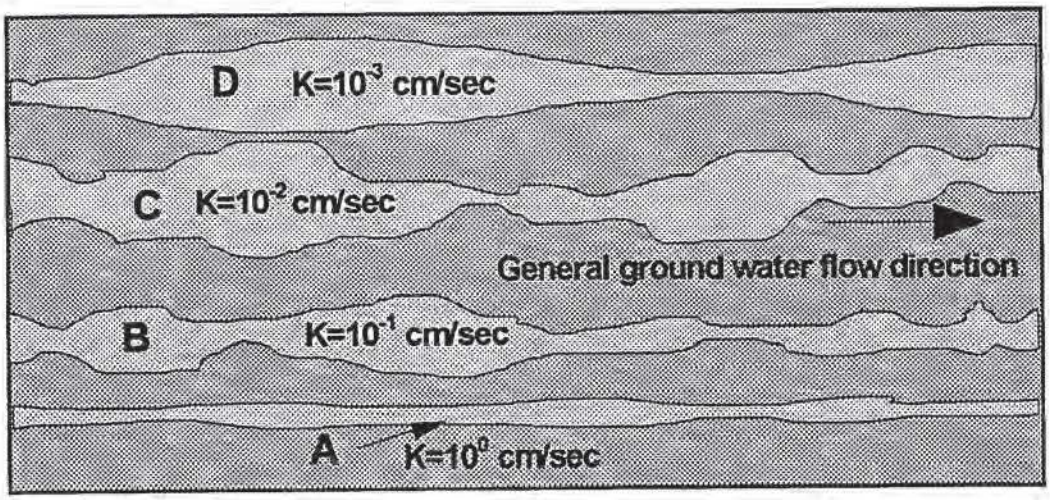

(a)

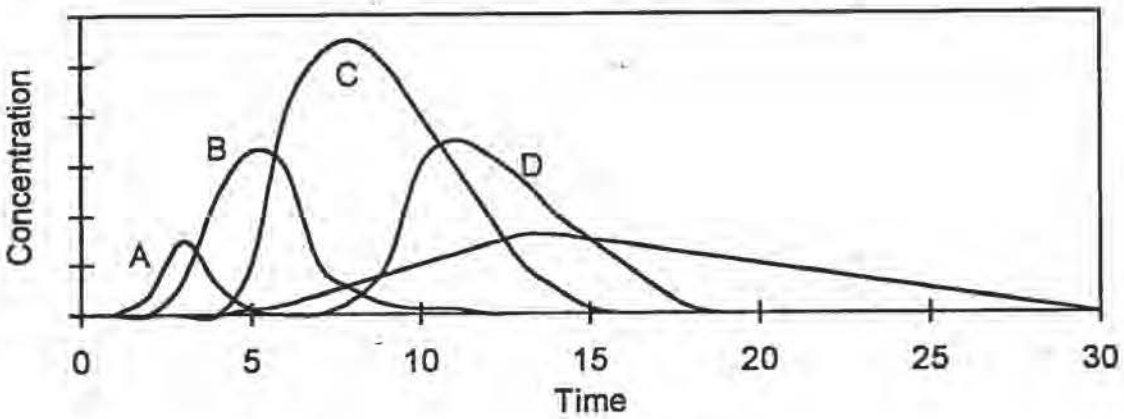

(b)

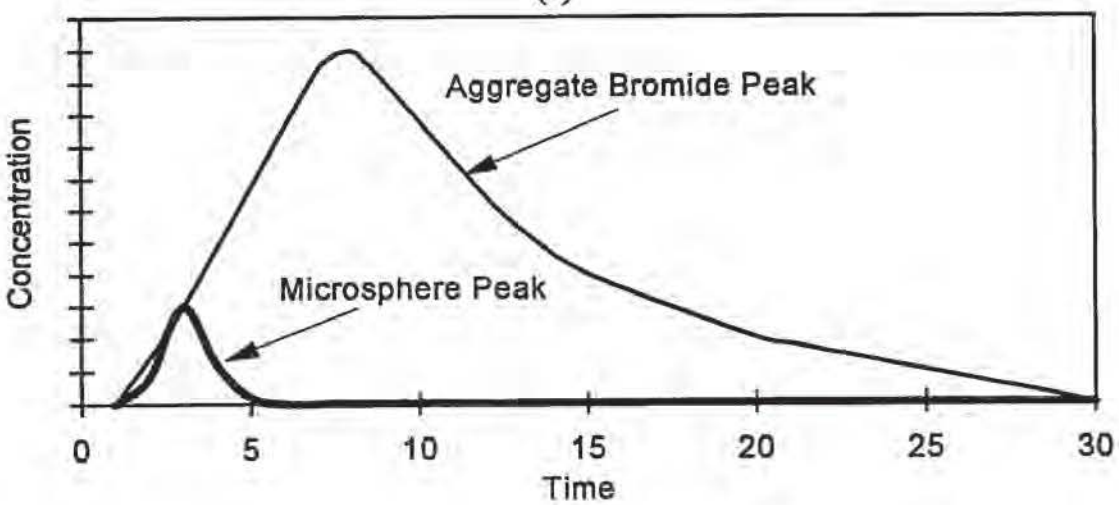

(c)

Figure 11.4-1: Hypothetical flowpath model (see text for explanation).

Fewer 5-μm-diameter spheres than 2-μm spheres were observed in monitoring well samples, and no 15-μm-diameter spheres were observed. Several 15-μm spheres were, however, observed in sediments removed from the bottom of MW-21, which indicates that some transport of 15-μm spheres occurred. Transport of particles as large as 15-μm or larger would have been expected in homogeneous materials on the basis of media and grain-size relationships described in Chapter 2 (see Figure 2.5-1).

Lower concentrations of larger diameter spheres may be attributed to (1) particle filtration, (2) particle sorption, (3) particle settling, and/or (4) insufficient injection concentration. First, polystyrene microsphere filtration may have occurred in places where the spheres were too large to pass through aquifer materials. Second, adsorption may have occurred because of interaction between the spheres and surrounding materials, although plain latex microspheres are thought to have relatively neutral surface characteristics. Third, sphere settling may have occurred in areas with insufficient ground water velocities to keep the spheres in suspension. Some settling was observed in well casing sediments.

Finally, the injection concentrations of the larger spheres may have been too low. Injection concentrations for 5-μm spheres were approximately two orders of magnitude less than the 2-μm injection concentrations; the 15-μm injection concentrations were approximately two orders of magnitude less than the 5-μm injection concentration. Injecting similar concentrations for each sphere size was prohibitively expensive. Peak concentrations for 5-μm spheres ranged from approximately 0.3 (MW-21, tracer test 3) to 14 (MW-18, tracer test 1) beads/ml; observing 15-μm spheres was therefore unlikely because the injection concentration was 2 orders of magnitude less than that of the 5-μm spheres.

Polystyrene microsphere C_{max}/C_o ratios decreased with distance (from the tracer injection well) more than bromide C_{max}/C_o ratios. This difference may also be the result of particle filtration, sorption, and/or settling. Invasive sampling and/or coring may have allowed a better description of particle fate in the aquifer sediments.

11.5 The Role of Particle Tracers in a Heterogenous Environment

This section provides a discussion of observed bromide and particle tracer patterns in the context of general transport parameters. The purpose of the section is to consider the role of particle tracers in evaluating transport patterns in a heterogeneous environment.

The movement of conservative ground water tracer in a homogeneous, isotropic aquifer has been described in terms of advection and dispersion by Bear (1972) and Freeze and Cherry (1979). The next several paragraphs provide a brief review of transport theory as a base for considering the role of particle tracers in heterogeneous aquifers.

Advective transport, or convection, is the process of contaminants being carried along with flowing ground water (Fetter, 1993). The amount contaminant being moved by advection depends on the contaminant's concentration and the quantity of flowing ground water.

Dispersion is primarily caused by the mechanical mixing of ground water flowing through tortuous aquifer pore spaces. Three factors affect the dispersion of a contaminant in moving ground water (Bear, 1972; Fetter, 1994): (1) pore space sizes, (2) flow path length (water moves along flowpaths of varying lengths in the same flow environment), and (3) friction in individual pores (water moves faster in the center of pores than along the edges).

Two-dimensional solute transport by advection and dispersion in a homogeneous medium with a uniform flow field (with the direction of flow parallel to the x-axis) can be described by the following equation (Fetter, 1993):

$$D_L\frac{\partial^2 C}{\partial x^2}+D_T\frac{\partial^2 C}{\partial y^2}-v_x\frac{\partial C}{\partial x}=\frac{\partial C}{\partial t}$$

where

D_L = the longitudinal hydrodynamic dispersion (L^2/T)

D_T = the transverse hydrodynamic dispersion (L^2/T)

v_x = average ground water velocity along the x-axis

C = solute concentration

The hydrodynamic dispersion coefficient, D, in the advection-dispersion equation is defined by the following formulas (Fetter, 1993):

$$D_L = \alpha_L v_i + D^*$$

$$D_T = \alpha_T v_i + D^*$$

where

D_L = hydrodynamic dispersion coefficient parallel to the principal direction of flow (longitudinal) (L^2/T)

D_T = hydrodynamic dispersion coefficient perpendicular to the principal direction of flow (transverse) (L^2/T)

v_i = average linear flow velocity (L/T)

α_L = longitudinal dynamic dispersivity (L)

α_T = transverse dynamic dispersivity (L)

D^* = effective diffusion coefficient (L^2/T) = ωD_d

where

ω = flowpath tortuosity factor

D_d = molecular diffusion

The hydrodynamic dispersion represents the processes of mechanical dispersion in moving ground water ($\alpha_L v_i$) and molecular diffusion. The hydrodynamic dispersion coefficient is generally dominated by mechanical dispersion in a flowing ground water environment. Longitudinal or transverse dispersivity values, defined as media properties, are often estimated on the basis of the transport patterns of a conservative, dissolved solute tracer. As such, the dispersivity values represent averaged estimates; tracer concentrations at any one point in the aquifer represent tracer moving in a variety of flowpaths.

Dispersivity values have been shown to depend on the scale of measurement (Pickens and Grisak, 1981; Gelhar, 1986). The differences between small scale measurements and field scale measurements depend on the range of flow conditions encountered. For instance, a field scale environment generally will have a greater range

of hydraulic conductivities and ground water flowpaths than a micro-scale flow domain consisting of only a few pore lengths. The greater range of flow conditions are thought to contribute to greater dispersion at field scale lengths (Fetter, 1993).

Aquifer transport parameter values may depend not only on the measurement scale but also upon the flowpath domain in which tracers are migrating. Significant differences in transport patterns were observed in this project between assumed conservative solute and polystyrene microsphere tracers. Particle tracer migration appeared to be defined by flowpaths capable of transmitting the particles. The larger the particles, the fewer the flowpaths that appeared able to transmit them.

The flowpaths capable of transmitting particles are a subset of those capable of transmitting a conservative dissolved solute. This subset of flowpaths also appeared to control the initial arrival of the dissolved tracer (bromide) at the Plant Science Farm site, since the bromide and polystyrene microsphere tracers appeared to arrive at approximately the same time. The subset of flowpaths capable of transmitting particles could also be expected to have significant influence on the initial spread of a contaminant.

On the basis of the experiments conducted for this project, the use of both conservative solute and particle tracers may represent a method for evaluating transport characteristics in the subset of flowpaths that influence the initial spreading of a contaminant plume. Estimates of dispersivity values could be made for an aquifer as a whole, or for aquifer portions capable of transmitting particles of varying diameters.

A numerical model could be used to evaluate averaged transport parameters at the site. A calibration process using deterministic or stochastic numerical models is frequently used to estimate transport parameters in the advection-dispersion equation (Fetter, 1993). The models allow the estimation of advection-dispersion parameters through an iterative calibration process. Iterative calibration using transport models is often necessary because of the number of variables and the frequent lack of discrete parameter measurements (e.g., it is generally not possible to obtain discrete D_L and D_T measurements).

A numerical model also could be used to evaluate transport characteristics for different flowpath groups, on the basis of observed particle and dissolved tracer transport characteristics. Such a numerical model, focusing on transport characteristics of a heterogeneous environment with multiple ground water flowpaths, was outside the scope of this project, but should be considered for future work.

11.6 Encapsulated Cell Transport

On the basis of polystyrene microsphere transport patterns it would be expected that encapsulated cells in the low end of the size range shown in Figure 2.3-1 (e.g., less than approximately 10-μm in diameter) would also have been transported in the Plant Science Farm aquifer. However, very low concentrations of encapsulated cells were observed in monitoring well samples. Encapsulated cell transport, as observed with the PCR analysis, was retarded with respect to bromide and polystyrene microsphere tracers.

Low apparent encapsulated-*Flavobacterium* transport rates could be caused by several factors. These include (1) filtration, (2) analysis error and/or method limitations, (3) loss of small size fractions during encapsulated cell staining, (4) interaction between encapsulated cells and aquifer sediments, and/or (5) insufficient injection quantities.

First, it may be possible that encapsulated cells were filtered in aquifer materials. The larger encapsulated cells (which were as large as 80-μm in diameter; see Figure 2.3-1) likely would be filtered. However, polystyrene microspheres as large as 15-μm were transported to MW-21 (observed in casing sediments), and thus it would be expected that at least some transport of the smaller encapsulated cells would have occurred (casing sediments were not analyzed for encapsulated cells).

Second, analysis error and/or limitations may have resulted in apparent low encapsulated cell transport rates. Microscopy was not an adequate screening technique for analyzing multiple samples.

Injection well samples and internal controls provided confidence in the PCR method, but only a limited number of ground water samples were analyzed using the PCR technique because of the technique complexity. Short spikes in the encapsulated

cell concentrations may have existed in samples not analyzed. However, this seems unlikely since samples taken a short time after injection were negative; retarded transport would probably lead to concentration peaks of longer duration, which would have been detected in the ground water samples analyzed with PCR.

The PCR technique was also only used for ground water samples obtained from monitoring well MW-21 (tracer test T3) and the associated injection well. Transect C well samples may have exhibited different transport patterns. Samples from Transect C wells were not analyzed with PCR because of the complexity and cost (in time) of the PCR technique.

Third, it may have been possible that significant numbers of smaller encapsulated cells were inadvertently lost during the acridine-orange staining and decanting process (See Section 5.10.3). The smallest diameter particles are the least prone to particle filtration, all other factors being equal, and decanting may have resulted in the inadvertent loss of some of these smaller particles.

Fourth, interaction between encapsulated cells and aquifer sediments may have resulted in significant retardation of the encapsulated cells with respect to the more conservative tracers. No literature reports were found describing agarose interaction with subsurface sediments. The possibility of encapsulated cell interaction with aquifer materials merits further study.

Finally, insufficient injection quantities may have led to low concentrations at the monitoring wells. The initial injection quantities of encapsulated cells could not be determined from injection well samples. A probable reason for low 2-μm and 5-μm polystyrene microsphere concentrations was that injection quantities were too low.

Quantifying encapsulated cells under a microscope or detecting encapsulated cells with PCR was not practical for large quantities of ground water samples. A better method for evaluating the effectiveness of *in situ* bioremediation using encapsulated cells might be to monitor degradation products resulting from encapsulated cell activity.

The encapsulated cell transport results did not provide a full understanding of encapsulated cell migration at this field site. Furthermore, encapsulated cell transport patterns could not be correlated with those of polystyrene microspheres. Preliminary

results suggest that the transport of agarose-encapsulated *Flavobacterium* was retarded with respect to polystyrene microspheres. Greater retardation may indicate that encapsulated cells were filtered by or adsorbed to aquifer sediments more than polystyrene microspheres.

General polystyrene microsphere transport characteristics, such as the observed transport patterns in a heterogeneous environment, help to suggest some possible encapsulated cell transport patterns. Tracer test results revealed that 2-μm-, 5-μm-, and 15-μm-diameter polystyrene microspheres were transported at least some distance in the Plant Science Farm aquifer. Analysis of sediments removed from the bottoms of wells revealed that 5-μm spheres had been transported to most wells; 15-μm spheres were observed in well bottom sediments removed from MW-21.

Particle transport appeared to have been restricted to preferential aquifer flowpaths. Preferential flowpath thicknesses, estimated on the basis of tracer transport velocities, indicate particle transport in less than approximately 0.5 to 5% of the assumed 152-cm aquifer thickness. On the basis of these observations it is likely that encapsulated cell transport would also be limited to those preferential aquifer flowpaths capable of allowing the passage of polystyrene microspheres. Encapsulated cells migrating in preferential flowpaths would thereby be excluded by size from other portions of an aquifer containing contaminants.

In summary, encapsulated cell transport patterns at the Plant Science field site could not be defined well on the basis of the encapsulated cell transport results. Polystyrene microspheres do not appear to represent an acceptable analogue for the encapsulated cells, since encapsulated cell transport appeared to be retarded with respect to microspheres. However, it appears that the use of polystyrene microspheres can be very helpful in defining general transport patterns, such as the migration in specific preferential flowpaths. Using polystyrene microspheres to evaluate the role of aquifer heterogeneities may thus assist in the use of both encapsulated cell and free cells for *in situ* bioremediation efforts.

11.7 The Use of Encapsulated Cells for *In Situ* Bioremediation

The general purpose of this project was to investigate particle transport characteristics to aid in the development of encapsulated cell biodegradation methods. This section addresses the potential use of encapsulated cells for *in situ* biodegradation on the basis of the transport studies described above.

The design of an *in situ* bioremediation system in a heterogeneous field environment using encapsulated cells must take into account the influence of aquifer heterogeneities and encapsulated cell transport characteristics. Factors influencing a bioremediation design using encapsulated cells would depend on specific aquifer and contaminant characteristics.

There are, however, some general considerations for the use of encapsulated cells in a heterogeneous environment that can be drawn from the results of this research. Encapsulated cell microbeads or the encapsulated cells themselves would need to come into contact with the ground water contaminant. This means that ground water carrying a dissolved contaminant would need to come into contact with encapsulated cell microbeads contained in (by filtration or adsorption) preferential flowpaths, or individual cells from the microbeads would need to be released from the microbeads so that they can be transported to aquifer zones from which microbeads are excluded.

There are several ways in which this might be done. Strategies for using encapsulated cells in a heterogeneous environment might include (1) establishing a recirculating flow system, (2) designing encapsulated cell beads for microbial release, and (3) using encapsulated cell beads in a "microbial curtain" design.

First, a recirculation system, such as the system used in the tracer tests conducted for this project, would allow for the repeated contact of encapsulated cells and contaminated water. Encapsulated cell microbeads could be designed for continued transport, or they could be designed with encapsulation materials that would lead to filtration and/or adsorption. Contaminated, recirculating water would come into contact with encapsulated cells even if the microbeads containing encapsulated cells were

transported a only very short distance from the injection well, and if the microbeads were limited to preferential ground water flowpaths. A recirculating flow system would also allow for above-ground treatment of other contaminant constituents.

A second strategy might be to design microbeads containing encapsulated cells for the eventual breakdown and release of the encapsulated cells. Temporary encapsulation might allow a sufficient acclimation period for newly-introduced cells in the subsurface. Released individual cells might then migrate to portions of the aquifer that would exclude the entire encapsulated cell microbeads. However, the encapsulated materials could eventually break down, leading to the further transport of microbead fragments or released cells. Also, some cell reproduction may occur on the bead exterior. These processes could lead to the release, further transport, and numeric amplification of cells capable of contaminant degradation.

Third, encapsulated cells could possibly be injected into the ground to form a "microbial curtain" in advance of a migrating contaminant plume. Contact between the contaminant and the encapsulated cells would occur as the contaminant migrated toward and into the microbial curtain. Nutrient and/or energy sources contained in the encapsulated cell microbeads would help maintain cell survival until the arrival of the contaminant plume.

In summary, preliminary results of these experiments indicate limited transport of encapsulated cells. A recirculating treatment system design, such as that used for this project, would allow for repeated contact between a dissolved contaminant and filtered and/or adsorbed encapsulated cells. The effectiveness of such a system might be tested with a pilot-scale system at a contaminated site. This might allow the effectiveness of encapsulated cell degradation to be monitored by actual contaminant degradation rates.